Investigating the Relationship between Lung Cancer and the Infection with the Parasite *Toxoplasma gondii*

Muyassar K. Tarabulsi

School of Science, Engineering and Environment

University of Salford, Salford, U.K.

Submitted in Fulfilment of the Requirements

of the Degree of Doctor of Philosophy

2020

Table of Contents

List of Figures

List of Tables

Acknowledgement

I would like to express my sincere gratitude to my supervisor Professor Geoff Hide, for providing his invaluable guidance, comments, suggestions and constant motivation throughout the course of the project. I would also like to thank Dr Dave Singh, Dr Thomas Southworth, Dr Josiah Dungwa and my co-supervisor Dr Lucy Smyth for providing the human lung cancer samples.

A special thanks to Dr Paul Denny, University of Durham, for kindly providing the *Toxoplasma gondii* parasites, and my colleague Bader Alwafi for the cultured cells. Also, I would like to thank Ms. Manishadevi Patel for her motivation and assistance in the lab, Mrs. Catherine Hide, for her assistance with sample preparation, Dr David Greensmith and Matthew Jones.

A special thanks to the Saudi Arabian cultural bureau for funding. Special thanks to all the staff of the school of Science, Engineering and Environment and my colleagues for constant motivation and support.

Last but not least, I am very thankful to my parents for their love, prayers caring, and sacrifices for educating and preparing me for my future. I am very thankful to my daughter Sariya for motivating me to always work harder. Finally, my deepest gratitude to my caring husband Dr Mohammed Nagshabandi, for his love, support and encouragement when times got rough.

Abbreviations

Acute Myeloid Leukaemia (AML)

Adventitia (Ad)

Alkaline Phosphatase (AP)

Antibody-Dependent Cellular Cytotoxicity (ADCC)

Arginase 1 (Arg-1)

Bronchiole (Br)

Bronchoalveolar Lavage (BAL)

Central Nervous System (CNS)

Cerebrospinal Fluid (CSF)

Chronic Obstruction Pulmonary Disease (COPD)

Diaminobenzidine (DAB)

DNA Damage Response (DDR)

Environmental Protection Agency (EPA)

External Elastic Lamina (EEL)

FITC-Dolichos biflorans (FITC-DB)

Fluorescein Isothiocyanate (FITC)

Haematoxylin Eosin Staining (HE)

Hepatocellular Carcinoma (HCC)

Horseradish Peroxidase (HRP)

Immunohistochemistry (IHC)

Immunofluorescence (IF)

Immunoglobulin G (IgG)

Immunoglobulin M (IgM)

Indoleamine 2, 3-Dioxygenase (IDO1)

Inducible Nitric-oxide Synthase (iNOS)

Interferon γ (IFN-γ)

Internal Elastic Lamina (IEL)

Lewis Lung Carcinoma (LLC)

Macrophages (Mg)

Manders Correlation Coefficient (MCC)

Multi-Locus Sequence Typing (MLST)

Nicotinamide Adenine Dinucleotide Phosphate (NADPH)

Nested Polymerase Chain Reaction (n-PCR)

Nitric Oxide (NO)

Nitic-Oxide Synthase (NOS)

Non-Small Lung Cancer (NSCLC)

Ornithine Decarboxylase (ODC)

Pearson's Correlation Coefficient (PCC)

Polymerase Chain Reaction (PCR)

Recombinant Human Arginase (rhArg)

Restriction Fragment Length Polymorphism (RFLP

Rhoptry Kinase (ROP16)

Small Cell Lung Cancer (SCLC)

Smooth Muscle (SM)

Surface Antigen Gene (SAG)

Toxoplasma Perforin-like Protein1 (TgPLP1)

Type I Pneumocytes (Type I)

Type II Pneumocytes (Type II)

Vascular Smooth Muscle (VSM)

Declaration

I hereby declare that the work that is presented in this thesis is my own work. Except where states otherwise by reference or acknowledgment, the work presented is entirely my own. I declare that I have not submitted this work for a degree or any other qualification at this or any other university.

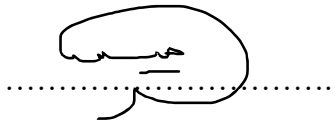

Muyassar K. Tarabulsi

March 2020

Abstract

Toxoplasma gondii is an obligate intracellular organism that has a worldwide distribution and is highly prevalent among animals and humans. Although usually asymptomatic, it can cause serious diseases in immunocompromised individuals such as pneumonia, ocular toxoplasmosis and abortions. Many studies have investigated *T. gondii* among cancer patients. However, none have addressed the significance of the infection with this ubiquitous parasite among this group. We aimed to investigate the relationship between *T. gondii* infection and lung cancer. In a study done at Salford University (published, 2019), 72 lung samples from patients with lung cancer were investigated for *T. gondii* infection by nested PCR and immunohistochemistry (IHC), and it documented a striking 100% prevalence. We recruited ten lung samples via bronchoalveolar lavage from healthy individuals to be used as a control group for the lung cancer patients study. Samples were tested with nested PCR targeting five *T. gondii* specific markers (B1, SAG1, SAG2 3′, SAG2 5′ and SAG3) and only one sample was positive for *T. gondii* infection with all five markers and then was further confirmed by IHC. Statistical analysis revealed an extremely significant difference between the lung cancer patients and the non-cancerous control group ($P<0.0001$). Previous studies on mice and rats have demonstrated the involvement of iNOS and Arginase gene expression in *T. gondii* infection. Nothing is known about the role of iNOS and Arginase in human lung tissue infected with *Toxoplasma*. We have established and optimised an IHC protocol to detect iNOS and Arg-1 in lung cancer samples and established a double immunofluorescence (IF) protocol to colocalise and measure the degree of colocalisation of Arg-1/*T. gondii* and iNOS/*T. gondii* parasite in 51 lung cancer samples. IHC results revealed expression of Arg-1, iNOS and *T. gondii* in the bronchiolar epithelium, smooth muscle cells of blood vessels, alveolar macrophages and type I and II pneumocytes. IF results revealed, at the alveolar macrophage level, Pearson correlation coefficient (PCC) measurement documented a significantly higher Arg-1/*T. gondii* colocalisation than iNOS/*T. gondii* ($P<0.00001$), whereas at the *T. gondii* cysts, iNOS/*T. gondii* colocalisation was significantly higher than Arg-1/*T. gondii*($P<0.0031$). On the other hand, at the level of the alveolar knobs, no differences were established in the colocalisation between Arg-1/*T. gondii* and iNOS/*T. gondii (*$P=0.49$). The difference in the level of expression between Arg-1 and iNOS suggest differences in the functions of these two markers in relation to *T. gondii* infection.

Chapter 1: General Introduction

1.1 General Introduction

The broad aim of this project was to conduct a detailed investigation into the relationship between infection with the parasite *Toxoplasma gondii* and lung tissue in samples collected from lung cancer patients. Furthermore, the study aims to investigate the relationship between *T. gondii* infection in lung tissue with respect to the expression of two important enzymes involved in immunity to pathogens. These enzymes, inducible Nitric Oxide Synthase (iNOS) and Arginase-1, act antagonistically and have been shown to control *T. gondii* infection in laboratory rodents.

Cancer is a leading health problem that affects many parts of the world and has claimed the lives of many individuals from all different ages (Jemal et al., 2008). With the various types of cancer, lung cancer continues to be a leading cause of death, and it is estimated that 1.4 million deaths worldwide are due to lung cancer alone (Mong et al., 2011). Due to the increased blood supply to the respiratory system, lung cancer has a high frequency of metastasis (Arya, 2011). In addition to the characteristic diminished oxygenation of this type of cancer, it exerts a tremendous burden on the quality of life (Arya, 2011). For therapeutic purposes, lung cancer is differentiated histologically and can be classified into two major groups, Small Cell Lung Carcinoma (SCLC) and Non-Small Cell Lung Carcinoma (NSCLC) (Travis, 2011). (SCLC) are epithelial tumours consisting of small cells with scant cytoplasm (Travis et al., 2004). It is a rapidly growing tumour and is the most aggressive (Travis et al., 2004), and accounts for 10%-15% of all lung cancers (Travis, 2011). Although smokers can develop all type of lung cancer, (SCLC) is strongly related to cigarette smoking and can metastasise rapidly to various sites within the body, which unfortunately is usually only discovered after it has spread extensively (Travis, 2011).

(NSCLC) is the most common type of lung cancer and accounts for about 85% of all lung cancer cases (Travis et al., 2015). (NSCLC) can be further divided into three subgroups differentiated by the type of cells found in the tumour: squamous cell carcinoma, large cell carcinoma and adenocarcinoma (Travis, 2011). Adenocarcinomas consist of glandular tumour cells that produce mucous and mostly arise in the peripheral areas of the lungs (Travis et al., 2015). On the other hand, squamous cell carcinomas, also known as epidermoid carcinomas, are malignant epithelial tumours which arise in the central chest area with a close relationship to the large bronchi (Travis et al., 2004). Large cell carcinomas are undifferentiated non-small cell carcinomas that lack the cellular features of small cell carcinoma or squamous carcinomas (Travis et al., 2015).

Smoking is a major risk factor for many diseases and plays a significant role in the development of lung cancer (Gasperino, 2011). A study revealed that in England, 81,400 deaths in 2009 were attributed to smoking, where 35% died from different respiratory diseases and 29% due to different types of cancers with lung cancer accounting for the highest number of deaths (Denman et al., 2015). Smoking is considered to be the primary cause of lung cancer, where 85% of lung cancer cases are due to smoking and passive smoking (Mong et al., 2011). The second leading cause of cancer in the lungs is radon, a naturally occurring radioactive odourless gas, which according to the United States Environmental Protection Agency, (EPA), causes 21,000 cases of lung cancer each year (Denton and Namazi, 2013). Other risk factors include gender, family history of lung cancer and radiation therapy to the chest (Gasperino, 2011).

Cancer patients in general, including lung cancer individuals, are subjected to various types of infections (Perlin et al., 1990). In the majority of lung cancer cases (50-70%), the course of the disease is complicated by pulmonary infections irrespective of lung tumour histology (Perlin et al., 1990). Some aspects including age >70, and advanced stages of lung cancer have been implicated in higher infection rates (Sarihan et al., 2005). Different factors can predispose patients with lung cancer to infections (Sarihan et al., 2005). Including, dysfunction of the humoral and cellular immunity, dysfunction of central nervous system and medical interventions (Lehrnbecher and Laws, 2005).

In some cancers arising from immune cells, e.g. Leukaemia and lymphoma, the susceptibility to infection could be due to the underlying malignancy itself (McDonald and Atkins, 1990). In addition to those deficiencies created by the malignant process, many patients acquire deficiencies in host defence mechanisms as a consequence of their therapy (McDonald and Atkins, 1990). The majority of chemotherapeutic drugs are designed to target the rapidly dividing tumour cells (Behl et al., 2006). However, the dividing cells of the immune system are also affected by these drugs, leading to lymphopenia with decreased percentage of circulating T cells (Behl et al., 2006). Antitumor agents can have tremendous effects on humoral and cellular defence mechanisms, even at doses that do not cause myelosuppression (Gerald, 1986). Major immune processes could be inhibited by chemotherapeutic agents including antigen recognition by precursor T and B lymphocyte, antigen uptake and processing by macrophages, lymphoblastoid transformation and proliferation, and antibody production (Gerald, 1986).

One common side effect of chemotherapy is neutropenia, the decreased number of neutrophils, which is a major factor contributing to infections in patients undergoing chemotherapy (Sarihan et al., 2005). The severity and the frequency of the infections depend on duration and the severity of neutropenia.

Moreover, damage to anatomical barriers is common after chemotherapy and radiation therapy. Patients with lung cancer often take corticosteroids for various reasons, including management Chronic Obstructive Lung Disease, COPD (Akinosoglou et al., 2013). As a result, suppressed cellular immunity due to the chronic use of corticosteroid favours opportunistic pathogens, including pathogens of the genus *Aspergillus* and *Pneumocystis jiroveci* (Akinosoglou et al., 2013). All these factors could predispose cancer patients to not only bactria and fungus but also opportunistic parasites (Yuan et al., 2007). One of the major opportunistic infections that can cause life-threatening manifestations in cancer and other patients is the parasite *T. gondii* (Scerra et al., 2013).

1.2 History of *Toxoplasma*

It has been more than a hundred years since the first identification of the parasite, *T. gondii*, in 1908 by Nicolle and Manceaux (Dubey, 2009). *T. gondii* was accidentally discovered while working with the parasite *Leishmania* and some viruses (Dubey, 2009). *T. gondii* was first isolated from a hamster-like rodent, *Ctenodactylus gundi*, from where the parasite got its species name. While the genus name was derived from the Greek word toxon = bow due to the crescent shape of the parasite (Black & Boothroyd 2000). Parasite transmission remained a mystery until 1970, the year its full life cycle was discovered (Dubey, 1996) and the cat was implicated as the only definitive host – the host in which the parasite can complete its full sexual life cycle (Frenkel, 1970). Gundis inhabit the southern Tunisian mountains and were used by scientists for research on leishmaniasis (Dubey, 2009). Since the parasite was found in the blood of the host, it was speculated that the mode of transmission involves arthropods (Dubey, 2009). However, it was later observed that *C. gundi* was not infected in the wild but had caught the infection from the laboratory (Dubey, 2009). This once obscure protozoan parasite of an obscure African rodent has become one of the most interesting subjects whose importance has been revealed by many years of research. *T. gondii* is a member of the phylum Ampicomplexa, which includes intercellular parasites that have a distinctive polarised cell structure and an apical complex (Dubey et al. 1998). *T. gondii* is related to the causative agent

of coccidiosis (*Eimeria* spp.) and *Plasmodium* spp., the causative agent of malaria (Boothroyd & Grigg 2002).

1.3 Life cycle of *T. gondii* and disease manifestations

T. gondii is an obligate intracellular protozoan parasite (Black and Boothroyd, 2000), which is considered to be one of the most successful eukaryotic parasites ever known to date (Su et al., 2010). That is due to many reasons, such as the wide range of warm-blooded vertebrates that it infects, the ability of the parasite to infect any nucleated cell, the characteristic persistent infection of the parasite and the high worldwide prevalence in humans of up to 30% (Hide et al., 2009). It is estimated that up to one-third of the world's population is chronically infected (Tenter et al., 2000), although there are national differences in prevalence (Pappas et al., 2009). Different factors such as, environmental and eating habits, climate conditions and host age, all contribute to the difference in prevalence around the world (Leal et al., 2007). In Europe, 30 to 60% of the *T. gondii* prevalence is probably due to the habit of eating undercooked meat (Halos et al., 2010). In France, since the consumption of undercooked meat is higher than any other region in Europe, 43.8% of tested pregnant women are seropositive (Halos et al.2010).

The sexual life cycle of *T. gondii* takes place in members of the Felidae family, which involves cats and its relatives, making them the only known definitive host for *T. gondii* (Frenkel, 1978), (Figure 1.1).The environmentally resistant oocyst is shed with the faeces of the infected cat, which can shed approximately 100 million oocysts per day (Dubey, 1996). Various factors such as humidity and temperature, aid in the sporulation of the oocyst outside the host to form the infective stage (Fritz et al., 2012). It is estimated that mostly all warm-blooded vertebrates are intermediate hosts, including marine mammals, birds, rodents and humans (Dubey et al., 2013). Intermediate hosts get infected through oral ingestion of oocysts harbouring the sporozoites either from water, soil or plants, where the asexual life cycle of the parasite takes place (Dubey et al., 2013). Sporozoites are released not long after the ingestion of the oocysts and differentiate into tachyzoite after penetrating the intestinal epithelium (Robert-Gangneux and Dardé, 2012). Tachyzoites form bradyzoites filled tissue cysts and localise into different tissues, including muscular and neural tissue (T. Wang et al., 2014). Definitive hosts, (cats), acquire the infection through the direct ingestion of sporulated oocysts, or by preying on infected intermediate hosts with tissue cysts (Frenkel, 1978). The human host can get infected either through the consumption of contaminated food or water, eating undercooked or raw meat products that harbour the tissue cyst, or handling contaminated environmental samples

such as cleaning cat litter boxes (Dubey, 2004). Another route of transmission is via blood transfusion or organ transplantation (Robert-Gangneux and Dardé, 2012), and finally, the infected mother can transmit the infection through the placenta to her unborn foetus (Tenter et al., 2000). The well-understood life cycle of *T. gondii* parasite identifies the main three routes of transmission, ingestion of oocysts shed by cats, consuming undercooked or raw meat containing the tissue cysts and finally, vertical transmission (Hide et al., 2009; Hide, 2016).

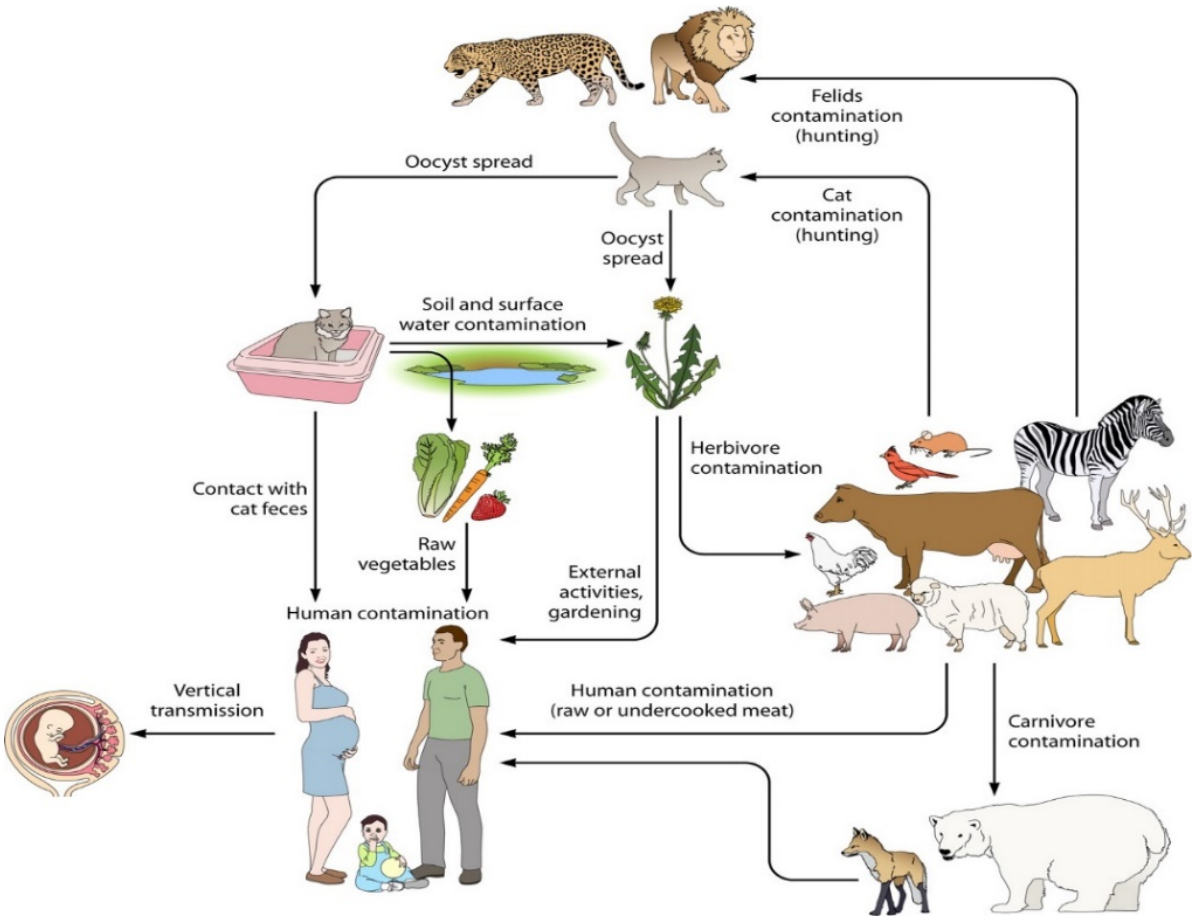

Figure 1.1 The life cycle of *T. gondii* parasite (Robert-Gangneux and Dardé, 2012). The intestinal tract of felines is the only source for the production of *T. gondii* oocysts. The human host obtains the infection either through the ingestion of undercooked meat that harbours the tissue cyst or by the ingestion of oocysts from contaminated sources (e.g., water, soil, vegetables and cat litter). Congenital infection is the transmission of the infection with *T. gondii* from the infected mother to her unborn fetus transplacentally.

If a mother developed an acute *T. gondii* infection during her pregnancy, her developing foetus would most probably be affected (Cortina-Borja et al., 2010). This is termed congenital

toxoplasmosis and can lead to catastrophic outcomes (Cortina-Borja et al., 2010). While the majority of the neonatal cases are presented without symptoms, a proportion result in deformities and unfortunately sometimes, death (Dubey and Jones, 2008). A number of babies are born supposedly healthy but later in life develop ocular toxoplasmosis (Dubey and Jones, 2008). While other babies are born with apparent manifestations, including hydrocephalus, retinochoroiditis, mental retardations and intracranial calcifications (Cortina-Borja et al., 2010). An infection with *T gondii* during pregnancy could end by stillbirth or spontaneous abortions in both humans and animals (Weiss and Dubey, 2009). In fact, Sheep are considered highly susceptible to abortions, where they can reach epidemic proportions (Holec-Gąsior et al., 2015).

Fortunately, 80-90% of the cases are asymptomatic, many aspects influence this, including host species and susceptibility, acquired immunity status and the parasite virulence (Sheffield and Melton, 1974). When *T. gondii* infection causes symptoms, it can be acute, sub-acute or chronic infections (Dubey, 1996). Swollen and painful lymph nodes in various sites, (inguinal, cervical or supraclavicular regions) is the most common symptom of acute infections. Other flu-like symptoms such as fever, headache, myalgia and lung involvement could occur in acute infections and can be easily mistaken for the flu; however, it is self-limiting (Robert-Gangneux and Dardé, 2012). In sub-acute infections, tachyzoites damage tissues and form extensive lesions in the brain, liver, eyes or lungs. This occurs when the host immunity develops slowly, and the acute phase is prolonged (Weiss and Dubey, 2009) On the other hand, when the host's immunity is adequate enough to overcome the proliferation of tachyzoites, chronic toxoplasmosis occurs, where tachyzoites transform into bradyzoites, and a cyst can be formed. This stage can be asymptomatic or be without any clinical significance and can persist for years (Dubey, 1996). However, if the infected individual became immunocompromised, this could result in serious manifestations affecting various organs (McLeod et al., 2014). If the central nervous system was involved, encephalitis could develop with symptoms varying from poor coordination, lethargy, loss of memory, or seizures (Carruthers and Suzuki, 2007). Ocular toxoplasmosis occurs when the chronic or relapsing tachyzoites infect retinal cells and can result in blind spots, and sometimes complete visual impairment, adding to the list of severe outcomes of toxoplasmosis in immunocompromised hosts (Dubey, 1996). Cancer patients under chemotherapy, organ transplant recipients under immunosuppressive treatment, and AIDS/HIV patients, are all considered immunocompromised hosts (Gallego et al., 2006), and since infection with *T. gondii* in these individuals is an opportunistic infection, it can lead to serious complications, or even death (Khan et al., 2005). Studies carried out on HIV

asymptomatic individuals in the United Kingdom have shown that 27% were serologically positive for *Toxoplasma* (Rottenberg et al., 1997).

1.4 Lung toxoplasmosis

In immunocompromised hosts with toxoplasmosis, lungs are the second most common site for infection after the central nervous system (Pomeroy and Filice, 1992). Reactivation of previously acquired toxoplasmosis infection is usually the cause of toxoplasmosis (Rottenberg et al., 1997).

When lungs are involved in toxoplasmosis, there are two main classifications depending on the clinical presentation. If the main clinical presentation is pneumonia, it is termed toxoplasmic pneumonia, whereas, pulmonary toxoplasmosis is a term used to describe the involvement of other organs in addition to the pulmonary system but without clinical features of pneumonia (Pomeroy and Filice, 1992).

Lung toxoplasmosis is usually diagnosed is through the identification of the parasite at extra-pulmonary sites or by serology (Israelski and Remington, 1993). Another method for definitive diagnosis is through bronchoscopy, with Giemsa- or eosin/methylene blue-stained preparations of bronchoalveolar lavage (BAL) or tissue biopsy. Finally, BAL can be inoculated and cultured in animals. However, this method is not always practical and is time-consuming (Israelski and Remington, 1993).

The serious pathologies that *T. gondii* infection causes in immunocompromised hosts were revealed decades ago. However, *T. gondii* infection in cancer patients has received relatively little attention, and only a few reports are available (Yuan et al., 2007).

A recent study has evaluted the relationship between *T.gondii* brain infection and brain diseases including cancer (Ngô et al., 2017). The study has assesed wether chronic brain parasitism associates with other neurologic diseases such as Parkinson's and Alzheimer's diseases, epilipsy and cancer (Ngô et al., 2017). In order toevaluate the relationships between brain disorders and human *T. gondii* infections, the study analysed a unique cohort, the National Collaborative Chicago Based Congenital Toxoplasmosis Study (NCCCTS), and detected the human susceptibility genes and the serologic biomarkers of active brain disease (Ngô et al., 2017). The study revealed that important mechanisms such as that such as Wnt/Ca + pathway, may potentiate cancer development in the *T. gondii* infected brain (Ngô et al., 2017).

Studies that have measured *T. gondii* infection, in different types of cancer patients, revealed the highest seroprevalence with some types of cancer such as nasopharyngeal carcinoma (46.15%), and rectal cancer (63.64%), and a relatively low seroprevalence with other types of cancer including breast cancer and uterine cancer with (9.53%) and (12.50%) respectively (Yuan et al., 2007). Although the serological method of measuring *T. gondii* infection is widely used and might suggest a link between *T. gondii* and cancer, the quality of the interpretation of these methods could be questioned since they do not reflect whether the infection is active or not. Moreover, these studies do not measure localised infections within the cancer affected tissue but only measure the overall infection status for these individuals. Hence, the true significance of the effect of *T. gondii* infection in cancer patients might be underestimated or at least unknown.

1.5 Molecular diagnosis of *T. gondii* infections

Before the development of molecular-based methods, the identification of parasites was based on the morphology of the organism, as well as the immunological and medical factors associated with an infection (Hide and Tait, 1991). Although such approaches worked, however, with parasites that are morphologically similar, such techniques can be with little benefit (Hide, 2016). However, the past two decades have witnessed a major breakthrough in molecular-based techniques, and ever since, these techniques have been used widely to identify *T. gondii* parasite (Su et al., 2010). These methods can be classified into two major groups. The first group involves techniques that are used for the specific detection of *T. gondii* DNA in samples. Conventional PCR, with all its modifications that include, nested (n-PCR), and quantitative real-time (q-PCR), are examples of this category (Su et al., 2010). On the other hand, the second group of molecular methods includes PCR-Restriction Fragment Length Polymorphism (RFLP), microsatellite and Multi-Locus Sequence Typing (MLST), and others (Ivović et al., 2007; Gao et al., 2017). Such methods are useful in high-resolution identification of *T. gondii* (Su et al., 2010) and have enabled us to establish different *T. gondii* strains(Su et al., 2010). Although *T. gondii* is highly prevalent in both humans and animals, it is still unclear what are the reasons behind the ubiquitousness of this parasite (Hide et al. 2016). This implies that the information regarding the importance of the different transmission routes of *T. gondii* is inadequate (Hide et al. 2009). One aspect that could play an important role in answering such questions, is establishing the different strains of the parasite through

genotyping(Su et al., 2010). One of the common molecular techniques used for characterisation of *T. gondii* parasite is RFLP (Robert-Gangneux and Dardé, 2012). This technique is based on the enzymatic digestion of DNA by using enzymes known as restriction endonuclease, and each enzyme recognises a specific nucleotide sequence known as the restriction site and cuts at this site. The number and size of the fragments produced is dependent on many factors; the enzyme used for the endonuclease, nucleotide sequence of the strand being digested and its length. After the digestion process, the fragments are separated by size during gel electrophoresis. The nucleic acid bands in the gel are stained with a fluorescent dye such as ethidium bromide. This produces a restriction pattern of bands unique for each region of DNA analysed. The differences between restriction patterns are known as restriction fragment length polymorphism (Weissfeld et al., 2007).

In Europe and Northern America, the majority of *T. gondii* isolates have been arranged into one of three clonal lineages by PCR-RFLP based on 106 isolates from both animals and humans (Su et al., 2006; Dubey et al., 2013). *T. gondii* parasite has an unusual clonal population structure with three main strains known as, I, II and III (Khan et al., 2005). Strains that were non-type I, II, or III, were classified as uncommon and were grouped together as exotic or atypical types (Dubey et al. 2013). ToxoDB, which is a genome and functional genomic database for *T. gondii* parasite, contain a list of strains (over 190 genotypes) that have been identified with multilocus PCR-RFLP and other techniques based on the ten specific markers of *T. gondii* parasite (SAG1, SAG2 3′and 5′, Alt.SAG2, SAG3, BTUB, GRA6, c22-8, c29-2, L358, PK1 and Apico) (Gajria et al., 2008).

1.6 Immunohistochemistry

In the last few decades, the technique of immunohistochemistry has been utilised as a powerful tool for both research and diagnostic purposes (van der Loos, 2009), and has been widely employed in the diagnosis of *T. gondii* infection (Silva et al., 2013).

Immunohistochemistry staining combines histological, immunological and biochemical techniques by the use of specific antibodies that are labelled, to detect an antigen of interest in cells or tissue sections so that the sites of antibody-antigen binding (immune-attachment) becomes microscopically visible (Haines and Chelack, 1991). In that way, IHC makes it possible to visualise the distribution and localisation of specific cellular components within a cell or tissue (Haines and Chelack, 1991).

The concept of IHC has existed since the 1930s (Kaliyappan et al., 2012); however, the first IHC study was not reported until the early 1940s, when Albert H. Coons at Harvard Medical School, Boston, USA, pointed out the possibility of localizing antigens in tissue sections through fluorescein-labelled anti-bodies, (Brandtzaeg, 1998). That concept was built on earlier observations that the antibody molecule could be conjugated with simple chemical material without damaging its ability to specifically react with its antigen. (Coons and Kaplan, 1949). Coons and his colleagues used Fluorescein isothiocyanate (FITC)-labeled antibodies with a fluorescent dye to localise pneumococcal antigens in infected tissues, and that is how the history of immunostaining began (Brandtzaeg, 1998). Later on, a fundamental era of IHC was established by the introduction of enzymes as antibody labels, such as peroxidase, (Coons and Kaplan, 1949), and the use of alkaline phosphatase developed by David Y. Mason and his colleagues, Oxford, UK. (Mason and Sammons, 1978; Mason et al., 2000). This development has boosted various applications of immunostaining (Cordell, 1984). Enzyme-labelled antibodies and methods applicable to tissues fixed in standard fixatives such as formalin have also been described (Haines and Chelack, 1991). Considering the fact that the immunostaining methods allow the analysis of tissue morphology and antigen localisation and at the same time, they have become especially popular among pathologists (Brandtzaeg, 1998). These techniques have added a new dimension to diagnostic pathology by creating permanent stains demonstrating the distribution of antigens visible with ordinary light microscopy (Nakane, 1968).

1.7 Applications and Methods of Immunohistochemistry

Since the concept of IHC involves specific antigen-antibody reactions, it has apparent advantages over commonly used special enzyme staining procedures that only recognise a restricted number of enzymes, proteins, and tissue structures (Kaliyappan et al., 2012). Therefore, IHC is an essential technique and has become an extraordinarily powerful tool in the apparatus of many medical research laboratories as well as in clinical diagnostics (Kaliyappan et al., 2012). This powerful technique is widely employed in the diagnosis of major medical conditions, e.g. in the diagnosis of cancerous tumours by identifying the presence of abnormal cells (Eyzaguirre and Haque, 2008). Moreover, IHC can be used to determine the prognosis of different cancers by the use of markers that are specific to each tumour, classify the tumour as malignant or benign, to identify the grade as well as the stage of the tumour and to determine the cell type and site of metastasis (Blows et al., 2010).

Furthermore, IHC is of high importance in basic research to understand the distribution and localisation of biomarkers and differentially expressed proteins in different parts of a biological tissue (Schacht and Kern, 2015). In many instances, IHC has proven to show high specificity allowing the differentiation of morphologically similar microorganisms, and it is especially useful when microorganisms are difficult to identify by routine or special stains (Lepidi et al., 2004). During the last two decades, there has been an expanding interest in the use of specific antibodies to bacterial, viral, fungal, and parasitic antigens in the identification and detection of the causative organisms in many infectious diseases, including infection with *T. gondii* in both human and animals (Eyzaguirre and Haque, 2008). In cases of infection with *T. gondii*, IHC can be used to identify the parasite with its different life stages, including the tissue cyst and tachyzoites (Conley and Jenkins, 1981). In addition, a diagnosis of acute toxoplasmosis can be established when tachyzoites are demonstrated in tissue sections or smears of body fluid including cerebrospinal fluid (CSF), amniotic fluid and visualised by immunohistochemical procedures (Montoya, 2002). Furthermore, the use of IHC has proven both specific and sensitive in the diagnosis of *T. gondii* infection, and it has been used successfully to indicate the presence of the parasite in the central nervous system (CNS) of AIDS patients (Montoya, 2002).

There are two main types of IHC, direct and indirect methods. In direct staining, the primary antibody, which is used to detect the antigen of interest is labelled with an enzyme (Haines and Chelack, 1991). In this method, after the tissue is incubated with the labelled primary antibody, an enzyme substrate is added which causes a reaction at the sites of antibody binding in the tissue by the deposition of an insoluble coloured reaction product which are visible with light microscope (Haines and Chelack, 1991), (Figure 1.5). Although direct immunostaining are easy to perform, cost-effective and less time consuming, they have a disadvantage of providing little amplification of the visible signal; hence, their use is limited to the detection of antigens that are expected to be highly abundant in the tested sample (e.g. diagnosis of autoimmune skin diseases), and when the primary antibody has a high specificity (Haines and Chelack, 1991).

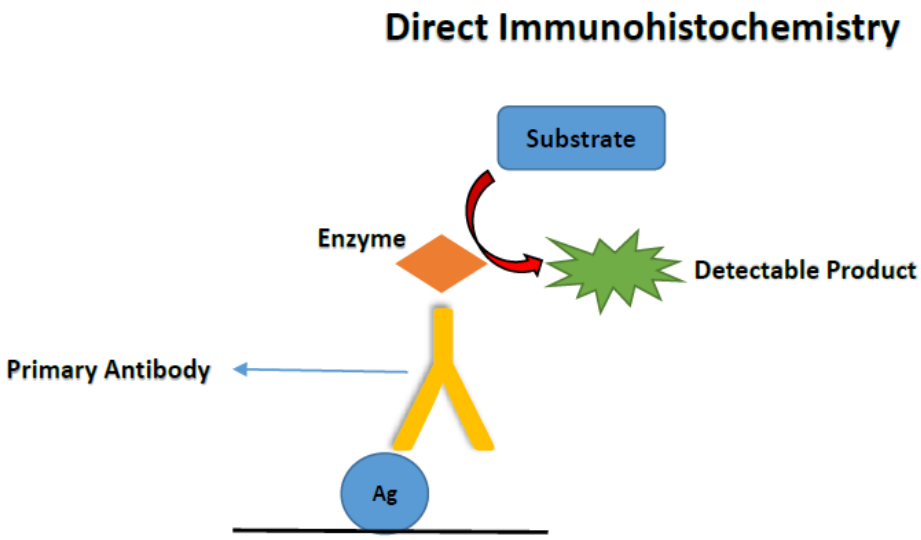

Figure 1.2 An illustration of direct Immunohistochemistry . In this method, the primary antibody is directly conjugated to the label, which reacts directly with the antigen in the histological preparation. The conjugate may be an enzyme or a fluorochrome. Although this method is fast, however, it lacks the sensitivity in antigen detection.

In indirect immunostaining methods, it utilises an unlabeled primary antibody to detect the antigen of interest in the tissue. A secondary labelled antibody is then used to bind to the primary antibody (Coons et al., 1955), (Figure 1.6). Despite the fact that indirect immunostaining approaches are relatively more complicated and labour intensive to conduct (e.g. extra incubation and wash steps are required), nonetheless, it is still a preferred method over direct methods for several reasons (Haines and Chelack, 1991). Since many secondary antibodies can bind to different antigenic sites of the primary antibody, indirect stains enhance the sensitivity of antigen detection, intensifying the visible signal produced by the binding of each primary antibody (Ramos-Vara, 2005). Moreover, indirect immunostaining methods could be performed on fixed tissues when the antigen of interest is relatively abundant since it has the ability to amplify relatively weak signals in a tested tissue (Haines and Chelack, 1991). In contrast to direct immunostaining methods, the indirect method of immunohistochemistry requires the use of a secondary antibody, which, unfortunately, may lead to non- specific binding of the secondary antibody (Ramos-Vara, 2005).

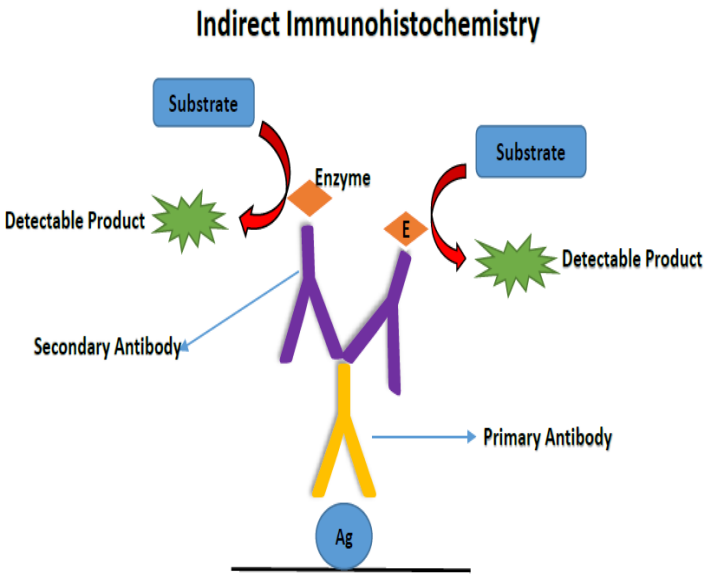

Figure 1.3 An illustration of indirect immunohistochemistry . In this method, two antibodies are used, a primary antibody which is unlabeled and specific to the antigen of interest, and a secondary antibody which is labelled and usually generated against the immunoglobulins of the primary antibody source. Indirect staining is more sensitive than the indirect technique because multiple secondary antibodies may bind to different antigenic sites on the primary antibody, thereby, increasing the signal amplification.

The antibody labels that are employed in immunostaining fall into two main categories; fluorescent and chromogenic (Warford et al., 2014). For the first 25 years of IHC, fluorescent labels were widely employed especially fluorescein (green) and rhodamine (red) being largely used by the end of this period. On an ideally, completely dark background, fluorescent labels give a bright visualisation of the antigen/antibody complex (Warford et al., 2014). Today, a broad range of fluorescent labels are available, and by incorporating these with proper detection systems, they can be used to discriminate between antigens co-located in the same region of a cell or tissue by changing excitation and emission filter combinations (Stack et al., 2014).

With chromogenic labels, an enzyme reacts with a substrate to produce a heavily coloured product that can be visualised with a standard light microscope. While the list of enzyme substrates is extensive, Alkaline Phosphatase (AP) and Horseradish Peroxidase (HRP) are the two most commonly used enzymes as labels for protein detection (Mason et al., 2000). Other enzymes include 3,3′-Diaminobenzidine (DAB), which, wherever the enzymes are bound, it will produce characteristic brown staining (Mason et al., 2000). Enzymatic chromogens have

the advantage of producing specimens that are permanently stained; hence; they are now broadly used among the biological sciences (van der Loos et al., 1993).

Although the main principle of IHC appears to be simple, however, the application of this procedure contains many drawbacks (Brandtzaeg, 1998). The advantage of immunofluorescence staining is that the amount of colour signal produced by the fluorescent dye relatively correlates with the concentration of the antigen of interest. Therefore, immunofluorescence is a better technique than light microscopy in quantitative analysis (Brandtzaeg, 1998). However, even though immunofluorescence is a widely used technique, and its accuracy is well established, this method still suffers from well-known drawbacks (Mason et al., 2000). Fading of the fluorescence signal due to poor storage of specimens (e.g. at room temperature) is not uncommon, quenching of the fluorescence signal at excitation (during microscopy) and the occurrence of auto-fluorescence caused by formaldehyde fixation (Mason et al., 2000).

1.8 Double Immunostaining

On many occasions, researchers have the need to detect more than one antigen in the same tissue specimen (van der Loos et al., 1993). Serial sections could be used for this purpose. However, this approach is considered extremely laborious (Brandtzaeg, 1998).

One of the main reasons for conducting double immunostaining experiments is the study of colocalisation (the visualisation of two markers in one cell or tissue constituent.), (van der Loos, 2009; Isidro et al., 2015). In a studied specimen, if the two antigens of interest are present in the same cellular compartment or tissue constituent, colocalisation is notable by the occurrence of a mixed colour (Nakane, 1968). On the other hand, when the two antigens are located in different cellular compartments (e.g. membrane, cytoplasm, and nucleus), colocalisation is expected to be observed as two separate colours (van der Loos et al., 1993).

In order to have a successful double-staining experiment, many factors must be in consideration, one of these factors is colour selection (Mason et al., 2000). It is of high importance to choose colours based on which colour combinations provide the best contrast between both individual colours and a mixed-colour at sites of colocalisation. Under ideal conditions, colocalisation can clearly be seen as a mixed colour that contrasts reasonably well against the two original colours (Mason et al., 2000). Nonetheless, if one of the two individual

colours overwhelms the other, the resultant mixed colour might be very faint or even missed (van der Loos, 2009).

Another main challenge that needs to be overcome for a successful double-staining protocol is cross-reactivity between the two individual antibodies (Lan et al., 1995). To avoid that, it is better to use two primary antibodies either raised in two different species (e.g., rabbit IgG and mouse IgG), or isotypes of the same species (e.g., mouse IgM and IgG), or isotype from the same species but with a different subclasses (e.g., mouse IgG1 and IgG3) (Lan et al., 1995; Isidro et al., 2015). Furthermore, the use of these antibody combinations facilitate the double immunostaining process by allowing the two primary antibodies and later on, the secondary antibodies incubation steps can be carried out at the same time (Isidro et al., 2015).

When it comes to dual colour analysis, several different techniques can be employed to calculated colocalisation (Humbert et al., 1992). In many biological studies, the simple overlay of RGB microscopy images for qualitative colocalisation assessments has been and continues to be a common practise (Humbert et al., 1992). Often, images of green and red fluorophores labelling distinct species are overlapped and evaluated in the joint image for the predominance of the merge of the red and green colours; - yellow pixels, which, to a first approximation, suggest the presence of interacting species. Even though overlaying images as a method for colocalisation is considered a relatively and easy and a quick method for identifying interactions between molecules; however, it is strictly qualitative (Comeau et al., 2006).

In general, colocalisation analysis includes two different aspects referred to as co-occurrence and correlation. Each approach has often contrasting strengths and weaknesses (Herce et al., 2013). Yet, neither method can be considered to always be preferable for any given application. Rather, each method is considered most applicable for answering different types of biological questions (Herce et al., 2013). The term co-occurrence is used to describes the extent to which two fluorophores are spatially overlapped (MANDERS et al., 1993). On the other hand, correlation refers to the extent to which the abundance of two spatially overlapping fluorophores are related to each other (MANDERS et al., 1993). The correlation and the overlap between images are useful tools to gain a quantitative idea of the underlying molecular interactions (Adler and Parmryd, 2010). For the measuring of the correlation between two fluorophores, Pearson's Correlation Coefficient (PCC) is a well-defined and commonly accepted method for assessing the degree of correlation between 2 coloured images (Pearson, 1895). PCC values vary from 1to -, where a value of 1is for two images whose fluorescence intensities are perfectly, linearly related, while a value of -1 represents two images whose

fluorescence intensities are perfectly, but inversely, related to one another. Moreover, a value near zero represents probes in which their distributions are uncorrelated with one another (Pearson, 1895).

On the other hand, For the quantitate measurement of co-occurrence, Manders and co-workers displayed a method to measure colocalisation coefficients, which accounts for the total number of fluorophores that overlapping with one another. This results in two coefficients, M1 and M2, which has become one of the most widely used techniques for quantitative colocalisation measurements through fluorescence microscopy (Manders et al., 1992). Values range from 0-1, where a value of 0 reflects no overlap, while a value of 1 represents perfect overlap (MANDERS et al., 1993).

1.9 Structure of an Antibody

Immunohistochemistry is based on the binding of antibodies to a specific antigen in tissue sections (Haines and Chelack, 1991). Antibodies are glycoproteins that are made in response to an antigen and can recognise and bind to the antigen that caused its production (Wootla et al., 2014). Antibodies are Y shaped molecules which have two arms called the Fab fragments (Breedveld, 2000), (Figure 1.7). These fab fragments contain identical antigen-binding sites at their tips, with the stem (the Fc fragment) joined to the Fabs by a flexible hinge (Davies, 1993). Each antibody molecule consists of four polypeptides– two identical heavy chains and two identical light chains Linked by disulphide bonds. Light chains are composed of 220 amino acid residues, while heavy chains are composed of 440-550 amino acids (Davies, 1993). Each chain has two different regions, constant and variable (Figure 1.7). Light chains are similar in all immunoglobulins, and they occur in two types, kappa and lambda. On the other hand, heavy chains can occur in five varieties (alpha, delta, gamma, epsilon or mu), and the difference in the heavy chain type is what determines the isotype of the antibody (IgA, IgD, IgG, IgE and IgM, respectively) (Schroeder and Cavacini, 2010). Because of polymorphisms occurring in the conserved regions of the heavy chain in some mammals, IgA and IgG are further subdivided into subclasses, referred to as isotypes, (Lipman et al., 2005).

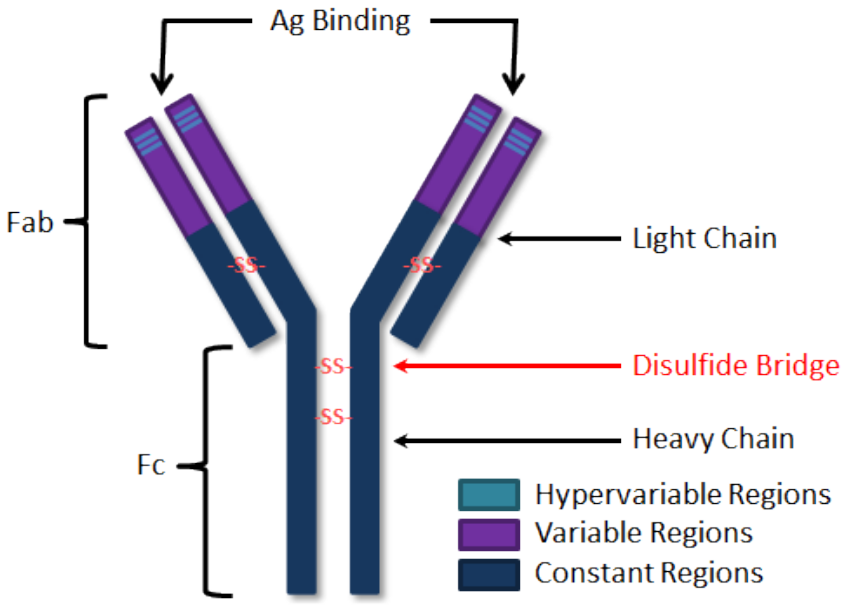

Figure 1.4 An illustration of the general antibody molecule structure (Lipman et al., 2005), which is composed of two types of protein chain: heavy chains and light chains. Each antibody molecule consists of two heavy chains, and two light chains joined by disulfide bonds. At the tips of the arms, is the two antigen-binding sites, which are attached to the trunk of the Y by a flexible hinge region. The Fab fragment contains the variable regions and binds antigen, and the Fc fragment contains the constant regions.

Natural antibodies play a fundamental role in the immune system; they have important functions in infectivity neutralisation, antibody-dependent cellular cytotoxicity (ADCC), complement-mediated lysis of infected cells or pathogens, and phagocytosis (Forthal, 2014). In fact, due to their ability to react with a broad variety of microbial components, these antibodies may play a major role in the primary line of defence against infections including, bacteria, viruses, protozoa and fungi (Forthal, 2014). When a pathogen invades the body of an immune-competent individual, the immune system has the genetic capability to generate a collection of antibodies that can target mostly any antigen (Wootla et al., 2014).

The high degree of affinity and specificity which antibodies have to bind to antigens, has led antibodies to be used extensively as a specific research, diagnostic and therapeutic reagent, which has had an undeniable impact on the improvement of health and welfare not only in humans, but also in animals (Lipman et al., 2005).

1.10 Types of Antibodies Used in Immunohistochemistry

In immunohistochemistry, there are different types of antibodies that can be used for specific detection, either monoclonal or polyclonal (Haines and Chelack, 1991). A monoclonal antibody is an antibody which is derived from a single antibody-producing B cell and therefore, they are monospecific and only bind with one unique epitope (Tabll et al., 2015). Polyclonal antibodies, on the other hand, represent a collection of antibodies which are made of different B cells that recognise multiple epitopes on the same antigen (Nakazawa et al., 2010; Tabll et al., 2015). Polyclonal antibodies are used more frequently in immunostaining techniques (Busby et al., 2016). In fact, in a study conducted to compare between the use of polyclonal and monoclonal antibodies in published research, it showcased that polyclonal antibodies are being used more often than monoclonal antibodies (54% of citations vs. 46%) respectively (Busby et al., 2016). This could be due to several reasons, but most importantly, with the nature of polyclonal antibodies to recognise various independent epitopes, they have a better chance of binding epitopes that are still available in fixed samples (Mighell, 1998). That being said, the use of polyclonal antibodies can result in unwanted nonspecific background staining that could interfere with the results (Haines et al., 1992). Furthermore, polyclonal antibodies are more practical to use, because, in order for monoclonal antibodies to work efficiently with immunostaining, it will require the screening of hundreds if not thousands of cultures for monoclonal antibodies which is quite impractical (Lipman et al., 2005).

The specificity of an antibody plays an important role in IHC. The specificity of an antibody can be defined as, to its capability to recognise a specific epitope in the presence of other epitopes. Hence, an antibody with high specificity would result in less cross-reactivity (Lipman et al., 2005).

In contrast to a monoclonal antibody which recognises a single epitope, a polyclonal antibody against a single molecular species of antigen have the advantage to recognise multiple epitopes on the target molecule (Nakazawa et al., 2010). This allows more than one antibody to bind through the antigen, thus amplifying the signal in indirect immunoassays, (Nakazawa et al., 2010).

Homogeneity and consistency are the main advantages of monoclonal antibodies (Davies, 1993). The characteristic mono-specificity exhibited by monoclonal antibodies allow them to be employed in many aspects, such as protein-protein interactions, evaluating changes in molecular conformation as well as phosphorylation states, and in identifying single members

of protein families (Lipman et al., 2005). Nonetheless, this mono-specificity of monoclonal antibodies may also serve as a disadvantage and limit their usefulness (Ramos-Vara, 2005). If an epitope showcased a small change in structure, either due to a genetic polymorphism, glycosylation, and denaturation, as a consequence, that could affect the function of monoclonal antibodies remarkably (Lipman et al., 2005). On the other hand, with polyclonal antibodies, the effect of the change on a single or a small number of epitopes is unlikely to be significant, that is due to the fact that polyclonal antibodies are heterogeneous and have the capacity to recognise a number of antigenic epitopes. Moreover, monoclonal antibodies are highly affected by small changes in pH and salt concentrations, whereas, polyclonal antibodies are considered more stable with a broad pH and salt concentration (Lipman et al., 2005).

1.11 The use of immunohistochemistry and immunofluorescence to localise *T. gondii*

The utilisation of immunohistochemistry and immunofluorescence has been widely used in the research field for the identification of *T. gondii* (Andres et al., 1981; Silva et al., 2013; Hanafiah et al., 2017). A study conducted on domestic cats to identify the presence of *T. gondii* infection in several tissue types via IHC (Hanafiah et al., 2017). Macrophages infected with *T. gondii* have been identified in several organs such as the liver, lungs, and kidney (Hanafiah et al., 2017). Moreover, *T. gondii* was found by IHC in the epithelial cells of kidneys and in the ileum (Hanafiah et al., 2017). In a study conducted on *T. gondii* seropositive sheep, different tissues, including heart, brain and liver, were tested for the presence of *T. gondii* (Silva et al., 2013). IHC showed a positive *T. gondii* infection, including the presence of *T. gondii* tissue cyst in all three tissue types (Silva et al., 2013). In a case study of an immunocompromised patient diagnosed with Hodgkin's disease, IHC was used to confirm the presence of *T. gondii* parasite infection (Andres et al., 1981). IHC demonstrated both free and encysted *T. gondii* within cerebral tissue in paraffin-embedded tissue sections of the brain (Andres et al., 1981).

The dormant stage of *T. gondii* is the tissue cyst and plays an important role in transmission and reactivation of the parasite (Sakikawa et al., 2012). Within the cyst, the fast multiplying bradyzoites are surrounded by a well-structured cyst wall; however, the function and composition of this layer in host-parasite interactions are not fully understood (Tu et al., 2019). A study has reported the utilisation of IF to identify the composition of *T.gondi* tissue cyst wall (Tu et al., 2019). Immunofluorescence has successfully localised the proteins located on

the cysts wall components, which most probably play a role in the parasite/host interface (Tu et al., 2019). Although *T. gondii* is asymptomatic in immunocompetent individuals, the studies suggest that chronic toxoplasmosis could have neuropathological and behavioural effects on these immunocompetent hosts (Pusch et al., 2009). As understanding tissue cyst behaviour could help address these consequences, a study has evaluated which neural cells *T. gondii* tissue cysts reside during chronic infection (Melzer and Carnston, 2012). By using double IF on infected brains of mouse models, targeting the astrocyte marker, the astrocyte-specific intermediate type cytoskeletal protein (GFAP), and *T. gondii* cysts marker FITC-*Dolichos biflorans* (FITC-DB), (Melzer and Carnston, 2012). It was reported that no *T. gondii* cysts were found in astrocytes. On the other hand, the specific neuron marker, microtubule-associated protein (MAP2), was double labelled with a *T. gondii* cysts marker. The assay revealed that neurons are most commonly the cell target in chronic infection for *T. gondii* cyst formation (Melzer and Carnston, 2012). Moreover, a study has documented the expression of Toxoplasma perforin-like protein1 (TgPLP1) gene in the bradyzoites within *T. gondii* cyst using both IHC and IF (Shan et al., 2015).

Some studies have documented the identification *T. gondii* in the lungs of some animals using IHC techniques. In China, a study reported lung toxoplasmosis in giant Pandas using IHC, which was represented by macrophages containing *T. gondii* tachyzoites in the alveoli (Ma et al., 2015). Furthermore, results were confirmed by conducting IF conducted on frozen tissues sections of giant panda lungs using monoclonal antibodies against the tachyzoite-specific surface antigen (SAG1) (Ma et al., 2015). The immunofluorescence assay has demonstrated the presence of *T. gondii* tachyzoites in the lungs (Ma et al., 2015). In a study conducted in New Zealand, IHC analysis has showed the presence of *T. gondii* in the lung of wild birds (Hunter and Alley, 2014). The IHC has identified both the intact tissue cysts and the *T. gondii* positive tachyzoites within the cytoplasm of the alveolar macrophages in the bird lung sections (Hunter and Alley, 2014). In South Africa, a study was conducted on Nicobar pigeons which revealed the presence of *T. gondii* infection in various organ, including the lungs. Various protozoal tachyzoites were identified by strong positive IHC labelling for *T.gondii.* (Last and Shivaprasad, 2008).

In the human host, few studies have reported the identification of *T. gondii* in the lungs by IHC and IF. A study has reported the presence of *T. gondii* infection in two cases of individuals with human immunodeficiency virus (HIV) by indirect IF (Kovari et al., 2010). The diagnosis was made by the identification of tachyzoites in bronchoalveolar lavages (BAL) samples of the two patients in association with Giemsa stain of the parasite (Kovari et al., 2010). As far

as we can tell, there are no detailed studies of immunofluorescence location of *T. gondii* in human lung tissue nor and publications that describe any partitioning of the parasites into a different cell or tissue types.

1.12 The roles of Inducible Nitric Oxide Synthase (iNOS) and Arginase-I

Inducible Nitric Oxide Synthase (iNOS) and arginase (Arg-1) are two enzymes that have been targeted for the detection via immunohistochemistry by different studies (Tousson et al., 2012; Choi *et al.*, 2012). Arginase is an enzyme that catalyses the hydrolysis of arginine to ornithine and urea (Ahn et al., 2012). In mammalian cells, there are two distinct isoforms of arginase, Arg-1 and 2 (Choi et al., 2012). Arginase-1 (hepatic arginase), is the fifth and final enzyme of the urea cycle and is expressed with high levels in the liver and to a lower extent in a few other tissues and cell types (Yu et al., 2003). On the other hand, the other form of the enzyme, arginase II, is a mitochondrial enzyme that is widely distributed in extrahepatic cells and tissues (Li et al., 2002). Interestingly, the two isoforms of arginase are encoded by two distinct genes and differ in many aspects, including immunological properties, tissue distribution, and regulation of expression (Jenkinson et al., 1996). Studies based on RT-PCR have reported that Arg-1 is especially abundant in the liver, while Arg-2 in the kidneys and intestines, hence, it has been implied that each arginase isoform plays a different role in each organ (Yu et al., 2003). Moreover, in comparison with other urea cycle enzymes, arginase enzymes have a much wider distribution in tissues, which suggests that arginase enzymes have important physiological roles apart from the urea cycle (Yu et al., 2003). Arginases have been suggested to be regulators of the synthesis of polyamines, glutamate and nitric oxide in endothelial and vascular smooth muscle cells (Morris Jr, 2009).

In recent years, interest in arginase has increased due to the expanding studies that demonstrated the involvement of arginase in the metabolism of the ubiquitous and complex molecule (NO) nitric oxide (Jenkinson et al., 1996).

Nitric Oxide (NO), a free gaseous molecule and one of the toxic constituent of air pollution, is now known to be synthesised enzymatically in a wide range of cells and tissues in a tightly regulated manner (Ermert, Ruppert, Günther, H. Duncker, et al., 2002). Although NO is a simple short-lived molecule, however, it mediates functions as diverse as cell-cell signalling and immune-mediated cytotoxicity (Ermert, Ruppert, Günther, H. Duncker, et al., 2002). Consequently, regulation of the timing and amount of NO produced, as well as of its location

of synthesis, all play a crucial role in the determination of the physiological effects of NO (Morris Jr, 2009). NO is the product of L-arginine by the enzyme nitric oxide synthase (NOS) (Hamal et al., 2008). Thus far, three different NOS isoforms have been identified, but it remains unclear whether additional isoforms exist (Hamal et al., 2008). The three isoforms differ in amino acid sequences, subcellular location, regulation, and thus, they provide different functions. Moreover, in NO synthesis, the different isoforms are differentially regulated and have different physiological roles (Ermert, Ruppert, Günther, H. Duncker, et al., 2002). Two of the isoforms are termed constitutive NOS because they are continuously present (Hamal et al., 2008). One of these types is endothelial (eNOS) also known as (human NOS 3), which has been localised to endothelium and plays an important role in the control of blood pressure and platelet aggregation (Michel et al., 1993). The second constitutive isoform is neuronal (nNOS), also known as (human NOS 1), has been localised to the cytosol of central and peripheral neurons (Zhou and Zhu, 2009). Furthermore, (nNOS) is also expressed in extra-neuronal sites such as skeletal muscle, kidney and pancreas (Zhou and Zhu, 2009).

NO is generated by these two types of NOS in small amounts when (calcium/calmodulin-binding permits electron transfer from NADPH (nicotinamide adenine dinucleotide phosphate) via flavin groups within the enzyme to a heme-containing active site (Jianling, 1993). This activation is short-lived, and the NO produced serves as a signalling molecule, mediating numerous physiological processes, including vasodilation and neurotransmission (Michel et al., 1993). A third isoform of the NOS family has been identified and in contrast with the previously mentioned types (eNOS and nNOS) which are constantly available, it is not expressed unless the cells have been induced by certain cytokines, microbes, or microbial products, thus it is termed inducible NOS (iNOS), also known as (human NOS 2) (Kroncke et al., 1998). Whenever iNOS is expressed, that results in a constant production of NO, which in mammalian tissues, exerts cytotoxic and cytostatic actions, as well as it has antimicrobial properties toward certain pathogens (Hammermann et al., 2001). In contrast to the two NOS isoforms eNOS and nNOS, iNOS remains activated and sustainably produces NO for the life of the active enzyme.

There is a tremendous parallelism between nitric oxide synthase (NOS) and arginase (Abdallahi et al., 2001). Both enzymes are co-induced at inflammatory sites, and have inducible and constitutive isoforms (Abdallahi et al., 2001). Moreover, in many cell types, including macrophages, nitric oxide synthase (NOS) and arginase share the same substrate, L-arginine (Chang et al., 1998). Inducible nitric oxide synthase (iNOS) produces NO through the utilisation of L-arginine, on the other hand, Arg-1 hydrolyses L-arginine to produce L-

ornithine and urea (Li et al., 2002). Arg-1 and iNOS are competitively related (Abdallahi et al., 2001). The production of NO is regulated by Arginase activity through reducing the availability of L-arginine to NOS, hence, decreasing the potential pathological effects of high levels of NO (Abdallahi et al., 2001). Furthermore, arginase produces ornithine, which is the precursor of the synthesis of polyamines, and since L-ornithine is a precursor for many polyamines through the ornithine decarboxylase (ODC) pathway, which is modulated by NO. Polyamines are crucial for the proliferation of normal and neoplastic cells (Abdallahi et al., 2001), and they support the growth of organisms, including the parasite (Zhao *et al.*, 2013). On the other hand, it has been reported that the production of NO by (iNOS) in tissues which are undergoing inflammation, is involved in the killing of intracellular pathogens including *Leishmania, Trypanosoma* and *Mycobacteria* (Abdallahi et al., 2001). In addition, NO also has implications for tissue injury and hemodynamics (Abdallahi et al., 2001).

iNOS and Arg-1 have become the interest of many researchers over the past decades (Li et al., 2012; Zhao et al., 2013a) A study has documented that the high activity and expression levels of iNOS and low activity an expression levels of Arg-1 in peritoneal macrophages of rats could be related to their resistance against *T. gondii* infection (Li et al., 2012). On the other hand, in mice, which are sensitive to *T. gondii* infection, demonstrated low iNOS and high Arg-1 activity and expression in the peritoneal macrophages (Li et al., 2012). Interestingly, when the same experiments were conducted on rat alveolar macrophages, they showed a level of sensitivity to *T. gondii* infection that resembles the mice peritoneal macrophages (Zhao et al., 2013b; Gao et al., 2015). It is still unclear if the balance between Arg-1 and iNOS plays a role in the susceptibly vs resistance in the human host. To our knowledge, there have not been studies that evaluated the expression of Arg-1 and iNOS in relation to the infection with *T. gondii* parasite in the human host. Specifically, we have been unable to find any publications that describe the spatial interactions of *T. gondii* infection and expression of either iNOS or Arginase-1 in human lung tissue.

In a recent study at Salford University (Bajnok, 2017), a total of 72 lung biopsies from lung cancer patients in Manchester, were tested for the presence of *T. gondii* infection. The cancer-free margins were used for DNA extraction and tested directly with nested (PCR) targeting five *T. gondii* specific markers (SAG1, SAG2 3′, SAG2 5′, SAG3 and B1). Furthermore, immunohistochemistry (IHC) was performed on the samples using specific *T. gondii* antibodies to detect the parasite as well as to determine the life cycle stage. Finally, the samples were tested by Haematoxylin and Eosin (H and E) staining to secondary confirm the presence of the parasite. The results showed astonishing data, where all tested samples were found to

be infected with *T. gondii* with all five PCR markers, giving a prevalence of 100%. IHC further confirmed the results with all 72 samples were successfully stained and showed variable parasite stages.

Although the 100% prevalence observed in the study is striking, it is hard to determine if the high frequency is only due to the immunocompromised status of these cancer patients, which alone acts as a huge risk for acquiring *T. gondii* infection, or whether there is a link between this ubiquitous parasite and lung cancer or lung disease in general. To better address such questions, we aimed to compare these data with a group of samples that represents the normal healthy population. Moreover, different studies are documenting that pulmonary toxoplasmosis is considered one of the most severe clinical signs of *T. gondii* infection in humans (de Souza Giassi et al., 2014a), we aimed to establish and optimise an IHC technique to detect iNOS and Arg-1 in 51 lung cancer samples. Moreover, we aimed to conduct a colocalisation analysis via establishing and conducting double immunofluorescence assay targeting *T. gondii* infection in relation to the expression of Arg-1 and iNOS in patients with lung cancer. Hopefully, this will enable us to gain a better understanding regarding the sensitivity/susceptibility to infection with *T. gondii* in the human host.

1.13 Objectives of this project

(1) Obtain samples from non-cancerous individuals to be used as a control group for the lung cancer clinical samples used in the previously mentioned study (Bajnok, 2017), and subsequently to follow the same diagnostic tools by nested PCR targeting the same five specific *T. gondii* markers (SAG1, SAG2 3′, SAG2 5′, SAG3 and B1), Immunohistochemistry and conduct RFLP on positive control samples.

(2) To establish and optimise an immunohistochemistry protocol using different rat tissues (heart, liver and lung), to detect iNOS and Arg-1, and to establish and optimise a double immunofluorescence procedure targeting Arg-1/*T. gondii* and iNOS/ *T. gondii* parasite. Then to optimise these processes for use in human lung tissue from the lung cancer patients.

(3) To conduct immunohistochemistry targeting Arg-1 and iNOS on lung cancer samples infected with *T. gondii*, and to conduct a quantitative colocalisation analysis on samples of lung cancer between Arg-1/iNOS expression in association with the infection with *T. gondii* via double immunofluorescence**.**

Chapter 2: Material and Methods

The aims of this thesis are (1) to test lung samples collected from healthy individuals to be used as a control group for lung cancer patient clinical samples tested in a previous study, (2) to establish and optimise immunohistochemistry (IHC) and immunofluorescence (IF) protocols to detect iNOS and Arg-1 in human lung cancer samples infected with *T. gondii* parasite and (3) to establish and conduct IHC and double immunofluorescent assays on lung cancer clinical samples to colocalise *T. gondii* infection in relation to Arg-1 and iNOS expression.

2.1 Ethical approval

The studies were approved by the NRES Committee North West – Greater Manchester South (06/Q1403/156, bronchoscopy sampling for controls) and the local South Manchester research ethics committee (03/SM/396, lung tissue collection). All subjects provided written informed consent. The University of Salford, Research Ethics and Governance Committee granted the ethical approval (ST16/124), see Appendix (B).

2.2 Lung cancer subjects and sample processing

A total of 10 bronchoalveolar lavage samples were collected through bronchoscopy from healthy individuals who had no previous history of lung cancer, in Manchester, UK. Control subjects were selected to cover a comparable age range as the lung cancer patients and were chosen from the same population catchments area. Only 10 control samples were obtained due to the difficulty of obtaining lung samples from healthy subjects. Data regarding age, gender, history of lung cancer and other lung conditions (COPD, asthma), smoking history and the use of inhaled medication including bronchodilators and inhaled corticosteroids were available, (Table 2.1 and 2.2). For data regarding the lung cancer patients, see Appendix C (Table 7.1).

For the lung cancer samples, a total of 72 tissue samples were recruited from patients undergoing lung resection as a part of their treatment in the National Health Service (NHS) at University Hospital of South Manchester. These lung samples were taken as a part of an exploratory investigation for suspected cancer and were taken prior to any anti-cancer treatment. Following all the subsequent diagnostic tests, all 72 patients were confirmed to have lung cancer. As determined by an NHS pathologist, tissue sections were obtained as far distal to the tumour as possible. None of the patients were tested for the presence of *T. gondii* infection as serological tests as *T. gondii* tests are not a part of the routine investigation for cancer patients. These subjects were recruited by (Thomas Southworth, Josiah Dungwa, Dave Singh, and Dr Lucy Smyth).

Table 2.1 Control subject demographics . COPD = Chronic Obstructive Pulmonary Disease, NS = never smoked.

Patient Number	Gender	Age	Smoking History	COPD	Asthma	Diagnosis
920	M	41	Never	No	No	Healthy NS no cancer
292	M	31	Never	No	No	Healthy NS no cancer
545	M	75	Never	No	No	Healthy NS no cancer
929	M	45	Never	No	No	Healthy NS no cancer
134	F	45	Never	No	No	Healthy NS no cancer
137	F	74	Never	No	No	Healthy NS no cancer
917	F	57	Never	No	No	Healthy NS no cancer
268	M	43	Never	No	No	Healthy NS no cancer
166	M	44	Never	No	No	Healthy NS no cancer
558	M	67	Never	No	No	Healthy NS no cancer
Summary/Mean	7m/3f	52.2	---	---	---	----

Table 1.2 Patient demographic summary

	Gender	Age	FEV1	FEV1 (%pred)	FVC	FEV1/FVC ratio	PYH	Lung Cancer Lesion	SAB	LAB	ICS
CCS	10/6	70.9 (60-82)	1.9 (0.9-3.5)	74.6 (53-96)	3.3 (1.7-5.4)	59.0 (46-75)	56.9 (9-124)	y	7	4	4
CEX	17/2	72.1 (60-80)	1.7 (1.3-2.5)	64.8 (45-118)	3.0 (2.4-4.5)	56.3 (42.5-69.3)	48.7 (11-112)	y	9	12	9
NCS	4/13	64.4 (44-78)	2.3 (1.6-3.3)	105.2 (70-131)	3.1 (2.1-4.4)	73.1 (66.9-82.5)	44.2 (15-90)	y	0	0	0
NEX	9/8	72.1 (57-84)	2.1 (1.2-3.2)	91.9 (47-127)	2.9 (1.8-4.1)	71.2 (55-85.8)	37.3 (2.1-117)	y	1	1	1
NS	0/3	68.3 (65-71)	1.9 (1.8-2.0)	108.3 (100-113)	2.7 (2.2-3.6)	82.5 (77-91)	0 (0)	y	1	0	1
Average for lung cancer group	40/32 (Total)	69.8 (44-84)	2.0 (0.87-3.5)	84.8 (45-131)	3.1 (1.69-5.4)	65.5 (42.5-90.9)	44.1 (0-124)	y	18	17	15
HNS Controls	7/3	52.2 (31-75)	3.3 (2.3-4.18)	107 (82.7-148.6)	4.3 (2.9-5.6)	78.6 (70.8-95.1)	0.0 (0)	n	0	0	0

Notes: Subject demographics of cancer patients (n=72) and healthy non-smoker control subjects (n=10). Gender: male/female. Groups: CCS, COPD current smoker; CEX, COPD ex-smoker; NCS, no airflow obstruction current smoker; NEX, no airflow obstruction ex-smoker, NS, never smoked; HNS, healthy never smoked. Characteristics: FEV1 (forced expired volume in 1 second), %pred (Percentage of the predicted value), FVC (Forced Vital Capacity), PYH (Pack Year History). patient medications include: SAB (short-acting bronchodilators), LAB (long-acting bronchodilators), ICS (inhaled corticosteroid). Average values are shown (range in brackets).

2.3 DNA isolation from control samples of human lung tissue

To extract DNA from the slides containing the samples, the protocol described by (Duncanson et al., 2001) was used with modifications to be applied on microscopic slides. First, a few drops of lysis buffer were added directly on the tissue on the slide. Then, with the sterile tip of the micropipette, by avoiding the wax around the tissue as much as possible, the tissue was gently scratched off and then put it into a sterile Eppendorf tube. After that, 4 µl of proteinase K (50mg/ml) or 10 µl of proteinase K (20mg/ml) was added to the samples and incubated at 56 °C for 3 – 4 hours. Next, 500 µl of tris buffered phenol/chloroform (pH8.0) was added and mixed for 10 minutes, and subsequently centrifuged at 13000rmp for 10 minutes. The resultant supernatant was removed into a fresh tube, and that process was repeated at least twice. Then, 90 µl sodium acetate (3M pH 5.3) and 900 µl 100% ethanol were added to the supernatant and then stored at 20 °C overnight. Samples were centrifuged at 13000rpm for 20 minutes, and the supernatant was discarded. Next, 500 µl 70% ethanol was used to wash pellets and then centrifuged at 13000rmp for 10 minutes, and the supernatant was discarded. Finally, for 10 minutes, pellets were air dried at room temperature and then dissolved in 100 µl of T.E buffer (pH8.0).

2.4 Mammalian Tubulin PCR to verify the quality of DNA

Extracted DNA was tested for mammalian tubulin to ensure the viability of PCR amplification. As described (Terry et al, 2001), the reaction was carried out in a final volume of 25 µl containing, 18.6 µl of PCR water, 2.5 µl of Bioline NH4Cl (excluding MgCl2), 1 µl of Bioline MgCl2 (50mM), 0.5 µl of forward primer (CGTGAGTGCATCTCCATCCAT) and 0.5 µl of reverse primer (GCCCTCACCCACATACCAGTG), 0.25 dNTP mix (25 mM) and 0.5 of *Taq* polymerase enzyme and 1 µl of the DNA samples. A Stratagene Robocycler was used to perform the amplification with the following cycling conditions: a starting denaturation step of 5 min at 95 °C, proceeded by 40 cycles of PCR carried out for 40 s at 94 °C, 60 s at 60 °C and 1.5 min at 72 °C, ending with a final extension step of 10 min at 72 °C. The PCR was resolved on 1% agarose gel electrophoresis containing GelRed with an expected band size of (1600) bp considered positive.

2.5 PCR detection of *T. gondii* in human lung control samples

T. gondii DNA extracted from sheep, Slovakia, SR (type II) was used as a positive control for all five markers (Bajnok et al., 2015) whereas, for the negative control, sterile water was used to detect any false amplification. Stratagene ROBOCYCLER™ (La Jolla, California, USA) was used to conduct all PCR reactions. Syngene G-BOX Gel Documentation and Analysis System (Cambridge, UK), was used to visualise the PCR products by gel electrophoresis.

To detect the presence of the parasite in samples, a nested PCR was performed targeting five specific markers of *T. gondii,* B1, SAG1, SAG2, (3′ and 5′ ends) and SAG3. All PCR reactions were performed three times with each marker. The samples were considered positive for *T. gondii* parasite if the PCR amplification was successful in all three reactions.

The nested PCR performed to amplify the B1 gene of *T. gondii* (Jeon and Yong, 2000) consisted of, for the first round of PCR, the amplification was carried out in a final volume of 25 µl consisting of, 18.6 µl of PCR water, 3.3 µl of Bioline KCl buffer, 0.25 µl of the forward primer and reverse primers respectively (GGAACTGCATCCGTTCATGAG), (TCTTTAAAGCGTTCGTGGTC), 0.25 of Taq polymerase enzyme, and 0.4 dNTP mix (25 mM). Three µl of the sample DNA was used as templates. A Stratagene Robocycler machine was used to accomplish the amplification. The thermal cycling conditions consisted of, 35 cycles at 93 °C for 10 s, at 57 °C for 10 s, at 72 °C for 30 s, and by a final extension step of 72 °C for 10 min. The second round of PCR, was performed in a final volume of 25 µl containing, 15.9 µl of PCR water, 5 µl of Bioline KCl buffer, 1.25 µl of forward and reverse primers respectively (TGCATAGGTTGCAGTCACTG) (GGCGACCAATCTGCGAATACACC), 0.2 of Taq polymerase enzyme, and 0.4 dNTP mix (25 mM), A volume of 2 µl of the first round products were used as templates. The first round of PCR cycling conditions were used for the second round as well, with the following adjustment; - the 30 s at 72 °C was decreased to 15 s. Eight µl of the second PCR product were run on a 2% agarose gel electrophoresis containing GelRed. All samples were tested three times, and samples are displaying a 96 bp band in all three reactions were considered positive.

As described by (Bajnok et al., 2015), a nested PCR was performed to detect the SAG1 gene of *T. gondii*, the reaction was carried out in a total volume of 25 µl, for the first round of PCR containing, 12.25 µl of PCR water, 2.5 µl of B-mercaptoethanol, 2.5 µl Bioline NH4Cl (excluding

MgCl2), 1 µl of Bioline MgCl2 (50mM), 2.5 µl of the forward primer, DS29 (TTGCCGCGCCCACACTGATG), and 2.5 of reverse primer, DS30 (CGCGACACAAGCTGCGATAG), 0.25 µl dNTP (25 mM) mix, 0.5 µl Taq polymerase enzyme and 1 µl of the DNA samples. A Stratagene Robocycler machine was used to perform the amplification with the following cycling conditions: a starting denaturation step of 5 min at 95 °C, followed by 40 cycles of PCR carried out for 40 s at 95 °C, 40 s at 63 °C and 1.10 min at 72 °C, ending with a final extension step of 10 min at 72 °C. The reaction and cycling conditions of the second round of nested PCR were the same as the first round with the exception of, PCR water was decreased to 11.25 µl, forward primer DS38 (CGACAGCCGCGGTCATTCTC) and reverse primer DS39 (GCAACCAGTCAGCGTCGTCC). Two µl of the first round of PCR was used as a template. The samples were run on a 1.5% agarose gel electrophoresis containing GelRed, and the expected band size was 522 bp. Samples exhibiting the expected size band in all three PCR reactions were considered positive.

The samples were tested with a nested PCR to detect SAG2 gene and was optimised as described by (Su et al. 2010). SAG2 locus has two different polymorphic sites, at 3′ and 5′ends, and each end was amplified separately (Bajnok et al., 2015). The initial round of amplification was carried out in a 25 µl mixture containing 14.9 sterile PCR water, 2.5 µl Bioline NH4Cl (excluding MgCl2) 1 µl of Bioline MgCl2 (50mM), 2.5 µl of each of the forward and reverse primers, (3′ end), (TCTGTTCTCCGAAGTGACTCC) and (TCAAAGCGTGCATTATCGC) respectively, 2.5 µl of the forward and reverse primers (5′ end), (GGAACGCGAACAATGAGTTT) and (GCACTGTTGTCCAGGGTTTT) respectively, 0.3 µl dNTP (25 mM) mix, 0.3 µl Taq polymerase enzyme and 2 µl of the DNA samples. Amplification was conducted at 95°C for 4 min followed by 30 cycles of 94°C for 30 s, 55°C for 1 min, and 72°C for 1.5 min, and a final extension step at 70°C for 10 min. The same cycling conditions were used as the first PCR round with the exception of primers, forward primer (ATTCTCATGCCTCCGCTTC), and reverse primer (AACGTTTCACGAAGGCACAC) for 3′ end, and forward primer (GAAATGTTTCAGGTTGCTGC), and reverse primer (GCAAGAGCGAACTTGAACAC) for 5′ end, and finally, the 55 °C was increased to 60 °C for 1 min. Two microliters of the first PCR products were used as templates for each end separately. Eight microliters of the second PCR products were examined on a 1.5% agarose gel electrophoresis stained by GelRed and visualised

under (UV) light. Samples showing a PCR product size of 222 bp for 3′ end, and 242 bp for 5′ end in all three reactions were considered positive.

A nested PCR was conducted to detect the specific SAG3 gene of *T. gondii* (Su et al., 2010). The same protocol for SAG2 nested PCR was applied to amplify SAG3 gene with specific SAG3 primers, forward primer (CAACTCTCACCATTCCACCC) and reverse primer (GCGCGTTGTTAGACAAGACA) for the first round of PCR, and a forward primer (TCTTGTCGGGTGTTCACTCA), and reverse primer (CACAAGGAGACCGAGAAGGA), for the second round of PCR. Second PCR products were resolved on a 1.5% agarose gel electrophoresis stained with GelRed and examined under UV light. The amplified PCR samples yielding a 225 bp product size in all three PCR reactions were considered positive.

2.6 Direct PCR-RFLP genotyping from DNA extracted from control human lung tissue slides

To display the RFLP pattern for the one positive control sample (558), 5 µl of the amplified second PCR product of the SAG2 (3′ and 5′ ends) were treated with restriction enzymes, *Hha*I for SAG2 3′ and *Mbo*I for SAG2 5′. One µl of the buffer recommended by the manufacturers and 0.5 µl of the restriction enzyme was added (Table 3.1). The digested products were resolved on a 2.5% agarose gel containing GelRed to display the different banding patterns. With reference to *Toxoplasma* Genomics Resource database (Gajria et al. 2008) http://www.ToxoDB.org, release 25, 23 July 2015), the patterns resolved after digestion were compared with the different genotypes for each marker to identify the strain.

Table 2.3 A Summary of restriction enzymes used in RFLP, NEB buffers and the incubation time and temperature for each marker.

Marker	Nested PCR product size (bp)	Restriction enzymes	NEB buffers, incubation temperature, and time, agarose gel%	Reference
SAG2 3′	222	*Hha*I	NEB4+BSA, 37°C, 1h, 2.5% gel	(Su et al. 2010)
SAG2 5′	241	*Mbo*I	NEB4+BSA, 37°C, 1h, 2.5% gel	(Su et al. 2010)

2.7 Detection of *T. gondii* using immunohistochemistry (IHC)

Immunohistochemistry was used to detect *T. gondii* parasite in control slides for the lung cancer study as well as to stain lung cancer clinical samples. IHC was performed on slides embedded with paraffin (Plumb et al., 2009) using commercial anti-*T. gondii* polyclonal antibodies produced in rabbits (Thermo Fisher Scientific, Catalogue number PA1-38789, Rockford, IL, USA). The tissue was cut into 5 µm sections and then mounted on positively charged glass slides. Then, slides were de-waxed in Histoclear (2 x 5 minutes), and then re-hydrated in ethanol, 100% for 5 minutes, 90% for 3 minutes, 75% for 2 minutes and in 50% for 1 minute. Finally, to remove the ethanol, slides were rinsed in tap water to for 5 minutes. In 1% trypsin/calcium chloride (pH 7.8) antigen retrieval was performed for 30 minutes at 37˚C in a humidified chamber (Roe et al., 2013). However, it was later modified to the use of Pretreatment (PT) Module (Thermo Scientific™ Lab Vision™**)** with 10 mM citric buffer (PH 6) for 20 mins followed by 20 mins cooling down. The slides were then left to cool down for 10 minutes at room temperature and then washed under running water for 7-10 minutes. Slides were incubated in 0.3% hydrogen peroxide for 30 minutes at room temperature and washed in TBS, to block endogenous peroxidase activity. In order to block non-specific antibody binding, normal goat serum (Vectastain ABC Systems, Vector Laboratories, UK) was used at room temperature for 30 minutes and followed by incubation in diluted (1/100) polyclonal rabbit anti- *T. gondii* antibodies at room temperature for 1 hour. Subsequently, the slides were washed in TBS-Tween for 3 x 3 minutes and incubated in biotinylated anti-goat secondary antibody (Vectastain ABC Systems, Vector Laboratories, UK) at room temperature for 30 minutes, and then washed again in TBS-Tween (3 x 3 minutes). Slides were incubated in ABC-Px mix (Vectastain ABC Systems, Vector Laboratories, UK) for 30 minutes, and then re-washed three times in TBS. To visualise the resulting complex, 3-3′-diaminobenzidine (DAB) was used for a maximum of 10 minutes. Using light microscopy, the intensity of the tissue staining was monitored, and when optimal staining was reached, the DAB reaction was damped in distilled water. (Slides were washed with running water for 5 minutes, counter-stained with haematoxylin for 45 seconds, re-washed with water for 5 minutes, de-hydrated with alcohols, 50 % for 1 minute, 75 % for 2 minutes, 95% for 4 minutes, and 100 % for 5 minutes, then cleared in Histoclear (2 x 5 minutes) and finally mounted in DPX using coverslips. For each staining, three negative controls were used. These were human lung sections with primary antibodies excluded, lung sections from wood mouse (*Apodemus sylvaticus*) which are

T. gondii negative, and cells derived from a C2C12 culture (mouse myoblast cell line, free of *T. gondii*) with both primary antibodies present and absent. No specific *T. gondii* staining was observed in any negative controls. For positive controls, a lung tissue from a *T. gondii* infected wood mouse was used (Bajnok et al., 2015), and specific *T. gondii* staining was observed in all positive controls.

2.8 Detection of Arginase-1 and Inducible Nitric Oxide Synthase (iNOS) expression using immunohistochemistry

Immunohistochemistry protocols were optimised to detect iNOS and Arg-1 in lung tissue sections from cancer patients infected with *T. gondii* parasite.

For the iNOS staining positive control, heart tissue of Sprague Dawley female Rats were used. For the Arg-1 staining positive control, liver tissue of Sprague Dawley female Rats were used. Tissues were supplied by Manchester University and were cut into small sections and placed for at least 24 hours in 10% buffered formalin at room temperature and embedded in paraffin, using a Leica TP1020 automatic tissue processor. After that, tissues were sectioned using a microtome machine (LEICA BIOSYSTEMS RM2125RT) into 5µm slices and lifted onto positively charged adhesive slides, and the tissue sections were dried on a slide warmer at 60˚C prior to immunostaining. The immunohistochemistry procedure was performed as follows; first, the samples were de-waxed in Histoclear 2x5 minutes, and then de-hydrated through placing the slides in decreasing concentrations of ethanol, (100%) ethanol for 5 minutes, (90%) ethanol for 3 minutes, (75%) ethanol for 2 minutes and finally (50%) ethanol for 1 minute. To remove the ethanol, the samples were rinsed with distilled water for 5 minutes. For antigen retrieval, slides were covered in 10 mM citric buffer (PH 6) and placed in a 700W microwave for 7 minutes for iNOS samples (Takir et al., 2016) and 3 minutes for Arg-1 samples (Choi et al., 2012), but was later modified to the use of PT Module (Thermo Scientific™ Lab Vision™**)** with 10 mM citric buffer (PH 6) for 20 mins followed by 20 mins cooling down. The slides were then left to cool down for 10 minutes at room temperature and then washed under running water for 7-10 minutes. To block endogenous peroxidase activity, tissues were covered with 3% hydrogen peroxide (Dako EnVision Detection Systems, Dual Endogenous Enzyme Block, code number K4065) for 30 minutes at room temperature and then washed in PBS Tween (PH 7.4) 3x3 minutes. After that,

slides were incubated with the commercial iNOS polyclonal antibodies produced in rabbits (Thermo Fisher Scientific, Catalogue number PA1-036, Rockford, IL, USA) with a dilution of (1:200) and commercial Arginase-1 polyclonal antibodies produced in rabbits (Thermo Fisher Scientific, Catalogue number PA5-29645, Rockford, IL, USA) with a dilution of (1:200) for at least 1 hour and 30 minutes in room temperature. Later on, slides were washed with PBS Tween 3 x 3 minutes and then incubated with a secondary antibody (Labelled Polymer - Dako REAL EnVision-HRP, Rabbit-Mouse, code number K4065) for 1 hour, and then re-washed with PBS Tween 3 x 3 minutes. To visualise the resulting complex, slides were incubated in 3-3'-diaminobenzidine (DAB) for a maximum of 10 mins and then washed under running water for 5 minutes. To counter-stain the tissue, slides were covered with hematoxylin for 45 secs and then washed under running water for 5 minutes. To re-hydrate the tissue, slides were placed in (50%) ethanol for 1 minute, (75%) ethanol for 2 minutes, (90%) ethanol for 3 minutes and (100%) ethanol for 5 minutes, and then placed in Histoclear 2x5 minutes. Finally, slides were left to dry and prepared for mounting with DPX and covered with cover slips. One negative control sample was used for each slide; these were lung cancer sections, rat heart, liver sections with the primary antibody excluded.

2.9 Lung cancer clinical sample slide preparation

In order to obtain thin and higher quality sections, tissue blocks of the lung cancer clinical samples were placed in ice-cold distilled water at least half an hour before cutting. Cold wax helps to achieve thinner sections by providing support for harder elements within the tissue specimen. Furthermore, the small amount of moisture that penetrates the block from the melting ice also makes the tissue easier to cut. A Microtome machine (LEICA BIOSYSTEMS RM2125RT) was used to make tissue slices of 5µm in thickness. As dull blades are one of the main reasons for poor quality sections, to the microtome blades were regularly changed, and use of the part of the blade that has been previously used for rough trimming was avoided. After a few rounds of cutting, a small paintbrush is used to handle cut sections. Fingers should not be used to remove tissue slices, as by this is a high risk of getting them close to the blade. Furthermore, the heat applied from hands will cause the supporting paraffin wax to melt. Instead, the paintbrush is rolled under the ribbon of sections, and is carefully lifted away from the blade. After that, the ribbons of sections

were picked up and floated on the surface of the water in a distilled water bath (shiny side down) by using tweezers. Floating samples on water helps to remove wrinkles and facilitates easy sorting. After briefly floating the sections, tweezers were used to separate the sections, and each individual section was placed onto a positively charged microscope slide and stored upright on a slide rack for a few seconds. Finally, slides were placed on a 37°C hot plate for 30 mins and then left to dry at room temperature overnight. With respect to the comparative nature of this study, tissue cuts were performed in a serial manner as much as possible. Once tissue slices were placed on the positively charged slides, they were labelled in serial numbers according to the consecutive cuts. In order to be used in both IHC and IF, at least nine sequential cuts were made from each lung cancer sample.

2.10 Preparation of *T. gondii* infected control cells

Human neural cells type (SH-SY5Y), were cultured by my colleague Bader Alawfi, and then infected with *T. gondii* parasites (Type1 RHΔKU8) and were used as a positive control for the *T. gondii* immunofluorescence staining. *Toxoplasma gondii* parasites were kindly provided by Dr Paul Denny, University of Durham. To fix the cells, the media was removed, and 4% Paraformaldehyde (PFA) is added and incubated for 15 min, followed by 2 washes with PBS. For permeabilisation, PBS+1% (Triton-X-100) was added and incubated for 5 min, followed by 2 washed with PBS. To prevent the non-specific binding of the antibody, blocking was achieved by covering the cells with PBS +1% Bovine serum albumin (BSA) for 1 hr at room temperature. Cells were then incubated with the unconjugated primary polyclonal antibody targeting the *Toxoplasma gondii* parasite (Thermo Fisher Scientific, Catalogue number PA1-7256, Rockford, IL, USA**)** diluted 1:200 in PBS + 1% BSA for 1 hr room temperature in the dark. After that, cells were washed 3 times in PBS each for 5 min. After that, cells were incubated with the secondary antibody targeting *T. gondii***,** Alexa Fluor 488-conjugated rabbit anti-goat secondary antibody **(**Thermo Fisher Scientific, Catalogue number A27012, Rockford, IL, USA**)**, was diluted in PBS + 1% BSA at 1:200 in the dark for 1 hr. The incubation was followed by a 3x5 min in PBS carried out in the dark. Cells were then covered with DAPI stain (VECTASHIELD® Vibrance™ Antifade Mounting Medium with DAPI, Cat. No: H-1200). Coverslips were then covered with slides and sealed with transparent nail polish to prevent drying as well as providing stability during

visualising by microscopy. Slides were stored in the dark at 4°C. Furthermore, a set of cultured but uninfected cells were used as a negative control which was stained in the same way as the positive control. Slides were then visualised by fluorescent microscopy.

2.11 Double immunofluorescence (*T. gondii* /Arg-1 and *T. gondii* /iNOS) on lung cancer clinical samples

To colocalise *T. gondii* with Arg-1/iNOS in lung cancer clinical samples, a double immunofluorescence procedure was conducted. To ensure no cross-reactivity between the two targeted antibodies, all staining steps were performed sequentially, and no mixing of the 2 primary antibodies nor the 2 secondary antibodies occurred. Furthermore, the two antibodies use in this double immunofluorescence procedure were raised in different species. In order to de-paraffinise the tissue sections, slides were submerged in the xylene for 5 mins. Subsequently, tissues were re-hydrated in graded alcohols (ethanol 100 % x3 min, 95% x1 min and 70 % x1 min) followed by a 2-min wash in running tap water. In order to achieve antigen retrieval, the PT Module (Thermo Scientific™ Lab Vision™**)** was used with 10 mM citric buffer (PH 6) for 20 min and then followed by 20 min cooling down. After washing in phosphate-buffered saline (PBS)/ 0.2% (Triton-X-100) for 3x5 mins, a PAP pen (ImmEdge Hydrophobic Barrier PAP Pen Catalogue number H-4000) was used to draw around the tissue to ensure proper incubation with solutions. To reduce non-specific staining, the tissue was covered with the first blocking solution, 10% normal rabbit serum **(**Vector laboratories catalogue number S-5000) and incubated at room temperature for 30min. After the incubation was done, absorbent paper was used to remove excess blocking solution from the slides. The unconjugated primary polyclonal antibody targeting *Toxoplasma gondii* parasite (Thermo Fisher Scientific, Catalogue number PA1-7256, Rockford, IL, USA**)** was diluted 1:200 in PBS/ 0.2% (Triton-X-100), and enough volume of this solution was added to each tissue section to cover the entire tissue for 1 hr at room temperature or at 4°C overnight. From this point onward, washes involved submerging slides for 5 min three times in PBS/ 0.2% (Triton-X-100), and absorbent paper was used to dry excess PBS from slides. After washing, the secondary antibody Alexa Fluor 488-conjugated rabbit anti-goat secondary antibody **(**Thermo Fisher Scientific, Catalogue number A27012, Rockford, IL, USA**)**, diluted 1:200 in PBS/ 0.2% (Triton-X-100) was added to each slide and incubated at room temperature in the dark for 1 hr and subsequently washed. All steps for the latter stages of the protocol were performed in the

dark **(**Simport Staintray System Black Lid, Code: MIC4162**).** For the second blocking step, 10% normal goat serum (Thermo Fisher Scientific, Catalogue number 50197Z) was added to the tissue and incubated for 30 min at room temperature. The second primary antibody targeting either Induced Nitric-oxide Synthase (iNOS) with the commercial iNOS polyclonal antibodies produced in rabbits (Thermo Fisher Scientific, Catalogue number PA1-036, Rockford, IL, USA) with a dilution of (1:200) or Arginase-1 polyclonal antibodies produced in rabbits (Thermo Fisher Scientific, Catalogue number PA5-29645, Rockford, IL, USA), with both a dilution of 1:200 in PBS/ 0.2% (Triton-X-100) was added to the tissue and incubated for 1 hr at room temperature and followed by a washing step. The second secondary antibody **(**Alexa Fluor 594- conjugated goat anti-rabbit secondary antibody **(**Thermo Fisher Scientific, Catalogue number A32740, Rockford, IL, USA) was added to slides and incubated for 1 hr room temperature and subsequently washed. Slides were then counter-stained with DAPI (VECTASHIELD® Vibrance™ Antifade Mounting Medium with DAPI, Cat. No: H-1200) and sealed with a coverslip with the appropriate size for the tissue. To prevent drying and movement under the microscope, coverslips were sealed with a transparent nail polish. Slides were stored at a temperature of 4°C in the dark until viewing under the fluorescent microscope. Positive controls were rat liver tissue slides for Arg-1, rat heart tissue slides for iNOS and *T. gondii* infected cells for *T. gondii* immunostained slides. Negative controls were lung cancer tissue slides stained with the same protocol as the tested samples with the exclusion of the primary antibodies. Immunoassayed slides were then visualised by fluorescence microscopy. A summary of the antibodies used and the detection agents are listed in (Table 2.4).

Table 2.4 Summary of antibodies and detection agents used in the double immunofluorescent procedure.

	Target	conjugation	Catalogue#	Company	Dilution	Origin Species
1st primary	*T. gondii*	unconjugated	PA1-7256	Thermo Fisher Scientific	1:200	Goat
1st secondary	Rabbit anti-goat	Alexa Fluor 488	A27012	Thermo Fisher Scientific	1:200	rabbit
2nd primary	iNOS/ Arg-1	unconjugated	PA1-036 PA5-29645	Thermo Fisher Scientific	1:200	Rabbit
2nd secondary	Goat anti-rabbit	Alexa Fluor 594	A32740	Thermo Fisher Scientific	1:200	Goat

2.12 Microscopy and Imaging

Immunohistochemically stained tissues were visualised using a light microscope and images were taken using the Leica Microsystems application. Lung tissue/cells types were identified with the aid of histology and histopathology books (Ross et al., 1989; Young et al., 2006). Immunofluorescent stained tissues were visualised on a ZEISS AxioVert.A1 inverted microscope (Zeiss, Oberkochen, Germany), equipped with triple DAPI/GFP/Cy3 filter. Sequential monochrome images captured with the DAPI, GFP, and Cy3 filters were placed in the blue, green, and red channels. Images were later merged together via the Zeiss software and stored as tiff files.

2.13 Statistical analysis

In order to compare infection status with *T. gondii* parasite between lung cancer patients (n=72) and non-cancerous control samples (n=10), 2 x 2 contingency table was used. Fisher's Exact Test was used to calculate the *P*-value. A value of less than 0.05 was considered to be statistically significant.

In order to compare between the percentage of infection with *T. gondii* and the percentage of expression of iNOS and Arg-1 in different lung tissue types/cells, 2x3 and 2x4 contingency tables were used. Fisher's Exact Test (or r x c analyses, if more than a 2 x 2 matrix) was used to calculate the *P*-value with $P<0.05$ was considered statistically significant.

Furthermore, 2x2 contingency tables were constructed to compare between the associations between the infection with *T. gondii* in relation to the expression of Arg-1 and iNOS across different lung tissue/cell types. Fisher's Exact Test was used to calculate the *P*-value with $P<0.05$ was considered statistically significant.

Spearman's rank correlation was used to evaluate the association between the percentage of *T. gondii* infected alveolar macrophages expressing Arg1/iNOS and the grade of *T. gondii* infection. On the other hand, a two-tailed Student's t-test was used to determine statistically significant differences between means of different groups, $P<0.05$ was considered statistically significant.

2.14 Test of significance for true colocalisation

Prior to measuring the amount of colocalisation with PCC and MCC in a particular region, it is important to check whether true colocalisation is present; hence a statistical significance test was performed (Costes et al., 2004). Costes randomisation test is a statistical significance test based on evaluating the probability (*P*-value) in which the calculated value of the correlation (r) derived from the original two colours is significantly greater than values of r that would be calculated if there was only random overlap or due to chance. The test is conducted by randomly scrambling the pixels in one image, while keeping the other images the same. After that, the correlation (r) of the scrambled image is measured with the other (unscrambled) image. As scrambling the pixels in one image will cause the two spatial distributions independently, this means that only the contribution to the correlation of the random overlap will be calculated. This is repeated for 200 times, and in each time the value of r is measured. By comparing the amount of correlation measured from the unscrambled image with this distribution determines whether significant colocalisation exists. A *P*-value of > 95% indicate significant true colocalisation. Only those images with true colocalisation were included in the quantitative colocalisation analysis.

2.15 Quantitative colocalisation analysis

In order to perform a quantitate colocalisation analysis, the JACoP plugin for Image J software (http://rsb.info.nih.gov/ij/ plugins/track/jacop.html) was used. The special tool of JACoP, Region Of Interest (ROI) was used to draw lines around the targeted cell or structure to ensure that only

the desired cell/tissue structure was included in the quantification analysis. Several metric measures were used, including Pearson's Correlation Coefficient (PCC) was used Menders Correlation Coefficient (MCC). For PCC calculation, the dependency of pixels in double-channel images (red and green channels) was measured, and a linear equation of the relation between the intensities of the two channels was measured via linear regression. The value of the PCC can vary from 1 to -1, with 1 corresponding to perfect correlation, while -1 corresponds to negative correlation and 0 stands for no correlation.

With the MCC which is based on the PCC, two split coefficients were obtained, M1 and M2, for the fraction of red pixels overlapping with the green pixels and for the fraction of green pixels overlapping with red pixels, respectively. Values range from 0 to 1, where 0 means non-overlapping images, while a value of 1 means complete colocalisation.

Chapter 3: *Toxoplasma gondii* infection in lung cancer patients: analysis of control samples

3.1 Introduction

The aims of this chapter were to analyse a set of control samples, to complement and contribute to a study on *Toxoplasma gondii* infection in lung cancer patients. Lung cancer is a serious disease and represented 11.6% of all cancers globally in 2018 (WHO, 2019). Furthermore, in 2014 in the UK, the incidence (age-standardised incidence) was 62/100,000, and the mean 5-year survival rate was as low as 14.7% (WHO, 2019).

Little is known about the contribution of infection by parasitic agents on the outcome of cancers, although parasites like *Toxoplasma gondii* are known to be found more frequently in patients with cancer (Yuan et al 2007). The purpose of this study is to conduct a detailed investigation into the prevalence and distribution of *Toxoplasma gondii* in lung biopsy samples from lung cancer patients. The initial outcomes of this study (Bajnok, 2017) showed that in the lung biopsies of 72 potential patients, who were in for diagnostic purposes, all (100%) appeared to be infected with *T. gondii*. Both PCR detection using 5 *T. gondii* specific markers and, in an independent technique, immunohistochemistry using *T. gondii* specific antibodies confirmed this diagnosis. This was a surprising result since the background infection prevalence in the UK population, from which the lung cancer patients were drawn, is estimated to be 10% (Pappas et al 2009). To validate and further investigate this association between lung cancer and *Toxoplasma gondii* infection, there was a need to obtain and characterise control tissue samples from subjects that had no history of lung cancer. This chapter describes the results from the investigation into those controls and contributes to a published paper on the overall investigation (Bajnok et al. 2019).

This raises the question as to whether the 100% detection rate of *T. gondii* in these lung cancer patients is typical of the natural infection rate in the general surrounding population. To test the hypothesis that there is no difference between the infection rate in these lung cancer patients and the background population, a set of control lung tissues were examined using the same approaches.

3.1.1 Objectives

1. Obtain a collection of control lung tissue samples from subjects without lung cancer.

2. Extract DNA from control lung tissue samples and test the quality of the DNA for potential PCR amplification with *T. gondii* specific PCR primers.

3. Use of the *T. gondii* specific marker, the B1 gene, to detect infection in the control lung samples.

4. Use of the *T. gondii* specific marker, the SAG1 gene, to detect infection in the control lung samples.

5. Use of the *T. gondii* specific markers, the SAG2 3' end gene and the SAG2 5' end gene, to detect infection in the control lung samples.

6. Use of the *T. gondii* specific marker, the SAG3 gene, to detect infection in the control lung samples.

7. To use immunohistochemistry as an independent technique to detect infection in the control lung samples.

8. To use RFLP analysis to investigate the *T. gondii* strain type(s) present.

3.2 Methods

Samples for the study were provided by Professor Dave Singh from the Medicines Evaluation Unit at Manchester University and Wythenshaw Hospital. Collection and processing of the samples were carried out by Josiah Dungwa, Dr Thomas Southworth and Prof Singh. The collection of control samples was approved by the NRES Committee North West – Greater Manchester South (06/Q1403/156). The study also received ethical approval from the University of Salford Research Governance and Ethics Committee (CST 12/37 (Bajnok, J) and ST16/124 (Tarabulsi, M)). Ten samples of lung tissue were obtained by bronchoalveolar lavage from a cohort of subjects undergoing normal diagnostic procedures to act as a comparative set of samples to examine alongside comparable tissues from lung cancer patients. Due to the difficulty, safety and ethical issues associated with obtaining lung samples from healthy subjects, only 10 control samples were obtained. DNA was successfully extracted from the slides of the non-lung cancer control samples (n=10) as described in Chapter 2. Extracted DNA was then tested by PCR amplification of mammalian tubulin, then a sequence of nested PCR amplifications targeting five specific *T. gondii* markers (B1, SAG1, SAG2 3′, SAG2 5′ and SAG3) was performed to detect infection.

3.3 Results

3.3.1 Collection of control samples from non-cancer patients

Individuals involved in this study were carefully selected and had to fulfil certain criteria in order to participate as a part of the control group. As a start, the most fundamental aspect was to exclude any previous history of lung cancer. Smoking history was documented, and any lung conditions such as Chronic Obstructive Pulmonary Disease (COPD) and asthma were excluded (see Table 2.1 in Chapter 2).

Furthermore, smoking history and lung function status were also documented (Table 3.1). The lung function tests are a valuable tool for investigating and monitoring lung health status (Behr and Furst, 2008). If the FEV1/FVC ratio was less than 70% and FEV1 is decreased more than FVC, that implies an obstructive lung disease, whereas if the FEV1/FVC ratio was more than 70%, but the FVC is decreased more than FVE1, which suggests a restrictive lung disease (Behr and Furst, 2008). All subjects included in the control group for this experiment have lung function tests that are within the normal range including the only infected sample (558) where the FEV1/FVC ratio was 72.02% which is more than 70%; however the FVC (4.25) was not decreased more than the FVE1 (3.09) which indicates a normal lung function.

Table 3.1 Control subject demographics : Lung function: FEV1 (forced expired volume in 1 second), %Pred (Percentage of the predicted value), FVC (Forced Vital Capacity).

Patient Number	FV1	FEV1%Pred	FVC	FEV1/FVC ratio
920	4.18	100.80%	5.57	75.04%
292	3.35	82.72%	4.12	81.31%
545	3.93	148.55%	5.5	71.45%
929	2.88	100.31%	3.55	81.12%
134	---	---	---	---
137	2.3	115.69%	3.25	70.76%
917	2.45	116.83%	2.91	84.19%
268	4.05	101.17%	4.26	95.07%
166	3.7	87.43%	4.83	76.6%
558	3.09	109.03%	4.29	72.02%
Mean	3.32	106.95%	4.25	78.61%

3.3.2Checking the quality of the extracted DNA by PCR amplification of the α-tubulin gene

In order to confirm viability for PCR, extracted DNA samples were PCR amplified using a mammalian α-tubulin PCR technique that amplifies any mammalian DNA species if the DNA is of good quality. After the PCR, samples were resolved on a 1% agarose gel electrophoresis containing gel red and visualised under UV light. The results are shown in Figure 3.1. The presence of a band at 1600bp showed that all extracted samples showcased successful amplification of the α-tubulin gene. This indicated successful DNA extraction and the absence of PCR inhibition. Furthermore, the absence of these specific bands in the negative control (water) and the negative extraction controls demonstrated that no contamination nor non-specific PCR amplification was occurring. This validation test using these generic primers is important in the interpretation of the *T. gondii* diagnostic markers because a negative amplification with the *T. gondii* markers could be explained as either non-infection or failure of the PCR reaction to work for that sample. This experiment demonstrates the capability of each sample to be amplified and therefore rules out the latter interpretation. This showed that these samples were suitable for use with *T. gondii* DNA detection using the five genetic markers B1, SAG1, SAG2 (3′ and 5′ ends) and SAG3.

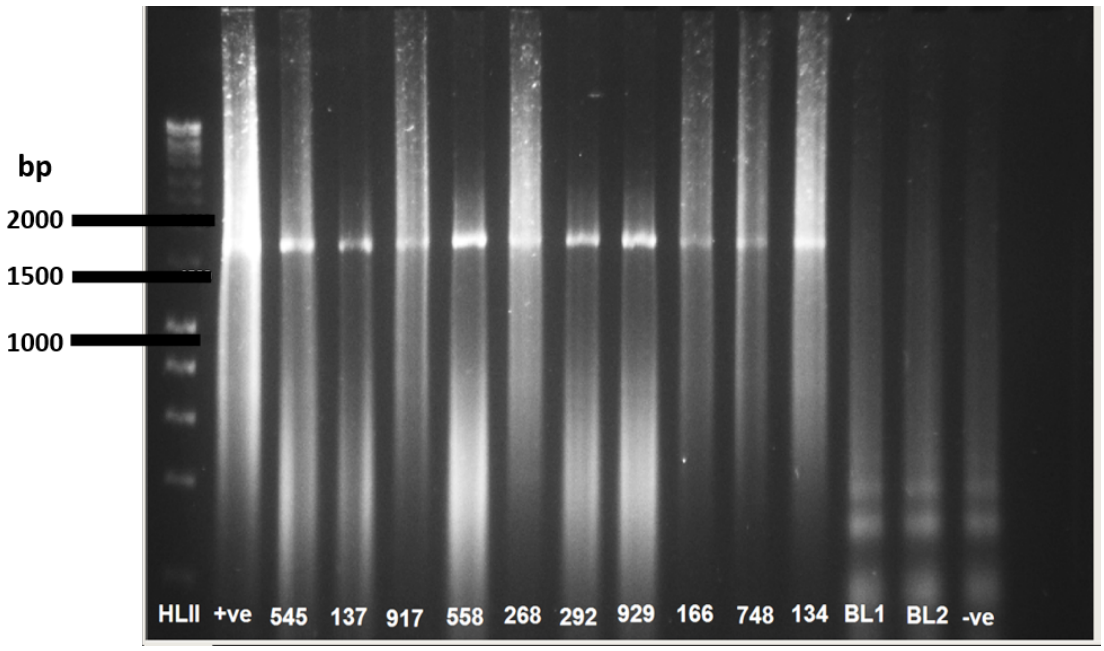

Figure 3.1 Agarose gel electrophoresis of PCR targeting the α-tubulin gene . HLll is the Hyper Ladder 2, +VE is the positive control (type II) strain, 545, 137, 917, 558, 268, 292, 929, 166, 784 and 134 are the tested samples, -VE is the negative control, BL1, BL2 are extraction negative controls. All the extracted samples, as well as the positive control, are displaying the expected band size of (1600) bp indicating the viability of samples and the absence of PCR inhibitors. Both negative and extraction controls are negative and thus exclude contamination.

Since the high number of gene copies plays a key role in the sensitivity of the detection of *T. gondii* parasite, highly repeated sequences are considered a good target for detection (Homan et al., 2000). The B1 gene is a 35 fold repetitive gene, which is used for a highly specific and sensitive PCR detection of *T. gondii* present in clinical specimens (Habibi et al., 2012). Moreover, the B1 gene has been used extensively for the detection of *T. gondii* infections, as well as in epidemiological studies, for its high sensitivity and specificity (Homan et al., 2000).

A nested PCR was performed to amplify the specific B1 gene for *T. gondii*. Each sample was tested three times, and the samples were considered positive for *T. gondii* parasite if the PCR amplification was successful in all three reactions. The second-round PCR products for each sample were resolved on a 2% agarose gel electrophoresis. Samples displaying a band size of

approximately 96 bp were considered positive. The first attempt at nested PCR was not reliable due to the presence of a band of the expected size in the negative control, as well the extraction control (Figure 3.2). Since sterile water is used to detect any false amplification, such results usually indicate contamination. Although nested PCR is used as a modification of the conventional PCR by using two sets of primers to increase the sensitivity and specificity of the amplification, however, a major limitation of nested PCR is the increased risk of contamination due to the post-PCR manipulation of samples between the two rounds of nested PCR (Haff, 1994). Studies have reported that B1 can detect as low as one parasite in an infected sample (Su et al. 2010), which might explain why contamination with B1 nested PCR is not uncommon.

To overcome the issue of contamination, further measures were taken when conducting the nested PCR. These measures included; ensuring that the second round of PCR was prepared in a different location than the first round of PCR, gloves were changed between the two rounds of PCR, the samples of the first PCR products were allowed to cool down on ice for at least 5-10 minutes before opening the PCR tubes, and finally, the outside surface of the PCR tubes were wiped after each round.

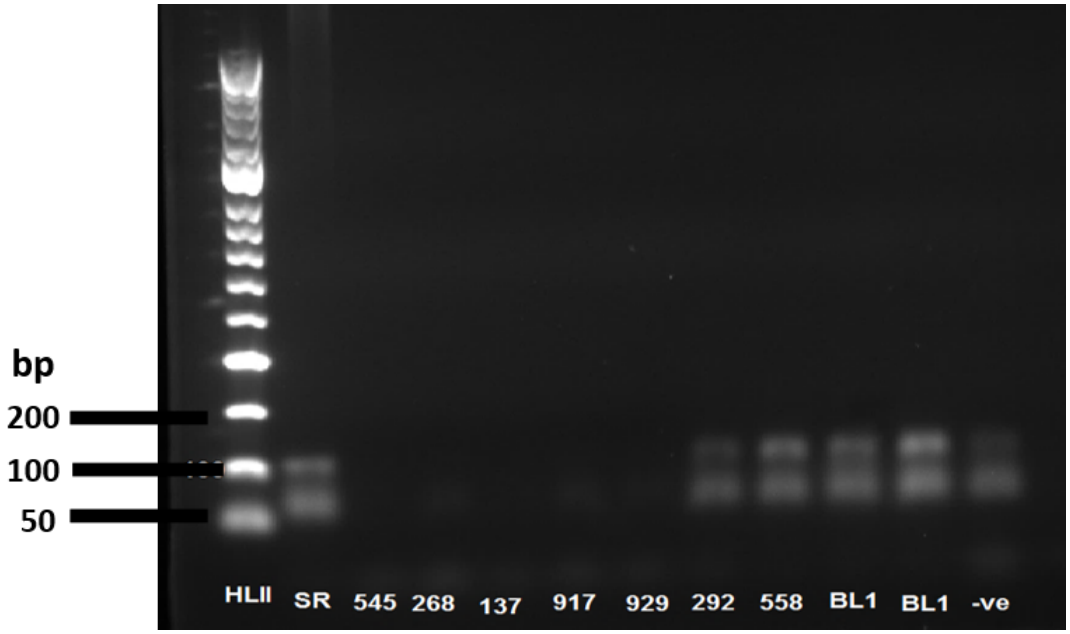

Figure 3.2 Agarose gel electrophoresis of nested PCR amplification targeting the B1 gene of *T. gondii* . HLll is the Hyper Ladder 2, SR is the positive control (type II) strain, 545, 268, 137, 917, 929, 292, and 558 are the tested samples, -VE is the negative control, BL1, BL2 are the extraction negative controls. Some of the samples, including the negative and extraction controls, are displaying the expected band size of 96 bp indicating contamination.

After the previously mentioned modifications had been considered, the B1 nested PCR was repeated. The positive control (SR), displayed a band at 98 bp, which is the predicted size for B1 gene amplification confirming that the PCR was working properly. Out of the 10 tested samples, only one sample (558), successfully amplified the B1 gene and showcased a band at the predicted size, 98 bp, indicating it is positive (Figure 3.3). On the other hand, the remaining tested samples (545, 268, 137, 917, 929, 292, 166, 748 and 134) failed to amplify the B1 gene of *T. gondii*. The negative control was negative, excluding the possibility of contamination, as well as the two extraction controls (BL1 and BL2).

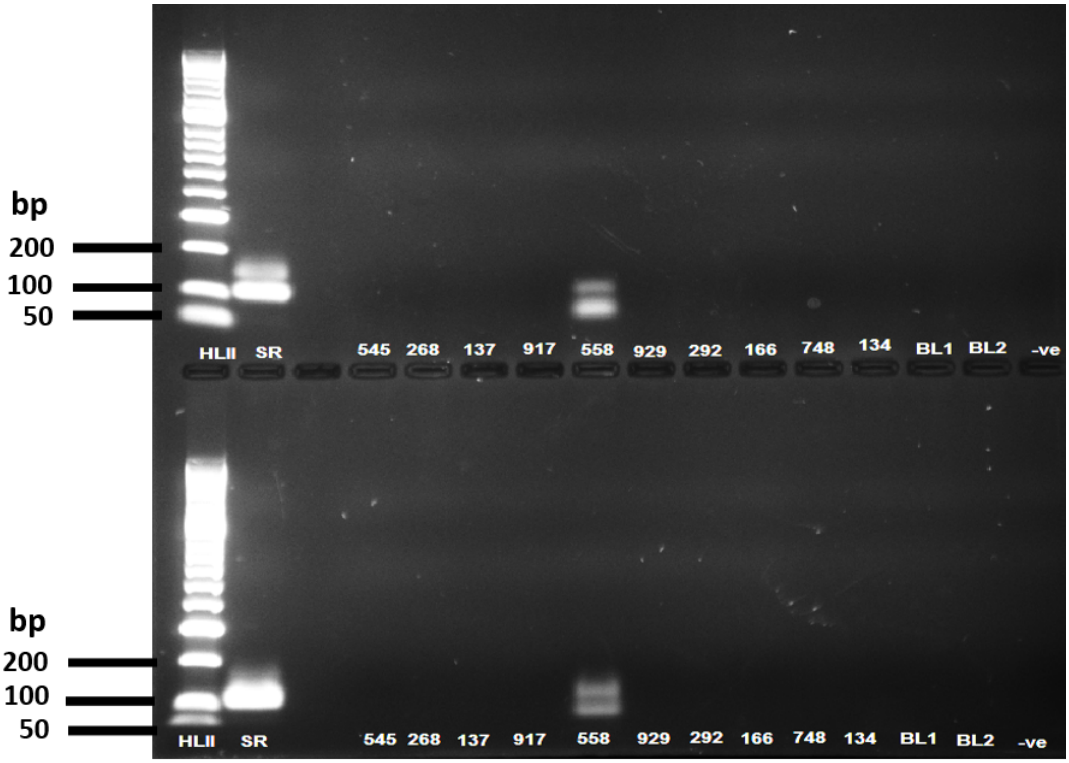

Figure 3.3 Gel electrophoresis of second PCR products of nested PCR targeting B1 gene for *T. gondii* parasite. HLll is the Hyper Ladder 2, SR = positive control (type II) strain, 545, 268, 137, 917, 929, 292, 166, 748, and 134 are the tested samples, BL1, BL2 are the extraction negative controls, -VE is the negative control. The positive control, as well as one sample (558), are displaying a band with the expected size of approximately 96 bp. Both negative and extraction controls are negative, excluding contamination.

3.3.4 PCR detection of the *T. gondii* SAG1 gene in control DNA samples

To further confirm the results obtained by the B1 amplification, a nested PCR targeting the specific Surface Antigen Gene 1 (SAG1), of *T. gondii* was conducted on the 10 samples. The PCR was performed three times for each sample, and it was considered positive for *T. gondii* infection only if the samples were successfully amplified in all three PCR reactions. The second PCR products for each sample were resolved on a 1.5% agarose gel electrophoresis. Samples showing a band size of approximately 522 bp were considered positive. Only one sample displayed the expected band size, which was the same sample that was positive with the B1 nested PCR, sample 558, hence, confirming the previous result, (Figure 3.4). Furthermore, samples (545, 268, 137, 917, 929, 292, 166, 748 and 134) did not display the expected band size indicating the absence of

T. gondii infection. No evidence of contamination was observed with the negative control as well as the extraction controls were all negative.

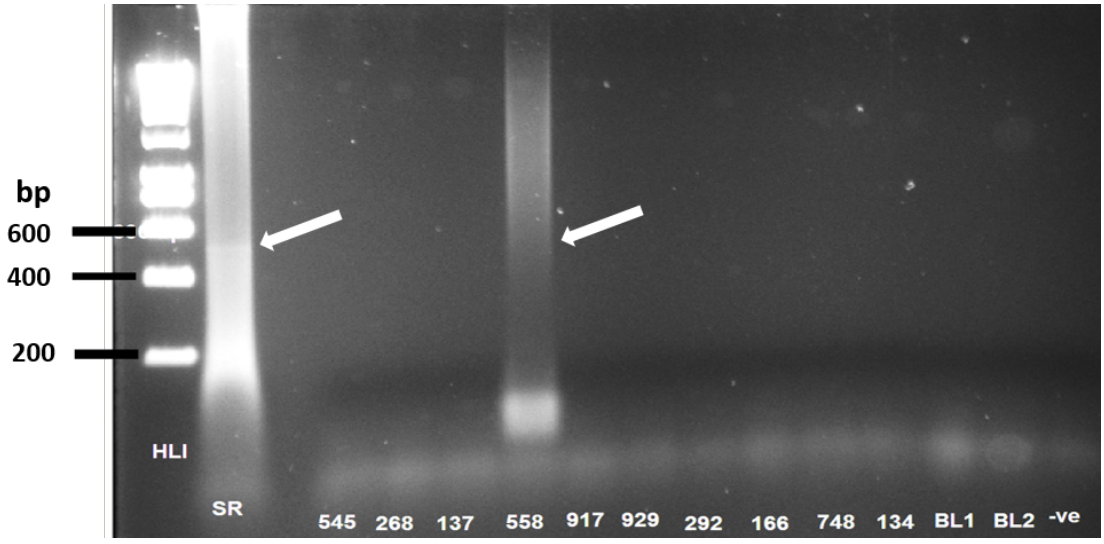

Figure 3.4 Gel electrophoresis of nested PCR amplification of SAG1 marker for *T. gondii* showing the 10 control samples . HLI is the Hyper Ladder 1, SR is the positive control (type II) strain, 545, 268, 137, 917, 929, 292, 166, 748, and 134 are the tested samples, -VE is the negative control, BL1, BL2 are the extraction controls. Second PCR products were resolved in a 1.5% gel containing GelRed. The positive control and only one sample (558), are displaying a product size of 522 bp (indicated by the white arrow). A negative control and extraction controls are negative, excluding contamination. Note, although the band of sample (558) is faint, it is more visible on the gel viewer).

3.3.5 PCR detection of the *T. gondii* SAG2 gene in control DNA samples

In addition to the SAG1 gene, nested PCR targeting the SAG2 gene to detect *T. gondii* parasite in clinical samples has been widely used due to its high sensitivity, where it has been reported that SAG2 nested PCR is able to detect as few as five parasites in a tested sample (Derouin et al., 1997).

Following the same methodology used for the lung cancer samples (Bajnok, 2017), a nested PCR targeting the SAG2 gene in two different loci SAG2 3′, and SAG2 5′ were done separately on the 10 samples. For the SAG2 3′ nested PCR, a 222 bp product at the end of the second round in all three times for each sample was considered positive. Samples were run on a 1.5% agarose gel

electrophoresis and visualised under UV light. Confirming the previous results obtained by B1 and SAG1 markers, the same sample (558) was the only sample that showcased the expected band size of this marker at 222 bp, (Figure 3.5), while samples (545, 268, 137, 917, 929, 292, 166, 748 and 134) were negative for *T. gondii* infection. No false amplification was documented since both negative and extraction controls were negative.

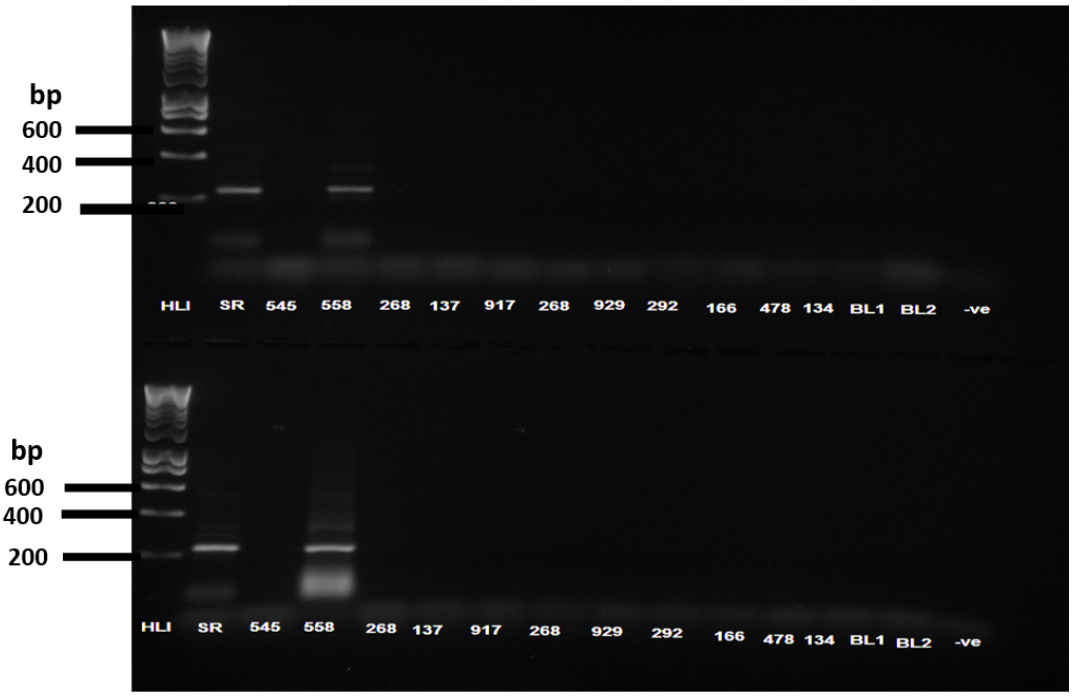

Figure 3.5 Gel electrophoresis of nested PCR amplification of SAG2 3′ marker for *T. gondii* of the 10 control samples . HLlis the Hyper Ladder 1. SR is the positive control (type II) strain, 545, 268, 137, 917, 929, 292, 166, 748, and 134 are the tested samples, -VE is the negative control, BL1, BL2 are the extraction controls. Second PCR products were resolved on a 1.5% gel containing GelRed. The positive control and one sample (558), are displaying a band with the expected size of approximately 222 bp.

To further confirm the results, nested PCR targeting the SAG2 5′ gene of *T. gondii* was conducted on all 10 samples three times for each sample, and a band size of 242 bp in any sample in all three reactions was considered positive. The second PCR products were run on a 1.5% gel electrophoresis and examined under UV light. Only one sample (558) displayed the expected band size of 242 bp (Figure 3.6), which matches previous results obtained by previous *T. gondii*

markers (B1, SAG1and SAG2'3). Whereas the remaining 9 samples (545, 268, 137, 917, 929, 292, 166, 748 and 134) did not exhibit the expected band indicating, they were all negative for *T. gondii* infection. No contamination was observed with both negative and extraction controls were negative.

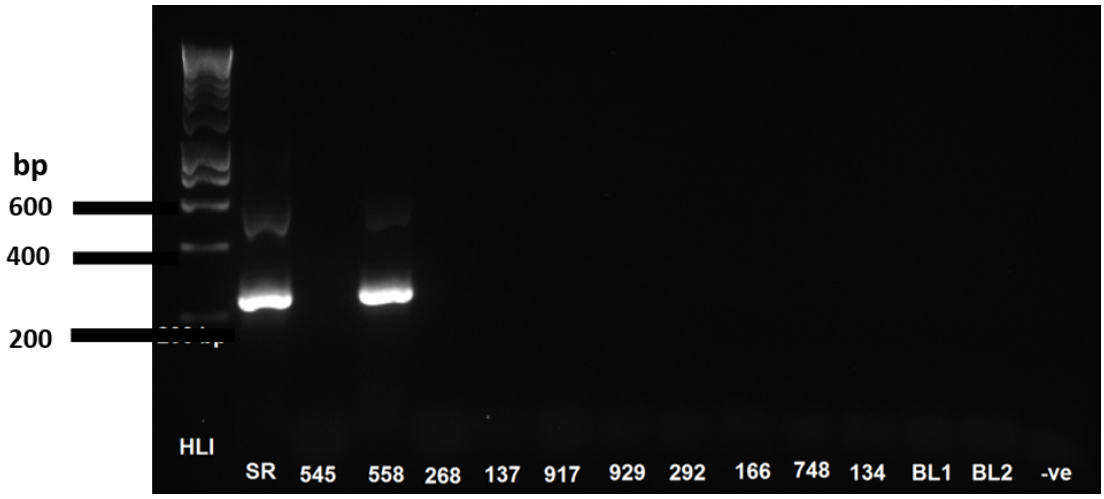

Figure 3.6 Gel electrophoresis of second PCR products of nested PCR targeting SAG2 5′ gene for *T. gondii* parasite . HLl is the Hyper Ladder 1, SR is the positive control (type II) strain, 545, 268, 137, 917, 929, 292, 166, 748, and 134 are the tested samples, BL1, BL2 are the extraction negative control, -VE is the negative control. The positive control and one sample (558), are displaying a band with the expected size of approximately 242 bp. Both negative and extraction control are negative, excluding contamination.

3.3.5 PCR detection of the *T. gondii* SAG3 gene in control DNA samples

To complete the set of markers used to detect *T. gondii* infection in the 10 samples, a SAG3 nested PCR was performed three times for each sample. A sample was said to be positive if it exhibited the expected band size of 242 bp in all three PCR reactions. Samples were visualised under UV light after they were run a 1.5% agarose gel electrophoresis. The same positive sample with the previous 4 *T. gondii* markers, sample (558), was displaying the expected band size for SAG3 of 242 bp, (Figure 3.7), while the remaining samples (545, 268, 137, 917, 929, 292, 166, 748 and 134) have failed to amplify indicating they are negative. Contamination was excluded by the fact that the negative control, as well as the extraction controls, were negative.

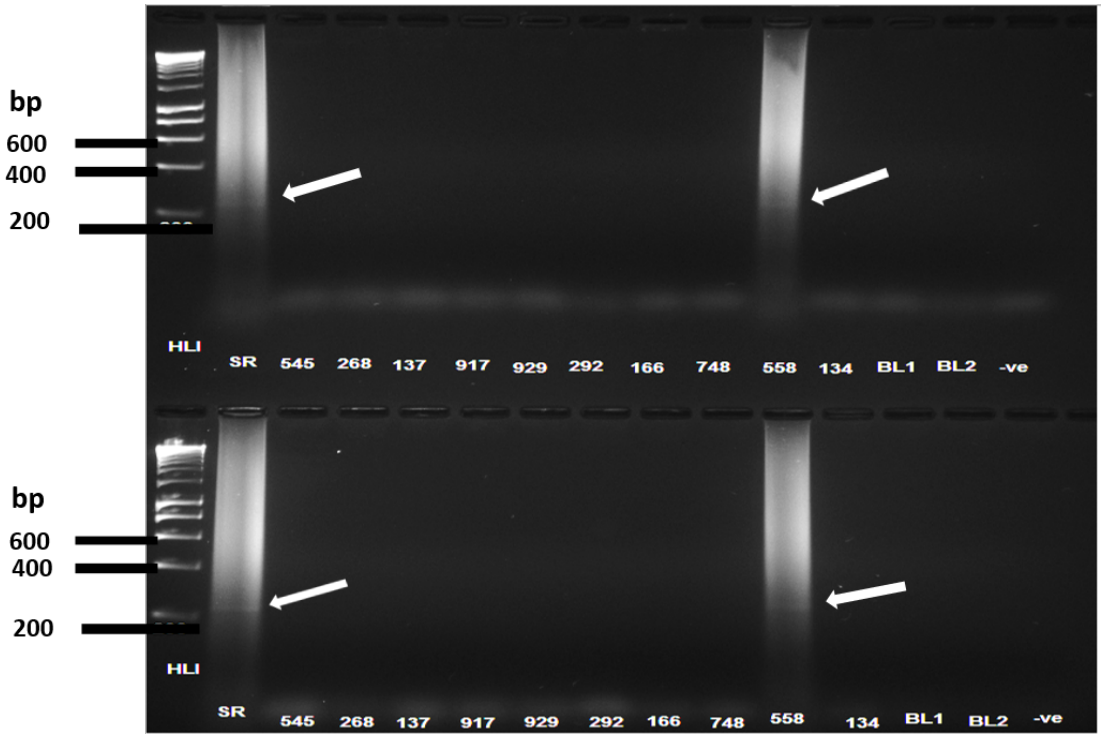

Figure 3.7 Agarose gel electrophoresis of nested PCR amplification of control samples targeting the SAG3 gene of *T. gondii* . HLl is the Hyper Ladder 1, SR is the positive control (type II) strain, 545-134 are the tested samples, -VE is the negative control. The positive control and one sample only (558) are displaying the expected band size of 225 bp (indicated by the white arrow). Both negative and extraction controls are negative, excluding contamination. Note, although the band of sample (558) is faint, it is more visible on the gel viewer).

3.3.6 Summary of the PCR detection results

Each control lung tissue sample was tested three times with each of the above markers. If a sample was amplified in all three replicates, they were considered to be positive for that marker. If the samples were negative in all three replicates BUT had been successfully amplified using the α-tubulin, they were considered negative. A summary of the aggregated nested PCR results of all the samples is listed in (Table 3.2). Only sample 558 was considered positive.

Table 3.2 A summary of nested PCR results for the 10 control samples with the five *T. gondii* specific markers (B1, SAG1, SAG2 3′, SAG2 5′ and SAG3).

Patient Number	B1 Marker	SAG1 Marker	SAG2 3′ Marker	SAG2 5′ Marker	SAG3 Marker
929	Negative	Negative	Negative	Negative	Negative
292	Negative	Negative	Negative	Negative	Negative
545	Negative	Negative	Negative	Negative	Negative
748	Negative	Negative	Negative	Negative	Negative
134	Negative	Negative	Negative	Negative	Negative
134	Negative	Negative	Negative	Negative	Negative
917	Negative	Negative	Negative	Negative	Negative
268	Negative	Negative	Negative	Negative	Negative
166	Negative	Negative	Negative	Negative	Negative
558	Positive	Positive	Positive	Positive	Positive

3.3.7 Use of Immunohistochemistry to detect the presence of *T. gondii* in the control lung samples

To be consistent with the analyses of lung cancer patients (Bajnok, 2017), immunohistochemistry was performed on the control samples to detect *T. gondii* infection. This work was performed by Jaroslav Bajnok) and is included here to reinforce the results obtained from the *T. gondii* specific PCRs. A specific anti-*T. gondii* antibody was used to detect the parasite antigen, as described in the Materials and Methods (Chapter 2), and following previously applied procedures (Plumb et al., 2009), immunohistochemistry protocol was conducted. For each sample, a negative and a positive control slide was used. For the negative control, these were lung cancer samples with the primary antibody omitted during the immunohistochemistry process to ensure the absence of contamination. Positive controls were lung tissue from a *T. gondii* infected wood mouse. Only one sample (558) in the control group (non-cancerous) exhibited specific staining with the anti-*T. gondii* antibody (Data produced by J. Bajnok, not shown). The positive sample was the same sample that showed positive amplification for the five *T. gondii* specific PCR amplifications B1, SAG1, SAG2 (3’ and 5’ ends), and SAG3.

3.3.8 Determination of the genotype of *T. gondii* in control lung tissues using RFLP Genotyping

In the ongoing study at Salford (Bajnok, 2017), they have tested the possibility of genotyping of *T. gondii* strains directly from infected lung tissue by PCR-RFLP on the positive samples. This has shown that the majority of the lung samples displayed a type II strain infection. Following that same methodology, RFLP genotyping was performed on the only control sample (558) that successfully amplified the five specific markers of *T. gondii* (B1, SAG1, SAG2 (3' and 5' ends) and SAG3) (Figure 3.8). The second-round PCR products of SAG2 3' were cut by the restriction enzyme *Hha*I while the SAG 5' end was digested with the restriction enzyme *Mbo*I and resolved on a 2.5% gel electrophoresis. The resulting restriction patterns were then compared to the database of genotypes known as ToxoDB and showed that the positive control sample (558) is displaying a type II strain of *T. gondii*.

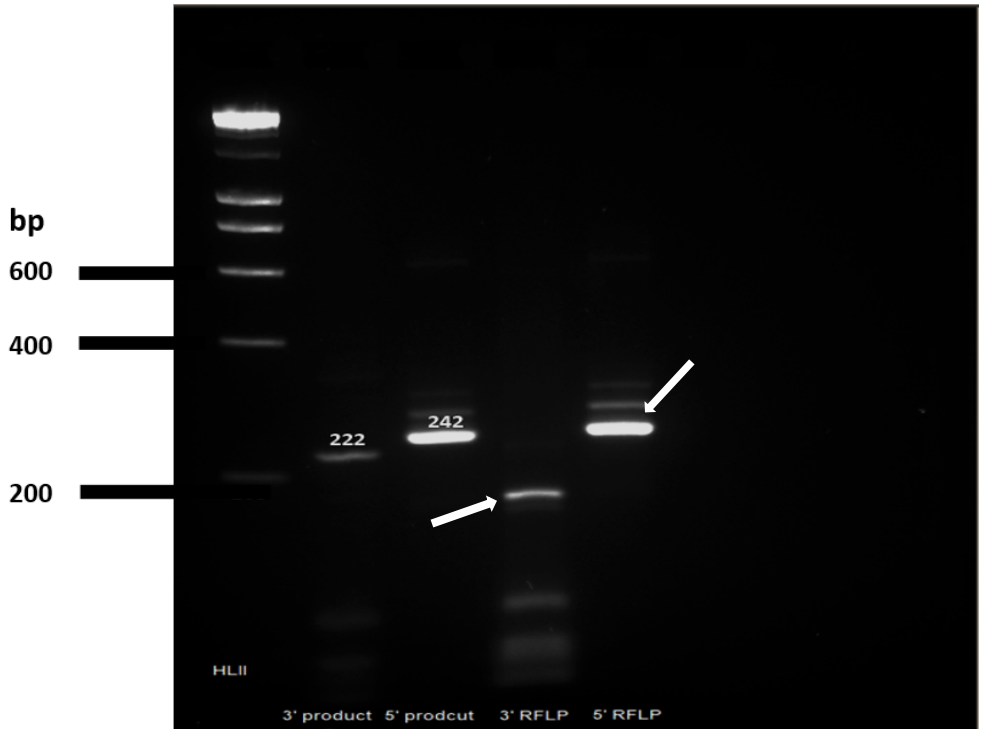

Figure 3.8. Gel electrophoresis of PCR-RFLP of the amplified second PCR products of SAG2 (3' and 5' ends) of the positive control sample (558), HL II is the hyper ladder 2, 3' product is the undigested second PCR product of nested SAG2 PCR 3' end, 5' product is the undigested second PCR product of nested SAG2 PCR 5' end, 3' RLFP is the result of 3' RLFP on sample (558), 5' RLFP is the result of 5' RLFP on sample (558). *T. gondii* strain. Second PCR products were digested by *Hha*I for SAG2 3'end product and by *Mbo*I SAG2 5' end product and resolved in a 2.5% gel electrophoresis containing GelRed. With reference to ToxoDB, sample (558), is displaying infection with type (II) strain of *T. gondii* (white arrows).

3.3.9 Analysis of the association between *T. gondii* infection in lung cancer patients and in the control samples.

The high prevalence of *T. gondii* infection observed in the previously mentioned lung cancer study of 100% prevalence (Bajnok, 2017) is striking. This study aimed to conduct the same diagnostic procedures on the samples recruited from healthy individuals to be used as a control group (n=10) for the lung cancer clinical samples (n=72). In order to investigate the difference between the two groups and to determine infection status, a 2 x 2 contingency table analysis was used (Table 3.3). Fisher's Exact Test was used to calculate the *P*-value, and a *P*-value of <0.05 was considered significant.

Table 3.3 A 2 x 2 contingency table for Fisher's Exact Test.

	Infected	**Non-infected**	**Total**
Cancer Patients	72	0	72
Control Group	1	9	10
Total	73	9	82

The null hypothesis is that there is no difference in infection status between the lung cancer group and the healthy control group. A *P*-value of less than 0.05 was considered statistically significant. The *P*-value was calculated and gave a result of (*P*=0.00001) which is less than 0.05. Hence, we reject our null hypothesis that there is no difference and state that there is an extremely significant difference in *T. gondii* infection status between the lung cancer group and the healthy control group.

3.4 Discussion

In conclusion, 10 samples were tested which were obtained by bronchoalveolar lavage from healthy individuals with no previous history of lung cancer to be used as a control group for the lung cancer patients study (Bajnok, 2017). After DNA extraction had been performed on the slides containing the samples, all 10 samples were tested by nested PCR targeting five specific *T. gondii* parasite markers (B1, SAG1, SAG2 3′, SAG2 5′ and SAG3) to detect *T. gondii* infection. Each sample was tested three times, and it was considered positive only if it exhibited the expected band of the specific marker in all three reactions. Out of 10 samples, only one sample (558) consistently showed successful amplification with all five markers indicating it was positive for *T. gondii* infection while the remaining samples (545, 268, 137, 917, 929, 292, 166, 748 and 134) failed to amplify with any of the markers, indicating they were negative for *T. gondii* parasite. The negative control excluded any contamination as well as the two extraction control samples (BL1 and BL2) in all reactions.

These results were further confirmed by IHC staining (conducted by Jaroslav Bajnok), with specific anti-*T. gondii* polyclonal antibodies produced in rabbit and designed to target intact *T.gondii* with reactivity to Protozoa, and only the same positive sample (558) identified by nested PCR with the five markers was positively stained with IHC. RFLP analysis suggested that sample 558 contained a type 2 *T. gondii* strain. The results of the comparison of *T. gondii* infection in the lung cancer and control patients (but not the genotyping) has been published with the author of this chapter as 2nd author (Bajnok et al 2019).

In this chapter, we have shown that it is possible to extract DNA directly from slides containing lung tissue samples and this can be used to produce PCR results, demonstrating that it is potentially a reliable and simple diagnostic approach for the detection of *T. gondii* from lung biopsy samples. Furthermore, the results that we have established from these lung tissue slides using nested PCR have been consistent with each marker targeting *T. gondii* and was supported by the IHC approach which demonstrated a consistent answer with the PCR results**.**

Various PCR-based techniques have been developed for the diagnosis of toxoplasmosis using several clinical specimens, including blood, amniotic fluid and tissue biopsy (Li et al., 2000). Among these techniques, nested PCR followed by hybridization of PCR products has been the

most sensitive method (Li et al., 2000). Nevertheless, the major drawback of these techniques is that they are time-consuming and fail to provide quantitative data. The recent advent of a real-time quantitative PCR technique has proven useful in several applications, including pathogen detection, gene expression and regulation, and allelic discrimination (Li et al., 2000). The use of q-PCR on our samples would be of benefit in obtaining a quantitative analysis of the infection load in each sample and then conduct a correlation analyse between parasite load and other aspects like gender, smoking and other diseases e.g. asthma and COPD.

The prevalence of *T. gondii* infection in the UK is 10- 12%, which, compared to the global infection rate of 30% (Pappas et al., 2009), is considered low. However, the results of this project represent a high infection rate in these cancer patients. In this chapter, we have recruited 10 healthy individuals with no previous history of cancer to be used as controls, and these were evaluated for *T. gondii* infection. It was also considered that the controls should have a similar age range as the cancer patients. In this case, they had a lower average range. We do recognise a few limitations involving the control group, however, with the difficulty and potential risks of lung biopsy techniques, it was challenging to accomplish a suitably sized and matched control group to the cancer patients. Moreover, the samples obtained from lung cancer patients were collected by cancer resection, and the cancer-free margins were used as lung tissue samples. On the other hand, control samples were obtained via bronchoalveolar lavage, which means that the comparison was between two relatively different tissues (lung versus bronchial tissue), nevertheless, since *T. gondii* has the capability to infect any nucleated cell type, and since both tissue types will experience a similar exposure to parasite infection, we expect a minimal influence of these limitations on the conclusions. We also acknowledge possible bias as a result of the relatively younger average age as well as the small control sample size of the control group, which is again attributed to the difficulty and risks accompanying the sampling process of healthy subjects. Despite these limitations, our results have demonstrated a high prevalence of *T. gondii* infection in lung cancer patients compared to the control group and compared to the expected UK prevalence in people without cancer.

Despite the fact that it is well documented that toxoplasmosis complicates patients with most types of cancer (Carey et al., 1973), as well as pneumonia and other respiratory diseases, (Rottenberg et al., 1997), only a few studies have described *T. gondii* infection complicating lung cancer. A case study in China, reported *Toxoplasma* in a 64-year-old patient with non-small lung

carcinoma (Lu et al., 2015). The condition was confirmed by detection of IgM antibodies, as well as the identification of tachyzoites in the bronchoalveolar lavage (Lu et al., 2015).

In a study conducted in China, a group of patients with different types of cancers were investigated for anti-*T. gondii* antibodies and they reported a high overall prevalence of (35.56%) compared to (17.44%) in the control group. The highest seroprevalence was reported with lung cancer (60.94%) followed by cervical cancer (50%) and (42.31%) for patients with brain cancer (Cong et al., 2015). On the other hand, when measuring the infection rate in patients with different cancers in China by nested PCR, the study reported a prevalence of 3.55%, while the same samples demonstrated 8.38% using serological prevalence (Wang et al., 2015). This suggests that there is some variation in the measurable outcomes when using different diagnostic approaches.

Toxoplasma has been reported to complicate different types of neoplastic diseases. A study reported, that out of 24 patients with toxoplasmosis, 14 patients had either leukaemia or lymphoma, and 9 patients had Hodgkin's disease (Carey et al., 1973). In a study conducted in the United States, they attempted to explore the associations between *T. gondii* infection and brain cancers in human populations from 37 different countries (Thomas et al., 2012). The countries that have increased prevalence of *T. gondii* infection had a 1.8 fold higher incidence of brain cancer compared to other areas where *T. gondii* infection was low or absent (Thomas et al., 2012). The majority of studies that have investigated *T. gondii* infection among cancer patients have used serological based approaches to measure the prevalence of *T. gondii* as opposed to direct tissue sample investigation. There are advantages and disadvantages of each approach. One of the key difficulties of the serological detection approach is that it only measures exposure to the parasite and gives no indication as to whether a current infection is present. One of the key difficulties of the direct detection approach is that the parasite must be detected directly from infected lung tissue samples – which are difficult to collect. In natural infections, some individuals are clearly highly infected, while others are not. This can lead to variability in the PCR detection systems used and in some cases, detection or lack of it depending on the random selection of parts of samples. Furthermore, all the studies that have reported toxoplasmosis in cancer patients, none have addressed the mechanism of the relationship between cancer and *T. gondii* infection. In this chapter, we directly aimed to study the association between lung cancer and *T. gondii* infection directly from tissue samples.

These types of studies shed light on the medical impact of *T. gondii* infection in cancer patients, e.g., routine serological testing for *T. gondii* infection in cancer patients, could help avoid the potentially fatal complications of this infection. Nonetheless, the mechanism of the interaction between *T. gondii* and lung cancer is far from clear. Data documenting *T. gondii* infection as a causative agent for cancer are unavailable, but the high frequency of toxoplasmosis among lung cancer patients (100%) compared to the controls does raise questions as to whether the two observations are linked. Furthermore, lung toxoplasmosis is not common among immunocompetent individuals (de Souza Giassi et al., 2014a), which supports the idea that *T. gondii* infection in these lung cancer patients could be due to their immunocompromised status which might be generated by the lung cancer. Furthermore, several types of cancer are documented to induce immunomodulatory effects on the cancerous tissue (Franklin et al., 2014). Moreover, since systemic *T. gondii* infection stimulates a long-term defect in the function and generation of naive T-lymphocytes, *T. gondii* infection could additionally be creating an environment of immunosuppression by affecting thymic related T-cell activity (Canessa et al., 1992; Kugler et al., 2016).

There is no doubt that toxoplasmosis is a life-threatening opportunistic infection in patients with lung cancer and with the high frequency observed in this study, many lung cancer patients could be at risk of developing toxoplasmosis. Early identification of *T. gondii* infection among lung cancer patients followed by adequate treatment of toxoplasmosis could help perhaps reduce symptoms, improve life quality and increase survival rate as well as contribute to the control of this disease. Clearly, further research is necessary to detect the linkage between *T. gondii* and lung tumours, as well as explore the mechanism of action.

It is still unclear how these lung cancer patients have become infected with *T. gondii* and what the reasons are behind their susceptibility, and many aspects need to be addressed. We aim to further evaluate the relationship between lung cancer and *T. gondii* infection by conducting more experiments on lung cancer samples as well as control samples. A good approach to achieve this would be to investigate the reasons behind what makes the humans host sensitive/susceptible. Previous research (Li et al., 2012; Zhao et al., 2013a; Gao et al., 2015) in mice and rats, suggests that host genes such as iNOS and Arginase might be associated with host resistance and susceptibility. This notion is further strengthened by studies in rats where peritoneal macrophages are resistant to *T. gondii* and expresses high levels of iNOS while alveolar macrophages are

sensitive and express low iNOS levels. Possible approaches could be, is to investigate *T. gondii* parasite distribution in lung tissues using histology on tissue sections by conducting double immunofluorescence and/or IHC staining of macrophages for both genes iNOS and Arg-1 and colocalise the expression of these two host genes (spatial gene expression) in relation to *T. gondii* parasite. Such an approach could aid in gaining a better understanding of the way the human host reacts to *T. gondii* infection and gain a better knowledge of lung toxoplasmosis.

In conclusion, although, it is still unclear what the dynamics between iNOS and Arg-1 are in determining susceptibility/sensitivity to *T. gondii* infection in the human host. Nevertheless, these types of studies may shed light on how we might understand the relationship between lung cancer and *T. gondii* infection.

Chapter 4: The establishment and optimisation of immunohistochemistry and immunofluorescence techniques to detect *Toxoplasma gondii* infection and the expression of the Arginase-1 and Inducible Nitric Oxide Synthase (iNOS) genes in human lung tissue

4.1 Introduction

The aims of this chapter were to develop and optimise immunohistochemistry (IHC) approach for detection of expression of the Arginase (Arg-1) and Inducible Nitric Oxide Synthase (iNOS) genes and infection with *Toxoplasma gondii*. In addition, to this, the aim was to establish and optimise an immunofluorescence (IF) protocol that could be used on lung cancer clinical samples for the purpose of conducting co-localisation analyses of infection with *T. gondii* and expression of the Arginase 1 and iNOS genes. In previous studies conducted on mice and rats, it was found that the balance between the level of expression of iNOS and the expression levels of Arg-1 determined the susceptibility/sensitivity to infection with *T. gondii* parasite (virulent RH strain) (Li et al., 2012). In peritoneal macrophages of rats, which are considered naturally resistant to *T. gondii* infection, it was found that the expression of iNOS was high while the expression of Arg-1 was low. On the other hand, mice that are considered naturally sensitive to *T. gondii* infection, Arg-1 expression was high, whereas iNOS expression was low in the peritoneal macrophages. Both iNOS and Arg-1 share the same substrate, L-arginine (Chang et al., 1998) and so these enzymes act antagonistically. We aimed to gain a better understanding as to whether the balance between Arg-1 and iNOS determines susceptibility/sensitivity in the human host. To achieve this, we aimed to develop and optimise both an IHC and an IF protocol to stain the human lung cancer samples and investigate colocaliaation of *T. gondii* in relation to Arg-1 and iNOS expression in tissues collected from a set of lung cancer subjects. As indicated before (Chapter 3), these human lung cancer tissue sections were previously tested for the presence of *T. gondii* infection using nested PCR detection of the five specific *T. gondii* markers B1, SAG1, SAG2 (3' and 5' ends), and SAG3, which showed 100% prevalence. Results were further confirmed by IHC staining with specific anti-*T. gondii* antibodies.

In addition to other animals, studies have shown that iNOS is extensively expressed in the hearts of rats, while Arg-1 is expressed profoundly in rat liver (Maier et al., 1976; Choi et al., 2012). Since a positive control should be a well-characterised sample that contains the antigen of interest, rat heart and liver tissue were used as positive controls and as good tissue models for the optimisation of iNOS and Arg-1 immunohistochemistry/immunofluorescence.

4.1.1 Objectives

1) To establish and optimise an IHC protocol to detect iNOS expression in rat heart tissue.
2) To establish and optimise an IHC protocol to detect Arg-1 expression in rat liver tissue.
3) To evaluate the iNOS and Arg-1 immunohistochemistry on rat lung tissue.
4) To evaluate *T. gondii* immunohistochemistry on *T. gondii* positive control slides.
5) To evaluate Arg1, iNOS and *T. gondii* IHC on human lung cancer tissue samples.
6) To establish and optimise an IF protocol to detect Arg-1 expression in rat liver tissue.
7) To establish and optimise an IF protocol to detect iNOS expression in rat heart tissue.
8) To establish and optimise an IF protocol to detect *T. gondii* on experimentally infected cells with *T. gondii* to be used as controls.
9) To test the double IF protocol to detect *T. gondii* infections and Arg-1 expression on a pilot lung cancer sample.
10) To test the double IF protocol to detect *T. gondii* infection and iNOS expression on a pilot lung cancer sample.

4.2 Methods

Liver, heart and lung tissues from Sprague Dawley rats and were prepared and cut using a into thin slices (5µm) and placed on slides and prepared for staining (as described in Chapter 2). Slides with liver tissue were used to optimise the IHC procedure using a polyclonal antibody targeting Arg-1. On the other hand, slides containing heart tissue were used to optimise an IHC procedure using a polyclonal antibody targeting iNOS. After the successful optimisation, Arg-1 and iNOS IHC protocols were conducted on lung rat tissue. The previously established IHC protocol (Bajnok, 2017; Bajnok et al 2019) targeting the *T. gondii* parasite was conducted on *T. gondii* positive control samples. After that, the Arg-1, iNOS and *T. gondii* IHC protocols were validated on a pilot lung cancer sample. Light microscopy was used to take images of slides. Furthermore, each marker (Arg-1, iNOS and *T. gondii*) was optimised individually to develop a protocol to study colocalisation in lung cancer clinical samples by performing a double IF procedure. IF targeting of Arg-1 expression was optimised on rat liver slides and developed to be used as positive controls, while IF targeting of iNOS expression was optimised on rat heart slides and developed to be used as controls. On the other hand, cultured *T. gondii* infected, and uninfected cells were used to optimise IF targeting of *T. gondii* infection. After full optimisation of the three markers separately, a double IF protocol was optimised and conducted on a pilot lung cancer sample targeting, separately, *T. gondii*/Arg-1 and *T. gondii*/iNOS. Stained tissues were visualised on a fluorescence microscope with each channel (red, iNOS or Arg-1, green, *T. gondii* and DAPI for nuclei of cells). Merged images were constructed using the software and saved as Tiff files.

4.3 Results

4.3.1 Development of Arginase-1 immunohistochemical staining of rat liver tissue

In a normal rat liver, the main structure of the liver comprises the hepatocytes which make up to 80% of the liver structure, and different studies have shown that Arginase-1 is profoundly expressed in rat liver (Choi *et al.*, 2012). This makes it a good tissue to examine to use to develop an immunohistochemistry (IHC) assay for Arg-1. IHC localisation of Arg-1 was performed on paraffin-embedded liver tissue of Sprague Dawley rats. After the completion of the staining procedure, slides were mounted and visualised by light microscopy. Different magnifications were used to analyse the immunostained slides (x400 and x100), and images were taken using Leica software. For the positive control, a primary antibody (anti-Arg-1 antibody) was used. Immunoreactivity was marked by the presence of a specific brown staining. The Arg-1 immunostaining was intense in both the nuclei as well as the cytoplasm of the hepatocytes (Figure 4.1). Negative control slides contained rat liver tissue sections which were stained with the same procedure as the positive control but with the omission of the primary antibody. No brown staining was detected on the negative control slides indicating successful staining of the positive control with Arg-1 antibody and false-positive results caused by non-specific binding of the secondary antibody system were excluded.

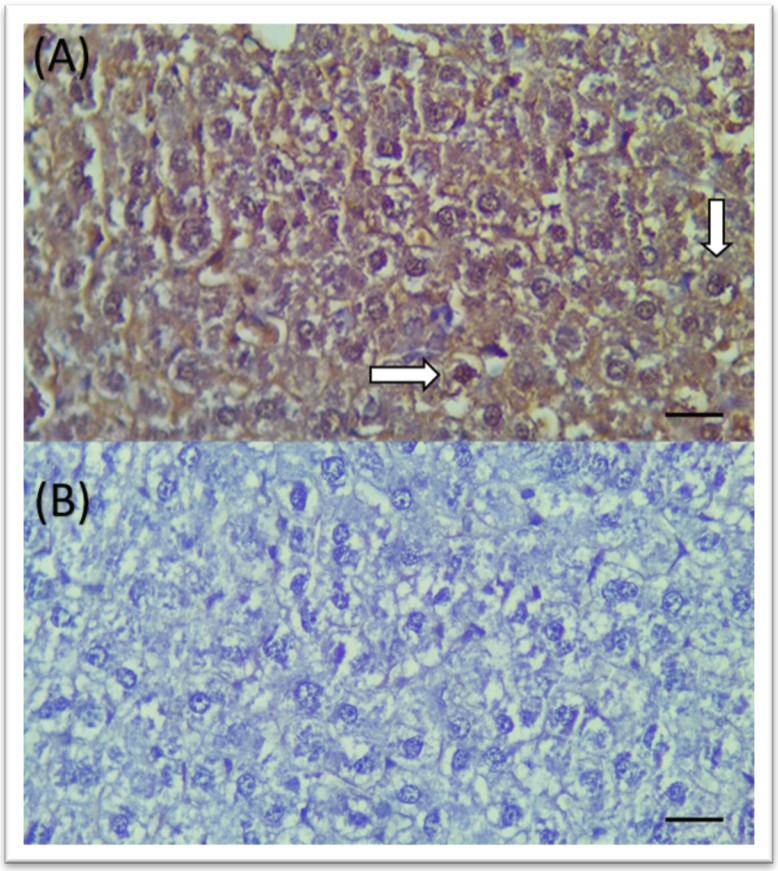

Figure 4.1 Immunohistochemical localisation of Arg-1 of paraffin-embedded liver tissue of Sprague Dawley rats . (A) Positive control of Arg-1 IHC using anti-Arg-1 antibodies, immunoreactivity can be seen (brown staining) in irregularly scattered hepatocytes in both nuclei and cytoplasm (Arrow), image magnification x400. (B) Negative control of the immunohistochemistry staining of Sprague Dawley rat liver with the primary antibody (anti-Arg-1 antibody) omitted to exclude contamination or false-positive result, image magnification x400. Scale bar = 20 μm.

4.3.2 Development of iNOS immunohistochemical staining of rat heart tissue

Immunohistochemical (IHC) staining using the specific iNOS antibody was conducted on paraffin-embedded heart tissue of Sprague Dawley rats. After the staining processes were complete, slides were visualised by light microscopy. A brown staining was observed in the positive control slide, which indicates successful staining of heart tissue with iNOS antibody. A negative control slide was used to exclude false-positive staining or contamination. Negative control slides were rat heart tissue sections that were stained exactly like the positive control

except for the incubation with the primary antibody, which was omitted (Figure 4.2). Immunoreactivity can be observed located at the vascular smooth muscle as well as the cardiac myocytes, which are elongated cylindrical cells with a single nucleus.

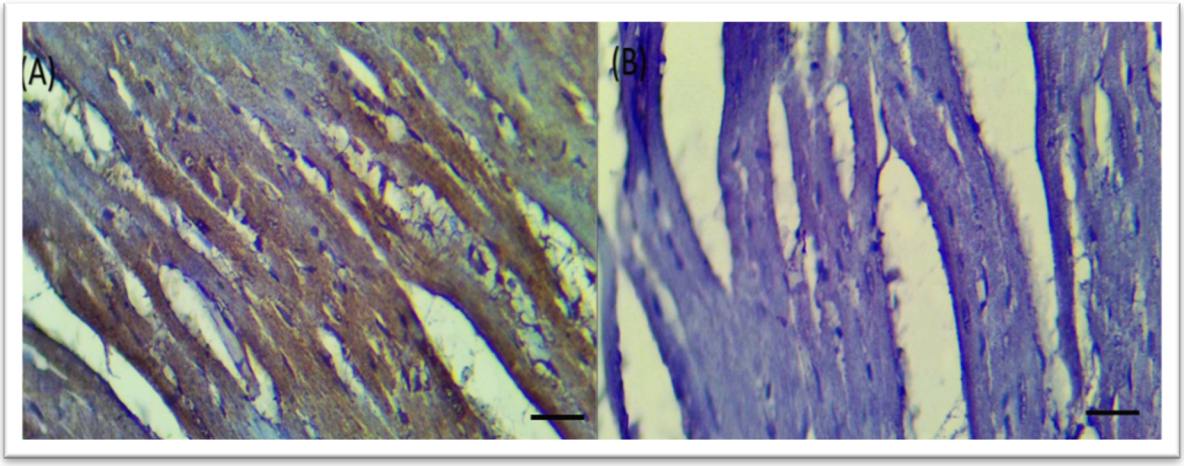

Figure 4.2 Immunohistochemical staining of iNOS on paraffin-embedded heart tissue of Sprague Dawley rat tissue . (A) Positive control of iNOS IHC using anti-iNOS antibodies. iNOS immune-reactivity can be observed in vascular smooth muscles and cardiac myocytes, image magnification x400. (B) Negative control, no immunohistochemical staining was detected in tissue sections in the absence of primary antibody, image magnification x400. Scale bar = 20 µm.

4.3.3 iNOS and Arg-1 IHC on rat lung tissue

After the IHC staining protocols of both iNOS and Arg-1 were optimised on paraffin-embedded liver and heart tissue of Sprague Dawley rats, and successful staining was achieved for both iNOS and Arg-1 expression, the protocols were used to localise iNOS and Arg-1 in rat lung tissue.

After the appropriate tissue preparation, paraffin-embedded rat lung tissue of Sprague Dawley rats was stained separately with the iNOS and Arg-1 antibodies. Light microscopy was used to visualise stained slides and images of different fields of view were taken.

Immunoreactivity was observed in slides stained with an anti iNOS antibody which was marked by the specific brown staining of the lung tissue. The iNOS localisation was observed mainly on

the cell linings, the bronchiole and the ciliated columnar epithelium (Figure 4.3). On the other hand, the negative control slides, which are rat lung tissue stained without the primary antibody (anti-iNOS antibody), did not show any brown staining confirming the successful staining and excluding false-positive immunoreactivity. The Arg-1 immunoreactivity was localised to the cells lining the bronchiole as well (Figure 4.4), while the negative control which was rat lung tissue section without the primary antibody, did not show any specific brown staining thus excluding contamination or false-positive results.

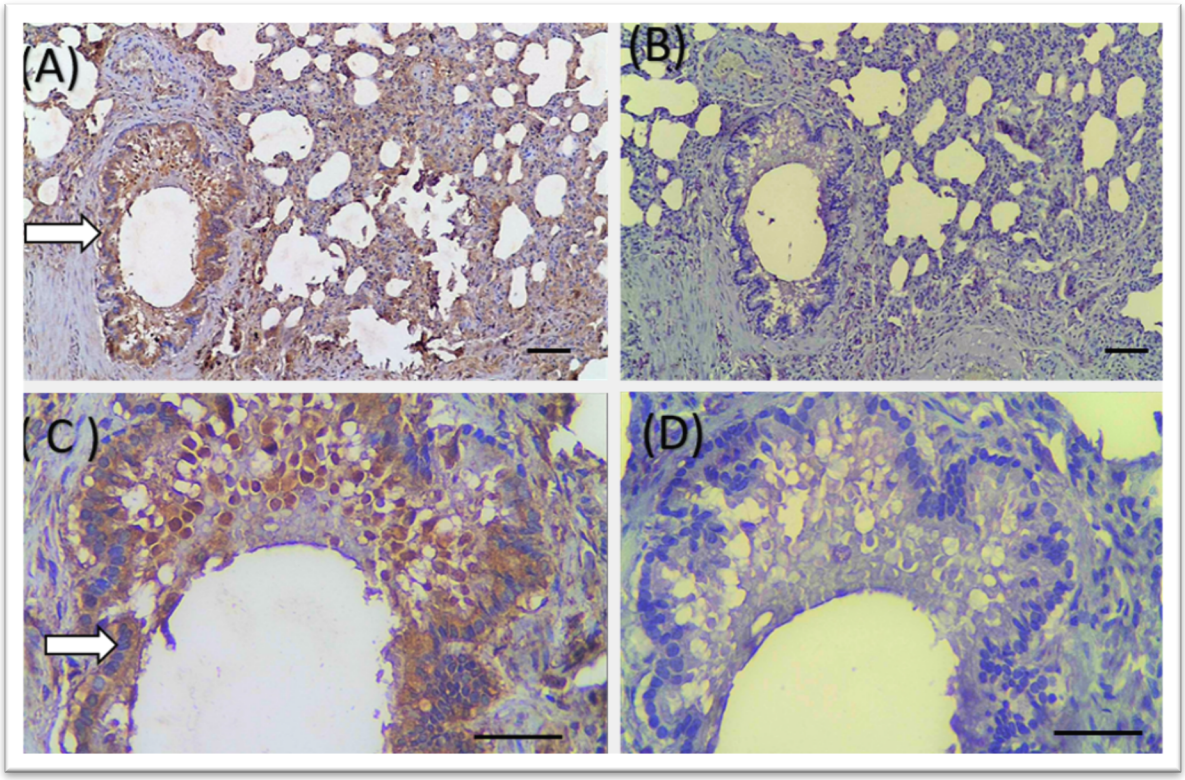

Figure 4.3 Immunohistochemical localisation of iNOS in paraffin-embedded lung tissue from Sprague Dawley rats **.** (A) Strong iNOS immunoreactivity was localised to bronchial epithelial cells (arrow) (x100 magnification). (B) Negative control of the lung sample: no staining is observed in negative control where the primary antibody is omitted, image magnification x100 (C) A higher magnification of the same slide with a clearer view of the stained lining of the bronchiole, image magnification x400 (D) higher magnification, (x400) of the negative control with the absence of iNOS staining. Scale bar = 20 µm.

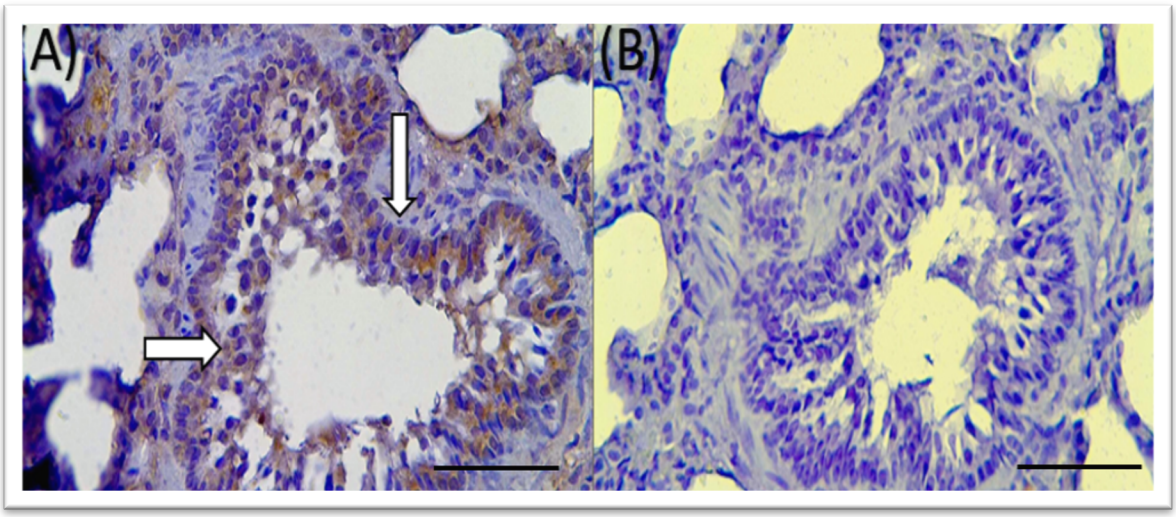

Figure 4.4 Immunohistochemistry of Sprague Dawley rat lung tissue stained with anti-Arg-1 antibodies . (A) Positive control shows successful staining (brown stain) of the lining of the bronchiole (ciliated columnar epithelium) showing high expression of Arg-1 in these cells (arrows), Image magnification x400. (B) Negative control, rat lung tissue with the primary antibody omitted, was conducted to ensure the absence of contamination. Image magnification x400. Scale bar = 20 µm.

4.3.4 Comparison of the use of the Pre-treatment (PT) module preparation method with the microwave heat method for antigen retrieval

Antigen retrieval is a rather simple laboratory technique, which is conducted to unmask the epitopes produced by the process of tissue fixation, either by heat (heat-induced epitope retrieval, HIER) or enzymatic degradation (proteolytic induced epitope retrieval, PIER) or through a combination of both approaches, which is infrequently used (Shi et al., 1991).

Initially, the microwave was used as a heating method for antigen retrieval, as suggested in various protocols. Using this approach, it has been noticed that the appearance of the morphology of the tissue was not optimal, especially when using the higher magnification of microscopy. Moreover, with microwave use, there is a need to make sure that the tissue slides are not overheated by frequently pausing the microwave; otherwise, tissue destruction is possible. We decided to try the PT Module (pre-treatment module) available in our lab, which by using gentle heat claims to offer consistent antigen retrieval results. Furthermore, with the precise temperature control, it has the advantage of maintaining the integrity of delicate tissue without the damaging effects of

temperature variations caused using the microwave method. To evaluate which is the best method of antigen retrieval, an IHC test was conducted on one of the trial lung cancer samples by using the microwave as an antigen retrieval method and using the same sample but with the PT Module, (Figure 4.5 and 4.6). With the microwave method, although that the IHC targeting iNOS was successful (Figure 4.5A) it was evident that there was a uniform brownish colour compared to the PT Module sample (Figure 4.5B), where the staining can be seen precisely to specific parts of the tissue. In addition, it was highly evident, especially with the higher magnification that the detailed architecture of the tissue was preserved much better (Figure 4.6B). While when using the microwave, the loss of the detailed morphology is obvious (Figure 4.6A). Based on these results, the PT Module was used in the subsequent IHC procedures, and the use of microwave as a heat method for antigen retrieval was discontinued.

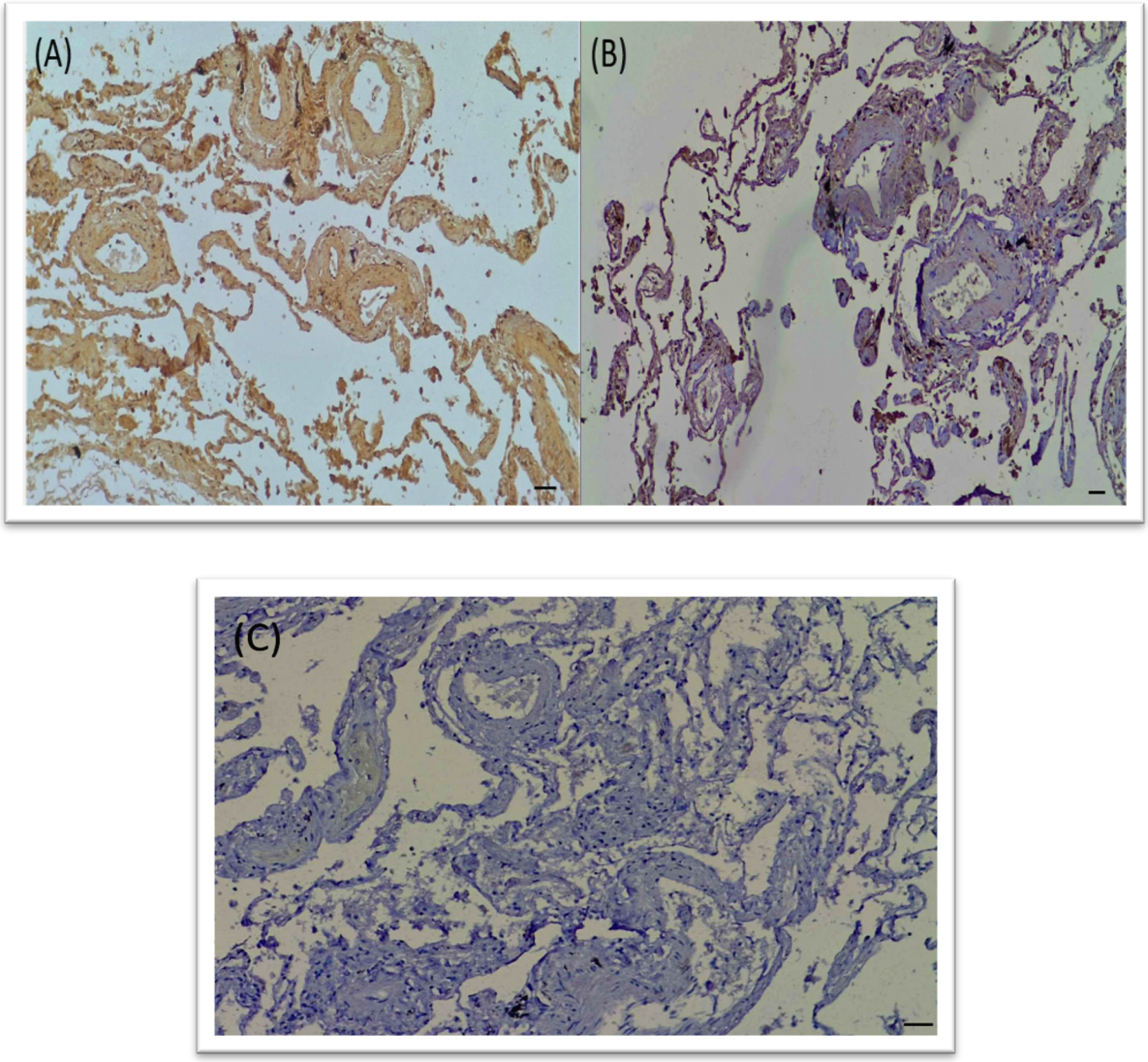

Figure 4.5 a comparative image of IHC of the same lung tissue sample performed with (A) the microwave used as an HIER method. A brown colour can be identified throughout the tissue giving a "microwave burn" pattern. Whereas (B) the PT module was used as the HIER technique, a more specific and settled staining is evident with the absence of the patchy burned appearance. Image magnification x100. (C) is the negative control. Scale bar = 20 μm.

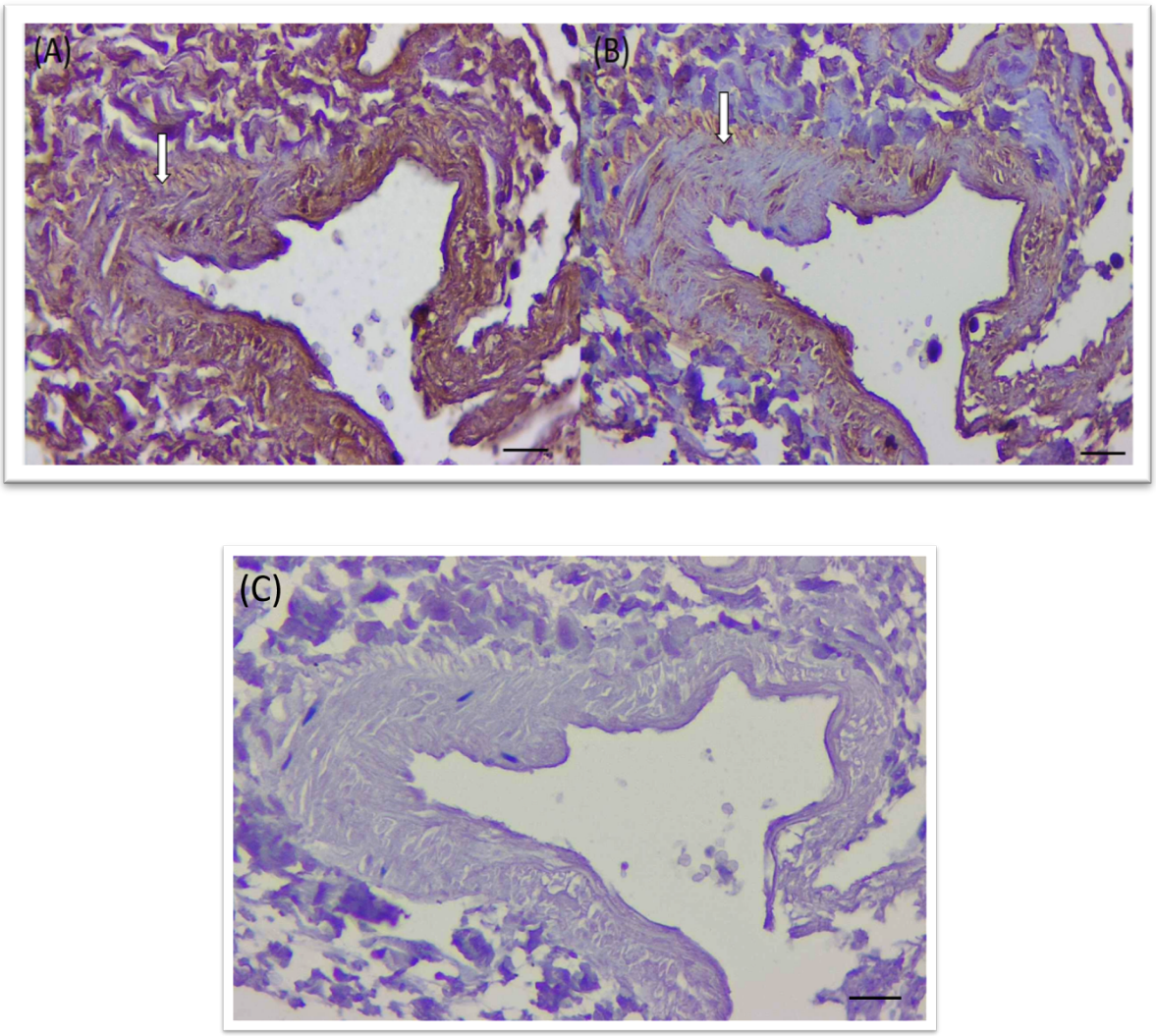

Figure 4.6 images showing different antigen retrieval methods (A) when using the microwave as a method for antigen retrieval could result in a level of loss of the normal architecture of the tissue (arrow). Whereas when using the PT module (B), it helps to preserve the architecture of the tissue, where a better presentation of the histology is evident (arrow), which will in result help in getting a better understanding of which tissue is expressing our protein of interest. Image magnification x400. (C) is the negative control. Scale bar = 20 µm

4.3.5 Optimisation and modification of microtome sectioning and tissue thickness

The lung tissue is considered one of the most difficult types of tissue to process with a microtome, and that is attributed to the nature of the anatomy of the lungs containing alveoli, holes and cavities resulting in structurally fragile tissue. A thickness of 7 µm was used to cut the tissue. However,

when visualising the slides under the microscope subsequent to IHC staining, the resultant images were somewhat blurry, and a satisfactory focus was hard to achieve for the entire field of view (Figure 4.7.A). Moreover, the staining quality was not optimal, as areas of background staining can be noticed (Figure 4.7.A). In order to ensure that the best quality images can be achieved, the lung tissue thickness cuts were lowered to from 7 to 5 μm as the recommended thickness of tissue section for IHC is mostly 4-5μm (Kim et al., 2016). After following a more robust approach in tissue sectioning with the microtome (see Chapter 2), the quality of images, as well as the staining, were enhanced (Figure 4.7.B). The areas of blurriness were no longer apparent, and a uniformed focus is achieved. Moreover, in addition to the better overall lung tissue architecture observed, the IHC staining is much more localised to tissue without background staining (Figure 4.7.B).

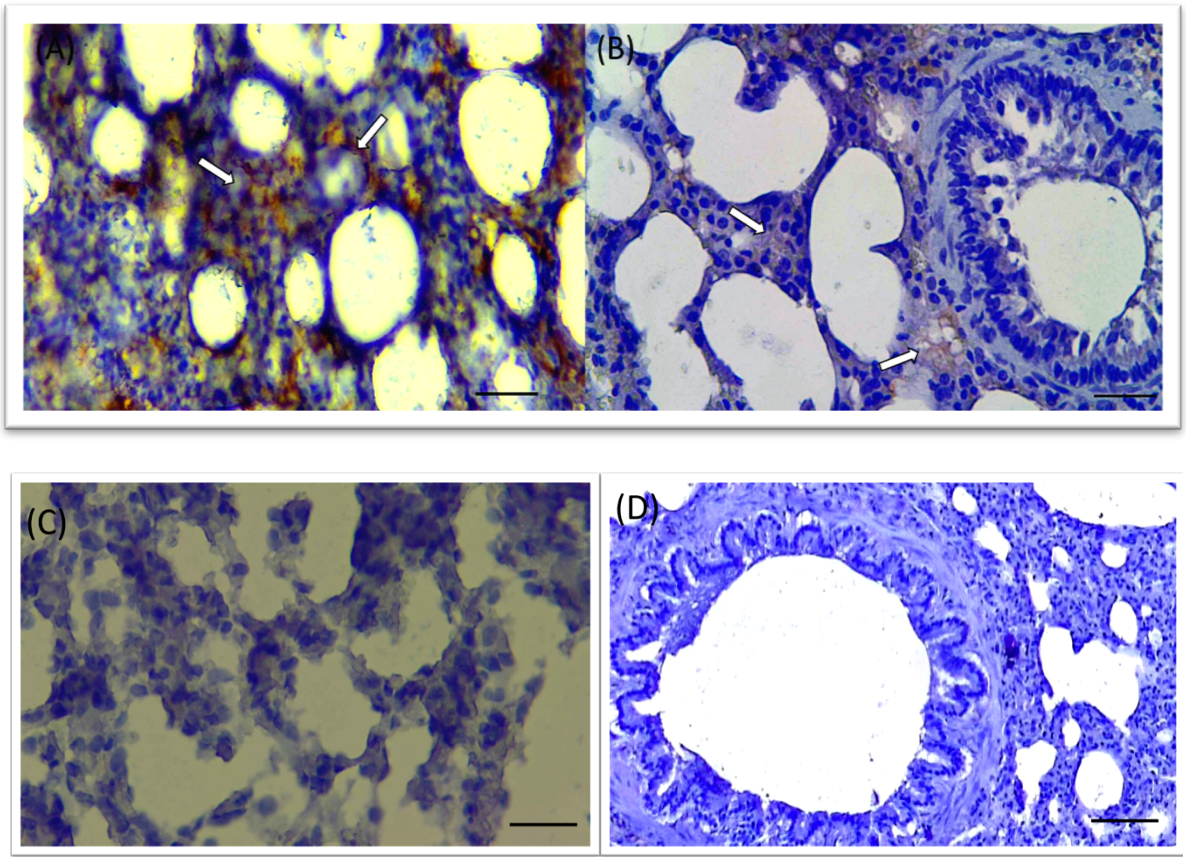

Figure 4.7 A comparative image of IHC of lung tissue stained with primary antibody targeting iNOS . (A) areas of blurriness, as well as background staining (arrows), is evident, image magnification x400. (B) lung tissue cuts were modified from 7 µm to 5 µm, the image obtained after staining shows better detail of the lung structure as well as an ability to achieve satisfactory focus. The quality of staining is also enhanced with much more localised staining (arrows) and the absence of background staining. Image magnification x400. (C) is the negative control of the 7 µm sample, and (D) is the negative control of the 5 µm sample. Image magnification x400, scale bar = 20 µm.

4.3.6 *T. gondii* immunohistochemistry on *T. gondii* positive control slides

A previously used IHC protocol (Bajnok, 2017; Bajnok et al 2019), targeting *T. gondii* to confirm positive infection, was used on commercially *T. gondii* positive control slides of mice liver, to ensure specificity. A polyclonal anti-*T. gondii* antibody was used to stain the control slides. A brownish colour indicates positive immunoreactivity. Stained slides were visualised by light microscopy and images collected. As shown in (Figure 4.8), two different stages of the parasite

could be identified: free tachyzoites (Figure 4.8.A) as well as, the dormant stage of the parasite (Figure 4.8.B), the *T. gondii* cyst.

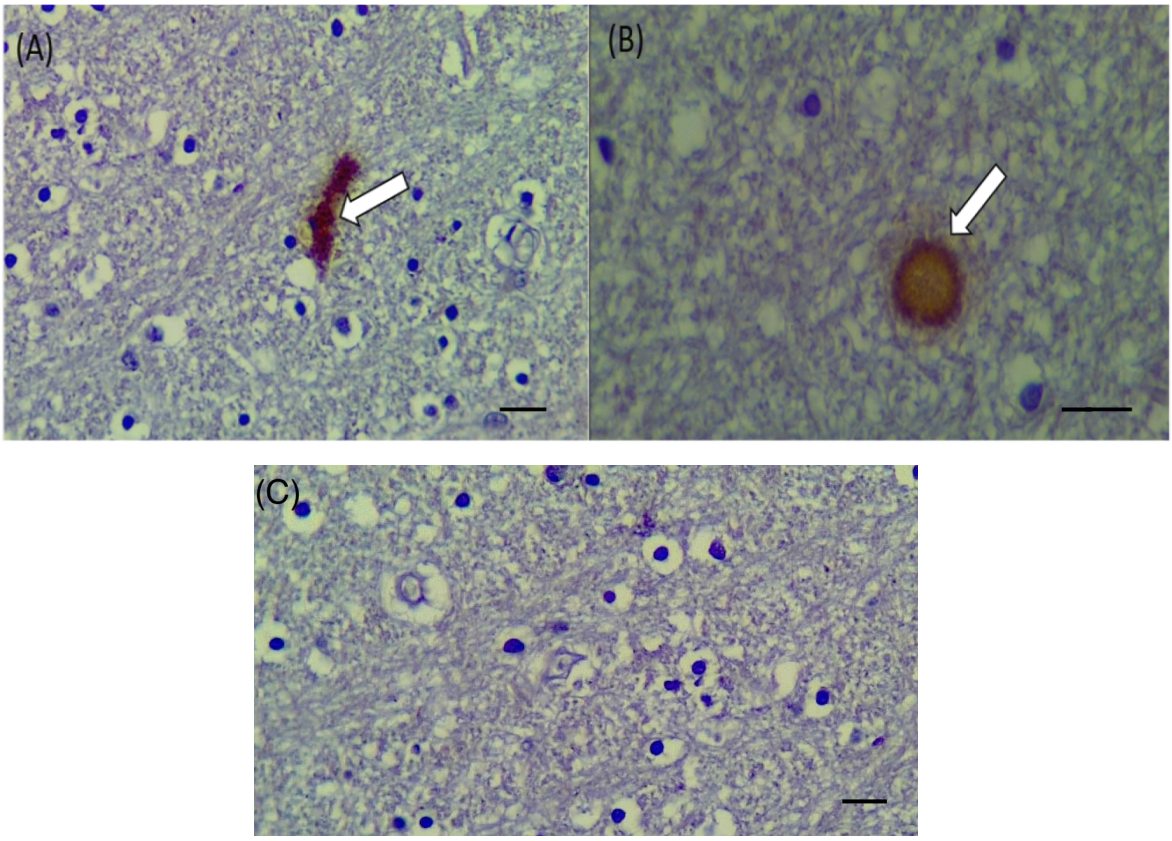

Figure 4.8 *T. gondii* positive control slides of mice liver tissue stained with polyclonal rabbit anti- *T. gondii* antibodies. (A) brownish staining can be observed (arrow) indicating the presence of tachyzoites, image magnification x400. (B) is showcasing a characteristic cyst stage of the parasite (arrow), 1mage magnification x1000. (C) is the negative control, image magnification x400.

4.3.7 Immunohistochemistry of iNOS, Arg-1 and *T. gondii* in lung cancer clinical samples

Following the optimisation of the iNOS and Arg-1 immunohistochemistry protocols on paraffin-embedded rat tissue (heart, liver and lung), the protocols were tested on a lung cancer sample (1004), which has previously tested positive for *T. gondii* infection by nested PCR targeting five specific *T. gondii* parasite markers (B1, SAG1, SAG2 3′, SAG2 5′ and SAG3) and by

immunohistochemistry using anti-*T. gondii* antibodies (Bajnok, 2017; Bajnok et al 2019). The same clinical sample (1004) was used to immunostain iNOS, Arg-1 and *T. gondii*. When cutting the paraffin-embedded lung cancer sample, it was performed in a serial manner as much as possible to ensure that the same field of view could be analysed for all three targets of immunohistochemistry (iNOS, Arg-1 and *T. gondii*).

The lung cancer sample was cut into 5 μm thin slices and prepared for immunohistochemistry staining using iNOS, Arg-1 and anti-*T. gondii* antibodies (see Chapter 2). Rat heart tissue was used as a positive control for iNOS immunostaining, whereas rat liver tissue slides were used as positive controls for Arg-1 immunostaining. Lung cancer tissue samples were used with the exclusion of primary antibodies as negative controls.

For immunolocalisation of iNOS, immune reactivity was marked by a specific brown staining which was observed mainly in the lining of the bronchiole, which is made of ciliated columnar epithelium cells, and to a lesser extent inside the lumen of the bronchiole (Figure 4.9.C). The negative control, which is the lung sample slides without the primary antibody (anti-iNOS antibody), failed to show any staining (Figure 4.9.D). Moreover, the same sample was tested with immunohistochemistry targeting Arg-1, immune-reactivity was not as intense as the staining with iNOS and was present faintly in the lining of the bronchiole as well as in the lumen (Figure 4.9.E). The negative control sample, which was the same lung sample without the primary antibody (anti-Arg-1 antibody), did not show any brown staining and thus excluded non-specific staining (Figure 4.9.F). For the immunohistochemistry to detect *T. gondii* infection, immunoreactivity was observed inside the lumen of the bronchiole, but unlike iNOS and Arg-1 immunohistochemistry results, no staining was observed at the ciliated columnar epithelium lining the lumen (Figure 4.9.A). The negative control was the same lung sample with the primary antibody (anti-*T. gondii* antibody) omitted, and it did not exhibit any specific brown staining confirming the successful staining and excluded contamination or false-positive results (Figure 4.9.B).

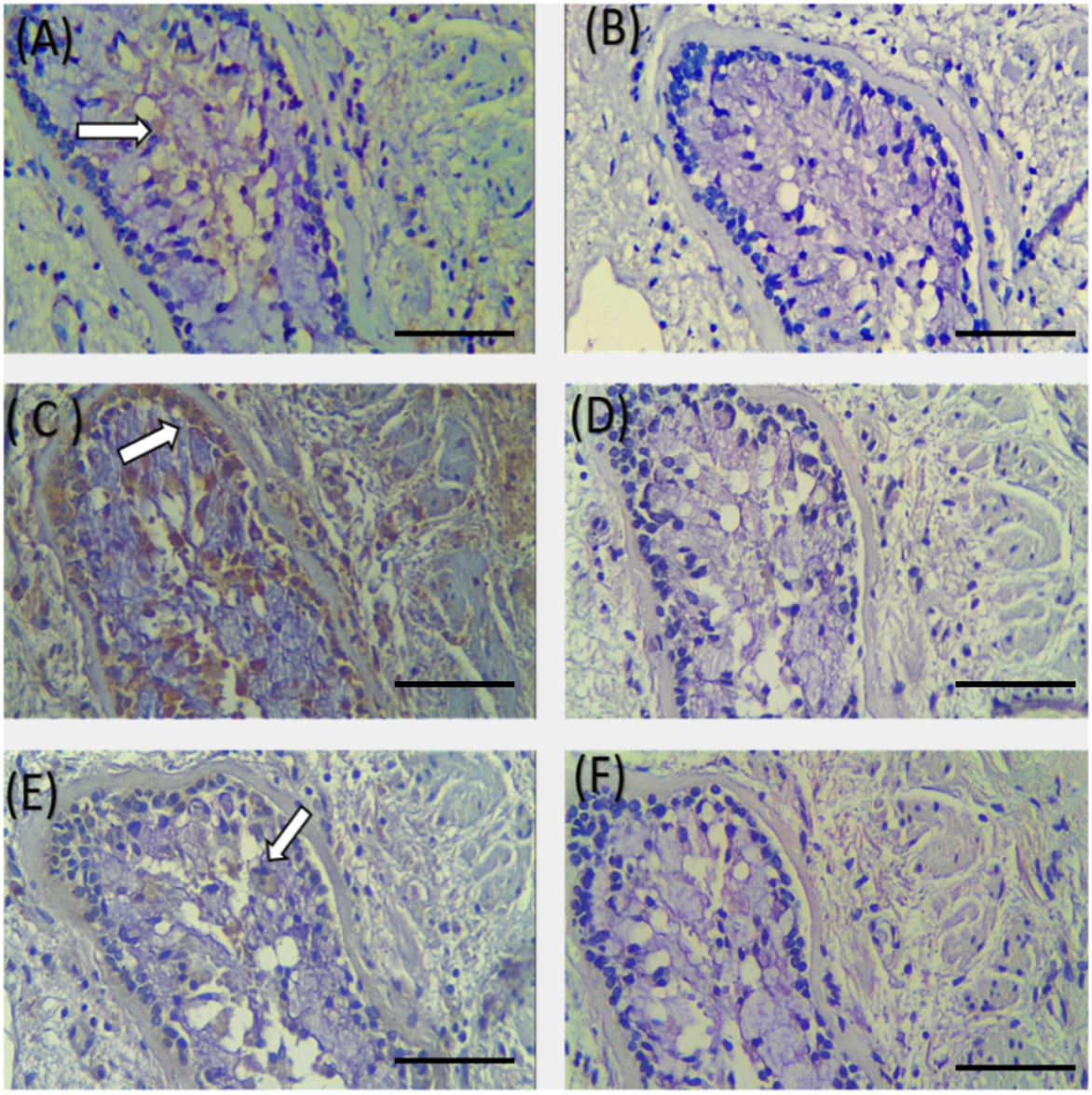

Figure 4.9 Immunohistochemical localisation of *T. gondii*, iNOS and Arg-1 in a lung cancer clinical sample (1004) (x400 magnification). (A) Immunohistochemistry using anti-*T. gondii* antibodies, brown staining indicating positive *T. gondii* infection can be observed inside the lumen of the bronchiole (arrow), while the negative control (B) showed no staining of *T. gondii* excluding false-positive results. (C) Immunohistochemical staining of iNOS, brown staining appeared to be intense in the ciliated columnar epithelium cells that are lining the lumen of the bronchiole (arrow) as well inside the lumen. (D) Negative control of iNOS staining with no apparent colour. (E) Immunohistochemical localisation of arg-1 on the lung cancer clinical sample, staining can be seen (arrow) inside the lumen of the bronchiole while the negative control (F) shows no sign of any staining. Scale bar = 20 µm.

4.3.8 Optimisation of iNOS, Arg-1 and *T. gondii* Immunofluorescence

Although immunohistochemistry is a well-established and informative procedure, it still has its own drawbacks (Brandtzaeg, 1998) especially whenever there is a need to observe two or more different types of sub-cellular structures simultaneously, immunofluorescence is usually a preferred option (van der Loos, 2009; Isidro et al., 2015). Moreover, the overlapping and combined fluorescence formed by colocalised targets is much easier to identify than overlapping IHC staining. To understand the dynamics between *T. gondii* infection and lung cancer, we have established and optimised a double immunofluorescence protocol to colocalise *T. gondii* infection in relation to either Arg-1 or iNOS in the same sample. As a start, each immunofluorescence protocol (Arg-1, iNOS and *T. gondii*) was optimised individually.

4.3.9 Colour combination selection for double immunofluorescence

A key factor in the success of a double immunofluorescence procedure is the accurate colour combination selection. When selecting fluorophores, the excitation and emission spectra must be carefully considered (Isidro et al., 2015). Overlapping ranges of excitation may lead to false-positive results as both fluorophores are triggered with the same light wavelength. In the same manner, overlapping emission spectra might make it difficult to differentiate unique probes. An important factor that must be considered is the Stokes shift, which is a phenomenon resulting in the emission of light at longer wavelength than the absorbed light (Jameson et al., 2003). The presence of considerable Stokes shift is mainly important for practical applications of fluorescence as it allows to separate (strong) excitation light from (weak) emitted fluorescence using appropriate optics (Jameson et al., 2003). With many types of dyes available in the research field, Alexa Fluor provides dyes with spectra that cover the entire visible range, but more importantly, these dyes and their conjugates haven been documented to be brighter and more photostable than the other analogues which are commonly used (Panchuk-Voloshina et al., 1999). Furthermore, Alexa dyes have been proven to be insensitive to pH in the 4–10 range (Panchuk-Voloshina et al., 1999). With respect to the need of choosing two colour combination which produces the best contrast between both individual colours and a relatively distinguishable mixed-colour at sites of colocalisation, without one of the two individual colours overwhelming the other, as the resultant mixed colour might be very faint or even missed (van der Loos, 2009). Hence, we

have selected Alexa Fluor 488 (green) and Alexa Fluor 594 (red) to be used for our double immunofluorescence protocol (Figure 4.10). The combination of red and green for double staining studies has been chosen by the majority of researchers (Isidro et al., 2015). Due to the high contrast between the two individual colours with a resultant yellowish colour at the site of overlap or colocalisation making it easy to identify. Finally, the blue-fluorescent DNA stain 4′,6-diamidino-2-phenylindole (DAPI), was used to counterstain the nuclei of cells.

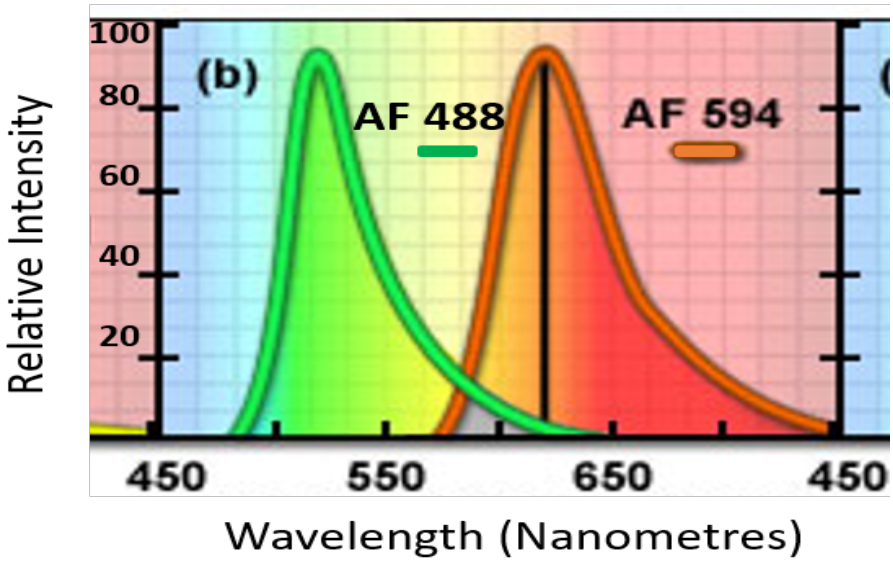

Figure 4.10 Spectral overlap in paired Alexa Fluor probes . Alexa Fluor 488 and fluorescent Alexa Fluor 594 demonstrate a low level of overlap. Both dyes are easily distinguishable to the human eye, and the low degree of spectral overlap should yield good results with minimal bleed-through in dual-labelling experiments, provided the concentrations of each probe are similar in the specimen.

4.3.10 Arg-1 Immunofluorescence on rat liver tissue

After the selection of the appropriate colour combination, as a start, each immunofluorescence protocol was optimised on its own. Since it is documented that Arg-1 is abundantly expressed in rat liver tissue (Choi et al., 2012), immunofluorescence targeting Arg-1 was optimised on tissue slides of rat liver, and these were also to be used as a positive control for Arg-1 immunofluorescence when testing the lung cancer clinical samples. After completion of the staining processes, slides were visualised by fluorescent microscopy. The channels were viewed

individually, and then a merged image was constructed by the software. Further confirming the previous results obtained by IHC targeting Arg-1, the same expected pattern of expression was obtained with immunofluorescence (Figure 4.11). Immunoreactivity was abundant in the liver cytoplasm as well as the nuclei of the hepatocytes.

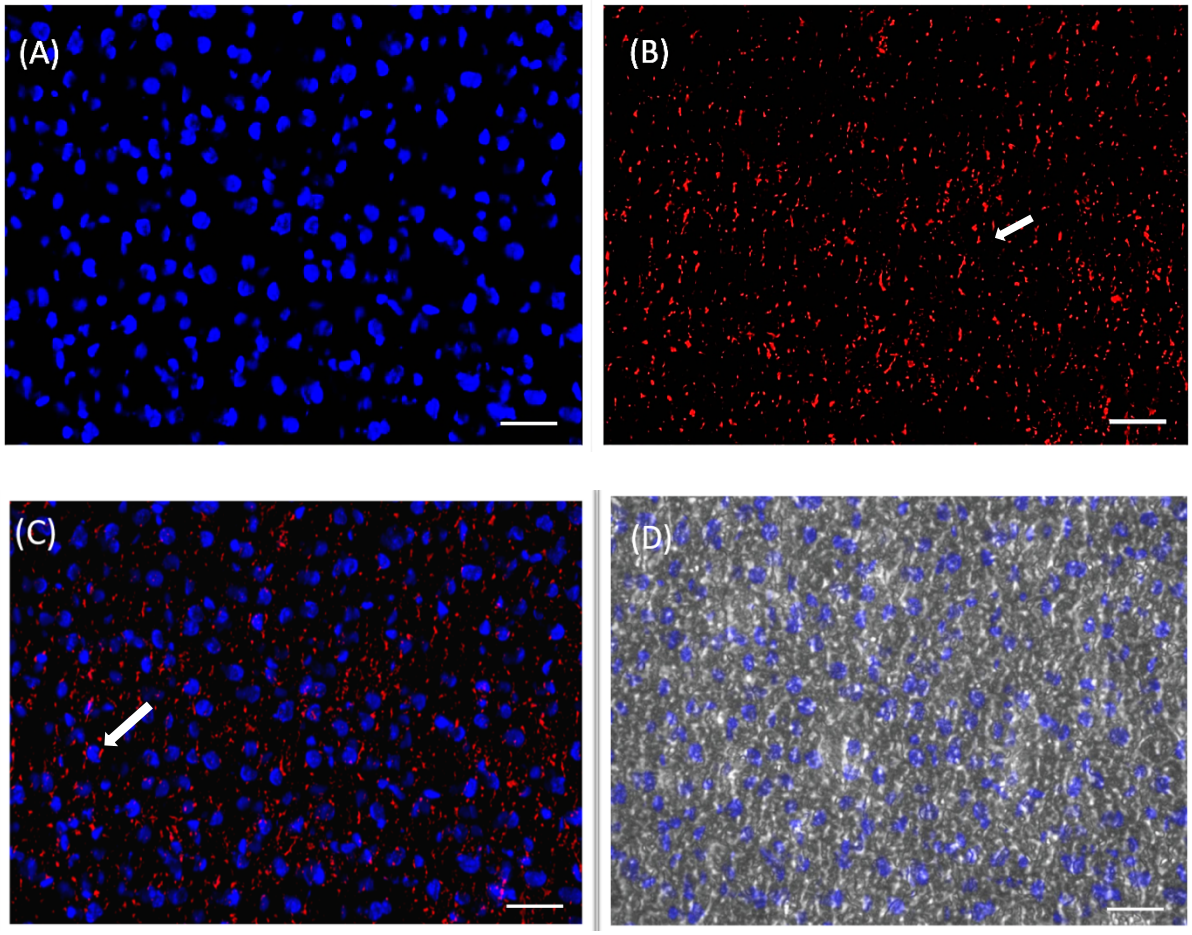

Figure 4.11 Immunofluorescence localisation of Arg-1 of paraffin-embedded liver tissue from Sprague Dawley rats . (A) DAPI staining of the hepatocyte nuclei. (B) Alexa Fluor 594 (red) of Arg-1, (C) merged DAPI and Arg-1, immunoreactivity can be seen (red colour) at the irregularly scattered hepatocytes in both nuclei and cytoplasm (arrow). (D) is the negative control. Image magnification x400. Scale bar = 20 μm.

4.3.11 iNOS Immunofluorescence on rat heart tissue

In order to establish and optimise immunofluorescence targeting iNOS and to be used later as a positive control for the iNOS marker, rat heart tissue slides were used. Stained slides were visualised by fluorescent microscopy with each channel viewed individually, and then the software was used to merge the images together. As previously documented with IHC, iNOS is expressed profoundly in rat heart tissue, and the pattern of expression mimics that of the results obtained by iNOS IHC of rat heart tissue (Figure 4.12). Immunoreactivity was observed within the vascular smooth muscle cells and the cardiac myocytes.

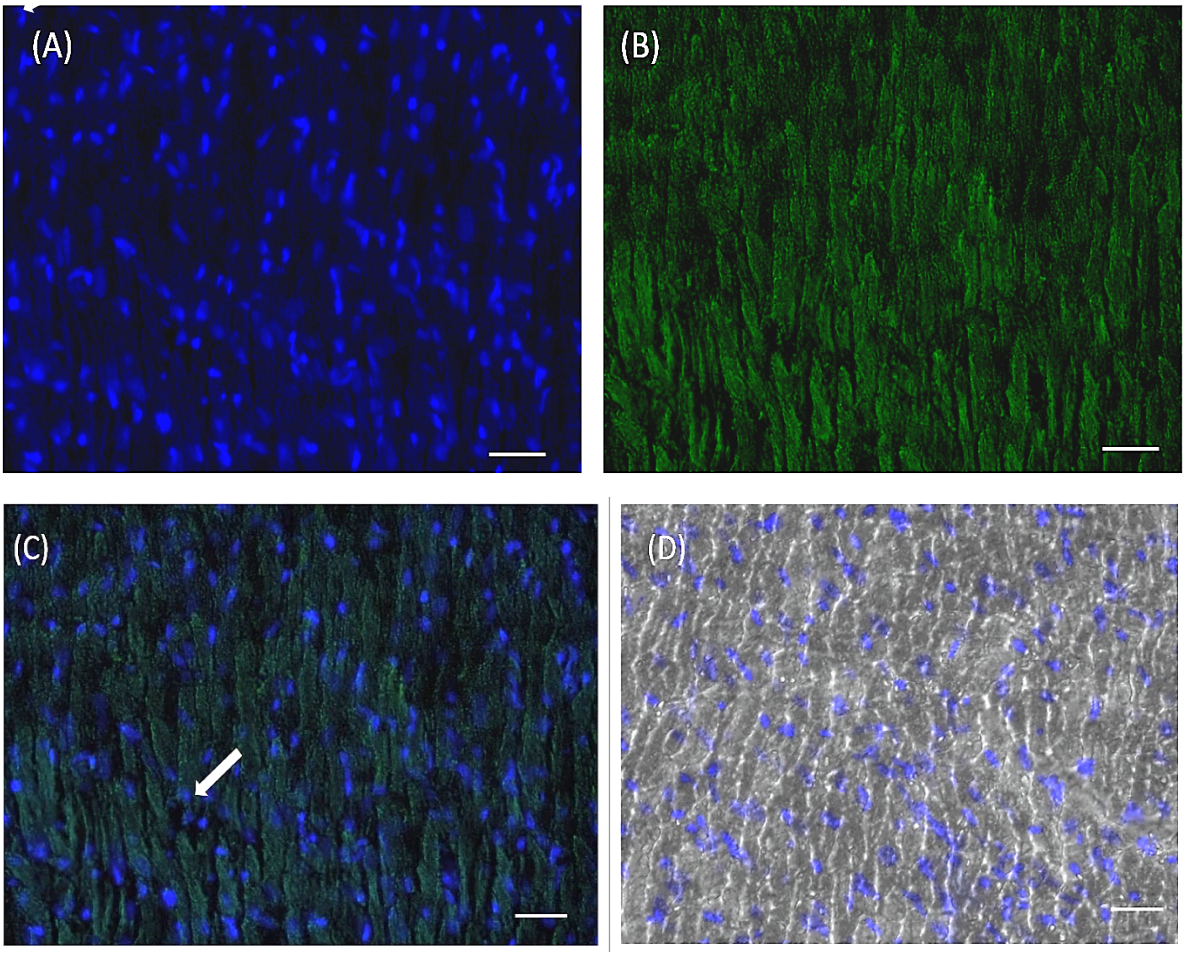

Figure 4.12 Immunofluorescence localisation of iNOS of paraffin-embedded heart tissue from Sprague Dawley rats . (A) DAPI staining of the nuclei. (B) Alexa Fluor 488 (green) of iNOS, (C) merged DAPI and iNOS, immunoreactivity can be seen (green colour) the cardiac myocytes (arrow). (D) is the negative control. Image magnification x400. Scale bar = 20 µm.

4.3.12 Immunofluorescence of *T. gondii* infected and uninfected cells

Human brain cells (SH-SY5Y) were cultured and infected with *T. gondii* (type1-RHΔKU8) by Bader Alawfi, a fellow colleague, to test them with the anti-*T. gondii* antibody, and to be used as a positive control for *T. gondii* when testing the lung cancer clinical samples. Furthermore, uninfected bovine brain cells were also cultured to be used as a negative control. After the cells were stained using anti-*T. gondii* antibodies, cells were visualised by fluorescent microscopy. While each channel was viewed individually, a merged image of the two channels was later constructed by the software. Human brain cells were successfully infected and showed positive immunoreactivity to *T. gondii* antibodies (Figure 4.13 A, B and C). *T. gondii* can be seen inside the brain cell (green) adjacent to the cell nucleus (blue) confirming the success of the immunofluorescent targeting of the *T. gondii* parasite. On the other hand, a culture of the same human cells but uninfected were also stained with *T. gondii* antibodies to ensure specificity of the protocol and to be used later as a negative control (Figure 4.13 E and F). No *T. gondii* staining can be observed with the uninfected cells where only the nucleus (DAPI) was positively stained.

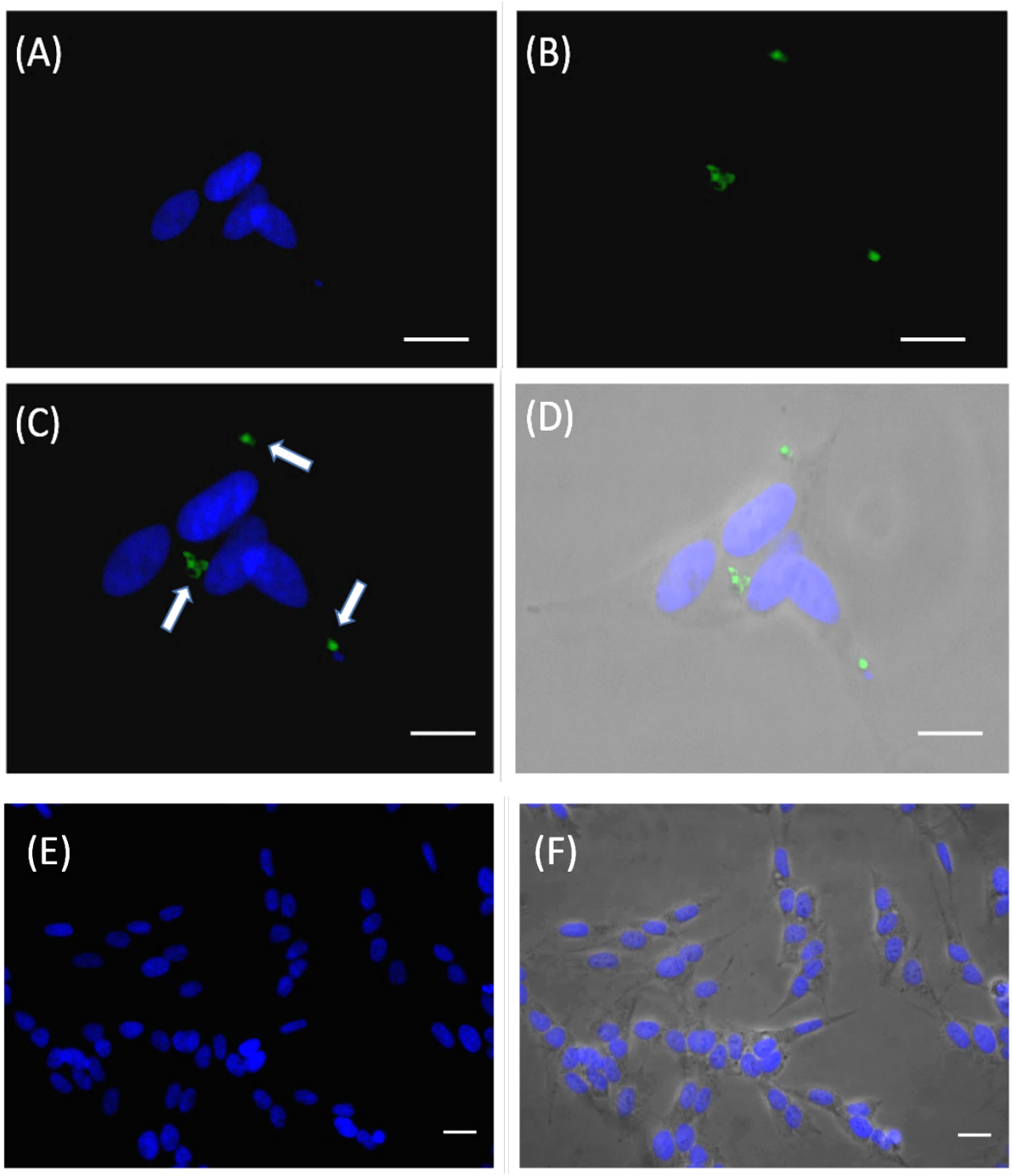

Figure 4.13 Immunofluorescence localisation of *T. gondii* in cultured human brain cells (SH-SY5Y) infected with *T. gondii* . (A) DAPI staining of the nuclei. (B) Alexa Fluor 488 (green) of *T. gondii*, (C) merged *T. gondii* and DAPI. *T. gondii* infection can be seen inside the brain cells (arrows). (D) is an overlay of the merged image of DAPI and *T. gondii* on a black and white image of the brain cells. Image magnification x400. (E) localisation of *T. gondii* on uninfected cultured bovine brain cells (SH-SY5Y) with DAPI staining of the nuclei. (F) an overlay of the merged image of DAPI and *T. gondii* (negative) on a black and white image of the brain cells. Image magnification x200. Scale bar = 20 µm.

4.3.13 Arg-1 immunofluorescence on lung cancer samples

After the immunofluorescence protocols were established on rat tissue and *T. gondii* infected cells, each marker was tested on a trial lung cancer sample. Immunofluorescence targeting Arg-1 was conducted on lung cancer samples and images were taken by fluorescence microscopy for each channel individually and then were superimposed by the software. Successful staining was achieved as positive Arg-1 immunoreactivity was observed at specific areas of the lungs (alveolar walls), (Figure 4.14) A full description of the pattern of expression of Arg-1 in lung cancer clinical samples will be discussed in chapter 5. Negative slides were the same lung cancer sample stained in the same way, but the primary antibody (Arg-1) was omitted.

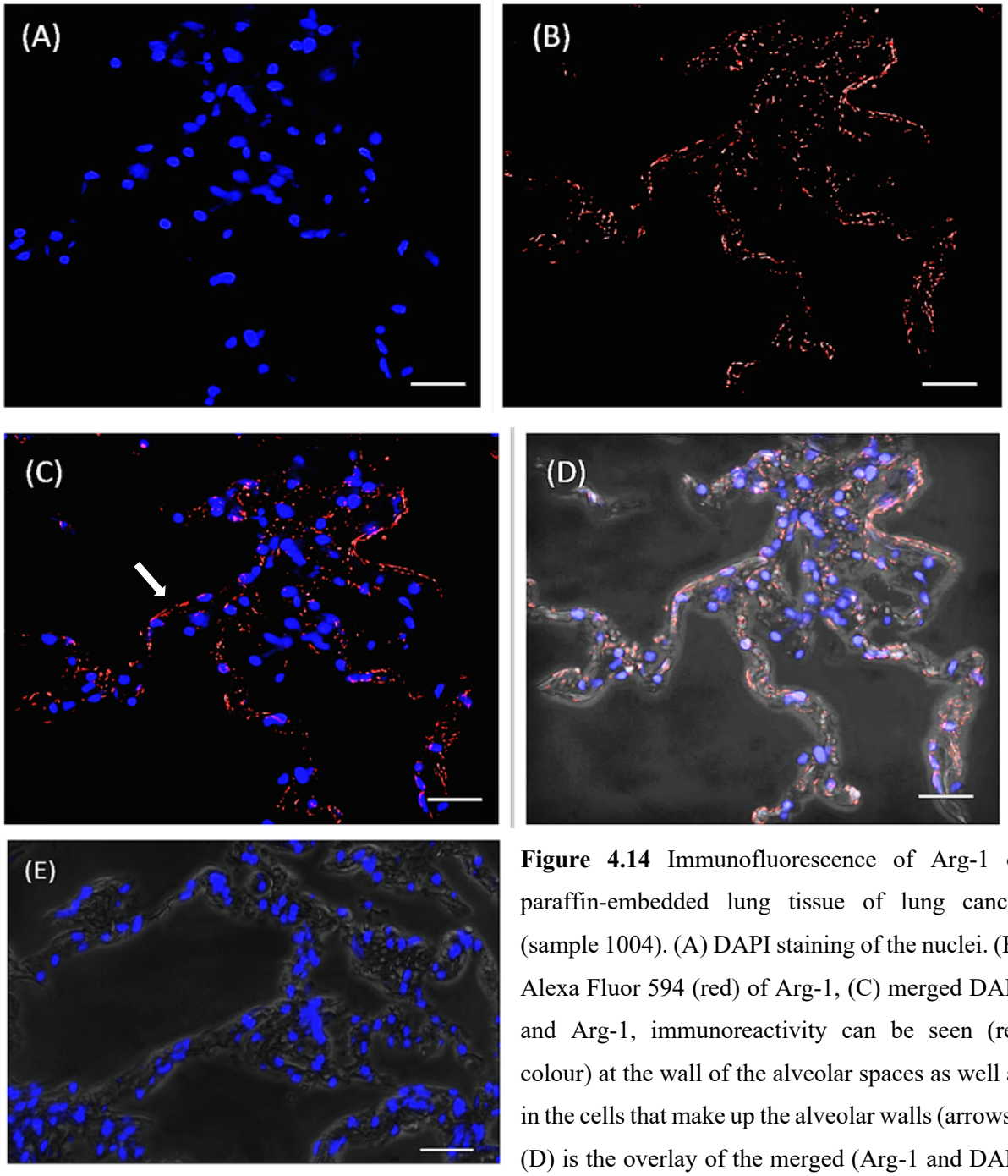

Figure 4.14 Immunofluorescence of Arg-1 of paraffin-embedded lung tissue of lung cancer (sample 1004). (A) DAPI staining of the nuclei. (B) Alexa Fluor 594 (red) of Arg-1, (C) merged DAPI and Arg-1, immunoreactivity can be seen (red colour) at the wall of the alveolar spaces as well as in the cells that make up the alveolar walls (arrows). (D) is the overlay of the merged (Arg-1 and DAPI stains) on a black and white image of the tissue. (E) is the negative control. Image magnification x400. Scale bar = 20 µm.

4.3.14 iNOS immunofluorescence on lung cancer samples

Before attempting to conduct double immunofluorescence analysis on lung cancer clinical samples, immunofluorescence protocol targeting iNOS alone was used to stain a trial lung cancer sample (1004). After the staining process was achieved, images were taken by fluorescent microscopy for each channel independently and then the software was used to overlay images. Positive immunoreactivity was observed in lung tissue (Figure 4.15). For a full description on tissue types expressing iNOS, please refer to chapter 5. Negative slides were the same lung cancer sample stained in the same way, but the primary antibody (iNOS) was omitted.

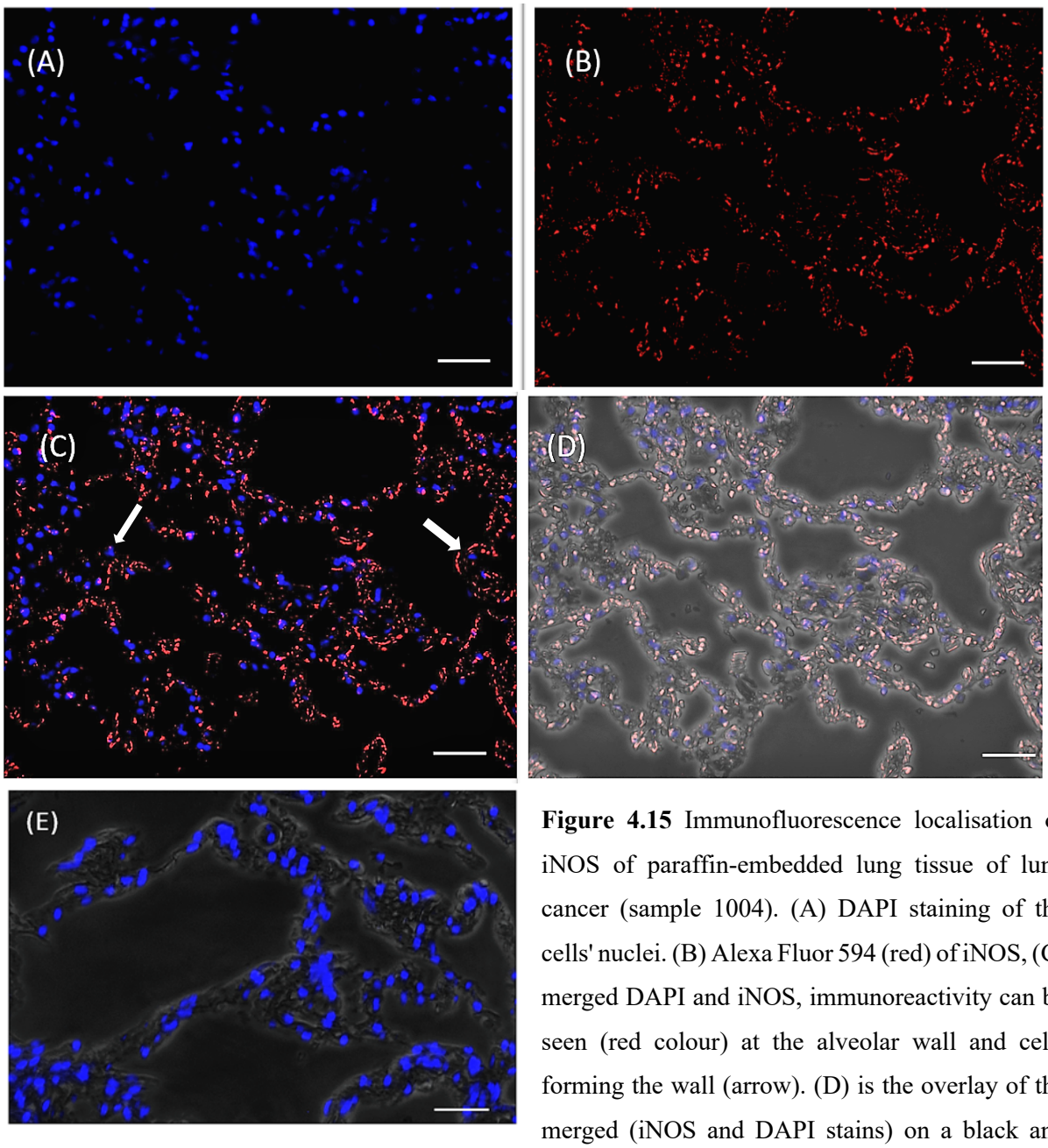

Figure 4.15 Immunofluorescence localisation of iNOS of paraffin-embedded lung tissue of lung cancer (sample 1004). (A) DAPI staining of the cells' nuclei. (B) Alexa Fluor 594 (red) of iNOS, (C) merged DAPI and iNOS, immunoreactivity can be seen (red colour) at the alveolar wall and cells forming the wall (arrow). (D) is the overlay of the merged (iNOS and DAPI stains) on a black and white image of the tissue. (E) is the negative control. Image magnification x400. Scale bar = 20 µm.

4.3.15 *T. gondii* immunofluorescence on lung cancer samples

As part of the aim to establish a double immunofluorescence protocol to colocalise *T. gondii* and Arg-1/iNOS, the immunofluorescence targeting *T. gondii* was conducted, on its own, on a trial lung cancer slide (sample 1004). After the staining process was accomplished, the slides were visualised by fluorescent microscopy with a merged image constructed after each channel was visualised separately. Negative control slides were the same lung cancer sample stained in the same way, but the primary antibody (*T. gondii*) was omitted. Immunoreactivity can be seen in the alveolar wall compartment of the lung, indicating positive *T. gondii* infection (Figure 4.16). A full descriptive analysis of the localisation of *T. gondii* in the lungs is described in chapter 5.

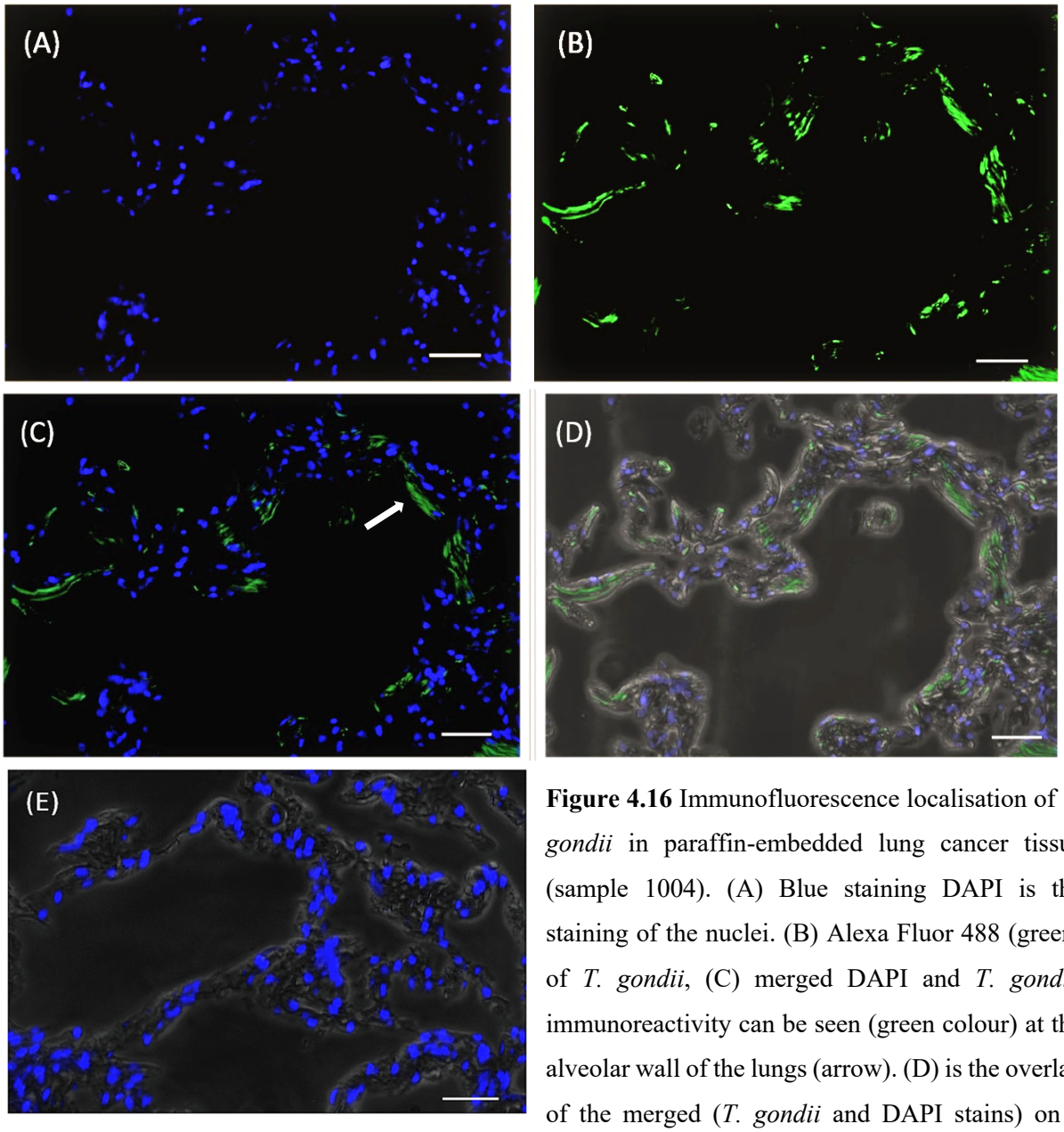

Figure 4.16 Immunofluorescence localisation of *T. gondii* in paraffin-embedded lung cancer tissue (sample 1004). (A) Blue staining DAPI is the staining of the nuclei. (B) Alexa Fluor 488 (green) of *T. gondii*, (C) merged DAPI and *T. gondii*, immunoreactivity can be seen (green colour) at the alveolar wall of the lungs (arrow). (D) is the overlay of the merged (*T. gondii* and DAPI stains) on a black and white image of the tissue. (E) is the negative control. Image magnification x400. Scale bar = 20 µm.

4.3.16 Double Immunofluorescence on a lung cancer trial sample targeting both *T. gondii* and Arg-1.

Once each protocol was established individually (Arg-1, iNOS and *T. gondii*), double immunofluorescence was developed on a trial lung cancer clinical sample to colocalise Arg-1 in relation to *T. gondii* infection Similarly this approach was developed to assay colocalisation between iNOS and *T. gondii* infection in the lung cancer clinical samples. As a start, a double immunofluorescence protocol targeting *T. gondii*/Arg-1 was conducted. Special measures were taken to ensure that no cross-reactivity between the antibodies will take place (see chapter 2). After the full process of immunofluorescence, staining was completed. Slides were left to dry and visualised the following day by fluorescence microscopy. Each channel (green, red and DAPI) was visualised independently, and the merged images were later constructed using the software. Colocalisation can be observed in the blood vessels of the lungs (Figure 4.17) with both *T. gondii* and well as Arg-1 being expressed in various levels of the blood vessel.

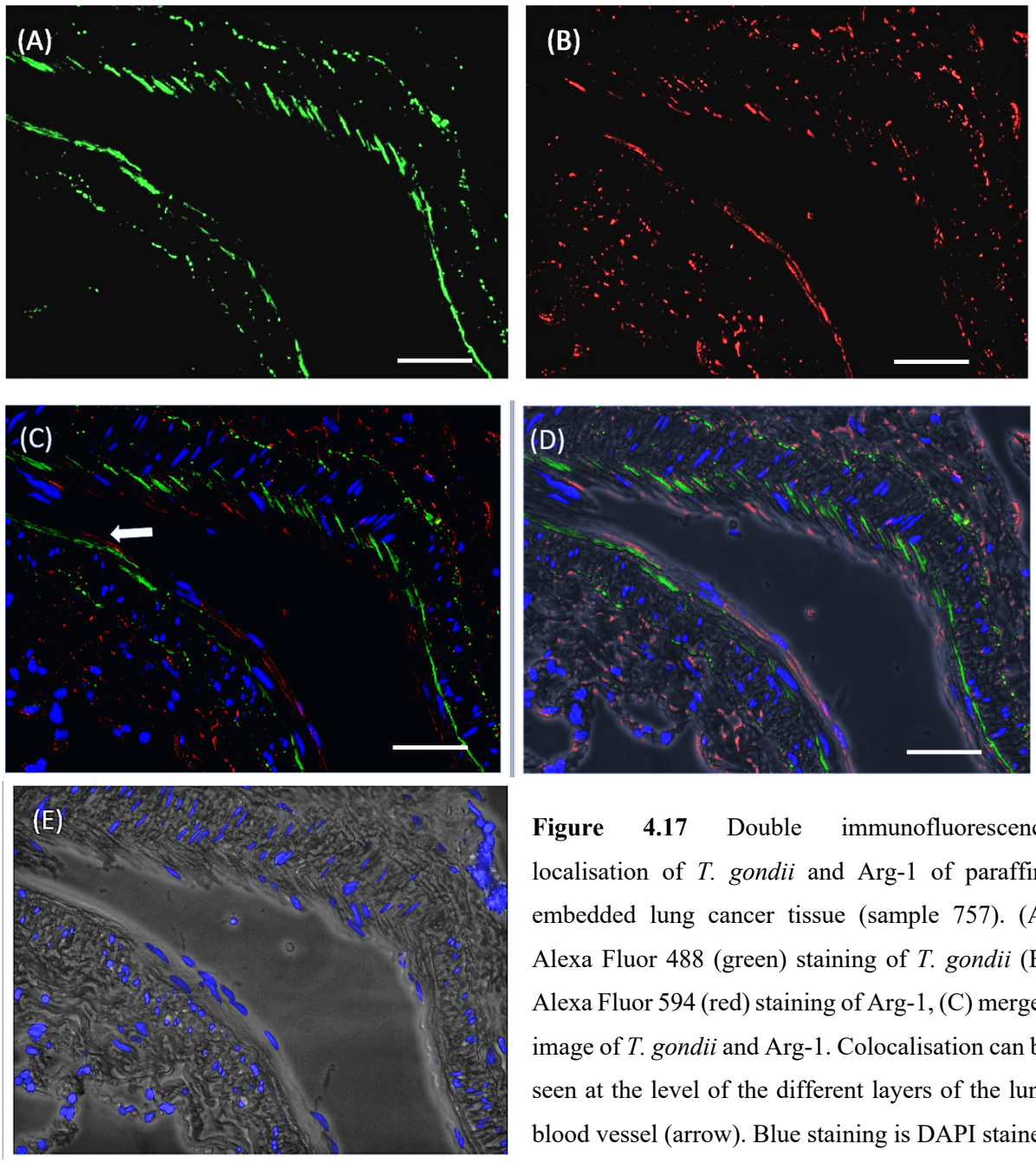

Figure 4.17 Double immunofluorescence localisation of *T. gondii* and Arg-1 of paraffin-embedded lung cancer tissue (sample 757). (A) Alexa Fluor 488 (green) staining of *T. gondii* (B) Alexa Fluor 594 (red) staining of Arg-1, (C) merged image of *T. gondii* and Arg-1. Colocalisation can be seen at the level of the different layers of the lung blood vessel (arrow). Blue staining is DAPI stained cell nuclei. (D) is the overlay of the merged (*T. gondii*, Arg-1 and DAPI stains) on a black and white image of the tissue. (E) is the negative control. Image magnification x400. Scale bar = 20 µm.

4.3.17 Double Immunofluorescence on a lung cancer trial sample targeting *T. gondii* and iNOS

For the purpose of colocalisation analysis, a double immunofluorescence targeting *T. gondii* and iNOS was conducted on the same lung cancer clinical sample (757) in which the double immunofluorescence of Arg-1 and *T. gondii* was conducted. To avoid cross-reactivity between the two antibodies, special measures have been taken (refer to chapter 2). Furthermore, after the staining procedure was accomplished and the slides were allowed to dry, slides were observed by fluorescent microscopy with every channel viewed independently, and the merged images were later formed using the software. Colocalisation of *T. gondii* and iNOS can be observed in the blood vessels of the lungs (Figure 4.18) with both *T. gondii* and well as iNOS being expressed in the different layers of the blood vessel.

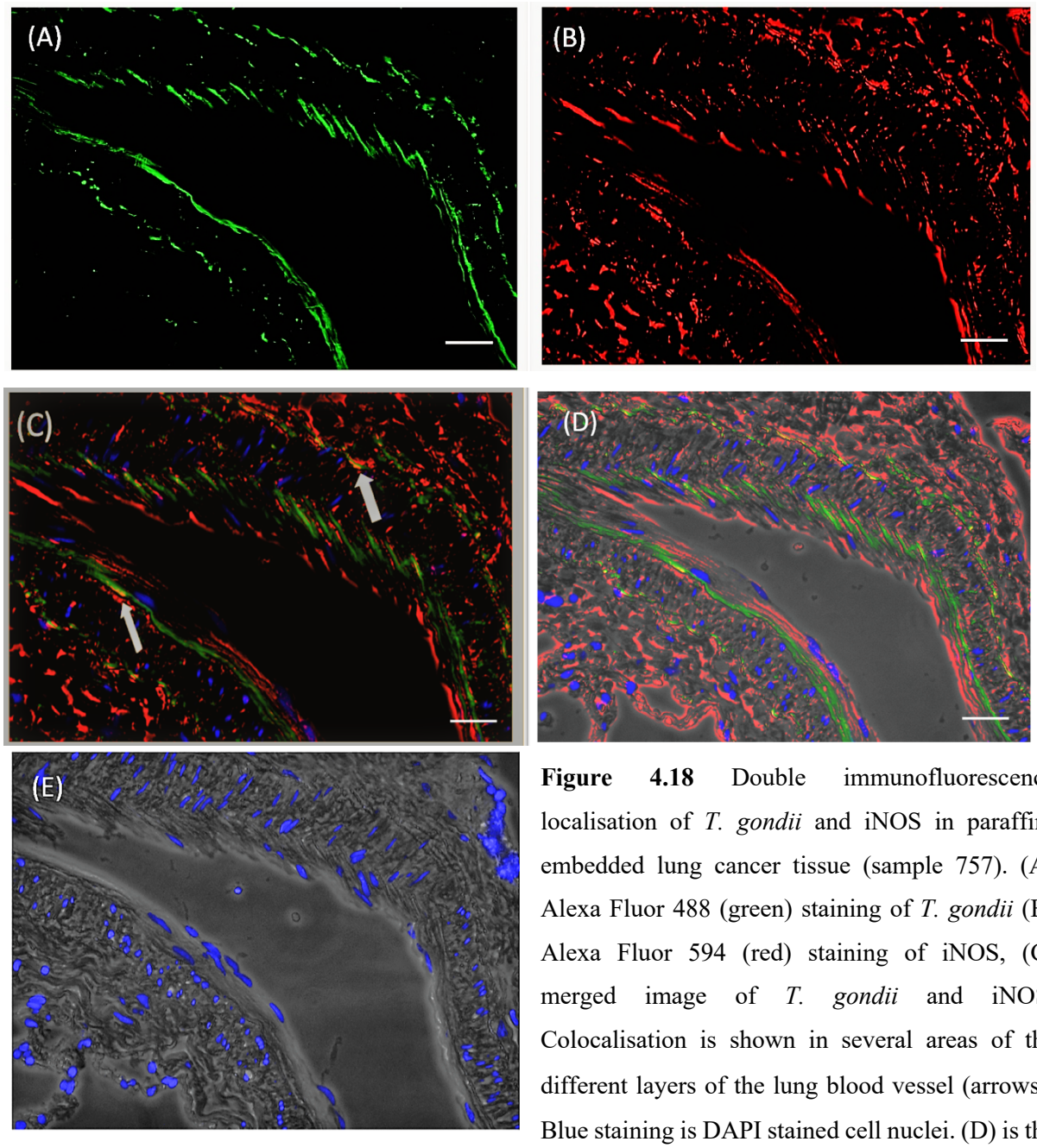

Figure 4.18 Double immunofluorescence localisation of *T. gondii* and iNOS in paraffin-embedded lung cancer tissue (sample 757). (A) Alexa Fluor 488 (green) staining of *T. gondii* (B) Alexa Fluor 594 (red) staining of iNOS, (C) merged image of *T. gondii* and iNOS. Colocalisation is shown in several areas of the different layers of the lung blood vessel (arrows). Blue staining is DAPI stained cell nuclei. (D) is the overlay of the merged (*T. gondii*, iNOS and DAPI stains) on a black and white image of the tissue. (E) is the negative control. Image magnification x400. Scale bar = 20 µm.

4.4 Discussion

In conclusion, we were able to establish and optimise an IHC protocol to identify the expression pattern of Arg-1 on rat liver paraffin-embedded tissue which showed high arg-1 expression in the hepatocytes as well as in the nucleus. IHC of iNOS on rat heart tissue was evident mainly in the cardiac myocytes. Furthermore, Arg-1 and iNOS IHC were tested on rat lung paraffin-embedded tissue which showed Arg-1 and iNOS expression in the bronchial epithelial cells but with stronger expression for the iNOS than the Arginase. On the other hand, the immunohistochemistry used in the previously used lung cancer clinical samples study (Bajnok et al., 2019), was tested on *T. gondii* positive control slides showing positive *T. gondii* staining of tachyzoites as well as *T. gondii* cysts.

Furthermore, in aiming to conduct the colocalisation analysis, we have established and optimised an immunofluorescence protocol that targets Arg-1, iNOS on rat liver and heart tissue respectively, which further confirmed the results obtained by IHC. The *T. gondii* immunofluorescence protocol was tested on *T. gondii* infected cells which showed positive staining of the *T. gondii* inside the human cultured brain cells. Each marker was then tested individually on lung cancer trial samples which showed expression of Arg-1 and iNOS in the alveolar wall of the lungs as well as positive infection with *T. gondii*. Finally, once each marker (Arg-1, iNOS and *T. gondii*) was optimised separately, a double immunofluorescence protocol was conducted targeting *T. gondii*/Arg-1 and *T. gondii*/iNOS on preliminary lung cancer tissue trial samples which displayed colocalisation of *T. gondii* and Arg-1 as well as *T. gondii* and iNOS in the tissue surrounding the lung blood vessels.

The discovery that high-temperature heating or strong alkaline treatment can reverse cross-linkages has formed the basis for the development of antigen retrieval techniques in 1991(Shi et al., 2001). The introduction of this technique has sparked a revolution throughout pathology practice and immunohistochemical research (Shi et al., 2001). For the first time, the observation of a wide variety of portions in formalin-fixed, paraffin-embedded (FFPE)-tissues has become possible (Shi et al., 2001).

The main principle of an antigen retrieval treatment is to eliminate the protein cross-links formed by the formalin fixation process. This procedure enables the antigens that are difficult or

impossible to stain to become more easily stainable by standardised immunohistochemical methods.

In this chapter, we have tested more than one heat method for antigen retrieval and have illustrated that previously tested protocols are not necessarily optimal, since the microwave method, when used, has been shown to exert a degree of damage to the tissue as well affected the end results of the staining pattern. Unfortunately, excessive tissue microwaving can result in the destruction of tissue antigenicity and morphology (Kim et al., 2016). Moreover, it may lead to the production of HIER lipofuscin, which is the appearance of fine yellow-brown pigment granules composed of lipid-containing residues which are artefacts of lysosomal breakdown (Kim et al., 2016). When using HIER, a "microwave burn" pattern can occur in loose connective tissue and fat.

On the other hand, when using the PT Module for antigen retrieval, the tissue was found to be better preserved in its morphology and therefore offering a more consistent and less damaging approach for fragile tissue (Gray et al., 2006). With the automated nature of the PT Module, we were able to achieve standardisation of antigen retrieval throughout the process as well as ensuring that a larger number of slides can be processed at the same time. Moreover, in this chapter, our results obtained by IHC on rat tissue (liver and heart) was further confirmed by the results obtained by IF on liver and heart rat tissue for Arg-1 and iNOS respectively, adding to the reliability and the specificity of the protocol we have used.

We could not obtain positive *T. gondii* slides to be used as positive controls for the IF procedure, instead cultured *T. gondii* infected cells were used. *T. gondii* infected cells have shown positive staining, which confirms that the antibody used to detect the *T. gondii* parasite is efficient and has produced reliable results. However, it would have been better to use the same type of tissue (i.e. infected human lung tissue) for both the controls and the tested sample. Unfortunately, we could not acquire *T. gondii* infected slides to be used as controls; hence, using cells were the only alternative option.

Arginase has two main isoforms Arg-1 and Arg-2 (Yu et al., 2003). Many studies have documented particularly high levels of Arg-1 but not Arg-2 in the liver by Western blot (Morris Jr, 2009; Wu et al., 2009). In a study that examined the protein levels and localisation of the two types of arginase (Arg-1 and Arg-2) by Western blot and immunohistochemistry in different rat tissues, they have documented that Arg-1 was expressed at high levels in the liver and at moderate

levels in other tissues including the pancreas and lower levels in the spinal cord and stomach (Choi *et al.*, 2012). In the liver, they have reported high immune-reactivity of Arg-1 in the hepatocytes nucleus and cytosol (Choi *et al.*, 2012), which was further confirmed by (Maier et al., 1976). Furthermore, they have reported small levels of Arg-2 in the liver by immunohistochemistry, which was not detected by the Western blot analysis, which they attributed the discrepancy in results to the detection limit of the Western blotting protocol used (Choi *et al.*, 2012). These results match our data where Arg-1 was detectable in high levels in both the nuclei and cytoplasm of hepatocytes.

Immunohistochemical analysis showed that Arg-1 and was expressed in alveolar macrophages and the bronchiolar epithelium (Choi *et al.*, 2012), matching our data regarding Arg-1 immunohistochemistry in the rat lungs where staining was found mainly in the lining of the bronchiole. Alveolar macrophages are documented to be the main cell type in the lungs responsible for expressing arginase and iNOS, which share the same substrate, l-arginine (Hammermann et al., 2001). Moreover, iNOS is responsible for most of the NO production from alveolar macrophages (Hey et al., 1995).

In rats, iNOS can be expressed in various cell types, including inflammatory cells, endothelial cells, and cardiac myocytes (Tousson et al., 2012). Moreover, in studies that measured the expression of different NOS isoforms in rat heart tissue, including iNOS by immunohistochemistry, have reported that iNOS was detectable in vascular endothelial cells and vascular smooth muscle cells (Toshiyuki et al., 1997). In this chapter, we used rat heart tissue to optimise an immunohistochemistry protocol to detect iNOS and to be used as a positive control tissue for further experiments. Our data showed positive immunoreactivity of iNOS in rat heart tissue in cardiac myocytes and smooth muscle cells, matching previous studies.

Moreover, in a study conducted on rat lung tissue to compare between cell expression types in the different NOS isoforms by IHC, they demonstrated strong iNOS immunoreactivity in the bronchial epithelial cells as well as the bronchial smooth muscle cells (Ermert, Ruppert, Günther, H. R. Duncker, et al., 2002). Furthermore, iNOS expression was also evident at the alveolar macrophage and cells within the alveolar septum (Ermert, Ruppert, Günther, H. R. Duncker, et al., 2002). Other moderate immunoreactivity was demonstrated in the smooth muscle cells of muscular blood vessels, and myocytes of large hilar veins. In another study, conducted on fetal

sheep, iNOS was localised in bronchial and bronchiolar epithelium as well as in the terminal and respiratory bronchioles, including the alveolar wall (Sherman et al., 1999). In addition, iNOS was detected in the vascular smooth muscle (Sherman et al., 1999).

For the diagnosis of *T. gondii* infection, a study has documented the use of a direct immunofluorescence assay to detect *T. gondii* in paraffin-embedded lymph nodes (Matossian et al., 1977). The diagnosis was made by the presence of Toxoplasma cysts and trophozoites in a cervical lymph node biopsy of a 24-year-old sailor. (Matossian et al., 1977). Furthermore, in a study conducted on 4 cases of pulmonary toxoplasmosis in patients with acquired immunodeficiency syndrome, indirect immunofluorescence was used to detect *T. gondii* parasite as a diagnostic tool (Derouin et al., 1989). Although indirect immunofluorescence is considered one of the most commonly used techniques for the diagnosis of toxoplasmosis in humans (Bernal-Guadarrama et al., 2014). few studies have explored pulmonary toxoplasmosis via immunofluorescence. Additionally, even though double immunofluorescence has been gaining more popularity in the research field (van der Loos et al., 1993), as far as we know, we could not find any studies documenting the study of *T. gondii* infection via double IF.

In conclusion, we were able to establish a double IF procedure to target iNOS and Arg-1 in relation to *T. gondii* infection in the same samples. To our knowledge, there are still no studies that have attempted to investigate the dynamics behind the high rate of infection with *T. gondii* in individuals with cancer. We aim to conduct our optimised double IF procedure on the lung cancer clinical samples to colocalise *T. gondii* infection of the lungs with Arg-1 and iNOS in the purpose of exposing the reasons behind the high rate of infection in lung cancer patients. Clearly, this area has not been explored enough, and there is still a need for more exploration to gain a better understanding of what are the dynamics behind *T. gondii* infection in relation to Arg-1 and iNOS.

Chapter 5: Immunohistochemistry and immunofluorescence detection of *T. gondii*, Arg-1 and iNOS in lung cancer clinical samples

5.1. Introduction

The aims of this chapter were to stain lung cancer clinical samples using immunohistochemistry (IHC) to identify the different lung structures and cell types that express Arg-1 and iNOS and are infected with *T. gondii*. Furthermore, to investigate colocalisation of expression of these genes, and parasite infection, in lung cancer clinical samples using immunofluorescence (IF) with *T. gondii*/Arg-1 and *T. gondii*/iNOS antibodies. Cancer patients are highly susceptible to opportunistic infections, including infection with the parasite *T. gondii*, (Carey et al., 1973). In immunocompromised individuals (including cancer patients), lungs are the second most common site for *T. gondii* infection after the central nervous system (Pomeroy and Filice, 1992). Nevertheless, the association between *T. gondii* infection and lung cancer remains relatively unexplored. In a recent study, involving our laboratory, analysis of lung biopsy samples from 72 lung cancer patients showed the presence of the parasite in all samples with 95% of samples showing evidence of active infections (Bajnok et al., 2019). This raises important questions about the locations of infection and the immune responses acting during infection.

Studies conducted on mice and rats have suggested the involvement of the two enzymes Arginase-1 (Arg-1) and inducible nitric oxide synthase (iNOS) and that the balance between their expression and activity might determine host susceptibility vs resistance (Li et al., 2012; Zhao et al., 2013a). In order to investigate whether this applies to the human host, we have conducted IHC staining as well as double immunofluorescence staining to identify the pattern of expression as well as colocalisation of Arg-1 and iNOS in relation to *T. gondii* infection in 51 lung samples from individual lung cancer patients. Quantitate analysis to measure the average percentage of *T. gondii* infection as well as the average expression of Arg-1 and iNOS across different lung tissue/cell types was conducted. Pearson's Correlation Coefficient (PCC) and Manders Correlation Coefficient (MCC) was used to quantify colocalisation between *T. gondii* infection and Arg-1 and iNOS enzymes. This chapter illustrates the outcome of the colocalisation study conducted on lung cancer subjects. To date, little is known about the nature or dynamics behind the reasons which make lung cancer patients highly susceptible to contract toxoplasmosis the lungs. The aim in this chapter is to test the hypothesis that the two markers Arg-1 and iNOS are colocalised with *T. gondii* infection and to investigate whether these two enzymes might be involved in aspects of the lung cancer patients' infection status.

5.1.1 Objectives

1) Histological description of lung tissue structures which are expressing Arg-1, iNOS and *T. gondii* by IHC.
2) Histological description of lung tissue structures which are expressing Arg-1, iNOS and *T. gondii* by double IF.
3) Quantitative determination of *T. gondii* infection in each lung tissue structure and exploration of the relationship between *T. gondii* and tissue/cell types.
4) Quantitative determination of Arg-1 expression in each lung tissue structure and exploration of the relationship between Arg-1 and tissue/cell types.
5) Quantitative determination of iNOS expression in each lung tissue structure and exploration of the relationship between iNOS and tissue/cell types.
6) Quantitative determination of the association between *T. gondii* infection in relation to the expression of Arg-1 and iNOS.
7) Statistical analysis of the association between *T. gondii* infection and Arg-1 in different lung tissue types.
8) Statistical analysis of the association between *T. gondii* infection and iNOS in different lung tissue types.
9) Statistical analysis of the association between the expression of Arg-1 and iNOS in different lung tissue types when infected with *T. gondii*.
10) Statistical analysis of the association between *T. gondii* infection and Arg-1 and iNOS in alveolar macrophages.
11) Quantifying the relationship between the intensity of infection with *T. gondii* in alveolar macrophages co-expressing Arg-1 or iNOS.
12) Quantification of the colocalisation between *T. gondii* infection and Arg-1/iNOS in alveolar macrophages using Pearson's Correlation Coefficient Pearson's Correlation Coefficient (PCC).
13) Establishing the differences in colocalisation between *T. gondii*/Arg-1 and *T. gondii*/iNOS, in the alveolar macrophages using Pearson's Correlation Coefficient (PCC).
14) Quantification of the colocalisation between *T. gondii* infection and Arg-1/iNOS in alveolar macrophages using Manders Correlation Coefficient (MCC).

15) Establishing the differences in colocalisation between *T. gondii*/Arg-1 and *T. gondii*/iNOS, in alveolar macrophages with Manders Correlation Coefficient (MCC).
16) Quantification of the colocalisation between *T. gondii* cysts and Arg-1/iNOS using Pearson's Correlation Coefficient (PCC).
17) Establishing the differences in colocalisation between *T. gondii*/Arg-1 and *T. gondii*/iNOS, in *T. gondii* cysts with Pearson's Correlation Coefficient (PCC).
18) Quantification analysis of the colocalisation between *T. gondii* infection and Arg-1/iNOS in *T. gondii* cysts using Manders Correlation Coefficient (MCC).
19) Establishing the differences in colocalisation between *T. gondii*/Arg-1 and *T. gondii*/iNOS, in *T. gondii* cysts with Manders Correlation Coefficient (MCC).
20) Quantification of the colocalisation between *T. gondii* infection and Arg-1/iNOS in alveolar wall knobs using Pearson's Correlation Coefficient (PCC).
21) Establishing the differences in colocalisation between *T. gondii*/Arg-1 and *T. gondii*/iNOS, in alveolar wall knobs with Pearson's Correlation Coefficient (PCC).
22) Quantification analysis of the colocalisation between *T. gondii* infection and Arg-1/iNOS of alveolar walls (knobs) using Manders Correlation Coefficient (MCC).
23) Establishing the differences in colocalisation between *T. gondii*/Arg-1 and *T. gondii*/iNOS, in the alveolar wall knobs with Manders Correlation Coefficient (MCC).

5.2 Methods

A total of 51 lung cancer tissue blocks from individual patients were cut and prepared on slides. Tissue slides were tested with IHC targeting *T. gondii*, Arg-1and iNOS individually and subsequently visualised under the light microscope. Images constructed by IHC were then analysed histologically to identify the different lung structures expressing/co-expressing Arg-1 and iNOS while infected with *T. gondii.* Furthermore, the same lung cancer slides were tested with double immunofluorescence targeting *T. gondii* and either Arg-1 or iNOS, and later visualised using a fluorescent microscope. The percentage of infection/expression across lung tissue types/cells for each marker was calculated individually in each lung structure. Statistical associations using 2x2 contingency tables were investigated, and Fisher's exact test was used to establish the significance for Arg-1, iNOS and *T. gondii* expression. In order to evaluate the associations between Arg-1 and iNOS expression in relation to infection with *T. gondii,* lung tissues/cells expressing Arg-1/iNOS and showing *T. gondii* infection in all of these structures were counted and documented. Again, 2x2 contingency tables were constructed for lung tissue co-expressing *T. gondii*/Arg-1, *T. gondii*/iNOS and Arg-1/iNOS, and Fisher's exact tests were later conducted. Pearson correlation coefficient (PCC) with Costes test of significance, and Mander's correlation coefficient (MCC) were used to quantify the degree of co-expression (colocalisation) between *T. gondii* infection and Arg-1/iNOS. This was conducted specifically with alveolar macrophages, with the cyst stage of the parasite and in the alveolar wall knobs. Student t-tests were later used to evaluate the significance of differences in the colocalisation between *T. gondii*/Arg-1 and *T. gondii*/iNOS in macrophages, *T. gondii* cysts and alveolar knobs.

5.3 Results

5.3.1 Immunohistochemical detection of Arg-1. iNOS and *T. gondii* in lung cancer patients

With the aim of understanding the dynamics behind the high prevalence of infection in lung cancer patients with the parasite *T. gondii* parasite, immunohistochemistry analysis targeting Arg-1, iNOS and *T. gondii* has been performed. During the sample preparation process, it was made sure that slides were cut, labelled and eventually stained in a serial manner to ensure that colocalisation of the three markers (Arg-1, iNOS and *T. gondii*) would be as accurate as possible (refer to chapter 2). Immunohistochemistry for the three markers were optimised and conducted individually on 51 lung cancer samples, which were previously tested for the presence of *T. gondii* infection by nested PCR (Bajnok, 2017).

Lung tissue slides were stained and subsequently visualised using a light microscope. For each sample, images of the same field of view for each slide were captured for the three markers (Arg-1, iNOS and *T. gondii*). Positive immunoreactivity was marked by the presence of a brown colour staining within the tissue compartments or specific cells. Lung tissue types/cells were identified for each marker individually. The bronchiole, which is considered a smaller branch of the bronchial airways in the respiratory system, showed moderate Arg-1 staining of the bronchiole lining and specifically the ciliated columnar epithelium (Figure 5.1.A), and a moderately faint immunoreactivity in the smooth muscle layer around the bronchiole. Moreover, inside the lumen of the blood vessel, Immunoreactive cells can be observed which, due to the absence of the nucleus, are most probably red blood cells (Figure 5.1.A). The connective tissue, which permits the lungs to inflate during inhalation and return to their original shape after exhalation, is showing little staining (Figure 5.1.A). On the other hand, strong iNOS immunoreactivity is observed mainly in the epithelial cells, which consists of ciliated columnar epithelium (Figure 5.1.C). In addition, moderate iNOS immunostaining was documented in the bronchial smooth muscle cells surrounding the bronchiole as well as the smooth muscle cells of the small blood vessel (Figure 5.1.C). Regarding the infection with *T. gondii* (Figure 5.1.E), the pattern of staining is resembling that of iNOS, where it is found predominantly in the ciliated columnar epithelium lining of the bronchiole, in the vascular smooth muscle of the blood vessels, in the smooth muscle surrounding

the bronchiole and in the connective tissue of the lung (Figure 5.1.E). In the negative controls (primary antibody excluded) for all three markers (Arg-1, iNOS and *T. gondii*) (Figures 5.1.B, D and F, respectively), there was an absolute absence of immunostaining in the bronchial epithelium and all other cell types, excluding false positivity or contamination. Moreover, in Figure 5.2, a higher magnification (x40) of the bronchiole, the same findings can be seen.

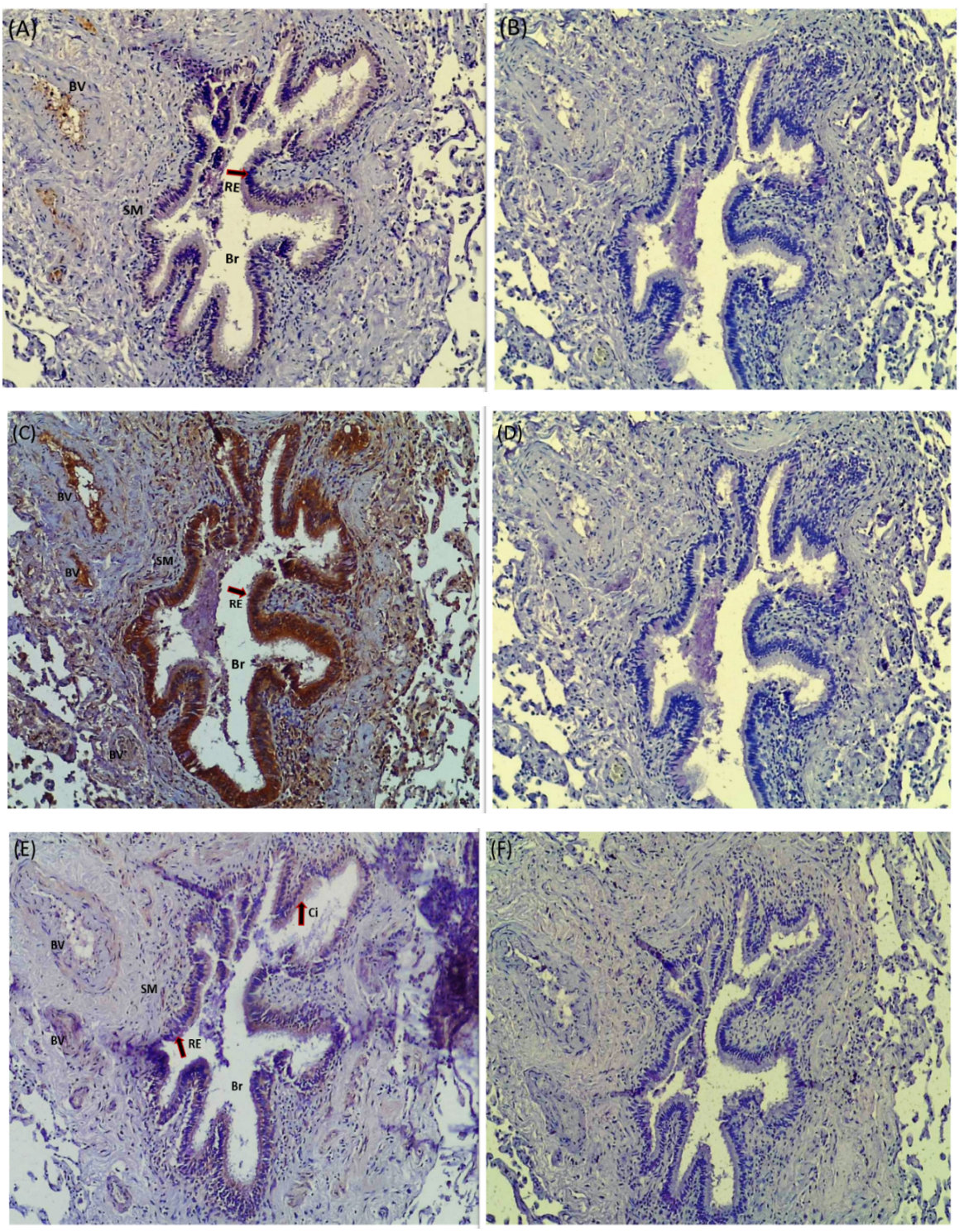

Figure 5.1 Immunohistochemistry of lung cancer tissue targeting (A) Arg-1, (C) iNOS and (E) *T. gondii.* The lining of the proximal bronchiole (Br), comprises the ciliated columnar epithelium (RE) cells. The lumen of the blood vessel (BV) and the smooth muscle layer (SM) are indicated. Negative controls for Arg-1 (B), iNOS (D) and *T. gondii* (F) which do not contain primary antibodies are not showing any brown staining excluding false positivity or contamination. Image magnification x20.

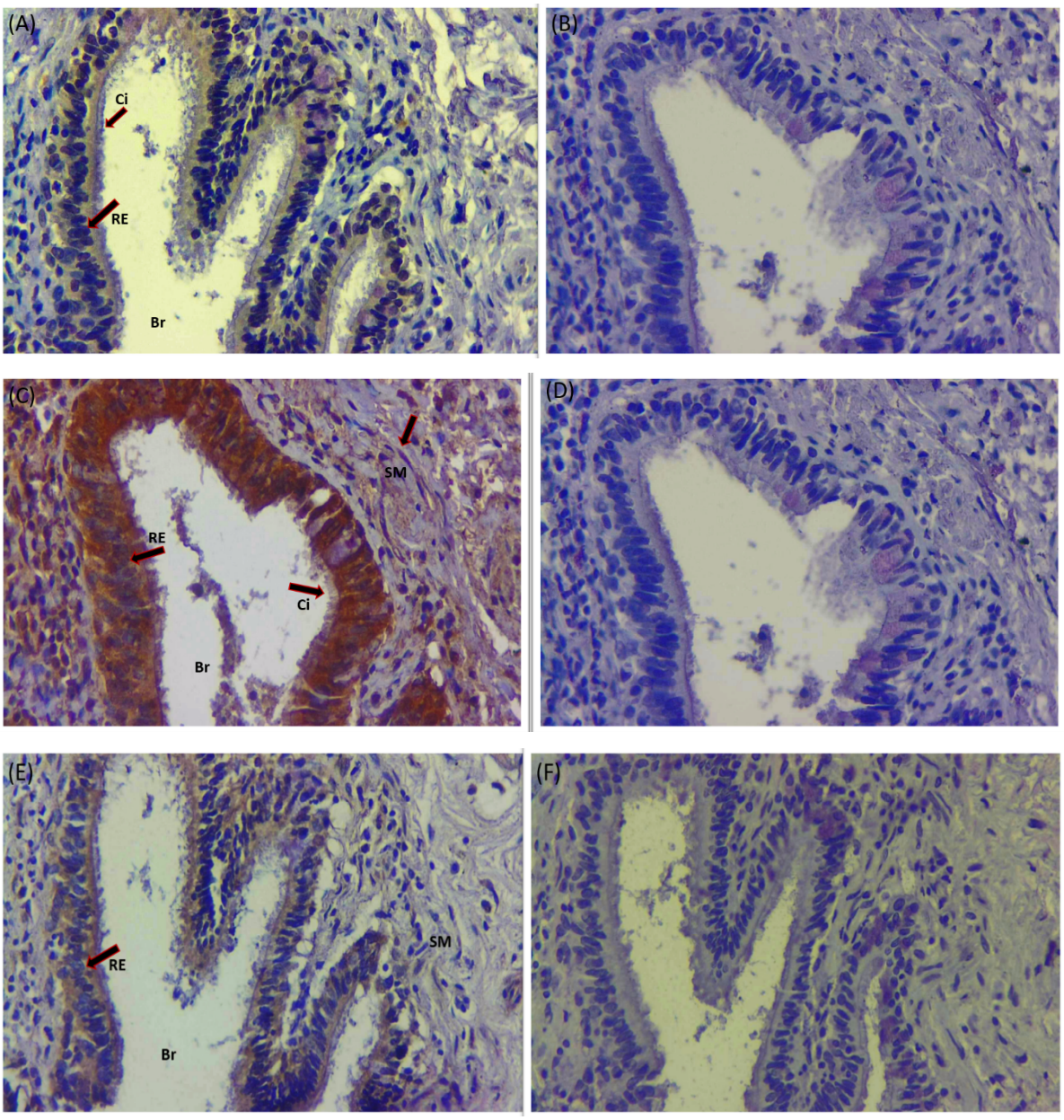

Figure 5.2 immunohistochemistry of lung cancer tissue samples targeting (A) Arg-1, (C) iNOS and (E) *T. gondii* parasite. The ciliated columnar epithelium cells (RE) lining the bronchiole (Br) and the smooth muscle (SM) cells surrounding the bronchiole are indicated. The cilia (Ci) can be seen, which are small hair like structures on cells lining the bronchi responsible of protecting the airways from being damaged or infected by particles of dust or foreign matter. Negative controls (B, D and F) for Arg-1, iNOS and *T. gondii* respectively, are absent of any staining excluding contamination or false-positive results. Image magnification x40.

Human lungs have a double blood supply through the pulmonary vascular system and the bronchial vascular system (Ellis, 2008). Blood vessels have shown positive staining for all three antibodies in our study, for example, a pulmonary artery shown in Figure 5.3. A relatively faint immunoreactivity was observed with Arg-1 (Figure 5.3.A), mainly in the smooth muscle cells of the tunica media and in the External Elastic Lamina. No staining was observed in the adventitia nor the endothelial cell lining of the blood vessel lumen.

On the other hand, a strong immunoreactivity was observed in the blood vessel with iNOS (Figure 5.3.C), where the different layers of the blood vessel including the External Elastic Lamina and the Internal Elastic Lamina were expressing iNOS as well as the endothelial cells lining the lumen of the artery (Figure 5.3.C). Furthermore, a relatively strong staining indicating iNOS expression was visible in the smooth muscle cells located in the tunica media layer as well as in the supporting collagen. Moreover, the adventitial layer consisting mainly of fibro-collagenous supporting tissue is moderately expressing iNOS (Figure 5.3.C).

Similar to the distribution of iNOS, *T. gondii* infection can be seen throughout the structures of the lung blood vessel (Figure 5.3.E). in the smooth muscle cell of the tunica media layer, external and internal lamina and the endothelial cells, however in contrast to iNOS expression. *T. gondii* was more prominent in the fibro-collagenous supporting tissue of the adventitial layer (Figure 5.3.E). All negative controls (Figures 5.3 B, D, F) did not show any staining for any marker.

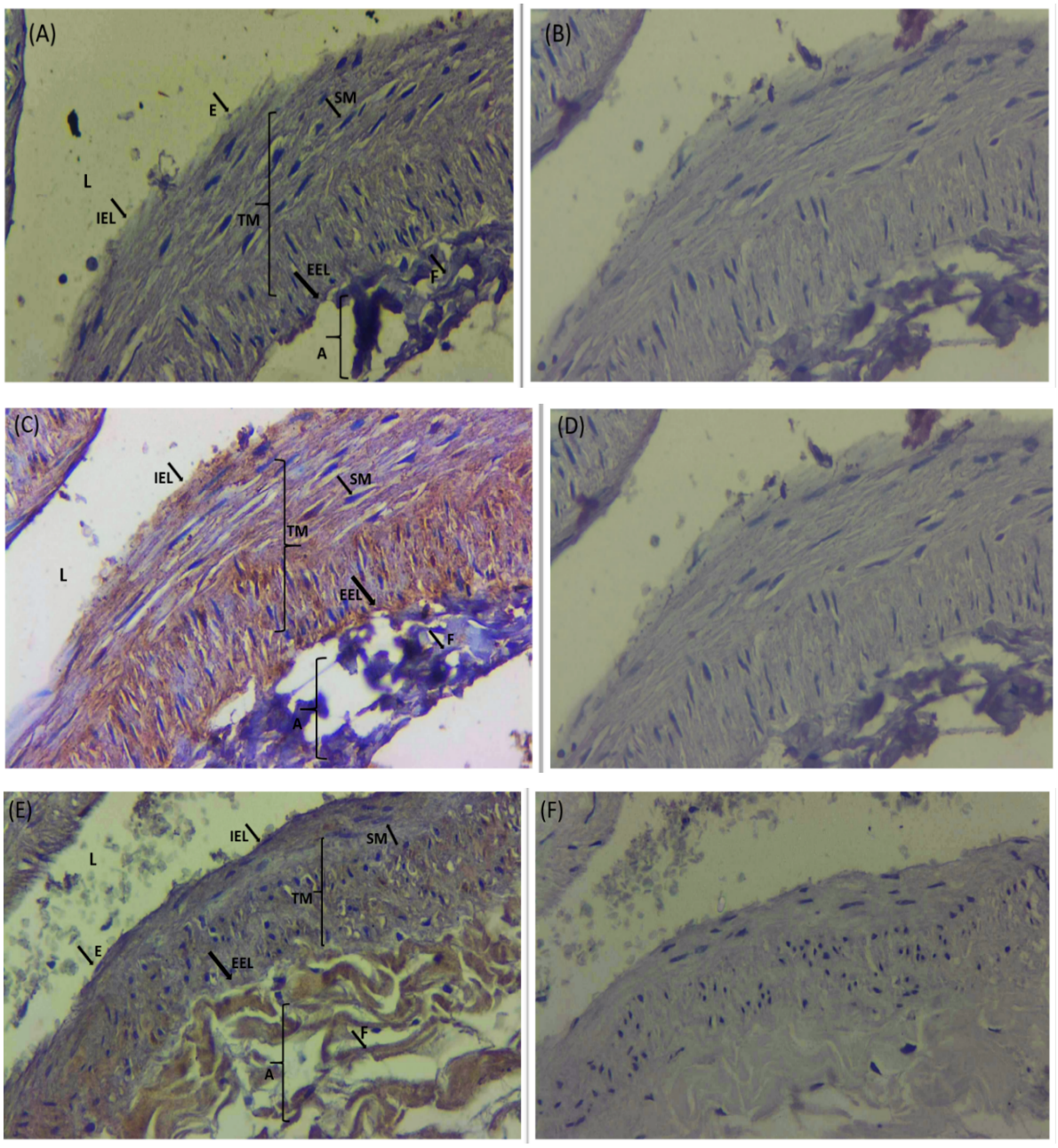

Figure 5.3 Immunohistochemical analysis targeting **(A)** Arg-1, **(C)** iNOS and **(E)** *T. gondii* infection in lung cancer subjects. The image is showing a pulmonary blood vessel where (SM) is the smooth muscle of the tunica media (TM), (ELL) is the External Elastic Lamina and (IEL) is the Internal Elastic Lamina (IEL), (E) is the endothelial cells and (A) is the adventitia. Negative controls (**B, D** and **F**) for Arg-1, iNOS and *T. gondii* respectively, are not showing any staining excluding contamination or false-positive results. Image magnification x40.

Moving towards the most distal parts of the lungs, which is mainly composed of alveolar spaces, the immunohistochemistry findings at the alveolar level are shown in Figure 5.4, Figure 5.5 and Figure 5.6 for Arg-1, iNOS and *T. gondii* respectively. The alveoli, which are small, balloon-shaped air sacs, are showing similar distribution of staining with all three markers (Arg-1, iNOS and *T. gondii*), at the alveolar wall, which consists mainly of type I (marked by the flat nucleus) and type II pneumocytes (with a characteristic cuboidal nucleus). These are showing positive staining in Arg-1(Figure 5.4.B), iNOS (Figure 5.5 .A) and *T. gondii* (Figure 5.6 .A). Smooth muscle fibres of the alveolar wall (knobs), which mark the opening of the alveolar sacs and assist in the process of expansion and recoil during breathing, are positively stained with Arg-1(Figure 5.4.A), iNOS (Figure 5.5.A) and *T. gondii* (Figure 5.6.B). Moreover, alveolar macrophages, which act primarily as phagocytes, often referred to as dust cells are located in the pulmonary alveoli adjacent to pneumocytes but separated from the wall. These exhibited strong immunoreactivity with the three markers evident as a cluster of macrophages in Arg-1 staining, (Figure 5.4.C), and with iNOS (Figure 5.5.B), and with *T. gondii* (Figure 5.6.A and B). Negative controls did not show any staining in any of the markers (Figure 5.6.D). A summary of the identified tissue/cell types expressing Arg-1 and iNOS and infected with *T. gondii* by IHC is listed in (Table 5.1).

Table 5.1 A summary of lung tissue/cell types expressing Arg-1, iNOS and infected with *T. gondii* . (Br) is the bronchiolar lining, SMb is the smooth muscle layer surrounding the bronchiole. IEL is the External Elastic Lamina of the blood vessel, VSM is the vascular smooth muscle, IEL is the External Elastic Lamina, and Ad is the adventitia. Type1 and Type II are pneumocytes and Mg is the alveolar macrophages.

	Br	**SM(b)**	**IEL**	**VSM**	**EEL**	**Ad**	**Type I**	**TypeII**	**Mg**
Arg-1	Yes	Yes	NO	Yes	Yes	NO	Yes	Yes	Yes
iNOS	Yes	Yes	Yes	Yes	Yes	Yes	Yes	Yes	Yes
T. gondii	Yes	Yes	Yes	Yes	Yes	Yes	Yes	Yes	Yes

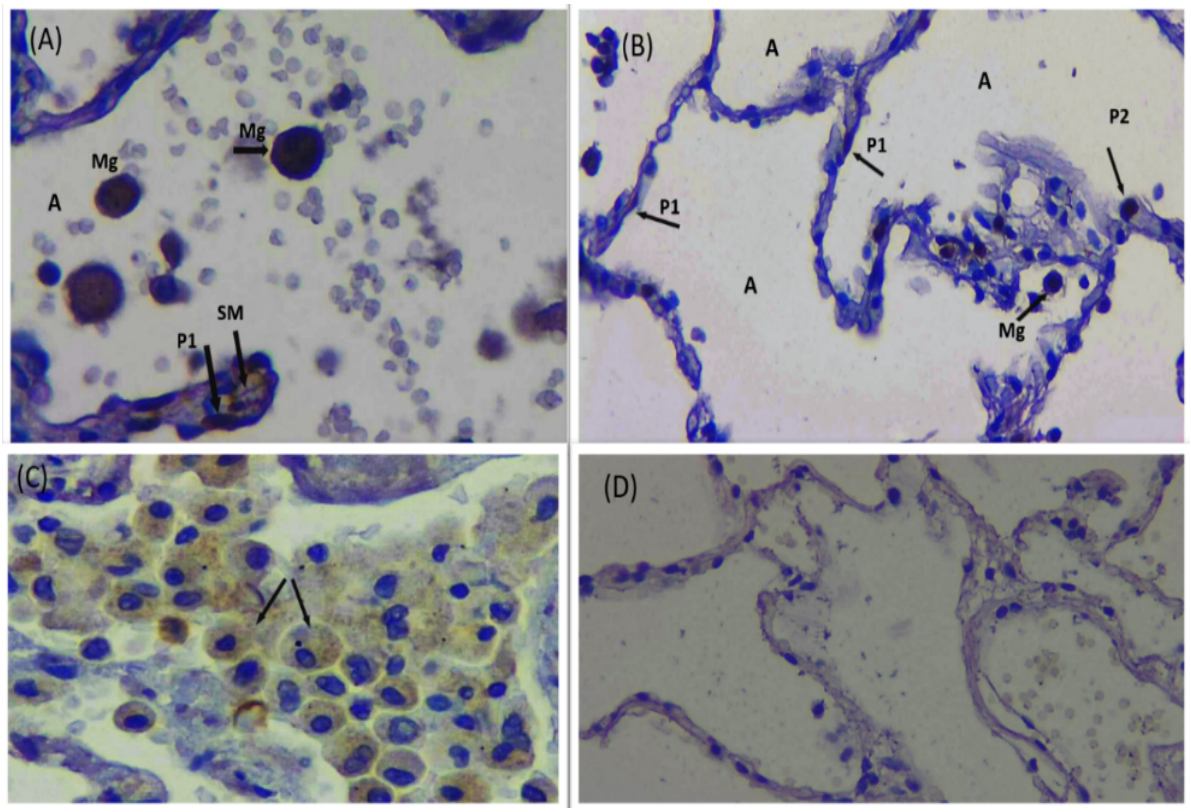

Figure 5.4 Immunohistochemical localisation of Arg-1 in lung cancer tissue . **(A)** in the alveolar macrophages (Mg), the smooth muscle fibres (SM) of the alveolar wall (alveolar knob) and the lining of the alveolar wall, type I pneumocyte (P1). **(B)** Immunoreactivity in the epithelial cells lining the alveolar wall type I pneumocyte (P1), and type II pneumocyte (P2). **(C)** a large cluster of alveolar macrophages (Mg) expressing Arg-1. **(D)** Negative control with no brown staining. Images magnification x40.

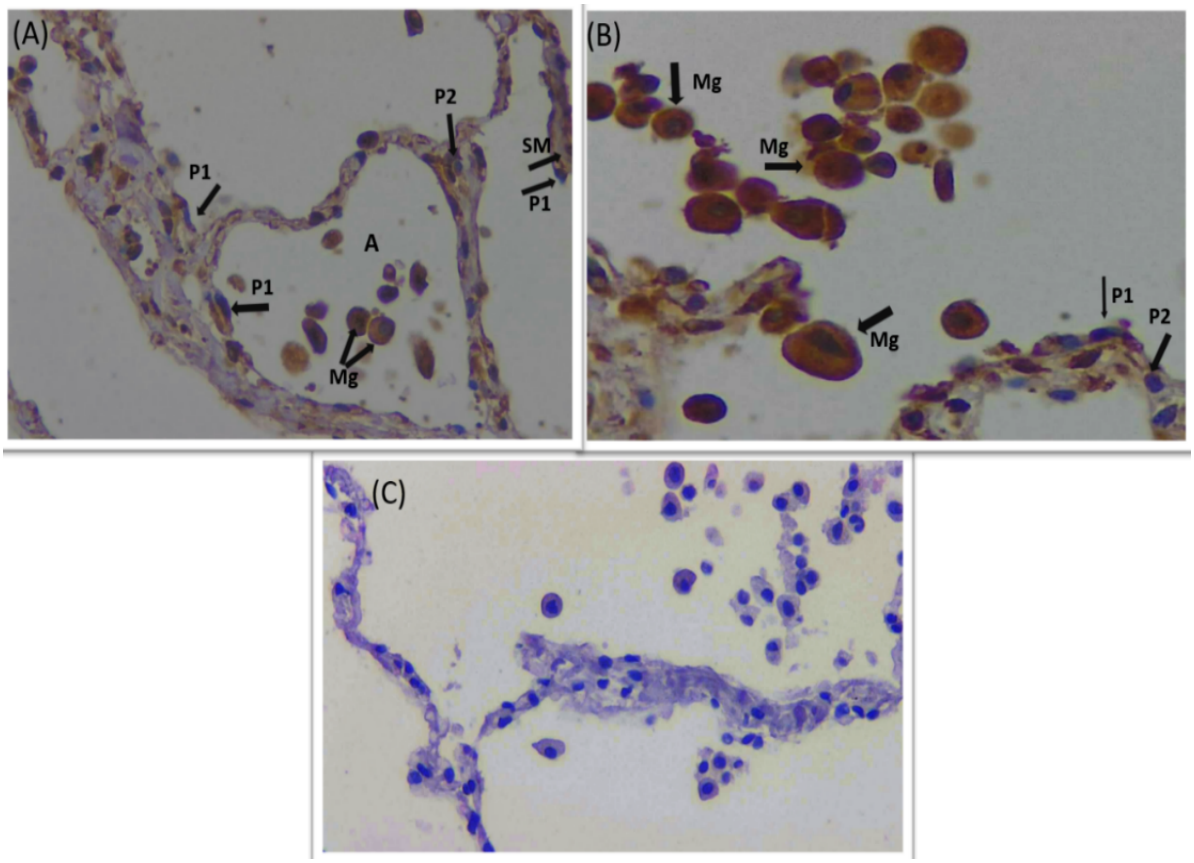

Figure 5.5 Immunohistochemistry of iNOS in lung cancer patients infected with *T. gondii* . **(A)** Alveolar spaces with the lining of the alveolar wall, pneumocyte type I (P1) as well as pneumocyte type II (P2). Smooth muscle fibres (SM) of the alveolar wall opening with its lining consisting of the flat nucleated epithelial cells (type I pneumocyte (P1) are indicated. Few macrophages (Mg) can be seen inside the (A) alveolus. **(B)** A cluster of macrophages (Mg), as well as type I (P1) and type II (P2) pneumocyte, are positively stained with iNOS. **(C)** Negative control with no staining. Images magnification x40.

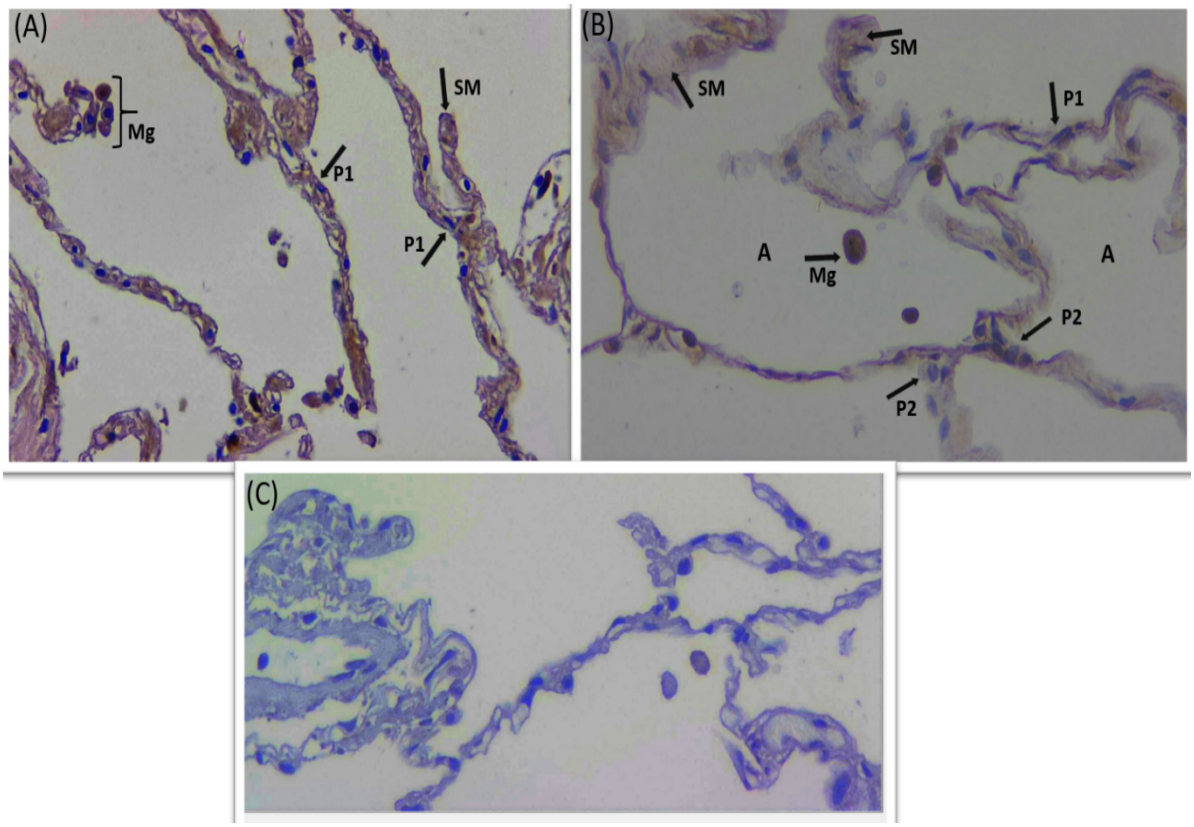

Figure 5.6 Immunohistochemistry staining of lung cancer tissue using polyclonal antibody targeting *T. gondii* parasite . **(A)** Immunoreactivity marking infection at epithelial cells lining the alveolar walls consisting of type I (P1) and type II (P2) pneumocytes and at the smooth muscle fibres (SM). A cluster of *T. gondii* infected macrophages (Mg) is seen at the top left. **(B)** Distal bronchiole marked by the thicker smooth muscle wall (SM), type I (P1), type II (P2) pneumocytes and a free macrophage (Mg) is indicated. **(C)** Negative control with no brown staining. Images magnification x40.

5.3.2 Double staining immunofluorescence of Arg-1, iNOS and *T. gondii* in lung cancer patients

To further confirm the results obtained by immunohistochemistry, and to establish a more detailed informative colocalisation analysis, double immunofluorescence was conducted on the 51 lung cancer samples. The first objective was to investigate colocalisation of Arg-1 with *T. gondii* infection of the lungs. Secondly, double immunofluorescence was also carried out to localise iNOS expression in relation to the localisation of infection with the parasite *T. gondii.* All 51 patients were examined using both techniques and examples of the types of immunofluorescence staining is shown in the following pages.

Supporting the results achieved by IHC in the lung tissues, double immunofluorescence targeting *T. gondii*/Arg-1 showed positive immunoreactivity in the bronchioles of the lungs (Figure 5.7). The outer most lining of the bronchiole, which is composed of columnar epithelium along with the cilia showed infection with *T. gondii* (Figure 5.7.A) and expression of Arg-1 (Figure 5.7.B). Moreover, the smooth muscle layer surrounding the bronchiole, which controls air flow, by contraction, showed a moderately heavy infection with *T. gondii* (Figure 5.7.A) while expressing Arg-1 faintly (Figure 5.7.B). Colocalisation of *T. gondii* infection and Arg-1 expression can be observed mainly in the epithelial layer of the bronchiole and faintly in the smooth muscle layer. On the other hand, the full thickness of the epithelium which is composed of pseudostratified columnar epithelium laying on a thin basement membrane is not expressing Arg-1 nor infected with *T. gondii*. This layer is evident with the heavily DAPI (blue) stained nuclei of these cells (Figure 5.7.C).

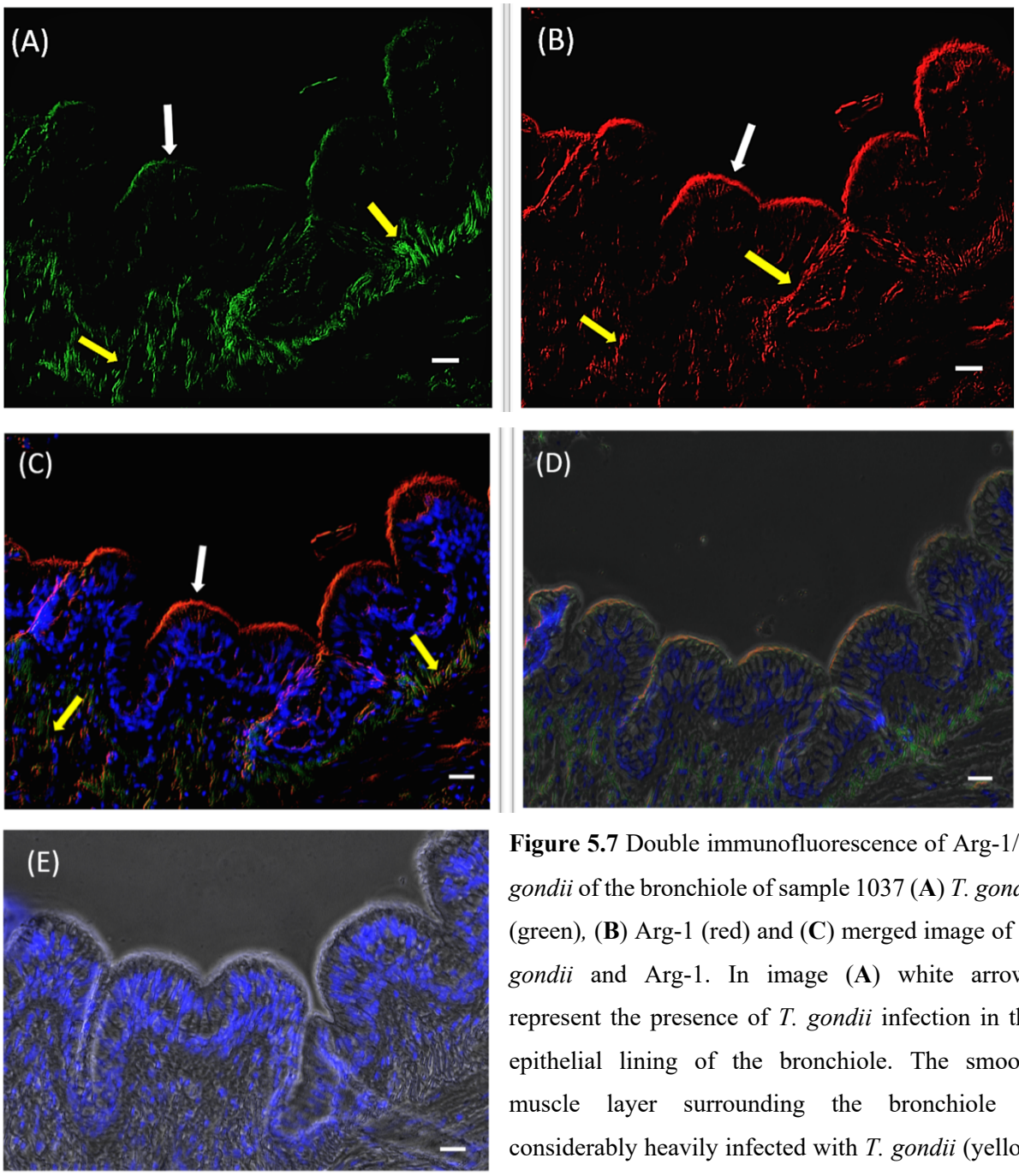

Figure 5.7 Double immunofluorescence of Arg-1/*T. gondii* of the bronchiole of sample 1037 (**A**) *T. gondii* (green), (**B**) Arg-1 (red) and (**C**) merged image of *T. gondii* and Arg-1. In image (**A**) white arrows represent the presence of *T. gondii* infection in the epithelial lining of the bronchiole. The smooth muscle layer surrounding the bronchiole is considerably heavily infected with *T. gondii* (yellow arrow). In image (**B**) immunoreactivity of Arg-1 is evident in the epithelial lining of the bronchiole (white arrow), while Arg-1 is faintly expressed in the smooth muscle layer surrounding the bronchiole (yellow arrow). (**C**) is the merged image of *T. gondii* and Arg-1 showing the colocalisation at the bronchiole lining (white arrow) and smooth muscle (yellow arrow). Blue staining is DAPI stained cell nuclei. (**D**) is the overlay of the merged (*T. gondii*, Arg-1 and DAPI stains) on a black and white image of the tissue. (**E**) is the negative control. Scale bar = 20 µm. Image magnification x20.

The same double immunofluorescent procedure was carried out targeting *T. gondii* in association with iNOS on all of the samples and images were taken and then analysed. The bronchiole section of the lung shows a strong expression of iNOS at the inner lining of the lumen which is composed of ciliated columnar epithelium (Figure 5.8.B) as well as infection with *T. gondii* (Figure 5.8.A). Furthermore, the expression of iNOS further extends to the surrounding smooth muscle layer (Figure 5.8.A) as well as the infection with *T. gondii* (Figure 5.8.A). It is evident that colocalisation between *T. gondii* and iNOS at the level of the bronchial is located at the lining of the bronchiole and extending to the surrounding smooth muscle layer (Figure 5.8.C), hence, mimicking the expression pattern of Arg-1 in relation to *T. gondii* infection at this level, however with a stronger pattern of expression. Moreover, the full thickness of the epithelium, which is composed of pseudostratified columnar epithelial cells are not infected with *T. gondii*, nor expressing iNOS. The cells of the epithelium is conspicuous by the presence of the DAPI stained nuclei (Figure 5.8.C).

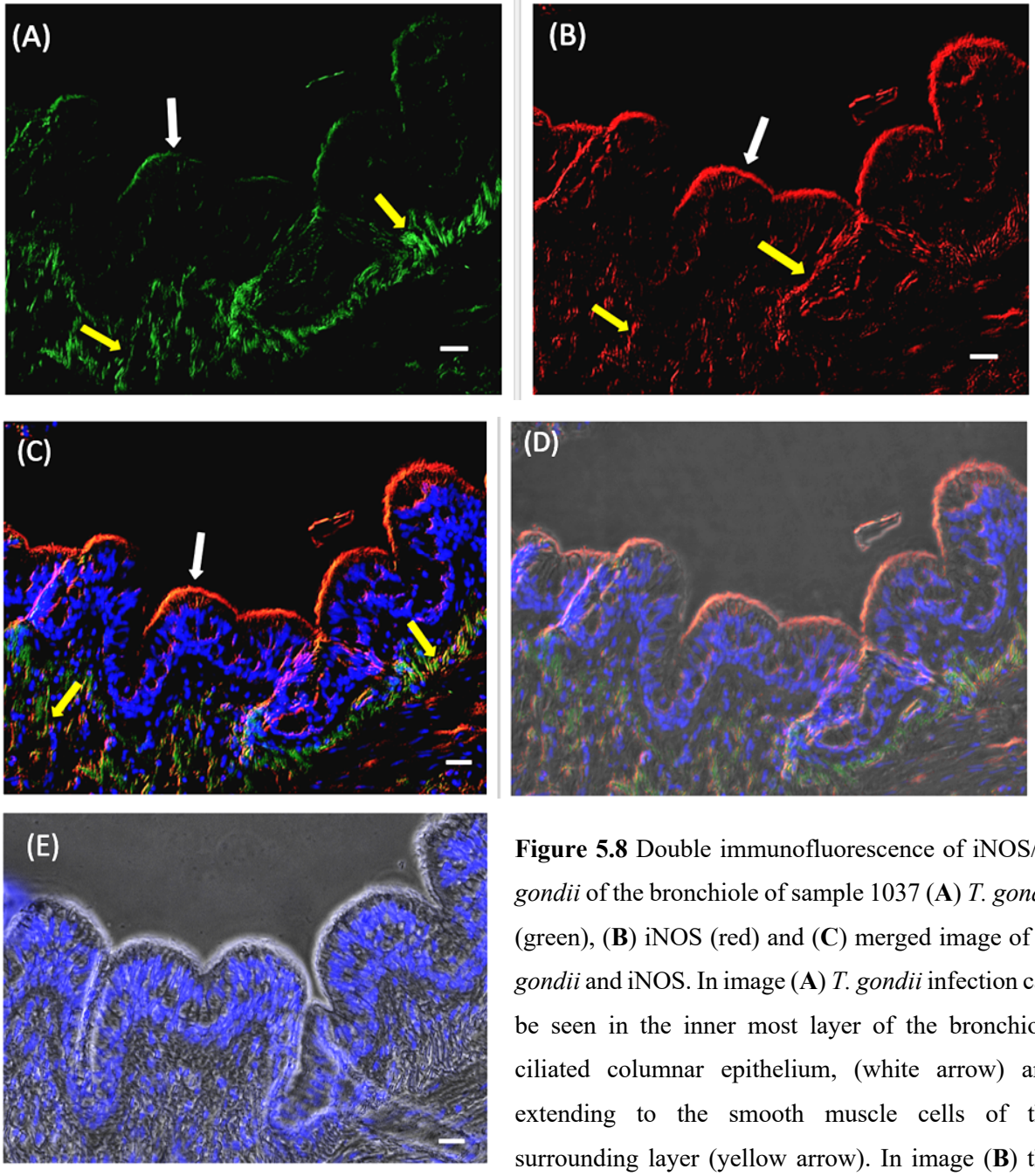

Figure 5.8 Double immunofluorescence of iNOS/*T. gondii* of the bronchiole of sample 1037 (**A**) *T. gondii* (green), (**B**) iNOS (red) and (**C**) merged image of *T. gondii* and iNOS. In image (**A**) *T. gondii* infection can be seen in the inner most layer of the bronchiole ciliated columnar epithelium, (white arrow) and extending to the smooth muscle cells of the surrounding layer (yellow arrow). In image (**B**) the expression pattern of iNOS can be seen strongly on the lining of bronchiole (white arrow), as well as at the surrounding smooth muscle layer (yellow arrow). (**C**) is the merged image of *T. gondii* and iNOS expression showing the colocalisation at the bronchiole lining (white arrow) and smooth muscle (yellow arrow). Blue staining is DAPI stained cell nuclei. (**D**) is the overlay of the merged (*T. gondii*, iNOS and DAPI stains) on a black and white image of the tissue. (**E**) is the negative control. Scale bar = 20 µm. Image magnification x40.

As established previously with IHC analysis, blood vessels of the lungs have showcased *T. gondii* infection as well as expression of both markers Arg-1 and iNOS but in different amounts. Double immunofluorescence analysis of the lung clinical samples has revealed the same results of IHC; however, colocalisation data can also be obtained. At the blood vessel level, double immunofluorescence targeting *T. gondii* infection and the Arg-1 marker (Figure 5.9), *T. gondii* infection is clearly observed to be specific to the External Elastic Lamina layer of the blood vessel (Figure 5.9.A) extending to the vascular smooth muscle as well. The Internal Elastic Lamina layer of the blood vessel is not infected with *T. gondii*. In contrast to *T. gondii* infection, heavy Arg-1 expression was evident at the Internal Elastic Lamina layer (Figure 5.9.B) and extending to the vascular smooth muscle layer of the blood vessel as well. Colocalisation at the level of the vascular blood vessel between *T. gondii* infection and Arg-1 is, therefore at the smooth muscle layer.

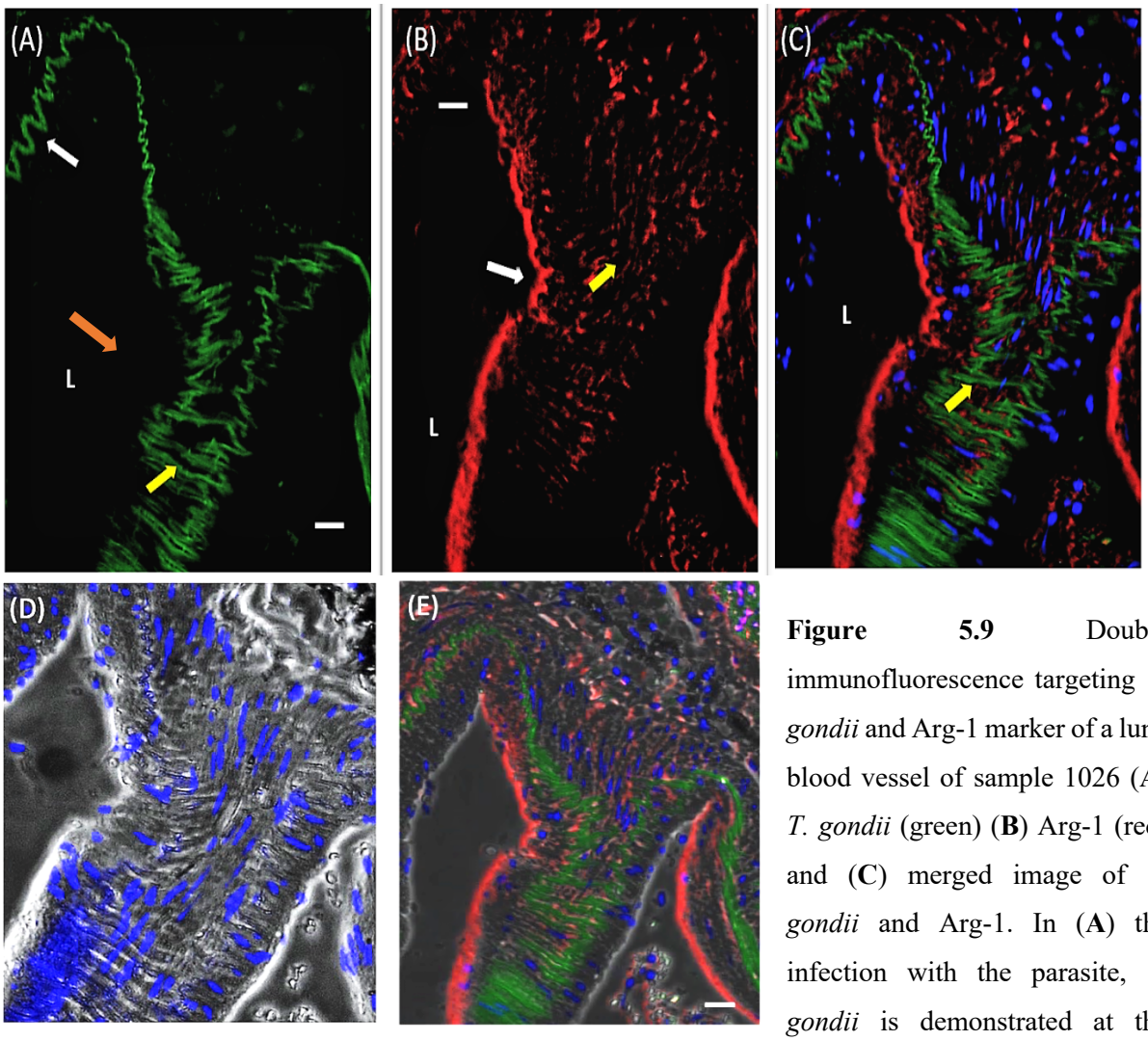

Figure 5.9 Double immunofluorescence targeting *T. gondii* and Arg-1 marker of a lung blood vessel of sample 1026 (**A**) *T. gondii* (green) (**B**) Arg-1 (red) and (**C**) merged image of *T. gondii* and Arg-1. In (**A**) the infection with the parasite, *T. gondii* is demonstrated at the External Elastic Lamina (EEL) layer (white arrow) and Vascular Smooth Muscle (VSM) (yellow arrow). No infection can be seen at the Internal Elastic Lamina (IEL) (orange arrow). In image (**B**) immunofluorescence reactivity of Arg-1 is evident at the Internal Elastic Lamina (IEL) which is the first layer in the blood vessel (white arrow) and the Vascular Smooth Muscle (VSM) (yellow arrow). (**C**) is the merged image of *T. gondii* and Arg-1 expression shows the colocalisation at Vascular Smooth muscle (VSM) (yellow arrow). Blue staining is DAPI stained cell nuclei. (**D**) is the negative control. (**E**) is the overlay of the merged (*T. gondii*, Arg-1 and DAPI stains) on a black and white image of the tissue. Scale bar = 20 µm. Image magnification x20.

Regarding the double immunofluorescence targeting *T. gondii* infection in relation to iNOS expression, the same lung blood vessel was analysed (Figure 5.10). *T. gondii* infection has a similar pattern of infection as that obtained from the previous sample (Figure 5.9.A), where the infection is seen mainly at the External Elastic Lamina and sweeping to the vascular smooth muscle layer but also reaching the Adventitial (Ad) layer in low intensity (Figure 5.10.A). As to the expression pattern of iNOS in relation to *T. gondii* infection, immunoreactivity can be observed in the Internal Elastic Lamina (IEL) spreading to the Vascular smooth muscle (VSM) and expressed faintly at External Elastic Lamina (EEL) (Figure 5.10.B). Moreover, iNOS expression is also visible at the Adventitial layer of the blood vessel (Figure 5.10.B). Colocalisation between *T. gondii* infection and iNOS is thereby is confined to 3 layers of the lung blood vessel, which are the EEL, VSM and Ad.

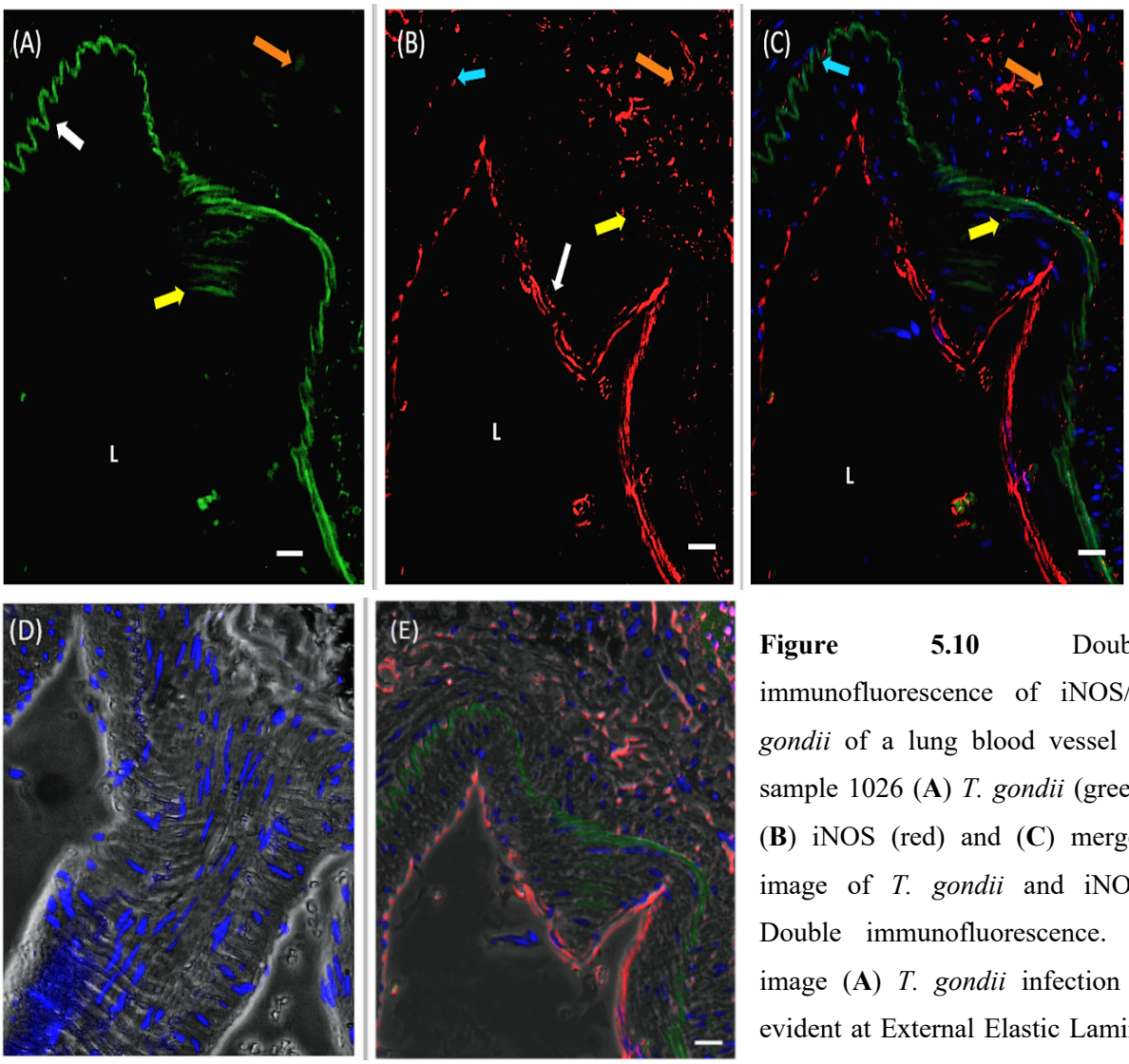

Figure 5.10 Double immunofluorescence of iNOS/*T. gondii* of a lung blood vessel of sample 1026 (**A**) *T. gondii* (green) (**B**) iNOS (red) and (**C**) merged image of *T. gondii* and iNOS. Double immunofluorescence. In image (**A**) *T. gondii* infection is evident at External Elastic Lamina (EEL) (white arrow), the vascular smooth muscle (VSM) (yellow arrow) and the Adventitia (Ad) (orange arrow). In image (**B**) the Expression of iNOS is evident at the Internal Elastic Lamina (IEL) (white arrow), the vascular smooth muscle (VSM) (yellow arrow), the External Elastic Lamina (EEL) (blue arrow) and the Adventitia (Ad) (orange arrow). (**C**) is the merged image of *T. gondii* and iNOS expression demonstrating the colocalisation at Vascular Smooth muscle (VSM) (yellow arrow), the External Elastic lamina (EEL) (blue arrow) and faintly at the Adventitia (Ad) (orange arrow). Blue staining is DAPI stained cell nuclei. (**D**) is the negative control. (**E**) is the overlay of the merged (*T. gondii*, iNOS and DAPI stains) on a black and white image of the tissue. Scale bar = 20 μm. Image magnification x20.

Moving more distally towards the end of the lung air spaces, as found with IHC analysis, double immunofluorescence analysis of *T. gondii* infection in relation to Arg-1 has revealed positive infection with *T. gondii* and expression of Arg-1 in the alveolar walls (Figure 5.11).

The alveolar spaces are composed mainly of two types of cells, type I, type II pneumocytes, and smooth muscle fibres at the opening of the alveolar spaces which contract to aid the breathing process. The smooth muscle fibres at the tip of the alveolar space (the knobs) show positive infection with *T. gondii* (Figure 5.11.A). Furthermore, type I pneumocytes, which form the epithelial lining of the alveolar wall, also exhibited infection with *T. gondii* (Figure 5.11.A). Arg-1 expression is found in the smooth muscle fibres of the (knobs) as well as the type I pneumocytes as characterised by their round nuclei (Figure 5.11.B). *T. gondii* infection and Arg-1 expression appear to be colocalised at the alveolar knobs and epithelial lining cells (Figure 5.11.C).

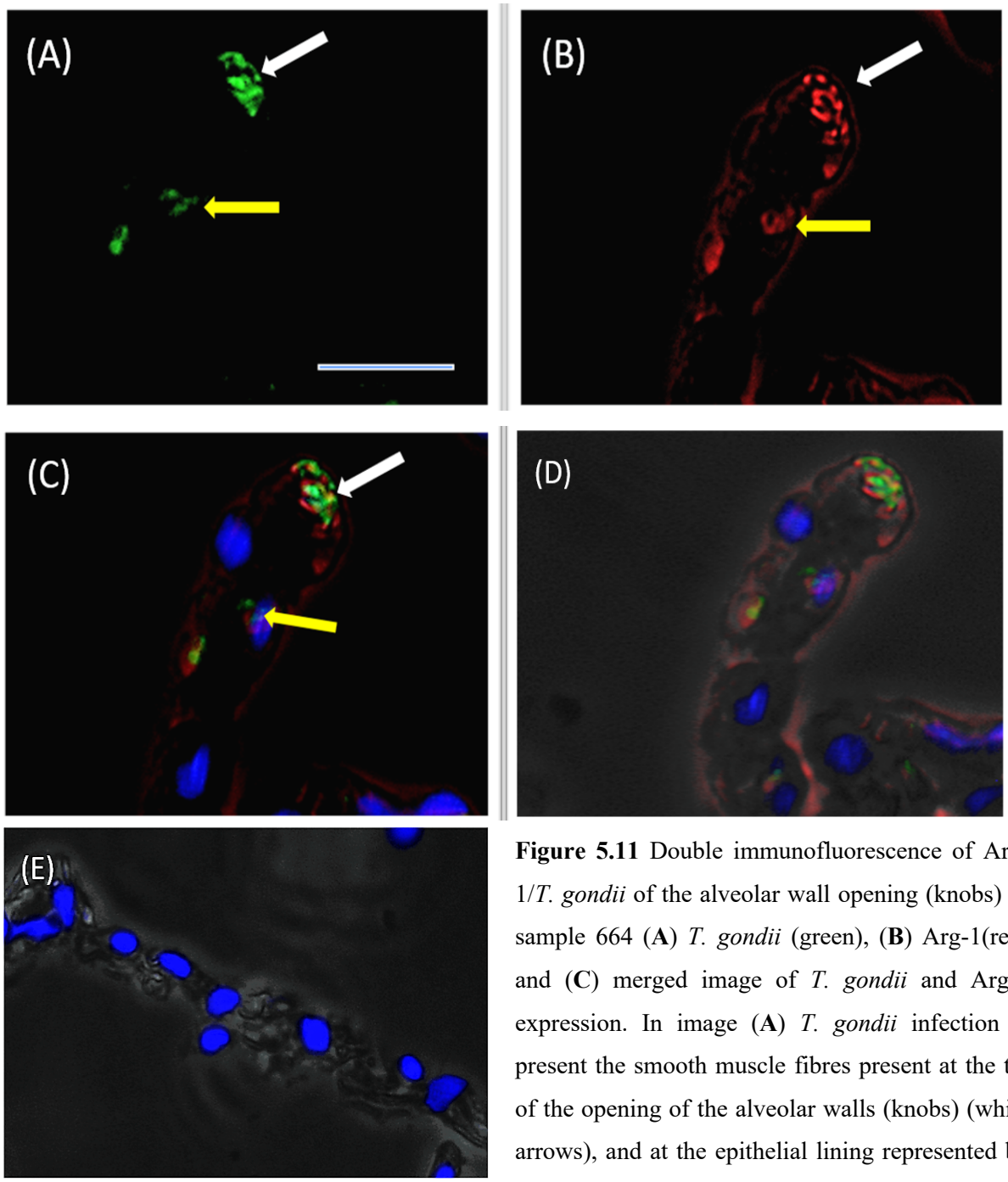

Figure 5.11 Double immunofluorescence of Arg-1/*T. gondii* of the alveolar wall opening (knobs) of sample 664 (**A**) *T. gondii* (green), (**B**) Arg-1(red) and (**C**) merged image of *T. gondii* and Arg-1 expression. In image (**A**) *T. gondii* infection is present the smooth muscle fibres present at the tip of the opening of the alveolar walls (knobs) (white arrows), and at the epithelial lining represented by type I pneumocytes (yellow arrow). In image (**B**) expression of Arg-1 can be evident the (knobs) smooth muscle fibres (white arrows), and at type I pneumocytes of the alveolar epithelial lining (yellow arrow). (**C**) is the merged image of *T. gondii* infection and Arg-1 expression demonstrating the colocalisation at the knobs (white arrow) and the type1 pneumocyte (yellow arrow). Blue staining is DAPI stained cell nuclei. (**D**) is the overlay of the merged (*T. gondii*, Arg-1 and DAPI stains) on a black and white image of the tissue. (**E**) is the negative control. Scale bar = 20 μm. Image magnification x40.

Double immunofluorescence targeting *T. gondii* in association with iNOS expression was analysed at the same alveolar level (Figure 5.12) in the distal lungs. Confirming previous results, *T. gondii* infection was observed at the tip of the knobs consisting of smooth muscle fibres (Figure 5.12.A). The pattern of iNOS expression, was located at smooth muscle fibres as well (Figure 5.12.B). Imitating the colocalisation pattern between *T. gondii* and Arg-1, iNOS and *T. gondii* are colocalised at the smooth muscle fibre of the alveolar wall tips (knobs) (Figure 5.12.C).

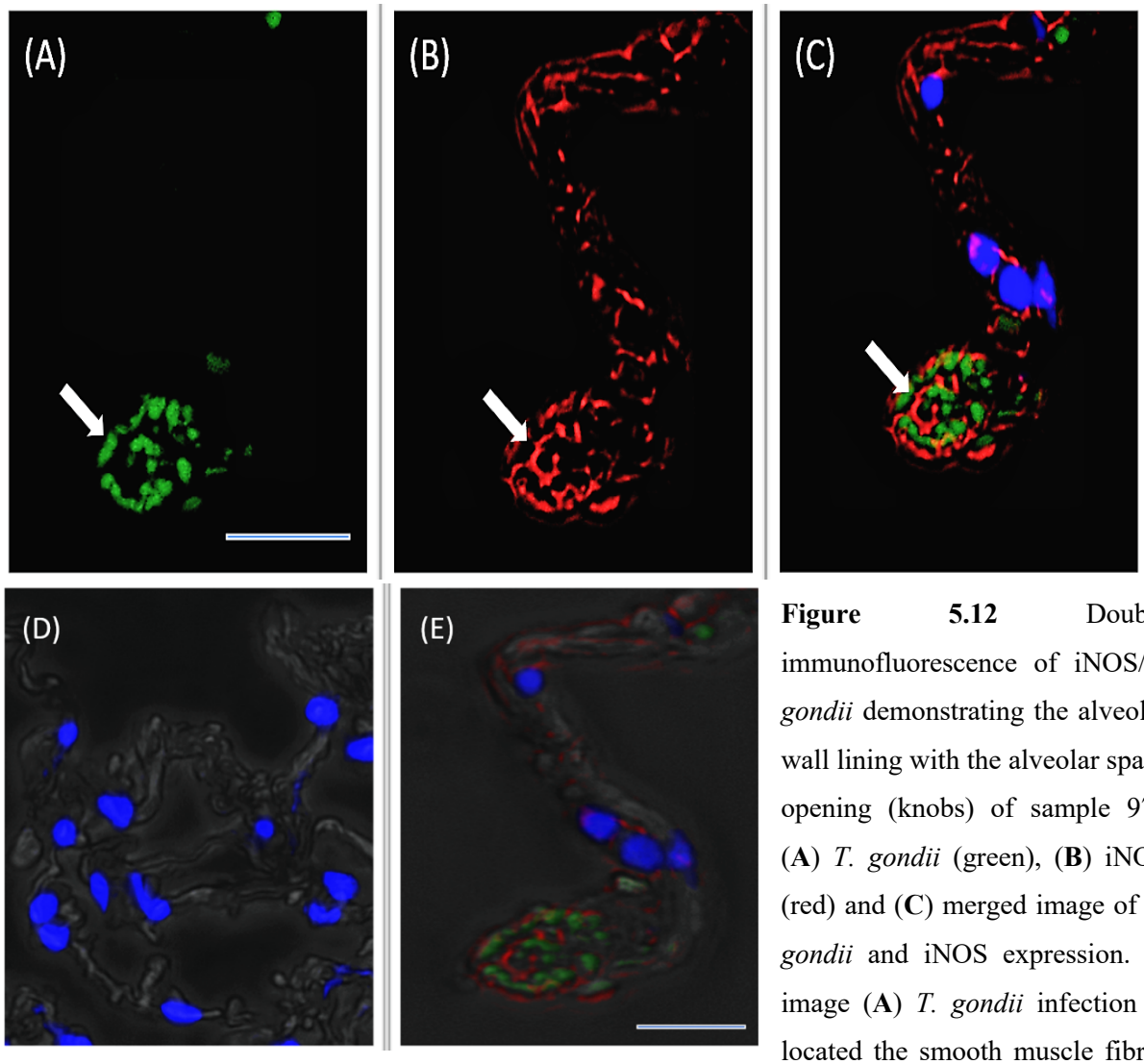

Figure 5.12 Double immunofluorescence of iNOS/*T. gondii* demonstrating the alveolar wall lining with the alveolar space opening (knobs) of sample 972 (**A**) *T. gondii* (green), (**B**) iNOS (red) and (**C**) merged image of *T. gondii* and iNOS expression. In image (**A**) *T. gondii* infection is located the smooth muscle fibres present at the tip of the opening of the alveolar walls (knobs) (white arrows). In (**B**) expression of iNOS is present at the smooth muscle fibres of the knobs (white arrows). (**C**) Merged image of *T. gondii* infection and iNOS expression demonstrating the colocalisation at the knobs (white arrow). Blue staining is DAPI stained cell nuclei. staining is DAPI stained cell nuclei. (**D**) is the negative control. (**E**) is the overlay of the merged (*T. gondii*, iNOS and DAPI stains) on a black and white image of the tissue. Scale bar = 20 µm. Image magnification x40.

Alveolar macrophages are highly prevalent in the alveolar spaces and are usually found roaming freely away from the wall. Matching the results obtained by IHC, double immunofluorescence of *T. gondii* and Arg-1 have shown positive *T. gondii* infection as well as positive immunoreactivity in the alveolar macrophages (Figure 5.13). All of the macrophages apparent are expressing Arg-1 while being infected with *T. gondii.*

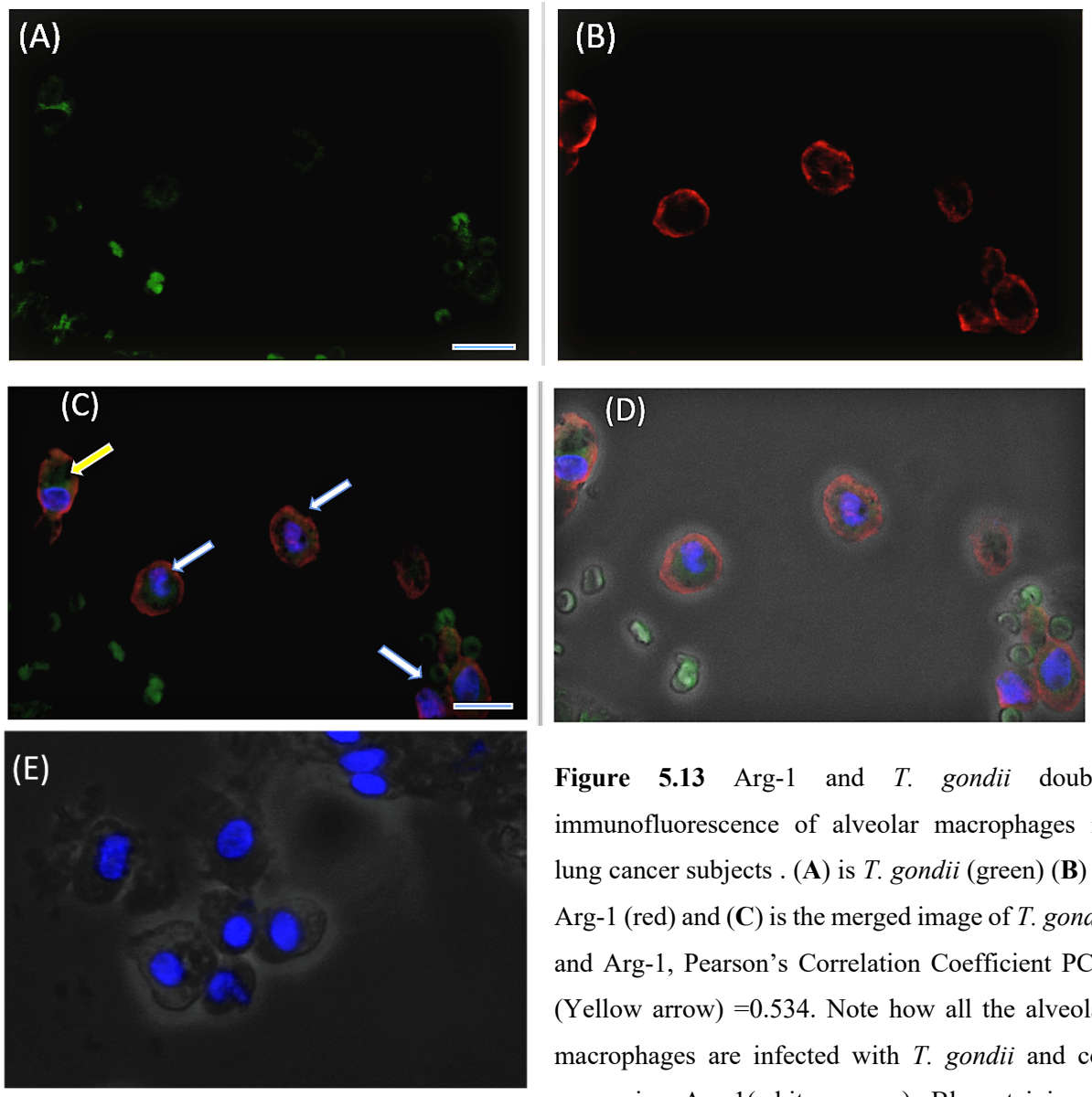

Figure 5.13 Arg-1 and *T. gondii* double immunofluorescence of alveolar macrophages in lung cancer subjects . (**A**) is *T. gondii* (green) (**B**) is Arg-1 (red) and (**C**) is the merged image of *T. gondii* and Arg-1, Pearson's Correlation Coefficient PCC (Yellow arrow) =0.534. Note how all the alveolar macrophages are infected with *T. gondii* and co-expressing Arg-1(white arrows). Blue staining is DAPI stained cell nuclei. (**D**) is the overlay of the merged (*T. gondii*, Arg-1 and DAPI stains) on a black and white image of the tissue. (**E**) is the negative control. Scale bar = 20 µm. Image magnification x40.

On the other hand, double immunofluorescence targeting *T. gondii* and iNOS has also showcased positive iNOS expression in most of the alveolar macrophages (Figure 5.14); however, only one is positively infected with *T. gondii*, while two macrophages are not expressing iNOS nor are they infected with *T. gondii*. A detailed quantification of alveolar macrophages infected with *T. gondii* and co-expressing iNOS is discussed later in this chapter. A summary of the identified tissue/cell types expressing Arg-1 and iNOS and infected with *T. gondii* by IF is listed in (Table 5.2).

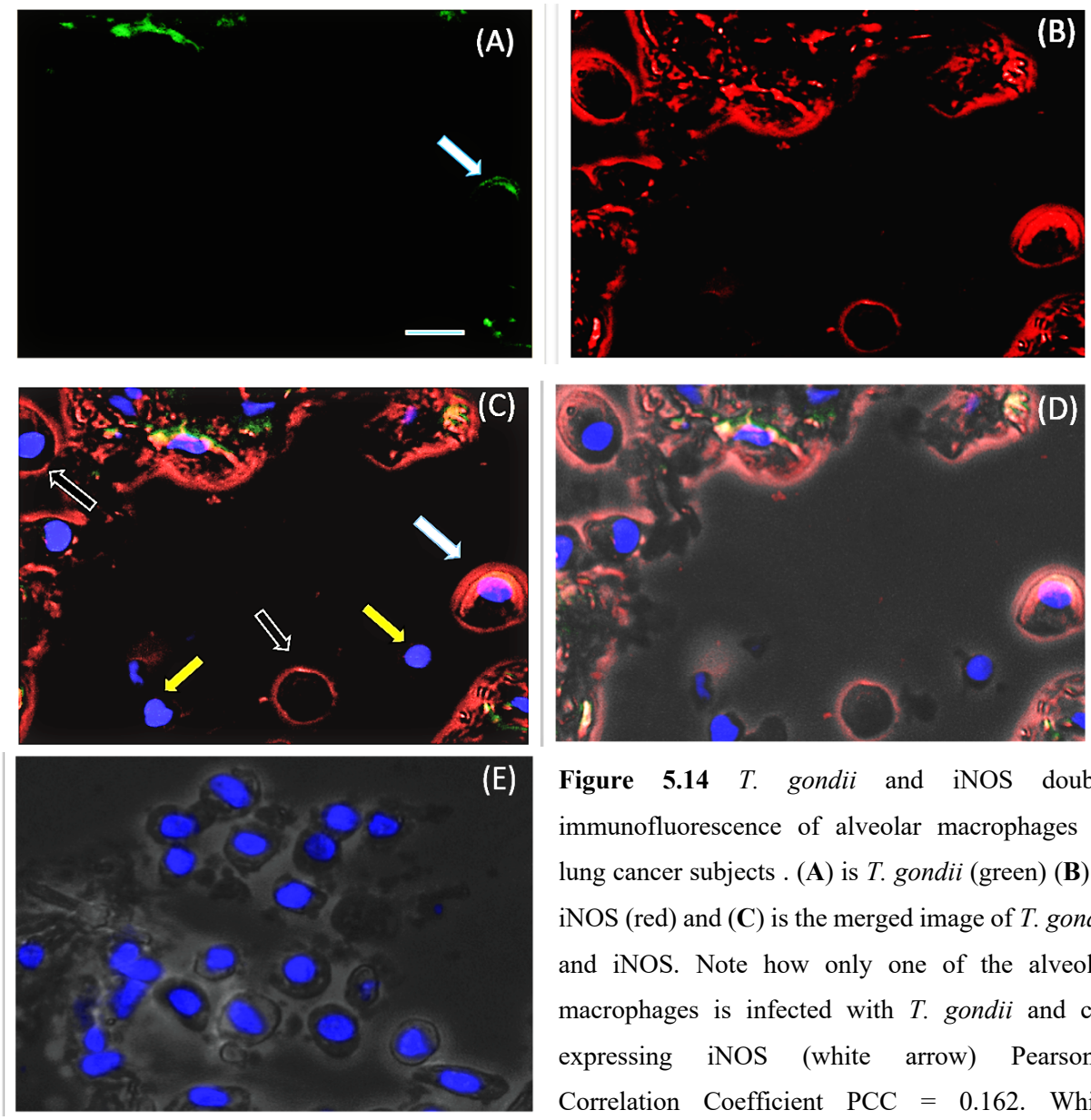

Figure 5.14 *T. gondii* and iNOS double immunofluorescence of alveolar macrophages in lung cancer subjects . (**A**) is *T. gondii* (green) (**B**) is iNOS (red) and (**C**) is the merged image of *T. gondii* and iNOS. Note how only one of the alveolar macrophages is infected with *T. gondii* and co-expressing iNOS (white arrow) Pearson's Correlation Coefficient PCC = 0.162. While macrophages are expressing iNOS only (black arrows) and two other macrophages are not infected with *T. gondii* nor expressing iNOS (yellow arrows). Blue staining is DAPI stained cell nuclei. (**D**) is the overlay of the merged (*T. gondii*, iNOS and DAPI stains) on a black and white image of the tissue. (**E**) is the negative control. Scale bar = 20 µm. Image magnification x40.

Table 5.2 A summary of lung tissue/cell types expressing Arg-1, iNOS and infected with *T. gondii* by IF . (Br) is the bronchiolar lining, SMb is the smooth muscle layer surrounding the bronchiole. IEL is the External Elastic Lamina of the blood vessel, VSM is the vascular smooth muscle, IEL is the External Elastic Lamina, and Ad is the adventitia. Type1 and Type II are pneumocytes, and Mg is the alveolar macrophages.

	Br	**SM(b)**	**IEL**	**VSM**	**EEL**	**Ad**	**Type I**	**TypeII**	**Mg**
Arg-1	Yes	Yes	Yes	Yes	Yes	Yes	Yes	Yes	Yes
iNOS	Yes	Yes	Yes	Yes	Yes	Yes	Yes	Yes	Yes
T. gondii	Yes	Yes	NO	Yes	Yes	Yes	Yes	Yes	Yes

5.3.3 Investigation of the proportion of *T. gondii* infections in each lung tissue structure and the relationship between *T. gondii* and tissue/cell types.

In order to estimate the level of infection with *T. gondii* across different lung tissues, and to measure the frequency of occurrence of *T. gondii* infection, the presence or absence of *T. gondii* infection was documented for each sample. This was performed on each lung tissue/cell type individually, and the percentage of infection with *T. gondii* was calculated on the 51 samples in different histological lung structures, (Figure 5.15). The percentage of infection was considered relatively high across the different lung tissue types, however it was highest in the EEL with 93% followed by 88%, 82%, 71,4%, 66,6% and 58.6% for type I pneumocytes, type II pneumocytes, the Ad, VSM, and the Mgs respectively. On the other hand, no *T. gondii* infection was documented at the IEL in any of the tested 51 samples.

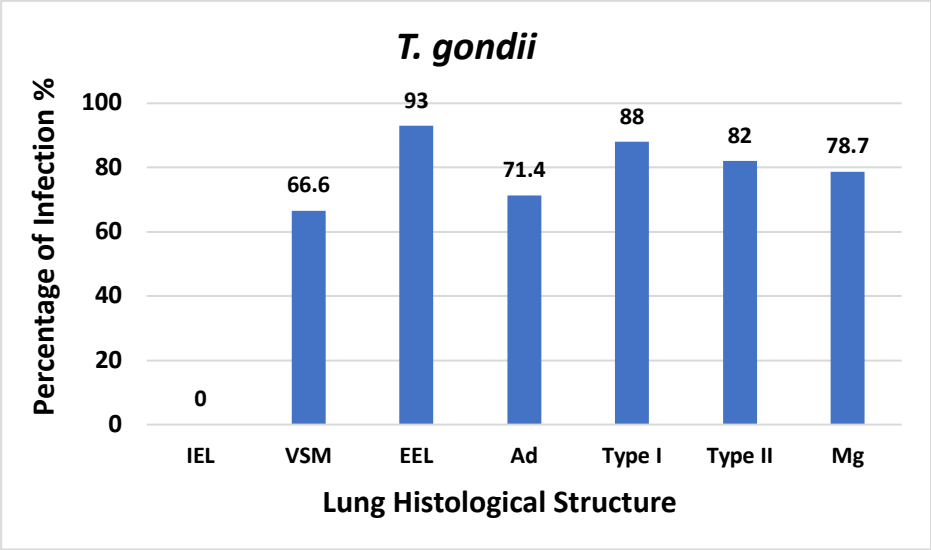

Figure 5.15 A graph illustrating the proportion of infection with *T. gondii* across different lung tissue types , IEL is Internal Elastic Lamina, VSM is Vascular Smooth Muscle, EEL is External Elastic Lamina, Ad is Adventitia, Type I pneumocytes, Type II pneumocytes and Mg is macrophages.

To evaluate whether the difference in the frequency of *T. gondii* infection across the various lung tissue types/cells shows a significant difference, a 2x4 contingency table was constructed (Table 5.3), and an R x C contingency table analysis was conducted to produce a *P-value*.

Table 5.3 A 2x4 contingency table of *T. gondii* infection frequency at the different layers of lung blood vessels.

	IEL	**VSM**	**EEL**	**Ad**	**Total**
***T. gondii*+**	0	28	39	30	97
***T. gondii*-**	42	14	3	12	71
Total	42	42	42	42	168

The analysis gave a *P-value* of $p = 1.0E-21$, ($p < 0.001$) indicating there is a very highly significant difference in the frequency of infection with *T. gondii* in the various blood vessels tissue types.

Since the IEL was not infected with *T. gondii* in any of the samples, it has been excluded to determine whether the other lung tissue types differ in the infection with *T. gondii*. A 2x3

contingency table was established to evaluate whether the difference in the frequency of *T. gondii* infection across the other lung tissue types is significant (Table 5.4), and an R x C contingency table analysis was conducted to produce a *P*-value.

Table 5.4 A 2x3 contingency table of *T. gondii* infection frequency at the different layers of lung blood vessels (excluding IEL).

	VSM	**EEL**	**Ad**	**Total**
***T. gondii*+**	28	39	30	97
***T. gondii*-**	14	3	12	29
Total	42	42	42	126

The analysis gave a *P*-value of p =0.006 hence there is a significant difference in the frequency of infection with *T. gondii* across the other lung tissue types (VSM, EEL and Ad) and it's not only due to the absence of infection at the level of the IEL.

In addition, a 2x3 contingency table was established to evaluate whether the difference in the frequency of *T. gondii* infection across the different lung cell types is significant (Table 5.5), and an R x C contingency table analysis was conducted to produce a *P*-value.

Table 5.5 A 2x3 contingency table of *T. gondii* infection frequency at the lung cell types.

	Type I	**Type II**	**Mg**	**Total**
***T. gondii*+**	30	28	137	195
***T. gondii*-**	4	6	37	47
Total	34	34	174	242

The analysis gave a *P*-value of, p =0.50 indicating there is no significant difference in the frequency of infection by *T. gondii* between the different lung cell types.

5.3.4 Establishing the proportion of Arg-1 expression in each lung tissue structure and exploring the relationship between Arg-1 and tissue/cell types.

To evaluate the level of Arg-1 expression throughout the lung structures, the presence or absence of Arg-1 expression across the lung tissue/cell types was documented. After that, the percentage of Arg-1 expression was calculated for the 51 samples across distinct lung tissue types, (Figure 5.16). While the highest percentage of expression was documented in Type I pneumocytes with a percent of 91%, followed by the alveolar Mg 87.4% and Type II pneumocytes 85.2%, the lowest expression was documented in the VSM 7.1% and followed by the EEL with 9.5%. In contrast to *T. gondii* infection, the expression in the IEL 64,2%, which is considered reasonably high compared to the absolute negative infection with *T. gondii* at this layer.

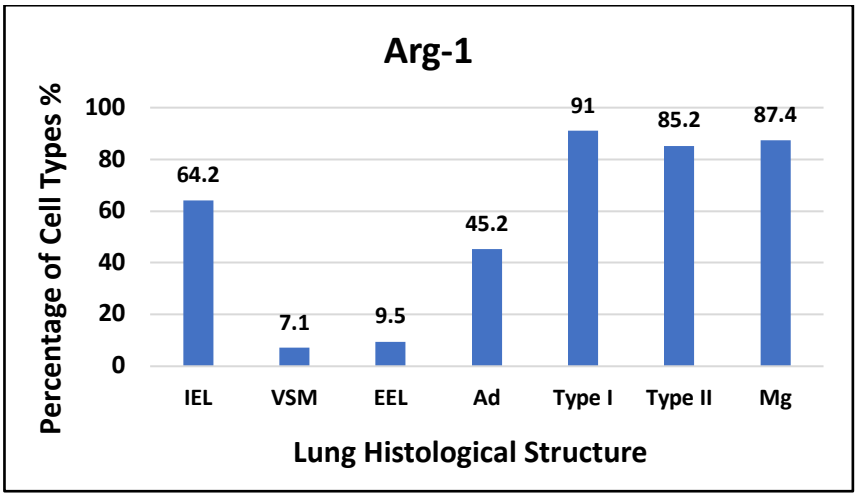

Figure 5.16 A graph illustrating of the percentage of expression of Arg-1 across various lung tissue structures of lung cancer patients infected with *T. gondii* . IEL is Internal Elastic Lamina, VSM is Vascular Smooth Muscle, EEL is External Elastic Lamina, Ad is Adventitia, Type I pneumocytes, Type II pneumocytes and Mg is macrophages.

In order to estimate whether the difference in the expression of Arg-1 across the different lung tissue types specifically (at the different layers of the lung blood vessels) is significantly different, a 2x4 contingency table was created (Table 5.6) and an R x C contingency table analysis was conducted to produce a *P*-value.

Table 5.6 A 2x4 contingency table listing the frequency of Arg-1 expression at the different layers of lung blood vessels.

	IEL	VSM	EEL	Ad	Total
Arg-1+	27	3	4	19	53
Arg-1-	14	39	38	23	114
Total	41	42	42	42	167

The analysis gave a *P*-value of p = 9.0E-11, ($p < 0.001$) revealing that there is a very highly significant difference in the frequency of expression of Arg-1 in the various blood vessel layers.

In order to asses whether the extremely high significant difference in Arg-1 expression is not only due to the low values of (VSM and EEL), a 2x2 contingency table was established (Table 5.7) with the remaining to tissue types (IEL and Ad). Fisher's exact test was conducted to produce a *P*-value.

Table 5.7 A 2x2 contingency table listing the frequency of Arg-1 expression at the different layers of lung blood vessels.

	IEL	Ad	Total
Arg-1+	27	19	46
Arg-1-	14	23	37
Total	41	42	83

Fisher's exact test, $P = 0.07$ indicating that the frequency of Arg-1 expression between IEL and Ad lung tissue types is not statistically significant, and the low *T. gondii* infection rate in (VSM and EEL) was causing the *P-value* to be extremely low.

Moreover, a 2x3 contingency table was created to estimate whether the difference in the frequency of Arg-1 expression across the different lung cell types is significant (Table 5.8), and an R x C contingency table analysis was conducted to produce a *P*-value.

Table 5.8 A 2x3 contingency table of Arg-1 expression frequency at the different lung cell types.

	Type I	**Type II**	**Mg**	**Total**
Arg-1+	31	29	146	206
Arg-1-	4	5	25	34
Total	35	34	171	239

The analysis gave a *P-value* of $P = 0.91$, indicating there is no significant difference in the frequency of Arg-1 expression in the different lung cell types.

5.3.5 Establishing the percentage of iNOS expression in each lung tissue structure and exploring the relationship between iNOS and tissue/cell types.

To evaluate the extent of iNOS expression across the distinct lung structures, the expression of iNOS across different lung tissue/cell types was documented for each in each of the samples. Then, the percentage of iNOS expression was calculated across the different lung tissue types for the 51 clinical samples, (Figure 5.17).

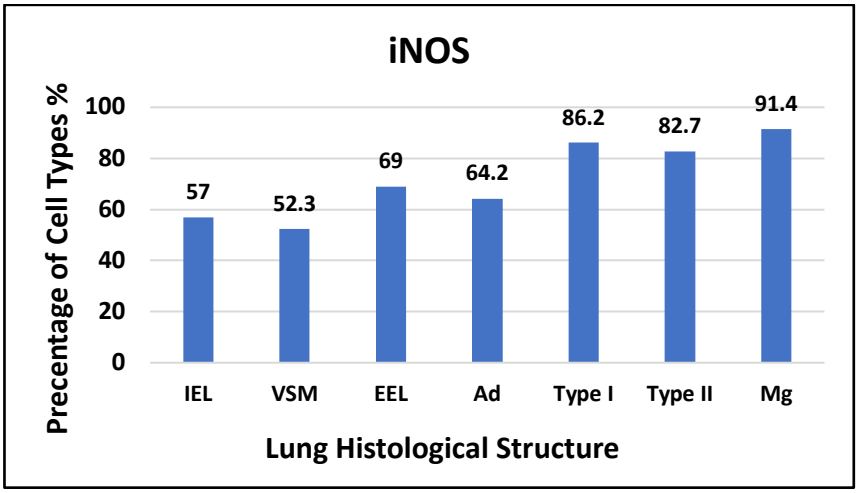

Figure 5.17 A graph illustration of the percentage of expression of iNOS across various lung tissue structures of lung cancer patients infected with *T. gondii* . IEL is Internal Elastic Lamina, VSM is Vascular Smooth Muscle, EEL is External Elastic Lamina, Ad is Adventitia, Type I pneumocytes, Type II pneumocytes and Mg is macrophages.

As illustrated from the graph, it is evident that the expression of iNOS is high across all of the tissue types/cells of the lungs with the highest expression in the Mg 91.4%, followed by Type I pneumocyte 86.2%, Type II pneumocyte 82.7%, EEL 69%, Ad 64.2. IEL 57% and the lowest at the VSM with a 52.3%.

Furthermore, a 2x3 contingency table was created to assess whether the difference in the frequency of iNOS expression across the different lung cell types is significant (Table 5.9), and an R x C contingency table analysis was conducted to produce a *P*-value.

Table 5.9 A 2x4 contingency table listing the frequency of iNOS expression at the different layers of lung blood vessels.

	IEL	**VSM**	**EEL**	**Ad**	**Total**
iNOS+	24	22	29	27	102
iNOS-	18	20	13	15	66
Total	42	42	42	42	168

The analysis gave a *P*-value of $p = 0.419$, stating that there is no significant difference in the frequency of expression of iNOS across the different layers of the lung blood vessels.

In order to estimate whether the difference in the frequency of iNOS expression across the different lung cell types is significant, a 2x3 contingency table was constructed (Table 5.10), and Fisher's exact test was conducted to produce a *P*-value.

Table 5.10 A 2x3 contingency table of iNOS expression frequency at the different lung cell types.

	Type I	**Type II**	**Mg**	**Total**
iNOS+	25	24	139	188
iNOS-	4	5	12	21
Total	29	29	151	209

The analysis gave a *P-value* of, $P = 0.20$; hence, there is no significant difference in the frequency of iNOS expression in the different lung cell types.

5.3.6 Evaluating the percentage of the association between *T. gondii* infection in relation to the expression of Arg-1 and iNOS

In the previous sections, the proportions of *T. gondii* infection and the expression of Arg-1 and iNOS across the various lung tissue/cells was established individually. To take this further and establish the degree of association between *T. gondii* infection and the expression of Arg-1 and iNOS, the percentage coinfection/co-expression between *T. gondii*/ Arg-1, *T. gondii*/ iNOS and Arg-1/iNOS was evaluated. (Figures 5.18, 5.19 and 5.20). To achieve that, each lung tissue /cell types expressing Arg-1 while infected with *T. gondii* or expressing iNOS while infected with *T. gondii* or co-expressing Arg-1 and iNOS was documented. This was conducted on the 51 clinical samples, and then the percentages were calculated. for all the 51clinical samples,

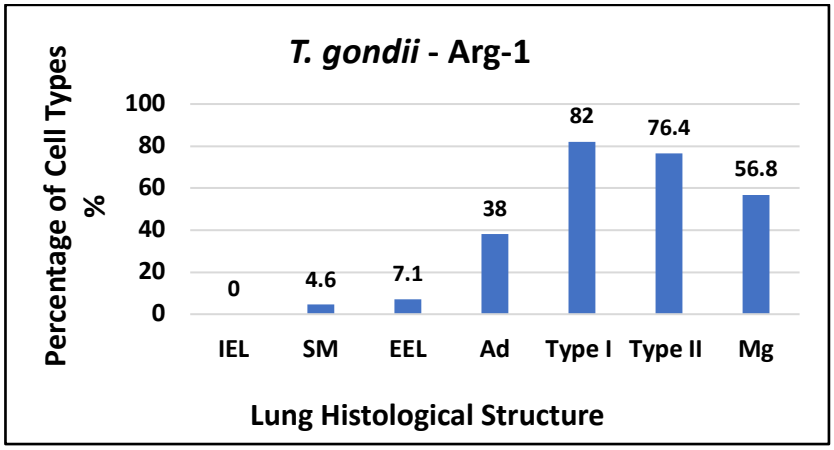

Figure 5.18 A graph illustrating the percentage of the association between the infection with *T. gondii* and the expression of Arg-1 across various lung tissue structures of lung cancer patients infected with *T. gondii* . IEL is Internal Elastic Lamina, VSM is Vascular Smooth Muscle, EEL is External Elastic Lamina, Ad is Adventitia, Type I pneumocytes, Type II pneumocytes and Mg is macrophages.

Regarding the association between *T. gondii* and the expression of Arg-1 (Figure 5.18), the highest co-expression percentage was at the Type I pneumocytes (82%) followed by 76.4%, 56.8%, 38% for Type I pneumocytes, Mg and Ad respectively. On the other hand, a much lower percentage of association was noticed at the EEL 7.1%, and the SM 4.6% and finally no association was found between the expression of Arg-1 and the infection with *T. gondii* at the IEL 0%.

With regards to the percentage of association between iNOS expression and the infection with *T. gondii* (Figure 5.19), considerably higher associations were documented than between *T. gondii* and Arg-1 expression. The highest association was documented with Type I pneumocytes (83.8%). The second highest association is marked by a 77% for Type II succeeded by 71.4% for the EEL. A relatively lower percentage of associations was established at the Ad 48%, SM 43% and Mg 25%. As with *T. gondii*/Arg-1, no association was found between the infection with *T. gondii* and the expression of iNOS at the level of the IEL.

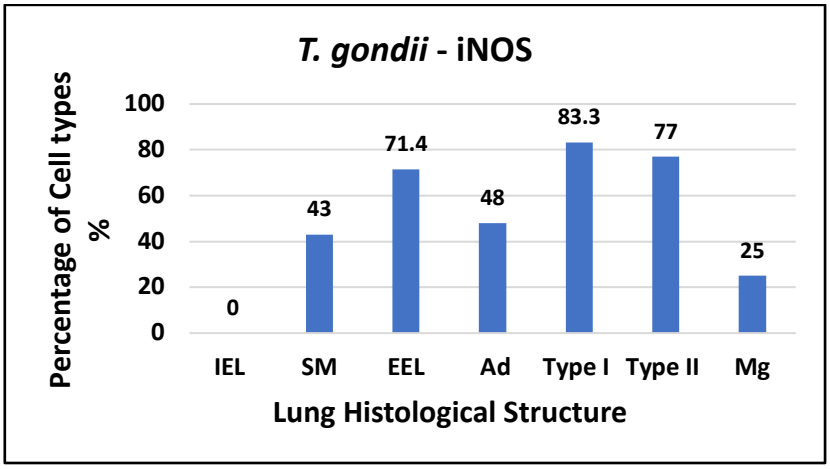

Figure 5.19 A graph illustrating the percentage of the association between the infection with *T. gondii* and the expression of iNOS across various lung tissue structures of lung cancer patients infected with *T. gondii* . IEL is Internal Elastic Lamina, VSM is Vascular Smooth Muscle, EEL is External Elastic Lamina, Ad is Adventitia, Type I pneumocytes, Type II pneumocytes and Mg is macrophages.

Finally, in order to evaluate the extent of the association between the expression of the two markers iNOS and Arg-1 in relation to *T. gondii* infection, the percentage of co-expression was calculated (Figure 5.20).

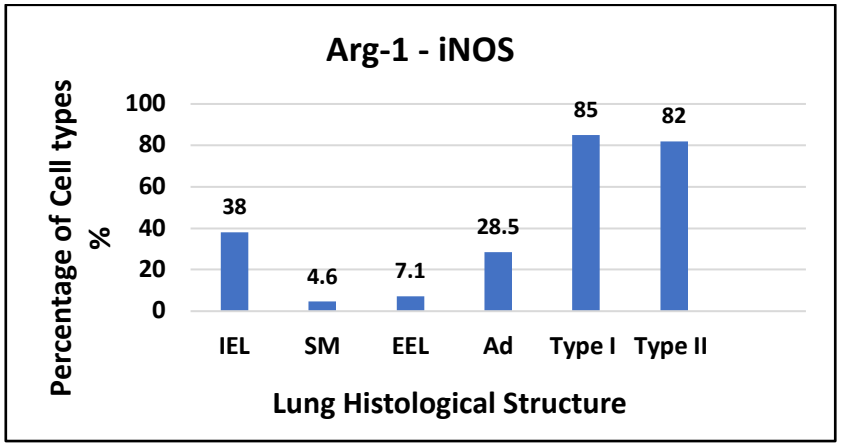

Figure 5.20 A graph illustrating the percentage of the co-expression between Arg-1 and iNOS across various lung tissue structures of lung cancer patients infected with *T. gondii* . IEL is Internal Elastic Lamina, VSM is Vascular Smooth Muscle, EEL is External Elastic Lamina, Ad is Adventitia, Type I pneumocytes, Type II pneumocytes and Mg is macrophages.

As noted with the previous analysis of the associations between *T. gondii*/Arg-1 and *T. gondii*/iNOS, the highest co-expression percentage was documented with Type I pneumocytes (85%) followed by Type II pneumocytes 82%. In contrast, other tissue types/cells have demonstrated a reasonably lower degree of co-expression with 38% at the IEL 28.5% and 7.1% at the Ad and EEL respectively. The lowest percentage of co-expression between Arg-1 and iNOS was documented at the SM, with only 4.6%. A summary graph of the percentage of the co-expressions established between Arg-1/*T. gondii*, iNOS/*T.gonddi* and Arg-1/iNOS across each lung tissue/cell types is listed below (Figure 5.21).

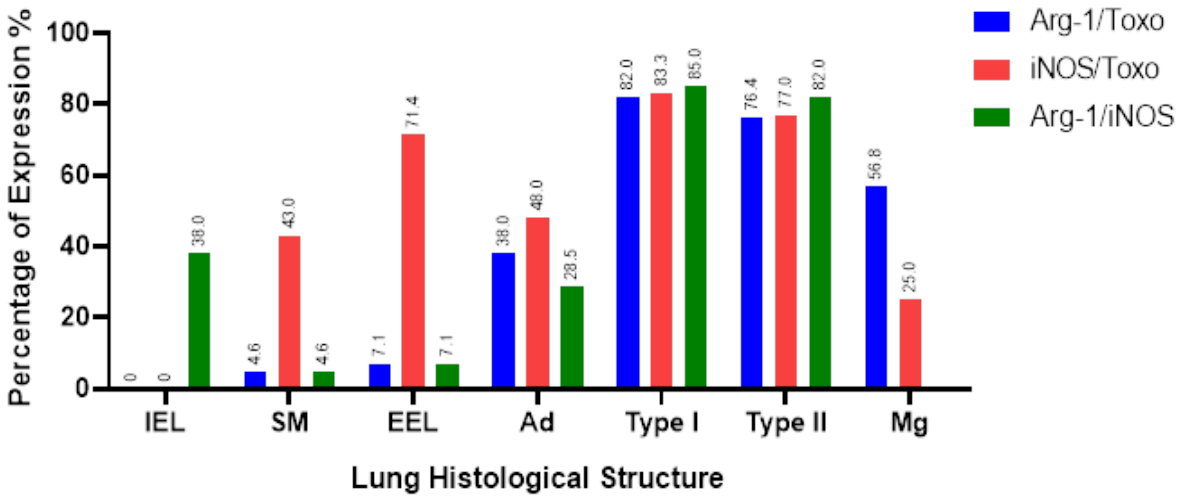

Figure 5.21 A summary graph illustrating the co-expression percentage between Arg-1/*T. gondii*, iNOS/ *T. gondii* and Arg-1/iNOS . IEL is Internal Elastic Lamina, SM is Vascular Smooth Muscle, EEL is External Elastic Lamina, Ad is Adventitia, Type I pneumocytes, Type II pneumocytes and Mg is alveolar macrophages.

5.3.7 Statistical analysis of the association between *T. gondii* infection and Arg-1 in different lung tissue types

In order to evaluate the significance of the associations established between the infection with *T. gondii* and the expression of Arg-1, and between the infection with *T. gondii* and the expression of iNOS, 2x2 contingency tables were constructed for each lung tissue type /cells in a total of 51

samples for the expression with Arg-1 iNOS and infection with *T. gondii*. Moreover, Fisher's exact test was conducted to evaluate the significance of these relationships.

The first layer of the blood vessel is the IEL, a 2x2 contingency table was constructed to assess the relationship between infection with *T. gondii* at the level of the IEL and the expression of Arg-1 (Table 5.11).

Table 5.11 A 2x2 contingency table with the frequency of infection of *T. gondii* in relation to Arg-1 expression at the IEL layer of the lung blood vessels **(Arg-1/*T. gondii*).**

	***T. gondii* +**	***T. gondii* -**	**Total**
Arg +	0	28	28
Arg -	0	18	18
Total	0	46	46

As noted from the table above, the IEL was not infected with *T. gondii* in any of the samples. Furthermore, Fisher's exact test *P*-value equals 1; hence, the association between the infection with *T. gondii* and the expression of Arg-1 at the level of IEL is not statistically significant.

The relationship between *T. gondii* infection and the expression of Arg-1 at the SM of blood vessels were assessed, and a 2x2 contingency table was produced (Table 5.12).

Table 5.12 A 2x2 contingency table with the frequency of infection of *T. gondii* in relation to Arg-1 expression at the SM layer of the lung blood vessels **(Arg-1/*T. gondii*).**

	***T. gondii* +**	***T. gondii* -**	**Total**
Arg +	2	0	3
Arg -	26	10	34
Total	25	12	37

Fisher's exact test *P*-value equals 1**,** establishing that the association between the infection with *T. gondii* and the expression of Arg-1 at the level of vascular SM is not statistically significant.

The third layer of the blood vessel that showcased infection with *T. gondii* and co-expressing Arg-1 is the EEL. In order to evaluate the link between *T. gondii* infection and the expression of Arg-1 at this layer, a 2x2 contingency table was constructed (Table 5.13).

Table 5.13 A 2x2 contingency table with the frequency of infection of *T. gondii* in relation to Arg-1 expression at the EEL layer of the lung blood vessels **(Arg-1/*T. gondii*).**

	***T. gondii* +**	***T. gondii* -**	**Total**
Arg +	3	1	4
Arg -	36	2	38
Total	39	3	42

Fisher's exact test with a *P* value of 0.26, establishing that the association between the expression of Arg-1 and the infection with *T. gondii* is not statistically significant at the level of the EEL.

The final layer of a blood vessel is the Ad, a 2x2 contingency table was created to estimate whether there is a relationship between *T. gondii* infection and Arg-1 expression at this layer (Table 5.14).

Table 5.14 A 2x2 contingency table with the frequency of infection of *T. gondii* in relation to Arg-1 expression at the Ad layer of the lung blood vessels **(Arg-1/*T. gondii*).**

	***T. gondii* +**	***T. gondii* -**	**Total**
Arg +	16	2	18
Arg -	12	9	21
Total	28	11	39

Fisher's exact test with a *P* value of 0.03**,** indicating that the association between the infection with *T. gondii* and the expression of Arg-1 is considered statistically significant at the level of the adventitia.

Three major cells of the alveolar spaces have demonstrated positive infection with *T. gondii* while expression Arg-1and/or iNOS are Type I pneumocytes, Type II pneumocytes and the alveolar

macrophages with both IHC and double immunofluorescence. As a means to establish the nature of the relationship between *T. gondii* infection and the expression of Arg-1 at these cells, a 2x2 contingency table was constructed (Table 5.15).

Table 5.15 A 2x2 contingency table with the frequency of infection of *T. gondii* in relation to Arg-1 expression in Type I pneumocyte **(Arg-1/*T. gondii*).**

	***T. gondii* +**	***T. gondii* -**	**Total**
Arg +	28	2	30
Arg -	1	2	3
Total	29	4	33

With a Fishers exact (P =0.03) the association between the infection with *T. gondii* and the expression of Arg-1 is considered statistically significant for Type I pneumocytes.

Additionally, for the purpose of evaluating if the association between the infection with *T. gondii* in Type II pyromucates and the expression of Arg-1 is significant, a 2x2 contingency table was constructed (Table 5.16).

Table 5.16 A 2x2 contingency table with the frequency of infection of *T. gondii* in relation to Arg-1 expression in Type II pneumocyte **(Arg-1/*T. gondii*).**

	***T. gondii* +**	***T. gondii* -**	**Total**
Arg +	26	3	29
Arg -	2	3	5
Total	28	6	34

With a Fishers exact (P =0.02) the association between the infection with *T. gondii* and the expression of Arg-1 is considered extremely statistically significant for Type II pneumocytes. A summary of the associations established between *T. gondii* infection and Arg-1 expression across the different lung/cell tissue types is listed in (Table 5.17).

Table 5.17 A summary table with the established relationships between *T. gondii* infection and Arg-1 expression across lung tissue/cells.

	Arg-1/*T. gondii*	***P-value***
IEL	No	$P=1$
SM	No	$P=1$
EEL	No	$P=0.26$
Ad	Yes	$P=0.03$
Type I	Yes	$P=0.03$
Type II	Yes	$P=0.02$

5.3.8 Statistical analysis of the association between *T. gondii* infection and iNOS in different lung tissue types

With the interest of assessing the nature of the relationship between infection with *T. gondii* and the expression of iNOS, and following the same approach on Arg-1/*T. gondii*, 2x2 contingency tables were constructed for each lung tissue type /cells in a total of 51 samples.

As evident before with IHC and double immunofluorescence analysis on lung cancer tissue samples targeting *T. gondii* as well as iNOS, the lung blood vessels showed infection and expression with iNOS. Assessing whether the association between the infection with *T. gondii* and the expression of iNOS at the first layer of blood vessels (IEL) is significant and 2x2 contingency table was created (Table 5.18) and Fisher's exact test was conducted.

Table 5.18 A 2x2 contingency table with the frequency of infection of *T. gondii* in relation to iNOS expression at the IEL layer of the lung blood vessels **(iNOS/*T. gondii*).**

	***T. gondii* +**	***T. gondii* -**	**Total**
iNOS +	0	24	24
iNOS -	0	19	19
Total	0	43	43

Fisher's exact test gave a (P = 1)**,** establishing that the association between the infection with *T. gondii* and the expression of iNOS at the level of IEL is not statistically significant.

Furthermore, a 2x2 contingency table was constructed to assess the association between *T. gondii* infection and the expression of iNOS at the smooth muscle layer of the blood vessel (Table 5.19).

Table 5.19 A 2x2 contingency table with the frequency of infection of *T. gondii* in relation to iNOS expression at the SM layer of the lung blood vessels **(iNOS/*T. gondii*).**

	***T. gondii* +**	***T. gondii* -**	**Total**
iNOS +	18	4	22
iNOS -	10	10	20
Total	28	14	42

Fisher's exact test with a (P =0.04)**,** establishing that the association between the infection with *T. gondii* and the expression of iNOS at the level of vascular SM is considered statistically significant.

Additionally, in aiming to assess the relationship between *T. gondii* infection and the expression of iNOS at the EEL layer of the blood vessels, a 2x2 contingency table was constructed (Table 5.20).

Table 5.20 A 2x2 contingency table with the frequency of infection of *T. gondii* in relation to iNOS expression at the EEL layer of the lung blood vessels **(iNOS/*T. gondii*).**

	***T. gondii* +**	***T. gondii* -**	**Total**
iNOS +	30	0	30
iNOS -	10	3	13
Total	35	3	43

Fisher's exact test with a (P =0.02)**,** demonstrating that the association between the infection with *T. gondii* and the expression of iNOS at the level of EEL is statistically significant.

Furthermore, in aiming to establish the association between *T. gondii* infection and the expression of iNOS at the Ad layer of the blood vessel, a 2x2 contingency table was created (Table 5.21).

Table 5.21 A 2x2 contingency table with the frequency of infection of *T. gondii* in relation to iNOS expression at the Ad layer of the lung blood vessels **(iNOS/*T. gondii*).**

	***T. gondii* +**	***T. gondii* -**	**Total**
iNOS +	20	7	27
iNOS -	10	6	16
Total	30	13	43

Fisher's exact test with a P = 0.5**,** demonstrating that the association between the infection with *T. gondii* and the expression of iNOS at the level of Ad is not statistically significant.

Moreover, in aiming to establish the association between *T. gondii* infection and the expression of iNOS in Type I pneumocyte, a 2x2 contingency table was created (Table 5.22).

Table 5.22 A 2x2 contingency table with the frequency of infection of *T. gondii* in relation to iNOS expression in Type I pneumocyte **(iNOS/*T. gondii*).**

	***T. gondii* +**	***T. gondii* -**	**Total**
iNOS +	25	2	27
iNOS -	1	2	3
Total	26	4	30

Fisher's exact test with a (P =0.03)**,** demonstrating that the association between the infection with *T. gondii* and the expression of iNOS in Type I pneumocytes is statistically significant.

Additionally, for the purpose of evaluating if the association between the infection with *T. gondii* in Type II pneumocytes and the expression of iNOS is significant, a 2x2 contingency table was constructed (Table 5.23).

Table 5.23 A 2x2 contingency table with the frequency of infection of *T. gondii* in relation to iNOS expression in Type II pneumocyte **(iNOS/*T. gondii*).**

	***T. gondii* +**	***T. gondii* -**	**Total**
iNOS +	21	2	23
iNOS -	1	3	4
Total	22	5	27

Fisher's exact test with a (P =0.01)**,** demonstrating that the association between the infection with *T. gondii* and the expression of iNOS in Type II pneumocytes is extremely statistically significant. A summary of the associations established between *T. gondii* infection and iNOS expression across the different lung/cell tissue types is listed in (Table 5.24).

Table 5.24 A summary table with the established relationships between *T. gondii* infection and iNOS expression across lung tissue/cells.

	iNOS/*T. gondii*	***P-value***
IEL	No	*P* =1
SM	Yes	*P* =0.04
EEL	Yes	*P* =0.02
Ad	No	*P* =0.5
Type I	Yes	*P* =0.03
Type II	Yes	*P* =0.01

5.3.9 Statistical analysis of the association between the expression of Arg-1 and iNOS in different lung tissue types while infected with *T. gondii*.

After establishing different associations between *T. gondii*/Arg-1 and *T.gondi*/iNOS at different lung tissue types/cells, there was a need to assess the relationships between the two markers Arg-1 and iNOS in relation to infection with *T. gondii* in the same tissue types assessed previously. In that aim, 2x2 contingency tables were established to evaluate the co-expression significance between Arg-1 and iNOS in lung cancer patients while infected with *T. gondii*.

Lung blood vessels have demonstrated positive expression of both Arg-1 and iNOS with both IHC and double immunofluorescence while infected with *T. gondii*. Assessing the significance of co-expression between Arg-1 and iNOS at the level of the first layer of lung blood vessels (IEL), a 2x2 contingency table was constructed (Table 5.25) and Fisher's Exact test was conducted.

Table 5.25 A 2x2 contingency table with the frequency of co-expression between Arg-1 and iNOS at the IEL layer of the lung blood vessels **(Arg-1/iNOS).**

	iNOS +	**iNOS -**	**Total**
Arg +	**16**	**10**	**26**
Arg -	**6**	**5**	**11**
Total	**22**	**15**	**37**

Fisher's exact test constructed a P value of 0.72, therefore, the co-expression between Arg-1 and iNOS at the level of the IEL is not statistically significant.

Moreover, co-expression of Arg-1 and iNOS was evaluated by a 2x2 contingency table at the vascular smooth muscle (Table 5.26).

Table 5.26 A 2x2 contingency table with the frequency of co-expression between Arg-1 and iNOS at the SM layer of the lung blood vessels **(Arg-1/iNOS).**

	iNOS +	**iNOS -**	**Total**
Arg +	**2**	**1**	**3**
Arg -	**20**	**18**	**38**
Total	**22**	**19**	**41**

Fisher's exact test with a P value of 1; thus, the co-expression between the two markers Arg-1 and iNOS is not statistically significant at the level of the vascular smooth muscle of the lungs.

Assessing whether there is an association between the expression of Arg-1 and iNOS at the level of EEL, a2x2 contingency table was constructed (Table 5.27).

Table 5.27 A 2x2 contingency table with the frequency of co-expression between Arg-1 and iNOS at the EEL layer of the lung blood vessels **(Arg-1/iNOS).**

	iNOS +	**iNOS -**	**Total**
Arg +	**3**	**1**	**4**
Arg -	**26**	**11**	**37**
Total	**29**	**12**	**41**

Fisher's exact test with a P value of 1**,** illustrating that the co-expression between the Arg-1 and iNOS the level of EEL is not statistically significant.

Finally, to establish the significance of the co-expression between Arg-1 and iNOS in the last layer of the lung blood vessels, the Ad, a 2x2 contingency table was constructed (Table 5.28).

Table 5.28 A 2x2 contingency table with the frequency of co-expression between Arg-1 and iNOS at the Ad layer of the lung blood vessels **(Arg-1/iNOS).**

	iNOS +	**iNOS -**	**Total**
Arg +	**12**	**6**	**18**
Arg -	**13**	**9**	**22**
Total	**25**	**15**	**40**

Fisher's exact test with a *P* value of 0.74**,** showing that the co-expression between the Arg-1 and iNOS the level of Ad is not statistically significant.

One of the major structures of the lung that demonstrated expression of Arg-1 and iNOS and infection with *T. gondii*, are the alveolar spaces, in particular, the alveolar wall which is made up of 2 types of cells (type I and II pneumocytes). 2x2 contingency tables were used to assess the relationship between the expression of iNOS and Arg-1 in relation to *T. gondii* infection in type I and type II pneumocytes (Tables 5.29-5.30), and a Fisher's Exact test was conducted.

Table 5.29 A 2x2 contingency table with the frequency of co-expression of Arg-1 and iNOS in Type I pneumocyte **(Arg-1/iNOS).**

	iNOS +	**iNOS -**	**Total**
Arg +	23	1	24
Arg -	1	2	3
Total	24	3	27

Fisher's Exact test *P* =0.02; hence, the association between the co-expression of Arg-1 and iNOS was found to be statistically significant in type I pneumocytes.

Finally, in aiming to establish the co-expression status between Arg-1 and iNOS in Type II pneumocytes, a 2x2 contingency table was created (Table 5.30) and Fisher's exact test conducted.

Table 5.30 A 2x2 contingency table with the frequency of infection of *T. gondii* in relation to Arg-1 expression in Type II pneumocyte **(Arg-1/iNOS).**

	iNOS +	**iNOS -**	**Total**
Arg +	23	1	24
Arg -	0	4	4
Total	23	5	28

Fisher's Exact test P =0.0002; hence, the association between the co-expression of Arg-1 and iNOS was found to be very highly statistically significant in type II pneumocytes. A summary of the co-expressions established between Arg-1 and iNOS expression across the different lung/cell tissue types is listed in (Table 5.31).

Table 5.31 A summary table with the co-expressions established between Arg-1 and iNOS expression across lung tissue/cells.

	Arg-1/iNOS	***P-value***
IEL	No	P =0.72
SM	No	P =1
EEL	No	P =1
Ad	No	P =0.74
Type I	Yes	P =0.02
Type II	Yes	P =0.0002

In summary, the associations established between *T. gondii* infection and the expression of Arg-1 were at the Ad, Type I and Type II pneumocytes. On the other hand, the links between the expression of iNOS and the infection with *T. gondii* was found to be significant at the SM, EEL, Type I, and Type II pneumocytes. Finally, co-expression between Arg-1 and iNOS relative to *T. gondii* infection was found to be significant only at Type I and Type II pneumocytes. A summary of the associations established is listed in the table below (Table 5.32).

Table 5.32 Summary table of the associations between Arg-1 and iNOS expression in relation to *T. gondii* infection in different lung tissue/cells of lung cancer samples.

	IEL	**SM**	**EEL**	**Ad**	**Type I pn**	**Type II pn**
***T. gondii*- Arg-1**	No	No	No	Yes	Yes	Yes
***T. gondii*- iNOS**	No	Yes	Yes	No	Yes	Yes
iNOS-Arg-1	No	No	No	No	Yes	Yes

5.3.10 Statistical analysis of the association between *T. gondii* infection and Arg-1 and iNOS in alveolar macrophages.

Alveolar macrophages are considered a major part of the immune system and play an important role in the defence against various organisms (Fraser, 2005). As previously established by IHC and double immunofluorescence targeting *T. gondii* infection in relation to iNOS and Arg-1, alveolar macrophages showed infection and expression of both Arg-1 and iNOS. With the purpose of evaluating the nature of involvement of alveolar macrophages in the process of *T. gondii* infection with respect to Arg-1 and iNOS expression, alveolar macrophages were identified with their characteristic mononuclear spherical shape. Cells were then counted according to whether they are independently expressing Arg-1, or independently infected with *T. gondii*, or both. A detailed table, below, shows the results (Table 5.33) obtained from those clinical samples where alveolar macrophages could be accurately determined.

Table 5.33 Counts of alveolar macrophages in clinical lung cancer samples stained with double immunofluorescence (Arg-1/*T. gondii).*

Sample	Total (Mg)	No expression	Arg-1	*T. gondii*	*T. gondii*/Arg-1	%*T. gondii* infected Mgs/Arg-1
988	4	1	2	0	1	25%
989	5	0	2	0	3	60%
1025	13	3	2	1	7	54%
1030	30	12	1	0	28	93%
1040	11	5	0	0	6	54%
1064	4	0	0	0	0	0%
664	15	1	12	1	1	2%
757	6	0	1	0	5	83%
813	7	0	4	0	3	43%
1004	24	0	18	0	6	25%
1068	11	3	1	0	7	63%
1069	22	0	5	0	17	77%
1072	15	0	3	1	11	73%
Total	167	25	51	3	95	56.88%

From the table above it can be established that the average percentage of *T. gondii* infected alveolar macrophages which are expressing Arg-1 is 56.88%.Nevertheless, in order to assess the significance of the co-existence between *T. gondii* infection and expression of Arg-1, a 2x2 contingency table was established (Table 5.34) and Fisher's exact test was conducted.

Table 5.34 A 2x2 contingency table of the frequency of alveolar macrophages infected with *T. gondii* in relation to Arg-1 expression in lung cancer clinical samples**.**

	T. gondii +	*T. gondii* -	Total
Arg-1 +	95	51	146
Arg-1 -	3	25	28
Total	98	76	174

Fisher's exact test was conducted, *P-value* (*P*=0.0001) suggesting that the association between the expression of Arg-1 in relation to *T. gondii* in the alveolar macrophages is very highly statistically significant.

In the interest of comparing the outcome of the co-existence between iNOS and *T. gondii* in alveolar macrophages, the same approach conducted on alveolar macrophages infected with *T. gondii* and expressing iNOS was done. The results are shown below (Table 5.35), listing the alveolar macrophage count according to whether they are independently expressing iNOS, independently infected with *T. gondii*, or both (Table 5.35). Only clinical samples where macrophages could be accurately identified were used.

Table 5.35 Counts of alveolar macrophages in lung cancer samples stained with double immunofluorescence (iNOS/*T. gondii)*.

Sample	**Total (Mg)**	**No expression**	**iNOS**	***T. gondii***	***T. gondii*/iNOS**	**%*T. gondii* infected Mgs/iNOS**
988	3	0	3	0	0	0%
989	5	0	4	0	1	20%
1025	10	1	8	0	1	10%
1030	16	2	14	0	0	0%
1040	5	0	4	0	0	0%
1064	2	0	0	0	2	100%
664	19	5	13	0	1	5.2%
757	12	0	4	0	8	66%
813	21	4	5	0	12	57%
1004	15	0	13	0	2	13%
1068	9	0	3	0	6	66%
1069	13	0	9	0	4	31%
1072	22	0	21	0	1	4.5%
Total	152	12	101	0	38	25%

As stated in the table above it can be noted that average percentage of *T. gondii* infected alveolar macrophages which are expressing iNOS is 25%, which is considerably lower compared to

average 56.88% of alveolar macrophages infected *T. gondii* co-expressing Arg-1. With the aim to appraise whether the co-existence between *T. gondii* infection in alveolar macrophages while expression iNOS is significant, a 2x2 contingency table was constructed (Table 5.36) and Fisher's exact test was performed.

Table 5.36 A 2x2 contingency table of the frequency of alveolar macrophages infected with *T. gondii* in relation to iNOS expression in lung cancer clinical samples**.**

	***T. gondii* +**	***T. gondii* -**	**Total**
iNOS +	38	101	139
iNOS -	0	12	12
Total	38	113	151

Fisher's exact test was conducted, *P-value* (P=0.03) indicating that the association between the expression of iNOS in relation to *T. gondii* in the alveolar macrophages is statistically significant.

5.3.11 Establishing the relationship between the percentage of infected alveolar macrophages co-expressing Arg-1 or iNOS and the overall grade of *T. gondii* infection using Spearman's rank correlation

In order to evaluate the association between the percentage of *T. gondii* infected alveolar macrophages expressing Arg1 and the grade of *T. gondii* infection (established in a previous study by Bajnok, 2017), Spearman's rank correlation has been used (Table 5.37).

Table 5.37 A list of the percentage of *T. gondii* infected alveolar macrophages while co-expressing either Arg-1or iNOS and the grade of the overall *T. gondii* infection per sample.

Sample number	% of infected Arg-1	% of infected iNOS	Grade of *T. gondii* infection
988	25%	0%	2
989	60%	20%	3
1025	54%	10%	3
1030	93%	0%	3
1040	54%	0%	3
1064	0%	100%	1
664	2%	5.20%	1
757	83%	66%	3
813	43%	57%	2
1004	25%	13%	3
1068	63%	66%	3
1069	77%	31%	3
1072	73%	4.50%	3

T+he association between the percentage of macrophages expressing Arg-1 while infected with *T. gondii* and the grade of infection is considered statistically significant, $r_s = 0.76$, and a *P-value* of 0.002, indicating that the higher the percentage of *T. gondii* infected macrophages expressing Arg-1, the higher the grade of *T. gondii* infection.

On the other hand, Spearman's' rank was used to measure the association between macrophages infection with *T. gondii* while co-expressing iNOS with the *T. gondii* infection grade $r_s = -0.12$, *P-value* of 0.67, indicating that the association between the percentage of macrophages expression iNOS while infected with *T. gondii* parasite and the grade of infection is considered not statistically significant.

5.3.12 Quantitative analysis of the colocalisation between *T. gondii* infection and Arg-1/iNOS in alveolar macrophages using Pearson's Correlation Coefficient (PCC)

In order to measure actual colocalisation between the expression of iNOS/Arg-1 and *T. gondii,* JACoP software was used (Jacop ref). Different methods were used to measure colocalisation including Pearson's Correlation Co-efficient (PCC), Mander's Correlation Co-efficient (MCC) and Costes randomisation test. In this section, the use of PCC is discussed.

In the interest of establishing a quantitative analysis of the colocalisation between *T. gondii* infection and Arg-1 expression, as well as *T. gondii* infection and iNOS expression, co-localisation was measured for the 51 tested clinical samples. Each macrophage that is co-expressing Arg-1/*T. gondii* and iNOS/*T. gondii,* was outlined using a special tool of JACoP, Region Of Interest (ROI) to evaluate each macrophage individually. PCC was conducted on alveolar macrophages for the 51-lung cancer clinical samples. PCC is a metric method that measures the correlation between the signal intensities in one image and the equivalent values in another. The PCC values range from 1 to -1, where a PCC of 1 refers to two images in which their fluorescence intensities are perfectly, linearly related, whereas a PCC value of -1 reflects two images whose fluorescence intensities are perfectly, but inversely, related to one another. Values close to zero represent distributions of probes that are uncorrelated with one another.

After the measurement of PCC was performed, a randomisation test (Costes test) is conducted on each alveolar macrophage to determine whether the result obtained is true colocalisation (Costes et al., 2004). This approach offers a statistical comparison that may exclude colocalisation of pixels due to chance. The test is constructed by scrambling the pixels randomly in one image, and after that, the correlation (r) is measured with the other (unscrambled) image. This is performed 200 times, and at each sift the correlation (r) value is calculated and a *P-value* of >95% indicates significant true colocalisation.

In (Figure 5.22), a Costes test analysis was run on the alveolar macrophages, shown in Figure 5.22.A, is the randomisation test that was performed on colocalisation between *T. gondii* and Arg-1 and the PCC value for this image pair is high with a value of 0.534. The green signal, which represents *T. gondii,* was then randomly scrambled 200 times using pixel blocks and the PCC value was calculated for each shift. A histogram of the resulting PCC values was calculated for 200 scrambled green (*T. gondii*) versus the unscrambled red (Arg-1) image is shown in (Figure

5.22.A). The red arrow indicates the true (unscrambled) PCC value. In this case, the true PCC value exceeds all of those calculated for the randomly scrambled images. On the other hand (Figure 5.22.B) is the randomisation test performed on the colocalisation between *T. gondii* and iNOS for one of the alveolar macrophage and the PCC value for this image pair is relatively low with the red arrow representing the true value of PCC = 0.162 and the true PCC value exceeds all of those calculated for the randomly scrambled images. In both cases (Figure 5.22.A and B), representing the PCC of *T. gondii* and Arg-1, and *T. gondii* and iNOS respectively, the *P-value* for the Costes test gave a value of 1, therefore, indicating a high statistical confidence in the PCC results and a high probability that the colocalisation calculated for these images is significant and is not due to chance. A table with the colocalisation measurements listing the PCC and Costas values for the colocalisation between *T. gondii* and Arg-1 and between *T. gondii* and iNOS for each alveolar macrophage can be found at the supplementary appendix D (Table 7.2 and 7.3).

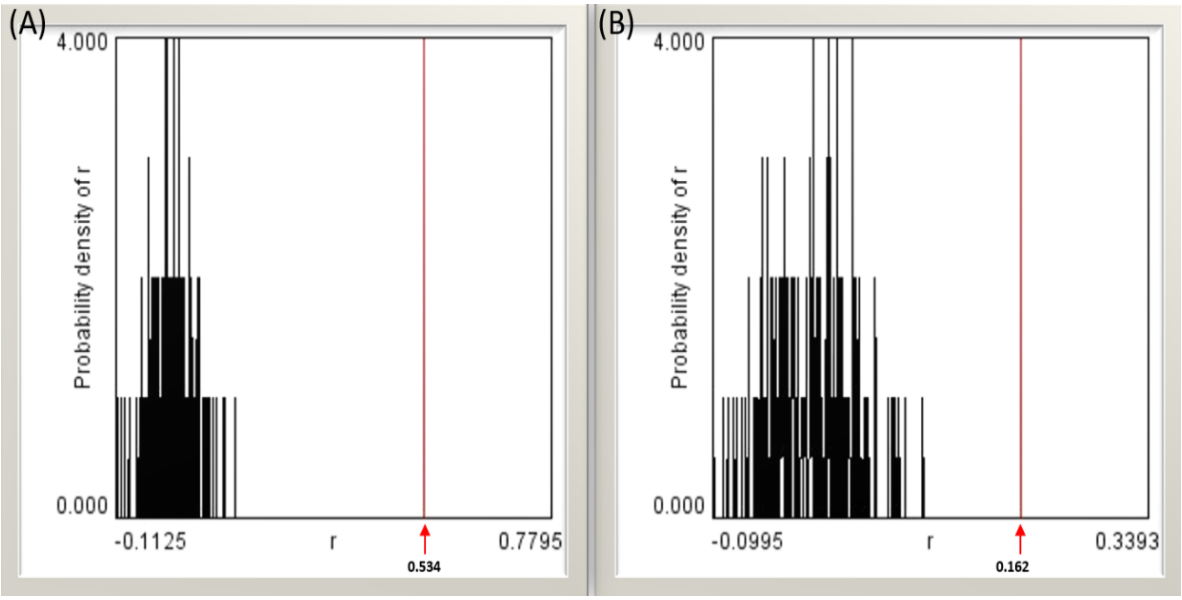

Figure 5.22 Plot of the distribution of the Pearson's coefficients (PCs) of randomised images (curve) and of the green channel image (*T. gondii*) indicated by the (red line) . The red line indicates the PC and the curve shows the probability distribution of the PCs of the randomised images. (A) is the randomisation test performed on colocalisation between *T. gondii* and Arg-1 of alveolar macrophages of lung cancer subjects PCC = 0.534. While (B), is the randomisation test performed on colocalisation between *T. gondii* and iNOS, PCC = 0.162. Note that the *P-value* for this analysis was 1 in both (A) and (B) indicating a high probability of colocalisation.

After the measurement of PCC and the Costes analysis was conducted, only the alveolar macrophages with true colocalisation were included and the average PCC was calculated for the colocalisation between *T. gondii* infection and Arg-1, as well as for *T. gondii* infection and iNOS.

5.3.13 Establishing the differences in colocalisation between *T. gondii*/Arg-1 and *T. gondii*/iNOS, in the alveolar macrophages using Pearson's Correlation Coefficient (PCC)

The average PCC of alveolar macrophages infected with *T. gondii* and expressing Arg-1 is 0.5 while the average PCC of alveolar macrophages infected with *T. gondii* and expressing iNOS is much lower with an average of 0.175 (Figure 5.23).

In order to determine whether the colocalisation between *T. gondii* and Arg-1 is statically significant compared to the colocalisation between *T. gondii* and iNOS in the alveolar macrophages of lung cancer subjects, a two-tailedd student t-test was performed to compare the averaged means of PCC of the two groups. The *P-value* is < 0.00001 (Figure 5.23), indicating that there is a an very highly significant difference in the colocalisation between *T. gondii* /Arg-1 and *T. gondii*/iNOS, thereby, the colocalisation of *T. gondii*/Arg-1 at the alveolar macrophages is higher than the colocalisation of *T. gondii* and iNOS in the alveolar macrophages.

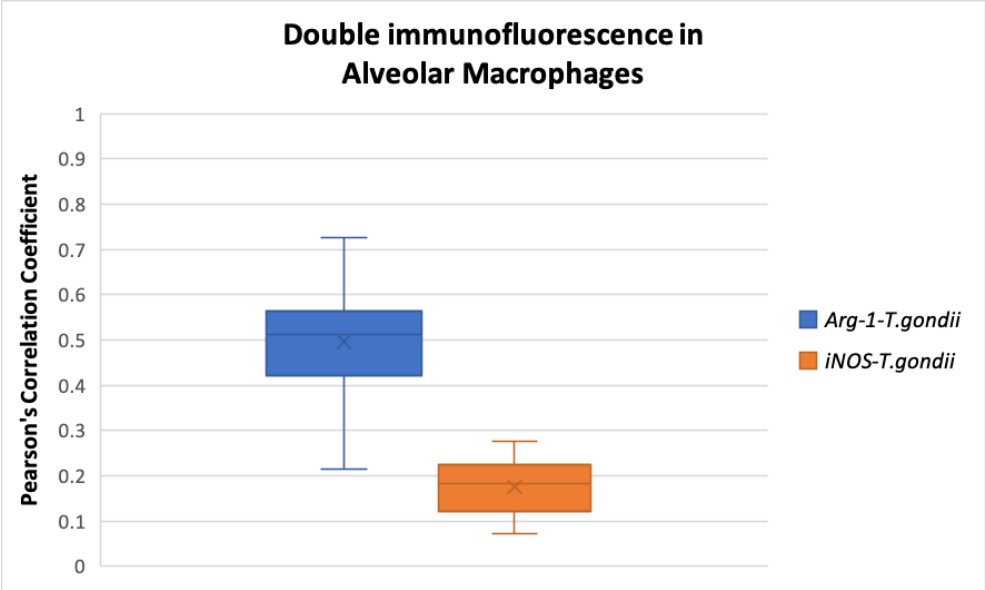

Figure 5.23 Quantitative colocalisation analysis of double immunofluorescence (PCC), comparing the distribution of *T. gondii* infecting with either Arg-1 or iNOS in alveolar macrophages of lung cancer subjects . The distribution of Arg-1 is much more highly correlated with *T. gondii* (r =0.5, n = 41) than with iNOS (r = 0.175, n = 34) at the alveolar macrophage level. Differences between the two groups were statistically significant, with *P-value* of < 0.00001.

5.3.14 Quantification of the colocalisation between *T. gondii* infection and Arg-1/iNOS in alveolar macrophages using Manders Correlation Coefficient (MCC)

Another method for measuring colocalisation that can be used is Manders correlation coefficient (MCC), with its split correlation co-efficient (M1and M2), in which it expresses the extent of co-occurrence between two images. The values range from 0-1, where a value of 1 means perfect overlap while a zero value represents no overlap between the two images.

MCC measurement was established on all of the samples, and the average values for the split co-efficient (M1) and (M2) were calculated for the colocalisation between *T. gondii* infection and Arg-1, as well as for *T. gondii* infection and iNOS. A table with the colocalisation measurements listing the values of (M1) and (M2) for each alveolar macrophage for the colocalisation between *T. gondii* and Arg-1 and between *T. gondii* and iNOS for each can be found at the supplementary appendix D (Table7.2 and 7.3).

In Figure 5.24, (M1-Arg-1) is the average proportion of red pixels (Arg-1) overlapping with green pixels (*T. gondii)* with a value of 0.69, while (M2-Arg-1) is the average proportion of green pixels (*T. gondii*) overlapping with red pixels *(*Arg-1) with a value of 0.74 in alveolar macrophages double labelled with Arg-1-*T. gondii.*

On the other hand, alveolar macrophages double labelled with iNOS-*T. gondii,* (M1-iNOS) is the average proportion of red pixels (iNOS) overlapping with green pixels (*T. gondii)* with a value of 0.53, while (M2-iNOS) is the average proportion of green pixels (*T. gondii*) overlapping with red pixels *(*iNOS) with a value of 0.56.

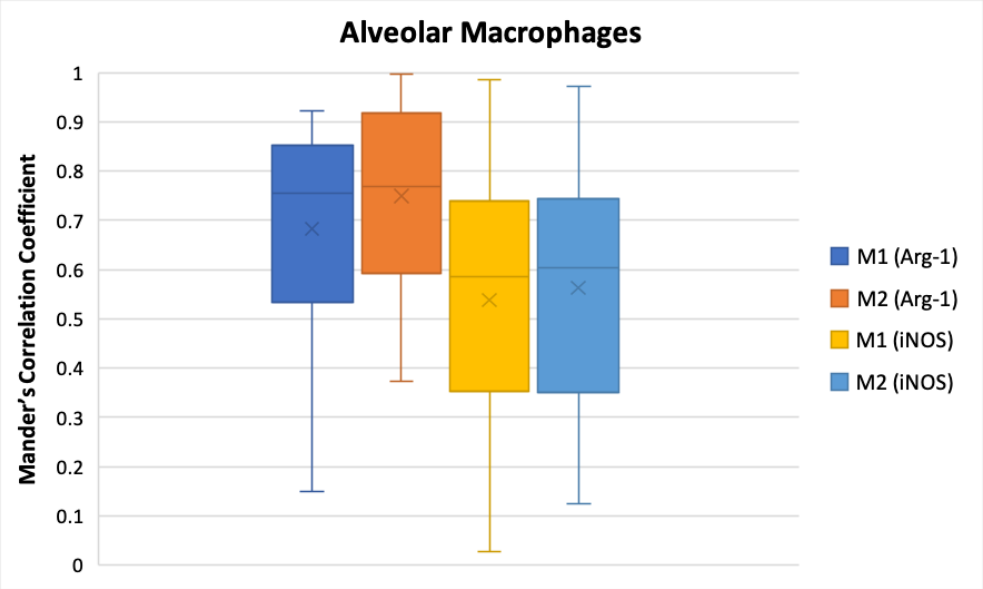

Figure 5.24 Quantitative colocalisation analysis of double immunofluorescence of *T. gondii* and Arg-1, and between *T. gondii* and iNOS in alveolar macrophages . (M1) is the fraction of red pixels overlapping with green pixels, while (M2) is the fraction of green pixels overlapping with green.

In the interest of establishing whether there is a significant difference between the averages overlap between *T. gondii*-Arg-1 double labelled alveolar macrophages, and *T. gondii*/-iNOS double labelled alveolar macrophages, a two-sample student t-test was conducted to compare between the average overlap of (M1) of samples double labelled with Arg-1-*T. gondii,* which is the proportion of red pixels (Arg-1) co-occurring with green pixels (*T. gondii*), with (M1) of samples double labelled with iNOS-*T. gondii,* which is the proportion of red pixels (iNOS) co-

occurring with green pixels. With a *P-value* of 0.008231, the result is very highly significant, indicating that there is a significant difference between the average overlap values (M1) and that the average Arg-1 (red) pixels overlapping with *T. gondii* (green) is significantly higher than the iNOS (red) pixels overlapping with *T. gondii* (green).

5.3.15 Establishing the differences in colocalisation between *T. gondii*/Arg-1 and *T. gondii*/iNOS, in the alveolar macrophages with Manders Correlation Coefficient (MCC)

Furthermore, to evaluate the difference between the split co-efficient (M2) averages in alveolar macrophages, a two-sample student t-test was conducted to compare between the average overlap of (M2-Arg-1) of samples double labelled with Arg-1-*T. gondii* which is the proportion of green pixels (*T. gondii*) co-occurring with red pixels (*Arg-1*), with (M2-iNOS) of samples double labelled with iNOS-*T. gondii,* which is the proportion of green pixels (*T. gondii*) co-occurring with red pixels (iNOS). With a *P-value* of 0.000402, the result is very highly significant, hence, here is a significant difference between the average overlap values (M2) and that the average *T. gondii* (green) pixels overlapping with Arg-1 (red) is significantly higher than the *T. gondii* (green) pixels overlapping with iNOS (red).

5.3.16 Quantitative analysis of the colocalisation between *T. gondii* infection and Arg-1/iNOS in *T. gondii* cysts using Pearson's Correlation Coefficient (PCC)

Out of the 51-lung cancer clinical samples analysed, a total of 3 cysts were found (image 5.25-5.26 and 5.27). Cyst represent the dormant stage of the parasite and have the potential to rupture and release thousands of bradyzoites. With the interest of establishing a quantitative analysis of the colocalisation between the expression of Arg-1 in the *T. gondii* cysts, as well as between iNOS expression and *T. gondii* cyst, each cyst was outlined by a special tool of JACoP, Region Of Interest (ROI) to evaluate each cyst individually, and the same colocalisation approach applied on the alveolar macrophages was applied to the *T. gondii* cysts. Correlation coefficients including PCC and MCC with its split co-efficient (M1 and M2) were measured. Additionally, the Costes randomisation test values were determined for the three *T. gondii* cysts. A table with the

colocalisation measurements listing the PCC and Costes values for the colocalisation between *T. gondii* cysts and Arg-1 and between *T. gondii* cysts and iNOS for each cyst individually can be found at the supplementary appendix D (Tables 7.4 and 7.5).

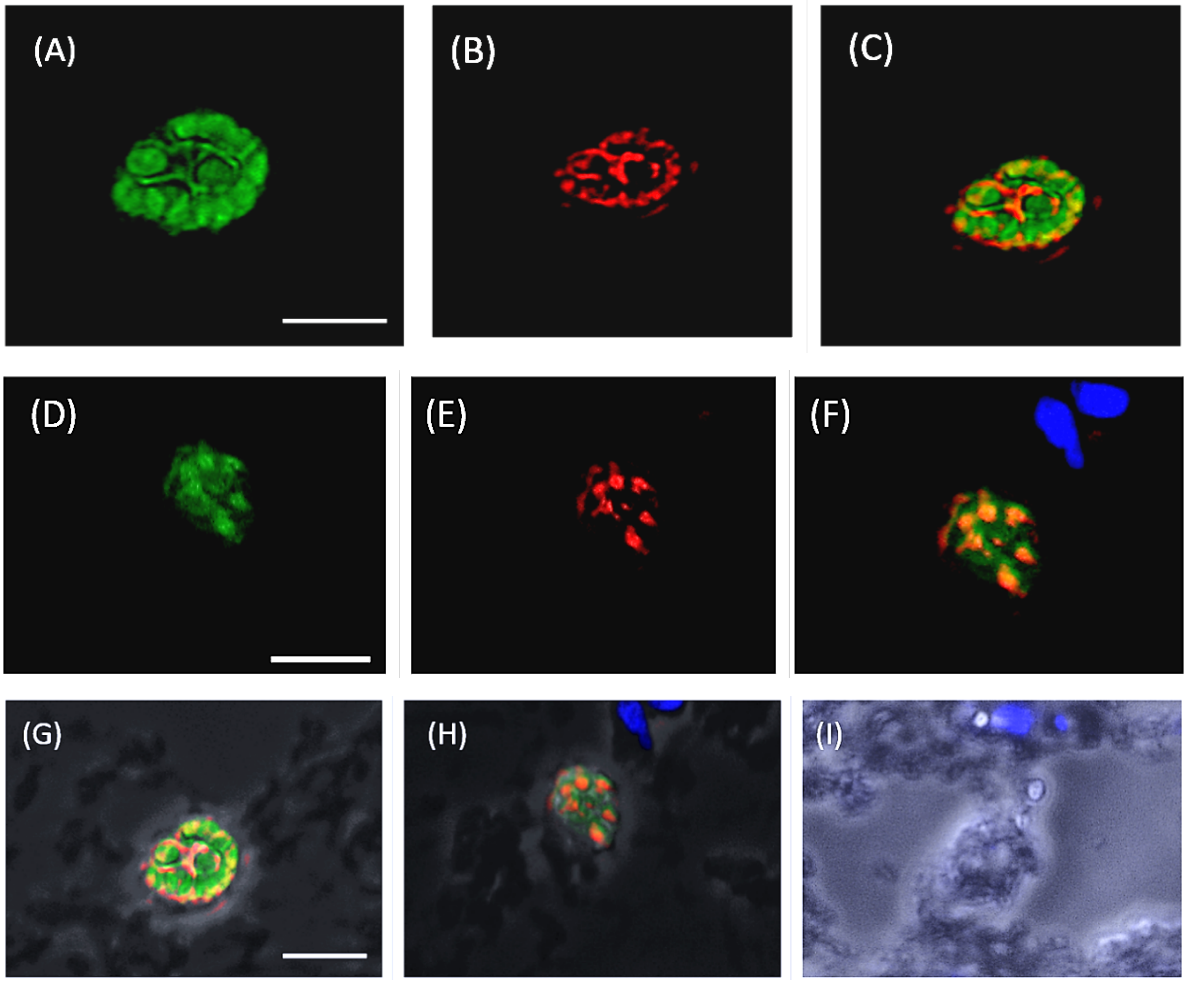

Figure 5.25 Arg-1 and *T. gondii* double immunofluorescent in a cyst from sample 1008. (**A**) is *T. gondii* (**B**) is Arg-1 and (**C**) is the merged image of *T. gondii* and Arg-1, the PCC is 0.116. The second panel of images is iNOS and *T. gondii* double immunofluorescent showing a cyst of the same sample 1008. (**D**) is *T. gondii* (**E**) is iNOS and (**F**) is the merged image of *T. gondii* and iNOS, the Pearson's Correlation Coefficient (PCC) is 0.671. (**G**) is the overlay of the merged (*T. gondii*, Arg-1 and DAPI stains) on a black and white image of the tissue. (**H**) is the overlay of the merged (*T. gondii*, iNOS and DAPI stains) on a black and white image of the tissue. (**I**) is the negative control. Scale bar = 20 μm. Image magnification x40.

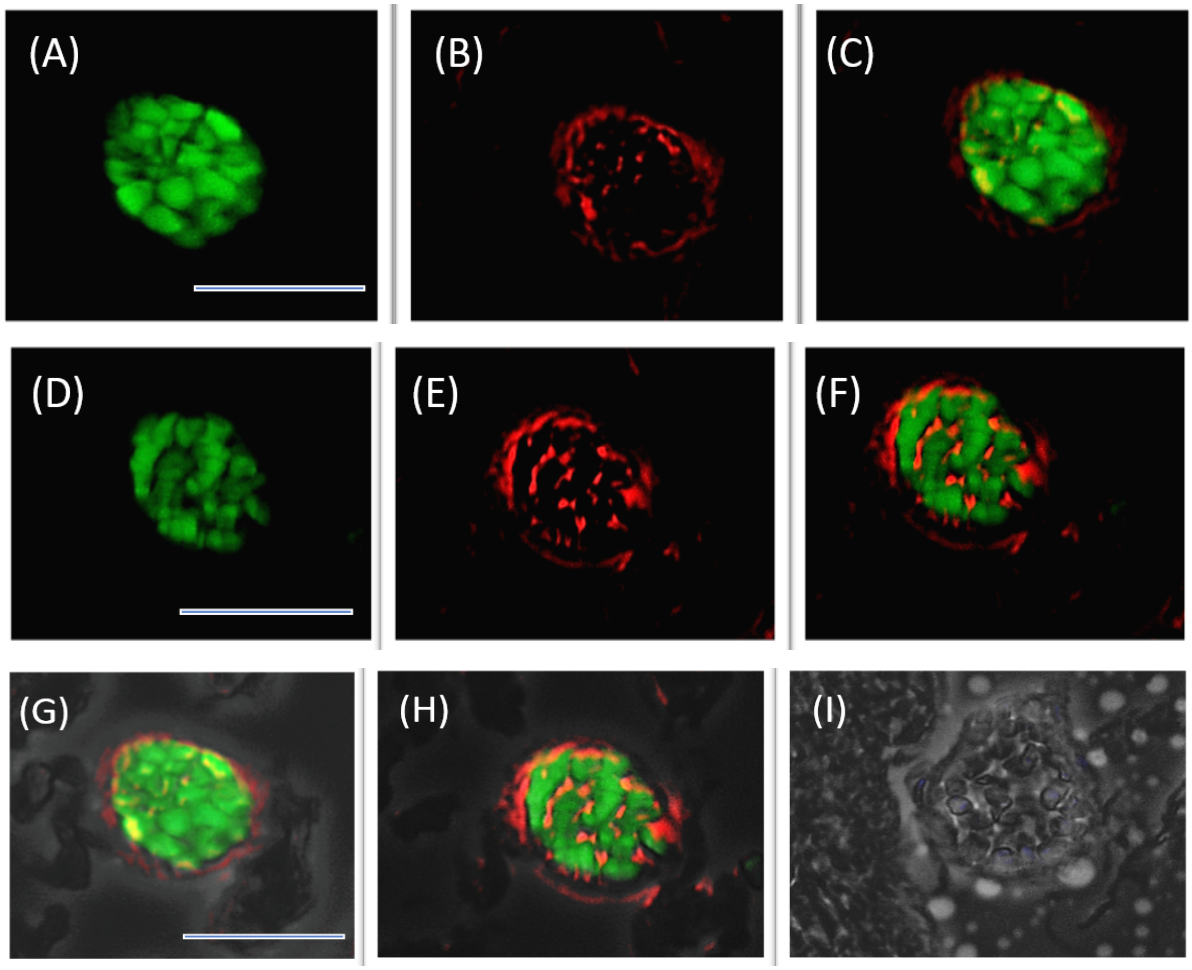

Figure 5.26 Arg-1 and *T. gondii* double immunofluorescent representing a cyst from sample 1045. (**A**) is *T. gondii* (**B**) is Arg-1 and (**C**) is the merged image of *T. gondii* and Arg-1, the Pearson's Correlation Coefficient (PCC) is 0.076. The second panel of images is iNOS and *T. gondii* double immunofluorescent showing a cyst of the same sample 1045. (**D**) is *T. gondii* (**E**) is iNOS and (**F**) is the merged image of *T. gondii* and iNOS, the Pearson's Correlation Coefficient (PCC) is 0.435. (**G**) is the overlay of the merged (*T. gondii*, Arg-1 and DAPI stains) on a black and white image of the tissue. (**H**) is the overlay of the merged (*T. gondii*, iNOS and DAPI stains) on a black and white image of the tissue. (I) is the negative control. Scale bar = 20 µm. Image magnification x40.

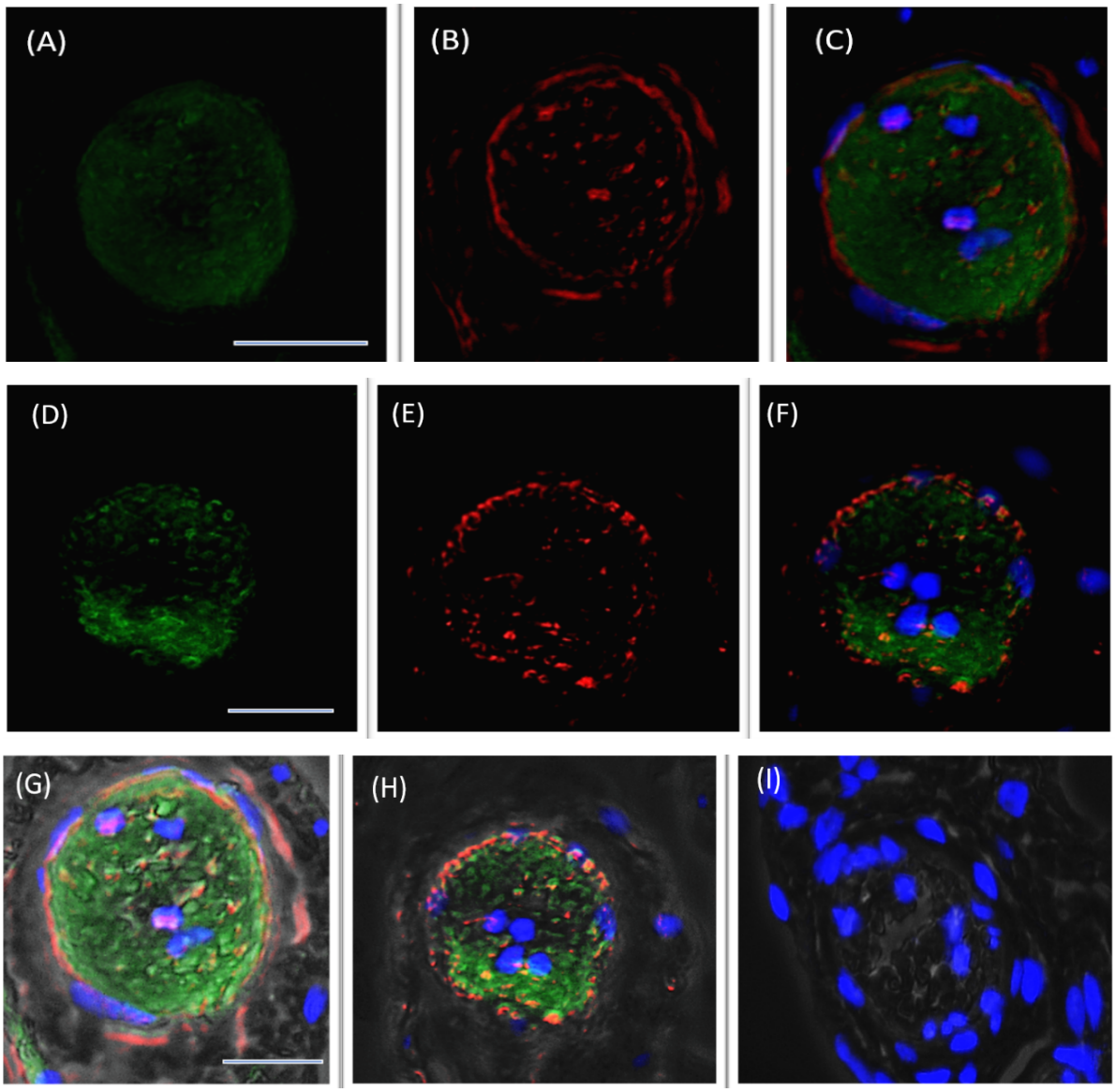

Figure 5.27 Arg-1 and *T. gondii* double immunofluorescent showing a cyst from sample 1028. (A) is *T. gondii* (B) is Arg-1 and (C) is the merged image of *T. gondii* and Arg-1, the Pearson's Correlation Coefficient (PCC) is 0.037. The second panel of images is iNOS and *T. gondii* double immunofluorescent illustrating a cyst of sample 1045. (D) is *T. gondii* (E) is iNOS and (F) is the merged image of *T. gondii* and iNOS, the Pearson's Correlation Coefficient (PCC) is 0.51. (G) is the overlay of the merged (*T. gondii*, Arg-1 and DAPI stains) on a black and white image of the tissue. (H) is the overlay of the merged (*T. gondii*, iNOS and DAPI stains) on a black and white image of the tissue. (I) is the negative control. Scale bar = 20 µm. Image magnification x40.

After the measurement of PCC was performed, to determine whether the result obtained is of true colocalisation, the randomisation test (Costes test) was carried out on the three *T. gondii* cysts. Figure 5.27 shows the Costes randomisation test conducted on one of the *T. gondii* cysts, where (A) is the randomisation test performed on colocalisation between *T. gondii* and Arg-1 in the *T. gondii* with a PCC value of 0.116. On the other hand regarding the randomisation test performed on the colocalisation between *T. gondii* and iNOS in the same *T. gondii* cyst (B) with a PCC value of 0.67. In both cases, the red line which represents the true colocalisation value highly exceeds the randomised value *P-value* of 100, thereby, conforming that the PCC value obtained is of true colocalisation.

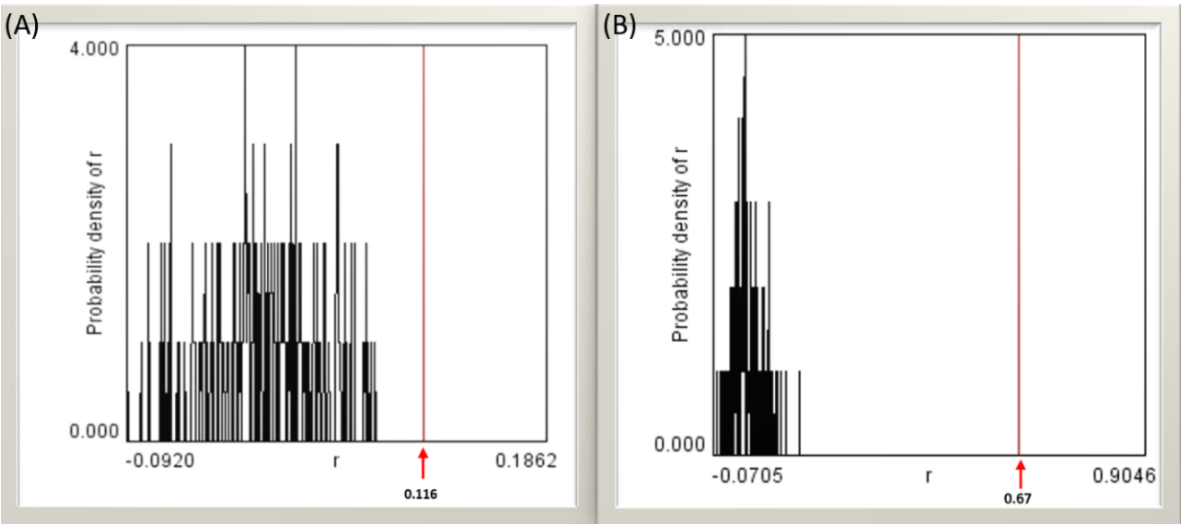

Figure 5.28 Plot of the distribution of the Pearson's coefficients (PCs) of randomised images (curve) and of the green channel image (*T. gondii*) indicated in the graph by the (red line). The red line indicates the PC and the curve shows the probability distribution of the PCs of the randomised images. (A) is the randomisation test performed on colocalisation between *T. gondii* and Arg-1 in the *T. gondii* cyst of subject (1008) the PCC = 0.116. While (B), is the randomisation test performed on colocalisation between *T. gondii* and iNOS in the *T. gondii* cyst of subject the same subject (1008) the PCC = 0.67. Note that the *P-value* for this analysis was 1 in both (A) and (B) indicating a high probability of colocalisation.

After the measurement of PCC and costs was established, and with the three cyst confirmed to have true colocalisation with Costes test, the average PCC was calculated for the colocalisation between *T. gondii* cyst and arg-1, as well as for *T. gondii* cysts and iNOS (Figure 5.29).

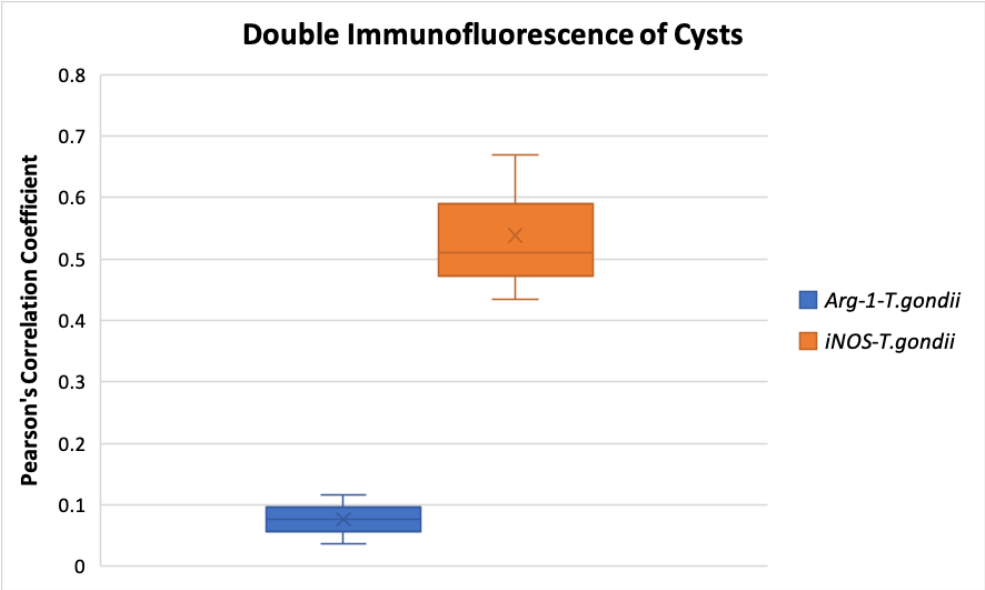

Figure 5.29 Quantitative colocalisation analysis of double immunofluorescence comparing the distribution of *T. gondii* infecting with either Arg-1 or iNOS in *T. gondii* cyst found in lung cancer subjects . The distribution of iNOS is much more highly correlated with *T. gondii* (r= 0.54, n = 3) than with iNOS (r = 0.076, n =3). Differences in between the two groups were very highly significant, with *p*= 0.0031.

5.3.17 Establishing the differences in colocalisation between *T. gondii*/Arg-1 and *T. gondii*/iNOS, in *T. gondii* cysts with Pearson's Correlation Coefficient (PCC)

The average PCC of *T. gondii* cysts and Arg-1 expression is 0.076, while the average PCC of *T. gondii* cysts and iNOS expression is 0.54 (Figure 5.29). It is obvious that the colocalisation is higher with iNOS than it is with Arg-1 at the *T. gondii* cysts level, however, is it statistically significant?

In order to address that question, a two-tailedd student t-test was performed to compare between the averaged means of PCC of the two groups. The *P-value* is < 0.003184, which is very highly significant (Figure 5.29), documenting that there is a significant difference in the colocalisation between *T. gondii* /Arg-1 and *T. gondii*/iNOS. Hence, we can establish that the colocalisation of *T. gondii*/iNOS is significantly higher than the colocalisation between *T. gondii* and Arg-1in *T. gondii* cysts.

5.3.18 Quantitative analysis of the colocalisation between *T. gondii* infection and Arg-1/iNOS in *T. gondii* cysts using Manders Correlation Coefficient (MCC)

Following the same approach conducted on the study of colocalisation of alveolar macrophages, MCC, with its split correlation co-efficient (M1and M2), was used as another method to evaluate colocalisation by establishing the level of overlap between the two images involved in double immunofluorescence. The values range from 0-1 where a value of 1 means perfect overlap while a zero value represents no overlap between the two images.

MCC measurement was established on the three *T. gondii* cysts and the average values for the split co-efficient (M1) and (M2) were calculated for the colocalisation between *T. gondii* cysts and Arg-1, as well as for *T. gondii* cysts and iNOS (Figure 5.30). A table with the colocalisation measurements listing the values of (M1) and (M2) for the three *T. gondii* cysts for the colocalisation between *T. gondii* and Arg-1 and between *T. gondii* and iNOS for be found at the supplementary appendix D (Table7.4 and 7.5).

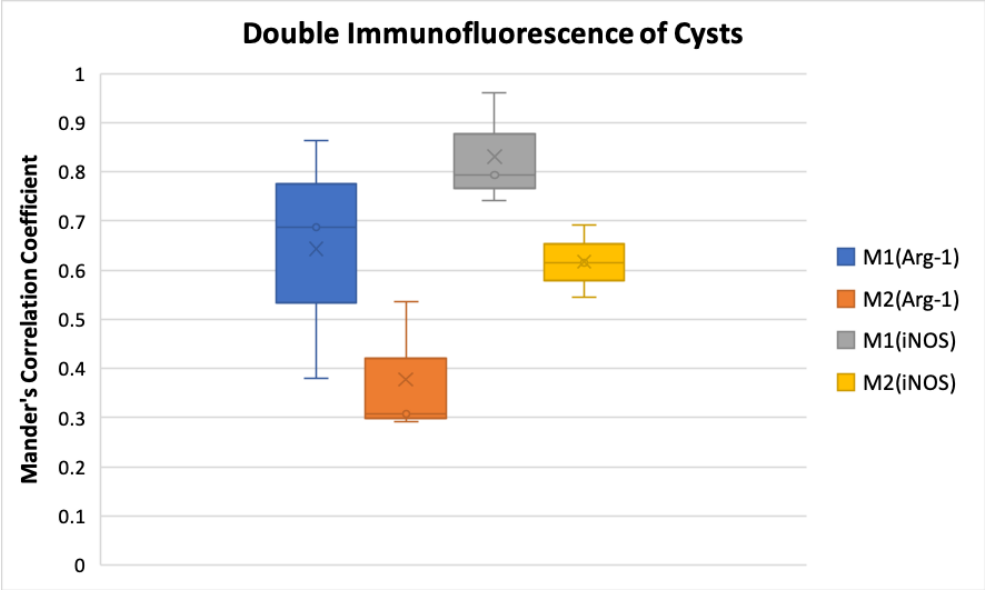

Figure 5.30 Quantitative colocalisation analysis of double immunofluorescence of *T. gondii* and Arg-1, and between *T. gondii* and iNOS in Cysts found in three subjects (1008,1028 and 1045). (M1) is the fraction of red pixels overlapping with green pixels, while (M2) is the fraction of green pixels overlapping with green pixels (*T. gondii*).

In Figure 5.30, (M1-Arg-1) represents the average proportion of red pixels (Arg-1) overlapping with green pixels (*T. gondii)* with a value of 0.64, while (M2-Arg-1) is the average proportion of green pixels (*T. gondii*) overlapping with red pixels *(*Arg-1) with a value of 0.37 in *T. gondii* cysts double labelled with Arg-1-*T. gondii.*

On the other hand, in *T. gondii* cysts double labelled with iNOS-*T. gondii,* (M1-iNOS) represents the average proportion of red pixels (iNOS) overlapping with green pixels (*T. gondii)* with a value of 0.83, while (M2-iNOS) is the average proportion of green pixels (*T. gondii*) overlapping with red pixels *(*iNOS) with a value of 0.61.

5.3.19 Establishing the differences in colocalisation between *T. gondii*/Arg-1 and *T. gondii*/iNOS, in *T. gondii* cysts with Manders Correlation Coefficient (MCC)

To assess if there is a significant difference between the average overlap between *T. gondii*-Arg-1 double labelled *T. gondii* cysts, and *T. gondii*/-iNOS double labelled *T. gondii* cysts, a two-sample student t-test was conducted to compare between the average overlap of (M1) of cysts double labelled with Arg-1-*T. gondii* which is the proportion of red pixels (Arg-1) co-occurring with green pixels (*T. gondii*), compared to (M1) of *T. gondii* cysts double labelled with iNOS-*T. gondii,* which represents the proportion of red pixels (iNOS) co-occurring with green pixels. With a *P-value* of 0.29, the result is not significant; hence, there is no significant difference in the average Arg-1 (red) pixels overlapping with *T. gondii* (green) and the iNOS (red) pixels overlapping with *T. gondii* (green).

Moreover, with the aim to evaluate if the difference between the split co-efficient (M2) averages in *T. gondii* cysts, a two-sample student t-test was conducted to compare between the average overlap of (M2-Arg-1) of *T. gondii* cysts double labelled with Arg-1-*T. gondii* which is the proportion of green pixels (*T. gondii*) co-occurring with red pixels (Arg-1), with (M2-iNOS) of the same *T. gondii* cysts double labelled with iNOS-*T. gondii,* which is the proportion of green pixels (*T. gondii*) co-occurring with red pixels (iNOS). With a *P-value* of 0.01, the result is significant, hence, here is a significant difference between the average overlap values (M2) of *T. gondii* (green) pixels overlapping with Arg-1 (red) and the *T. gondii* (green) pixels overlapping with iNOS (red).

5.3.20 Quantitative analysis of the colocalisation between *T. gondii* infection and Arg-1/iNOS of alveolar walls (knobs) using Pearson's Correlation Coefficient (PCC)

Confirming the results obtained by IHC of lung cancer subjects which revealed colocalisation of *T. gondii* with both Arg-1 and iNOS at the opening of alveolar walls, specifically in the smooth muscles fibres, the same results were documented with IF (Figure 5.11 and 12).

With the purpose of establishing a quantitative analysis of the colocalisation between the *T. gondii* infection and the expression of Arg-1at the level of the alveolar wall, as well as between iNOS expression and *T. gondii* infection, each alveolar wall was targeted individually. The outer most part of the alveolar walls, specifically the tip (knob), were outlined by the special tool of JACoP, (ROI) Region of Interest to evaluate each knob individually. The same colocalisation approach applied on the alveolar macrophages, and *T. gondii* cysts were applied. Correlation coefficients including PCC and MCC with its split co-efficient (M1 and M2) were measured, additionally the Costes randomisation test values were determined. A table with the colocalisation measurements listing the PCC and Costas values for the colocalisation between *T. gondii* infection and Arg-1 and between *T. gondii* infection and iNOS for each knob individually can be found at the supplementary appendix D (Tables 7.6 and 7.7).

Following the measurement of PCC and Costes was established, the average PCC of knobs with true colocalisation was calculated for the colocalisation between *T. gondii* infection and Arg-1, as well as for *T. gondii* infection and iNOS (Figure 5.31).

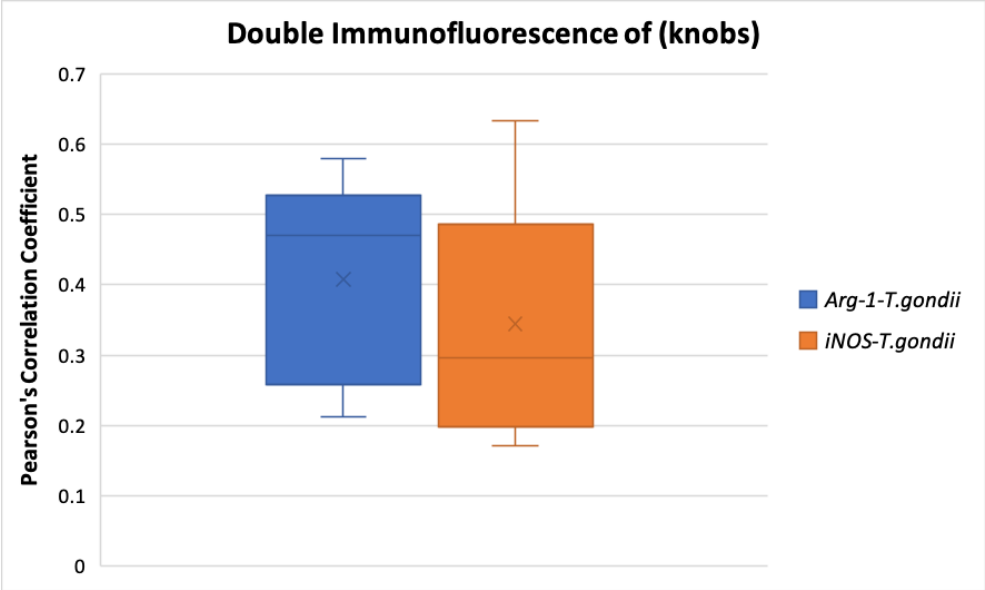

Figure 5.31 Quantitative colocalisation analysis of double immunofluorescence comparing the distribution of *T. gondii* infecting with either Arg-1 or iNOS in alveolar walls (knobs) in lung cancer subjects. No difference in the distribution between Arg-1/*T. gondii* and iNOS/*T. gondii, p*-=0.49.

5.3.21 Establishing the differences in colocalisation between *T. gondii*/Arg-1 and *T. gondii*/iNOS, in the alveolar wall knobs with Pearson's Correlation Coefficient (PCC)

The average PCC of *T. gondii* infection and Arg-1 expression is 0.41, while the average PCC of *T. gondii* infection and iNOS expression is 0.34 (Figure5.31). It is obvious that the colocalisation averages have values close to each other; however, is it statistically significant?

To address that question, a two-tailedd student t-test was performed to compare between the averaged means of PCC of the two groups. The *P-value* is 0.49, which is not significant (Figure5.31), documenting that there is no significant difference in the colocalisation between *T. gondii* /Arg-1 and *T. gondii*/iNOS at the level of the alveolar wall knobs.

5.3.22 Quantification analysis of the colocalisation between *T. gondii* infection and Arg-1/iNOS of alveolar walls (knobs) using Manders Correlation Coefficient (MCC)

Finally, to ensure methodological consistency, the same approach conducted on the study of colocalisation of alveolar macrophages and *T. gondii* cysts, MCC, with its split correlation co-

efficient (M1and M2), was used as another method to evaluate colocalisation by establishing the level of overlap between the two images.

MCC measurement was established on alveolar wall knobs, and the average values for the split co-efficient (M1) and (M2) were calculated for the colocalisation between *T. gondii* infection and Arg-1, as well as for *T. gondii* infection and iNOS (Figure 5.32). A table with the colocalisation measurements listing the values of (M1) and (M2) for the *T. gondii* infected knobs for the colocalisation between *T. gondii* and Arg-1 and between *T. gondii,* and iNOS can be found at the supplementary appendix D (Table7.6 and 7.7).

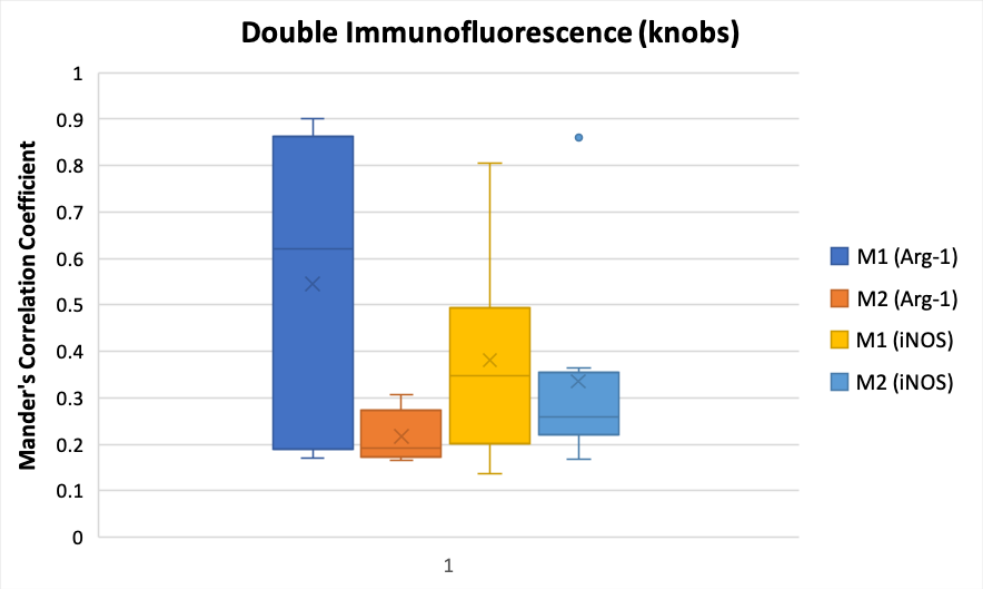

Figure 5. 32 Quantitative colocalisation analysis of double immunofluorescence of *T. gondii* and Arg-1, and between *T. gondii* and iNOS in alveolar wall knobs . (M1) is the fraction of red pixels overlapping with green pixels, while (M2) is the fraction of green pixels overlapping with green pixels (*T. gondii*).

In Figure 5.31, (M1-Arg-1) illustrates the average proportion of red pixels (Arg-1) overlapping with green pixels (*T. gondii)* with a value of 0.54, while (M2-Arg-1) is the average proportion of green pixels (*T. gondii*) overlapping with red pixels *(*Arg-1) with a value of 0.22 in *T. gondii* infected alveolar knobs double labelled with Arg-1-*T. gondii.*

Moreover, in *T. gondii* infected knobs double labelled with iNOS-*T. gondii,* (M1-iNOS) represents the average proportion of red pixels (iNOS) overlapping with green pixels (*T. gondii)* with a value of 0.38, while (M2-iNOS) is the average proportion of green pixels (*T. gondii*) overlapping with red pixels *(*iNOS) with a value of 0.34.

5.3.23 Establishing the differences in colocalisation between *T. gondii*/Arg-1 and *T. gondii*/iNOS, in the alveolar wall knobs with Manders Correlation Co efficient (MCC)

To assess if there is a significant difference between the average overlap between *T. gondii*-Arg-1 double labelled *T. gondii* infected knobs, and *T. gondii*/-iNOS double labelled *T. gondii* infected knobs, to address that, a two-sample student t-test was performed to compare between the average overlap of (M1) of knobs double labelled with Arg-1-*T. gondii,* which is the proportion of red pixels (Arg-1) overlapping with green pixels (*T. gondii*), compared to (M1) of *T. gondii* infected knobs double labelled with iNOS-*T. gondii* which represents the proportion of red pixels (iNOS) overlapping with green pixels. With a *P-value* of 0.30, the result is not significant; therefore, there is no significant difference in the average Arg-1 (red) pixels overlapping with *T. gondii* (green) and the iNOS (red) pixels overlapping with *T. gondii* (green).

Furthermore, with the interest in evaluating if the difference between the split co-efficient (M2) averages in alveolar wall knobs infected with *T. gondii*, a two-sample student t-test was conducted to compare between the average overlap of (M2-Arg-1) of *T. gondii* knobs double labelled with Arg-1-*T. gondii* which is the proportion of green pixels (*T. gondii*) co-occurring with red pixels (Arg-1), with (M2-iNOS) *T. gondii* infected knobs double labelled with iNOS-*T. gondii,* which is the proportion of green pixels (*T. gondii*) co-occurring with red pixels (iNOS). With a *P-value* of 0.063, the result is not significant; hence, there is no significant difference between the average overlap values (M2) of *T. gondii* (green) pixels overlapping with Arg-1 (red) and the *T. gondii* (green) pixels overlapping with iNOS (red).

5.4 Discussion

In conclusion, a total of 51 lung cancer tissue samples were prepared on slides in a serial manner with the aim of understanding the relationship between *T. gondii* infection and the expression of Arg-1 and iNOS in lung cancer. As a start, in order to understand the pattern of expression of Arg-1 and iNOS in relation to *T. gondii* infection of the lungs in relation to adjacent cells and tissues, slides of lung cancer patients (previously confirmed to be *T. gondii* positive) were tested with IHC targeting *T. gondii*, Arg-1 and iNOS. IHC results revealed co-expression of Arg-1, iNOS and *T. gondii* in bronchiolar epithelium, smooth muscle cells of blood vessels, alveolar macrophages and type I and II pneumocytes, (refer to Table 5.1). In order to have a more detailed quantitative colocalisation study between *T. gondii* and iNOS / Arg-1 and to further confirm the results obtained by IHC, double immunofluorescence was conducted on the same samples targeting (*T. gondii*/Arg-1) and (*T. gondii*/iNOS). Histologically, the results obtained by IF confirmed the findings of IHC (refer to Table 5.2).

The difference in the frequency of infection and expression across the various lung tissue types was established with Arg-1 and *T. gondii*. On the other hand, the expression rate of iNOS was relatively high across all tissue/cells types with no significant difference. Moreover, different links were established between the infection with *T. gondii* and the expression of Arg-1 and iNOS. The associations establishes between *T. gondii* infection, and the expression of Arg-1 were at the Ad, Type I and Type II pneumocytes, while On the other hand, the links between iNOS and the infection with *T. gondii* was found to be significant at the SM, EEL, Type I and Type II pneumocytes. Finally, co-expression between Arg-1 and iNOS relative to *T. gondii* infection was found to be significant only at Type I and Type II pneumocytes, (refer to summary Tables 5.17, 24 and 31).

Quantitative colocalisation analysis with both PCC and MCC revealed that the colocalisation between *T. gondii* and Arg-1 the level of the alveolar macrophages was higher than the colocalisation between *T. gondii* and iNOS. On the other hand, at *T. gondii* cysts, a higher colocalisation between *T. gondii* and iNOS was documented compared to *T. gondii*/Arg-1 with PCC, but no difference was documented with MCC. Finally, no difference in the colocalisation between *T. gondii*/iNOS and *T. gondii*/Arg-1 was documented at the level of the alveolar wall (knobs) With both PCC and MCC.

In this chapter, we were able to establish and conduct a double immunofluorescence procedure to establish and assess the relationship between *T. gondii* in lung cancer patients and between two markers which are considered important markers in the human immune defence mechanism, Arg-1 and iNOS. As far as we are aware, there is no study that has attempted to unlock the dynamics behind *T. gondii* infection in relation to Arg-1 and iNOS in lung cancer individuals.

We have approached this study by conducting an IHC targeting Arg-1, iNOS and *T. gondii* in aims of revealing the pattern of expression of Arg-1 and iNOS in relation to the sites of infection with *T. gondii*. Furthermore, we followed by performing a double immunofluorescence procedure to colocalise the two markers (Arg-1 and iNOS) in relation to *T. gondii*. Although the aims behind conducting these two procedures are not absolutely the same, however, the results optioned by IHC is followed by double immunofluorescence have complimented each other and collectively gave the same findings, further adding to the strength of our approach.

With the aim of colocalisation with IHC and IF, image collection was performed in a manner with respect to attempting to capture the same field of views in all slides of (*T. gondii*, iNOS, Arg-1 and the negative controls) for the same sample. This approach proved to be successful with the bigger structures of lungs, e.g. blood vessels which have more distinctive landmarks making it easier to recognise. On the other hand, with smaller structures and cells, the approach proved to be less attainable. Although if it was possible, it would have meant we would be able to specify if the same, e.g. alveolar macrophage is expressing Arg-1 or iNOS, or both at the same time while infected with *T. gondii* parasite.

Although using a conventional fluorescence microscope is widely accepted in the research filed, however, due to the high resolution and sectioning property of confocal microscopy, it is being widely used in the fields of materials and life sciences (Amos and White, 2003). With the 3-dimensional (3D) images that the confocal microscopy generates, it is considered a preferred option particularly when investigating complex structures that are not contained within a two-dimensional (2D) plane, such as neural tracts and vasculature (Kakimoto, 2018), and in our study, blood vessels and *T. gondii* cysts. Using a confocal microscope might have improved the quality of the images obtained and hence enhanced the outcome of the overall colocalisation analysis.

The tissue analysed in this study is a complex type of tissue involving various structures and cell types. Broad statistical analysis might fail to highlight the precise differences between complex

tissues as we have attempted with the expression of Arg-1 across the different lung tissue. When all the tissue types were included in the statistical analysis, the expression of Arg-1 was extremely different across these tissue types. However, when the two tissues with the lower expression rate were excluded (VSM and EEL), reanalysis with the remaining tissue did not showcase a significant difference. Hence, general statistical analysis in some cases could mask the true differences among certain data and separation of data that could be producing the shift of results and then reanalysis could be highly beneficial.

Arg-1 and iNOS are competitively related (Abdallahi et al., 2001). The production of NO is regulated by Arginase activity through reducing the availability of L-arginine to NOS, hence, decreasing the potential pathological effects of high levels of NO (Abdallahi et al., 2001). Furthermore, arginase produces ornithine, which is the precursor of the synthesis of polyamines and since L-ornithine is a precursor for many polyamines through the ornithine decarboxylase (ODC) pathway, which is modulated by NO. Polyamines are crucial for the proliferation of normal and neoplastic cells (Abdallahi et al., 2001), and they support the growth of organisms, including the parasite (Zhao *et al.*, 2013). On the other hand, it has been reported that the production of NO by (iNOS) in tissues which are undergoing inflammation, is involved in the killing of intracellular pathogens including *Leishmania, Trypanosoma* and *mycobacteria* (Abdallahi et al., 2001).

Several findings in our study have supports these facts, in this study, we have documented that the higher the percentage of alveolar macrophages expressing Arg-1 and infected with *T. gondii*, the higher is the overall grade of *T. gondii* infection, since Arg-1 promotes parasite. Although the exact reason is yet unknown, some species are more susceptible to the infection with *T. gondii* parasite while others are resistant (Gao et al., 2015). An example of the difference in susceptibility is rats and mice (McCabe and Remington, 1986). A study performed in 1986 had revealed that when the peritoneal macrophages of rats were exposed to *T. gondii* infection *in vitro*, 90% of the parasite was eliminated and the remaining parasites did not replicate in the next 72 hours that followed the infection (McCabe & Remington 1986). On the other hand, peritoneal macrophages of mice and other mammals such as pigs and hamsters did not demonstrate this resistance, and *T. gondii* can efficiently replicate (McCabe and Remington, 1986). The mechanism in which rat peritoneal macrophages exhibit resistance is still not well documented. However, many studies suggest the potential involvement of inducible nitric oxide synthase, iNOS, and Arg-1 (Li et al.,

2012). Many studies were performed to evaluate the role of nitric oxide (NO) in the natural resistance observed in peritoneal macrophages of rats (Li et al., 2012). (NO), is considered a major molecule in the regulation of the immune system and a fundamental cytotoxic mediator (Adams et al., 1990). Results showed a high expression and activity level of iNOS and low expression and activity level of Arg-1 in rat peritoneal macrophages (resistant hosts). On the other hand, it was the opposite in mouse peritoneal macrophages with high (Arg-1) and low iNOS (sensitive host) (Li et al., 2012). Interestingly, alveolar macrophages of rats did not show the same resistance as the peritoneal macrophages; In fact, it resembled susceptible mice peritoneal macrophages in the level of infection with *T. gondii* parasite (Zhao et al., 2013a). These results were attributed to the same low expression and activity of iNOS and in the result, low production of NO, and high expression and activity of Arg-1 (Zhao et al., 2013a). The interesting question is, why do peritoneal macrophages and alveolar macrophages show a different response to *T. gondii* infection within the same host? The fact that different rat inbred strains showed variation in the level of expression and activity of iNOS and Arg-1, suggests epigenetic differences in gene expression that causes alveolar macrophages to show a different level of susceptibility to *T. gondii* infection (Zhao et al., 2013a).

Our results of colocalisation with Pearson's Correlation Coefficient (PCC) and Manders Correlation Coefficient MCC on alveolar macrophages where the colocalisation between *T. gondii* and Arg-1 was significantly higher than that of iNOS and *T. gondii*, supports the findings of rat alveolar macrophages where they showed high Arg-1 expression activity and low iNOS expression and activity subjecting them to mimic mice sensitivity to infection. This might be one of the reasons behind the individuals we have included in our research being susceptible to *T. gondii* and could explain the striking 100% prevalence of these cancer patients obtained in a previous study (Bajnok 2017).

During acute *T. gondii* infection, and in response to stress signals such as the immune response or programmed spontaneous differentiation responses, tachyzoites differentiate into the slow-growing bradyzoite life cycle stage that remains latent in the host. Bradyzoites can form tissue cysts in various organs including the lungs and persist for years (Tomita et al., 2013). We have located 3 *T. gondii* cysts in our samples, and we successfully stained them with our two target markers (Arg-1 and iNOS) as well as with *T. gondii*. With respect to the low number of cysts found in our study, we do appreciate the limitation of this on our findings regrading *T.gondii*

tissue cysts. Nevertheless, the colocalisation analysis revealed significantly higher colocalisation between iNOS and *T. gondii* than Arg-1 and *T. gondii.* With respect to the fact that the cyst stage of the parasite represents the dormant stage, which hypothetically, means it requires to be maintained in the latent phase by the host immune system. Since iNOS plays an important role in the killing of the parasite, this supports our findings that iNOS is higher than Arg-1 on the *T. gondii* cyst level.

Different studies on rats and mice have documented that the balance between Arg-1/iNOS plays a role in determining the host being sensitive vs resistant to *T. gondii* infection. We have attempted to test this hypothesis on the human host and to assess whether the human cells react the same way to *T. gondii* infection in relation to Arg-1 and iNOS expression. We have documented high expression of Arg-1 and colocalisation with *T. gondii* inside the alveolar macrophages compared to the lower expression and colocalisation with iNOS. On the other hand, the opposite was found in the *T. gondii* cyst with high expression of iNOS and colocalisation with *T. gondii* and lower expression of Arg-1 and colocalisation with *T. gondii*.

These findings in our study supports our hypothesis that the balance between the activity and expression of Arg-1 and iNOS does play a role in the status of infection with *T. gondii*. Nevertheless, the colocalisation at the level of the alveolar knobs where there was no difference between Arg-1 and iNOS relative to the infection with *T. gondii*, contradicts our tested hypothesis. One possible reason that the alveolar knobs are not following our hypothesis could be due to the balance between Arginase and iNOS. Arginase and iNOS are two competitively related enzymes (Abdallahi et al., 2001), and depending on the concentration of either iNOS or Arg-1, the pathway could shift either way. Inducible nitric oxide synthase (iNOS) produces NO through the utilisation of L-arginine, on the other hand, Arg-1 hydrolyses L-arginine to produce L-ornithine and urea (Li et al., 2002). It could be that both Arg-1 and iNOS are present in nearly equal concentrations that caused the colocalisation analysis to have no difference between Arg-1 and iNOS in relation to *T. gondii* infection at the level of the alveolar knobs.

Alveoli represent the endpoint of the respiratory system. It is at this anatomical stage that oxygen molecules diffuse through a single cell in an alveolus and then a single cell in a capillary to enter the bloodstream (Ellis, 2008). Simultaneously, carbon dioxide (CO2) molecules, are diffused back into the alveolus where they are expelled out of the body via the nose or mouth (Zhang and Homer, 2016). Since the alveoli play a fundamental role in the process of oxygen and carbon dioxide

exchange to and from the bloodstream, alveolar compartments have extensive blood supply (Ellis, 2008). It could be that the increased blood supply to these compartments in general, and specifically (the alveolar knobs being at the tip), make them more exposed to the infection with *T. gondii*. In fact, lung toxoplasmosis mimics the presentation of pneumonia, which is the infection of the alveolar sacs (de Souza Giassi et al., 2014b).

Alveolar knobs represent the opening of the alveolar sacs and are formed mainly of smooth muscle fibers (ref). *T. gondii* infection was found strictly confined to the tip of the knobs while iNOS and Arg-1 expressions were at the knobs but also extend to the alveolar wall (Figure 5.11 and 12), which is made up of epithelial cells. The fact that muscular tissue/cells being specifically infected with *T. gondii* compared to the other cell types in the structure of the knob is quite interesting. In fact, many studies that have studied *T. gondii* infection, in general, have reported high rate of infection at muscular tissues (Dubey et al., 1998). Besides neurons, skeletal muscle cells are considered a favoured cell type for *T. gondii* infection and persistence by forming tissue cysts (Dubey et al., 1998). This might explain why *T. gondii* was found specifically in the smooth muscle cells compared to other cell types of the alveolar knob.

In this study, we have established a link between the expression of iNOS and the infection with *T. gondii* at the level of smooth muscle layer in lung blood vessels. On the other hand, no links have been established between *T. gondii* infection and the expression of Arg-1 at this level. Many studies have discussed the expression of iNOS in smooth muscle of arteries (Singh et al., 1996; Luoma et al., 1998; Kibbe et al., 2000). It has been documented that the overexpression of iNOS in vascular smooth muscle cells prevents the hyperplasia of the intimal layer through the production of nitric oxide (NO) and hence preventing intimal injury (Kibbe et al., 2000). Moreover, iNOS gene transfer has been employed successfully to lower balloon-injury–induced intimal hyperplasia in both rat and pig models as well as to decrease allograft vasculopathy in rodent models (Kibbe et al., 2000). Another study has documented the expression of iNOS in smooth muscle cells and macrophages in response to atherosclerosis in both humans and rabbits (Luoma et al., 1998). Expression of iNOS has been frequently documented to be associated with generalised or localised inflammatory response as a result of infection or tissue injury (Morris and Billiar, 1994). No other studies have documented the expression of iNOS in response to *T. gondii* infection, however, at the level of the lung blood vessels, iNOS could be expressed in relation to an inflammatory process undertaking in these blood vessels caused by *T. gondii* infection.

Whilst *T. gondii* can infect a wide variety of cell types; however, it ideally targets different types of host cells at different stages of infection. For instance, enterocytes of the Felidae family are the only cells that support sexual reproduction (Dubey, 1998). Similarly, blood monocytes permit the parasite to get to the extravascular space of the brain (Courret et al., 2006). While dendritic cells are infected for fast dissemination within the host (Lambert et al., 2006; Fuks et al., 2012). Furthermore, it has been suggested that compared to other blood leukocytes, dendritic cells as well as monocytes endure faster parasite replication (Channon et al., 2000). Finally, brain neurons are the main type of cell that promotes long-term parasite survival, in mice at least (Sims et al., 1989). With the diverse host cell types that *T. gondii* infects, will most probably result in specific host cell–parasite interactions which could influence distinct phenotypic traits of both the parasite as well as the host cell after infection. For example, although dendritic cells and monocytes are related host cell types, however, they strongly differ in their responses to infection with any pathogen, including *T. gondii* (Chaussabel et al., 2003). Such facts raise the question as what makes a specific type of host cell especially suitable as a host cell during a certain stage of toxoplasma infection. Moreover, following infection of a specific cell type, what are the functional consequences of specific host cell and parasite responses is an important question that still needs exploration.

To address such questions and other in the future, for example, since the alveolar knobs seems to contradict our hypothesis, it might be beneficial to attempt to obtain more answers by conducting colocalisation studies targeting other tissue/cell markers specific to the alveolar knobs (smooth muscle) in relation to *T. gondii* infection. Such studies could help in revealing which host cell types are involved with more precision. Furthermore, such an approach would aid in gaining a better understanding to the reason in which alveolar knobs does not follow our hypothesis of iNOS/Arg-1 balance, while both were expressed.

Although the number of the clinical samples tested in this study is reasonable, increasing the number of samples would increase the strength and add more confidence to the results. Moreover, with respect to the complexity of the tested tissue in this study, confocal microscopy would be an ideal technique for colocalisation analysis offering to construct 3-dimensional images of the sample with higher optical resolution.

Chapter 6: General Discussion

In this study, we have established a high rate of infection with the *T. gondii* parasite among lung cancer patients obtained by tissue biopsy when compared to the control group with no previous history of cancer. Moreover, we were able to develop and conduct an immunohistochemistry approach on lung cancer tissue slides targeting Arg-1 and iNOS expression in relation to *T. gondii* infection. Expression of Arg-1, iNOS and *T. gondii* infection was located in different lung tissue/cell types and further confirmed by immunofluorescence (IF). Double immunofluorescence quantitative colocalisation analysis has shown interesting results revealing that high Arg-1 expression and low iNOS expression are associated with alveolar macrophages. On the other hand, the opposite was found in *T. gondii* cysts, where high iNOS and low Arg-1 expression were seen. Finally, there were no differences found between iNOS and Arg-1expression in the alveolar knobs where *T. gondii* infection predominates.

In general, our aim was to investigate whether there is a relationship between lung cancer and *T. gondii* infection. We had the advantage of conducting our research on clinical samples obtained from lung cancer patients through tissue biopsy. While the utilisation of human clinical tissue has its benefits, using human lung cancer tissue to address our questions has its drawbacks. With respect to the complexity of lung tissue, there is the possibility of neighbouring tissues or cells influencing the outcomes to our questions. To overcome that, conducting our studies on cell cultures systems, e.g. different types of lung cells, might show whether these lung cells behave differently than when tested in association to the lung tissue as a whole. Moreover, will the expression patterns of Arg-1 and iNOS be different to that when related to lung cancer or when under the influence of *T. gondii* infection. Furthermore, performing our studies on cancerous/non-cancerous cell lines might help to address if Arg-1 and iNOS enzymes are expressed with cancer vs normal cells.

The lung cancer study in this research was conducted on 72 lung cancer patients from Manchester, UK, while the control group were 10 samples from Manchester as well. This study has revealed a surprisingly high prevalence of *T. gondii* infection in individuals with lung cancer compared with the healthy control group and in relation to expected UK prevalence in cancer-free individuals. Nevertheless, increasing the sample size of both tested and control samples will further add to the strength of our findings. The prevalence of *T. gondii* infection in the UK is

around 10 % (Pappas et al., 2009), which is reasonably low, yet, we have documented a 100% prevalence among cancer patients from Manchester. Investigating more samples with a wider geographical distribution could offer a better insight into the global extent of *T. gondii* infection in lung cancer individuals. An example of that would be to consider regions with documented high *T. gondii* prevalence and to compare it with our data from the UK. In some regions in Europe, the prevalence of *T. gondii* infection ranges from 30–63% (Blaga et al., 2019). In addition, in some countries in Latin America and Africa, the prevalence of toxoplasmosis is >60% (Nogareda et al., 2014)

With the high prevalence of *T. gondii* infection observed in this study compared to the control group, an important question remains as to what is the mechanism of infection with *T. gondii* in these lung cancer patients. The three main routes of transmission of toxoplasmosis, are the ingestion of oocysts shed by cats, consuming undercooked or raw meat containing the tissue cysts and vertical transmission (Hide et al., 2009; Hide, 2016). To the best of our knowledge, no other studies have documented that toxoplasmosis as an airborne infection, however, the high rate of lung toxoplasmosis in these patients raises the possibility of the infection being transmitted via air. Another possibility is the transmission of the infection systemically, after the consumption of an undercooked meat of an intermediate host harbouring the tissue cyst reaching the lungs via the blood circulation.

As far as we are aware, there is no reported data that documents *T. gondii* parasite as a causative agent for cancer, however, in these patients with lung cancer, the high frequency of *T. gondii* infection brings into question as to whether the two conditions are related. Cancer patients are considered immunocompromised and pulmonary toxoplasmosis is generally a rare form of toxoplasmosis in individuals who are immunocompetent (de Souza Giassi et al., 2014a). This supports the theory that the high rate of lung toxoplasmosis observed in our study could be due to the patients' overall immunocompromised state. Moreover, since systemic *T. gondii* infection can stimulate a long-term defect in the function and generation of naive T-lymphocytes, *T. gondii* infection could also be creating an environment of immunosuppression by affecting thymic related T-cell activity, (Canessa et al., 1992; Kugler et al., 2016).

Although the significant outcomes of *T. gondii* infection in immunocompromised hosts has been well established, *T. gondii* infection in cancer patients has received relatively little attention, and

only a few reports are available (Yuan et al., 2007). The majority of studies that measure the prevalence of *T. gondii* in relation to different types of cancers have relied mainly on serology. The highest seroprevalence was documented to be associated with nasopharyngeal carcinoma (46.15%), and rectal cancer (63.64%), and a relatively low seroprevalence with other types of cancer including breast cancer and uterine cancer with (9.53%) and (12.50%) respectively (Yuan et al., 2007). In a study conducted in Saudi Arabia on patients with several cancer types, the frequency of seropositivity of *T. gondii* infection was 30.6% (Imam et al., 2017). According to a study that measured the overall prevalence of *T. gondii* in Saudi Arabia has documented a prevalence of 32.7% (Tabbara et al., 1999). While another study in Saudi Arabia conducted on 203 pregnant women has documented an overall prevalence of 32.5% and 6.4% of IgG and IgM, respectively (Alghamdi et al., 2016). The conclusion from this is that, in Saudi Arabia, there seems to be no difference in parasite prevalence between cancer and non-cancer groups.

Many studies have documented an increase in the fatality rate of *Toxoplasma* patients with different types of cancer (Carey et al., 1973). A study reported, that out of 24 patients with toxoplasmosis, 14 patients had either leukaemia or lymphoma, and 9 patients had Hodgkin's disease (Carey et al., 1973). Yet, not many studies have assessed the complications caused by *T. gondii* infection in relation to lung cancer. In China, a patient with non-small lung carcinoma was reported to have lung toxoplasmosis on top of her cancer (Lu et al., 2015).

A study has evaluated the seroprevalence of *T. gondii* in cancer patients undergoing chemotherapy in relation to different types of malignancies (Ali et al., 2019). Using the ELISA method, anti-*T. gondii* IgG and IgM antibodies were measured in a total of 120 cancer patients receiving chemotherapy, in which 60 are diagnosed with solid organ tumours and 60 having haematological malignancies (Ali et al., 2019). *T. gondii* (IgG and IgM) were determined in (66.7% and 9.2%) of the cancer group while (33.3% and 6.7%) in the control group, which was a statistically significant difference (Ali et al., 2019). Moreover, it was documented that IgG seropositivity was significantly higher in patients with haematological malignancies than solid organ tumours (40% vs 26.7%) (Ali et al., 2019).

In a study conducted in the United States, they attempted to explore the associations between *T. gondii* infection and brain cancers in human populations from 37 different countries (Thomas et al., 2012). The countries that have increased prevalence of *T. gondii* infection had 1.8 fold higher

incidence of brain cancer compared to other areas where *T. gondii* infection was low or absent (Thomas et al., 2012). Moreover, in a study conducted in aims to address the relationship between *T.gondii* infection of the brain and brain disorders, cancer was the largest disease to correlate with the *T. gondii* brain infection (Ngô et al., 2017).

In China, a study conducted on a group of patients with different types of cancers were evaluated for anti-*T. gondii* antibodies and the overall prevalence was (35.56%) compared to (17.44%) in the control group. The highest seroprevalence was reported with lung cancer (60.94%) followed by cervical cancer (50%) and (42.31%) for patients with brain cancer (Cong et al., 2015). However, when measuring the infection rate in patients with different cancers in China by nested PCR, another study reported a prevalence of 3.55%, while the same samples demonstrated 8.38% serological prevalence (Wang et al., 2015).

Unfortunately, these methods of measuring *T. gondii* infection fail to distinguish whether the infection is active or not, although it is widely used and may indicate a relationship between *T. gondii* and cancer. The utilisation of serology as a method to measure *T. gondii* infection in cancer patients could be underestimating the true significance of the impact of *T. gondii* on cancer. The reason behind that is, such studies only measure the overall infection status rather than localised infections within the cancer affected tissue.

In general, many studies reported the expression of Arg-1 and iNOS in different animal and human tissues. The Nitric oxide synthase (NOS) enzyme has three main isoforms, the neuronal isoform nNOS (NOS-1) and an endothelial isoform eNOS (NOS-3) as constitutive isoenzymes, and an inducible isoform iNOS (NOS-2) (Kroncke et al., 1998). A study was conducted on rat lung tissue to evaluate the expression of the three isoforms via immunohistochemistry to reveal specific cell types before and after the exposure to endotoxin (Ermert, Ruppert, Günther, H. R. Duncker, et al., 2002). In normal rat lung tissue, iNOS immunoreactivity was localised to the epithelial cells of the first- and second-generation bronchi, alveolar macrophages and single cells within the alveolar septum (Ermert, Ruppert, Günther, H. R. Duncker, et al., 2002). In addition, smooth muscle cells of the bronchiole, smooth muscle cells of fully muscular and partially muscular vessels and myocytes of large hilar veins showed moderated iNOS staining. After exposure to endotoxin, iNOS expression was increased in all the cell types, which were stained in normal rat lung tissue (Ermert, Ruppert, Günther, H. R. Duncker, et al., 2002). The strong up-

regulation of iNOS described by this study evident in different cell types of the vascular and bronchial system, may play a role in provoking inflammatory events through the formation of peroxynitrite (Ermert, Ruppert, Günther, H. R. Duncker, et al., 2002). The same study was conducted but on fetal, newborn and maternal sheep lung tissue (Sherman et al., 1999). In all three age groups, iNOS expression was visible in epithelial cells; however, staining was absent in endothelial cells(Sherman et al., 1999). Moreover, in fetal lungs, staining of the airway epithelium and vascular smooth muscle was the highest, whereas airway smooth muscle staining was greatest in maternal lung (Sherman et al., 1999). A study attempted to evaluate the difference in iNOS expression in rabbit normal myocardium tissue and compare it with the expression in infarcted regions of the heart (Wildhirt et al., 1994). The activity of iNOS was measured by the conversion of L-arginine to L-citrulline and NO, which was significantly increased in the infarcted area of the rabbit myocardium (Wildhirt et al., 1994). With reference to these data, in this study, iNOS was found in several lung tissue types which matched the published data on mice and sheep. The expression of iNOS in this study was found relatively across most tissue cells including the epithelial lining of the bronchioles, vascular smooth muscle cells and alveolar macrophages. Hence the studies documenting the expression of iNOS in mice as well as sheep tissue do support our findings. On the other hand, to our knowledge, no studies have documented the expression of iNOS in humans.

Since IHC is a widely used technique to help address scientific questions through the study of various tissues in humans and animal models, Arg-1 expression was explored in many studies. IHC of Arg-1 has been reported in rat and mouse tissues to evaluate tissue expression (Hochstedler et al., 2013). A study reported the localisation of Arg-1 in murine liver tissue, and due to the abundancy of its expression, liver tissue was used as a positive control in our studies for IHC of Arg-1 (Hochstedler et al., 2013). In the liver, Arg-1 was localised to the hepatocytes as well as the bile ducts and gallbladder epithelium which showed weak to moderate staining. Expression of Arg-1 was detected in various tissues, including the pancreas, in solitary cells and along the pancreatic islets (Choi *et al.*, 2012). Other tissues included the surface epithelium of the intestines and duct epithelium of the salivary glands. In the lungs, Arg-1 expression was detected in submucosal glands and in the ciliated epithelium of the surface epithelium. However, the expression of Arg-1 in the airway epithelium is dynamic and could be upregulated (including Clara cells) in some disease circumstances such as mouse models of asthma (North et al., 2011).

We have used rat liver tissue as controls for our study, and the expression of Arg-1 was abundant in the cytoplasm of hepatocytes as well as in the and nucleus. These results matched other studied evaluating the expression of Arg-1 in rat/mice liver. Moreover, in the lungs, we have found Arg-1 to be expressed in various lung tissue cell types, including the ciliated lining epithelium of the bronchioles matching findings by other studies conducted on mice. On the other hand, we have not documented the Arg-1 expression in Clara cells, although some individuals tested do have asthma.

Many studies have evaluated iNOS and Arg-1 due to their competitive relationship (Abdallahi et al., 2001). Studies conducted on mice and rats have revealed interesting findings (McCabe and Remington, 1986; Li et al., 2012; Zhao et al., 2013a). Mice and rats have been selected to study Arg-1 and iNOS due to their difference in the susceptibility to *T. gondii* infection (McCabe and Remington, 1986). While laboratory mice are sensitive to *T. gondii* , rats are resistant (McCabe and Remington, 1986). Studies conducted on the peritoneal macrophages of rats have shown that high expression and activity levels of iNOS and low expression and activity levels of Arg-1 in rat peritoneal macrophages (Li et al., 2012). In contrast, the opposite was observed in mice peritoneal macrophages with high Arg-1 and low iNOS (Li et al., 2012). On the other hand, when the same studies were performed on rat alveolar macrophages (resistant host), it displayed a similar level of sensitivity to mice peritoneal macrophages (Zhao et al., 2013a). These results were linked to the same low expression and activity of iNOS leading to low production of nitric oxide (NO), and high expression and activity of Arg-1 (Zhao et al., 2013a). This suggests that there is epigenetic regulation of the iNOS and Arg-1 genes that determines the differences in behaviours between the peritoneal and alveolar macrophages.

A study was conducted on two different stains of mice C57BL/6 (a *T. gondii* susceptible strain) and BALB/c (a *T. gondii* resistant strain) infected with of *T. gondii*, to evaluate the role of NO in the production of Interferon γ (IFN γ) and apoptosis of splenocytes (Kang et al., 2004). After the mice were infected with *T. gondii*, an iNOS inhibitor (aminoguanidine) was injected. In the *T. gondii*-infected C57BL/6 mice, the number of brain cysts were increased whilst NO and IFNγ production was reduced by the iNOS inhibitor. On the other hand, in *T. gondii*-infected BALB/c mice, the number of brain cysts, NO and IFNγ production of splenocytes was not changed by treatment with iNOS inhibitor. The percentages of apoptotic splenocytes in both mice strains were not affected by the iNOS inhibitor treatment. These results imply that in *T. gondii*-infected

C57BL/6 mice, NO modulates IFNγ production, and that NO plays a role in mediating a protective response during acute infection in toxoplasmosis susceptible, but not resistant mice strains (Kang et al., 2004). Moreover, a study conducted on iNOS knockout mice infected with *T. gondii* , evaluated the role of iNOS in relation to *T. gondii* infection (Scharton-Kersten et al., 1997). Although they were able to control the acute infection, eventually they gave in to *T. gondii* infection at 3–4 weeks post-inoculation (Scharton-Kersten et al., 1997). Such data indicate that iNOS is crucial for host control of persistent but not acute infection with *T. gondii* parasite (Scharton-Kersten et al., 1997). This finding supports our data we documented of high expression of iNOS in *T. gondii* cysts compared to that of Arg-1. With respect to the cyst representing the dormant stage of toxoplasmosis, therefore iNOS expression could be higher to ensure persistence of the *T. gondii* cysts.

In mice, the anti-*T. gondii* role for iNOS, which is considered an IFNγ inducible protein, has been widely established (Bando et al., 2018). Nevertheless, its exact role in the IFNγ mediated interaction between humans and *T. gondii* remains unknown. A study suggested that unlike mice, iNOS could be a pro-*T. gondii* host factor that supports the growth of the parasite rather than an anti-*T. gondii* host factor (Bando et al., 2018). It has been suggested that *T. gondii* utilises the iNOS (NO)-dependent downregulation of indoleamine 2,3-dioxygenase (IDO1) through the secretion of effector GRA15 to enable the parasite to proliferate effectively in a wide range of human cell types (Bando et al., 2018). IDO1, which is induced by IFNγ, is an enzyme used in the catabolism of tryptophan, a fundamental nutritional amino acid for the intracellular growth of *T. gondii* in human cells (Pfefferkorn et al., 1986). Thus, by indirectly targeting IDO1, *T. gondii* can suppress the IFNγ -induced antiparasitic response (Bando et al., 2018). We have documented the expression of iNOS across the majority of lung tissue and cells types. With reference to the previous data suggesting iNOS as a pro-*T. gondii* rather than anti-*T. gondii*, it could be possible that iNOS expression in these many cell and tissue types is to aid in the growth of the parasite rather than to suppress it. Yet, further studies to evaluate this factor is required by possibly measuring IFNγ in relation to iNOS and *T. gondii*.

Since *T. gondii* infection is often asymptomatic, it is evident that this widespread parasite has established sophisticated ways to manipulate host immunity (Butcher et al., 2011). A study has been conducted on mouse bone marrow-derived macrophages, to evaluate the role of Rhoptry kinase (ROP16), a molecule which is discharged into the host cell cytosol during invasion, and

subsequently localises to the host cell nucleus (Butcher et al., 2011). The study has documented that ROP16 manipulates signalling pathways in host cells which determine the availability of arginine for parasite replication and dissemination, as well as NO production by the host (Butcher et al., 2011). Hence, ROP16 could possibly act as a central regulator of replication and transmission of the parasite by manipulating Arg-1 levels and consequently, arginine availability to both host and parasite (Butcher et al., 2011). In our study, we have documented a high expression of Arg-1 in the alveolar macrophages compared to iNOS. This matches the previously mentioned data on bone-marrow macrophages of mice, supporting the fact that Arg-1 could be expressed highly in the macrophages to facilitate *T. gondii* parasites growth. Moreover, our data matches the high Arg-1 expression and low iNOS in alveolar macrophages of rats documented by (Li et al., 2012; Zhao et al., 2013a), which are naturally resistant to *T. gondii* infection.

Different studies have evaluated the expression of Arg-1 and iNOS in relation to various diseases (Morris et al., 2004; North et al., 2009). Recent studies have suggested that Arg-1, which converts L-arginine into L-ornithine and urea, can play a significant role in the pathogenesis of many various lung diseases (Morris et al., 2004). It has been documented that in cystic fibrosis, asthma and chronic obstructive pulmonary disease (COPD), arginase induced a decrease in the production of NO which has bronchodilatory properties (de Boer et al., 1999). Therefore, elevated Arg-1 activity in the airway could contribute to the obstruction and hyper-responsiveness of the airway (North et al., 2009). Moreover, Arg-1 plays a role in the production of NO and superoxide anion by reducing the availability of L-arginine to iNOS (Xia and Zweier, 1997). Thus, enhancing the synthesis of peroxynitrite, which has pro-inflammatory and pro-contractile actions (Xia and Zweier, 1997). L-ornithine is a precursor for both metabolic products L-proline and polyamines, and these products may promote the production of collagen and enhance cell proliferation, respectively (Meurs et al., 2003). Thereby, increased synthesis of L-ornithine caused by Arg-1 may also contribute to airway remodelling in these pulmonary diseases. Finally, Arg-1 expression has been linked with both forms of pulmonary hypertension (primary and secondary), through decreasing the levels of NO, which has vasodilatation properties (Xia and Zweier, 1997). In this study, we did not find any associations between the expression of Arg-1 and COPD nor asthma; however, future studies regarding this matter would be beneficial.

On the other hand, a study documented that iNOS expression and activity is increased during acute as well as chronic inflammatory lung disorders (Huang et al., 2015). It suggested that

imaging iNOS expression could be a useful tool as an inflammation biomarker for monitoring lung disease activity (Huang et al., 2015). Furthermore, a study conducted on smoker COPD patients has documented that iNOS expression was significantly increased in the peripheral lung tissue in these patients compared with that in smokers without COPD or non-smokers (Jiang et al., 2015). By that, indicating the possibility that iNOS could play an important role in the pathogenesis of COPD and could be a potential marker to detect the smokers who are more liable to suffer COPD (Jiang et al., 2015). With reference to the disease and smoking history data we have on patients involved in this study, no links has been established between the expression of iNOS and smoking or COPD. Future evaluation of possible associations is required.

The involvement of Arg-1 and iNOS in the immune response against *T. gondii* is highly evident and established by different studies; however, the main question remains as how these two enzymes relate to cancer in general and to lung cancer specifically. In addition to various lung diseases, some studies have evaluated the expression of Arg-1 and iNOS in relation to different types of cancer, including lung cancer. A study has evaluated the expression of iNOS in the aim to assess the role of molecular pathways involved in inflammation-mediated carcinogenesis on lung rat modules (Blanco et al., 2007). The results indicated that the expression of iNOS in the inflammatory process is associated with DNA damage response (DDR) and p53, a DDR marker, accumulation in pre-neoplastic epithelial cells. Furthermore, p16, which is another marker of DDR, is also induced in the early steps of tumorigenic progression, followed by a clear loss of expression in late dysplastic bronchiolar lesions (Blanco et al., 2007). In this study, we have reported the expression of iNOS in the columnar epithelial cells as well as in the in smooth muscle cells of the bronchiole. Nonetheless, in order to establish the difference of iNOS expression before and after the involvement of cancer would require a healthy pre-cancer sample, or more realistically a healthy control lung sample.

The expression of Arg-1 was evaluated in different cancer types but specifically hepatocellular carcinoma (HCC). A study aimed to study the clinicopathological significance of Arg-1 in HCC and has established that the expression of Arg-1 was downregulated in HCC tissue and was correlated with prognosis of patients (You et al., 2018). Moreover, the study has suggested that ARG1, which encodes Arg-1 expression, operates as an oncogene in HCC, since knockdown of ARG1 may decrease cell proliferation activity and motility of HCC cell (You et al., 2018). On the other hand, ARG1 overexpression may promote tumour-related phenotypes in HCC cells (You et

al., 2018). Whether that is applicable in lung cancer is still unknown; however, further evaluation of the clinicopathological effects of Arg-1 expression in lung cancer in correlation to prognosis and the evaluation of Arg-1 as an oncogene for lung cancer might be helpful.

Recent studies established that Arg-1 expression is induced in alternatively activated (M2) macrophages and plays a role in anti-inflammation, tumour immunity, tumour proliferation, metastasis, and immunosuppression-related diseases (Secondini et al., 2017). Recently, Arg-1 depletion has been considered as a potential effective anticancer therapy in vitro (Mussai and Egan, 2015). Since acute myeloid leukaemia (AML) is dependent on Arg-1for proliferation and survival, a study suggested Arg-1 depression as a treatment for AML (Mussai and Egan, 2015). A study has revealed that the inhibition of Arg-1 expression suppresses the metastasis of breast cancer to the lungs (Secondini et al., 2017). The study suggested that Arg-1 inhibition should be further evaluated as a candidate anti-metastatic approach in aggressive breast cancer (Secondini et al., 2017). Recombinant human arginase (rhArg), has been documented to be an effective therapeutic approach for different types of cancer including the histological subtype of lung cancer, Non-small cell lung cancer (NSCLC) (Shen et al., 2017). It was documented that rhArg had an anti-tumour effect via inducing cytotoxicity and apoptosis in the therapy for NSCLC (Shen et al., 2017). In addition, rhArg induced the cytoprotective autophagy, which is a cellular response to external and internal stressors, serves as a metabolic process responsible for the degradation of organelles and dysfunctional proteins (Z. Wang et al., 2014). In order to establish weather Arg-1 expression in our lung cancer patients has anti-cancer effects, for the future it is possible to conduct a correlation study with our data in relation to patient prognosis. Moreover, conducting the same approach on lung cancer animal models to evaluate if Arg-1 has the same anti-tumour properties on lung cancer.

Many studies have assessed the expression of Arg-1 and iNOS, but to our knowledge, none have addressed the expression of these two enzymes in relation to *T. gondii* infection and cancer in humans. In this study, we have reported the expression of Arg-1 and iNOS in relation to the infection with *T. gondii* in lung cancer individuals. Lung carcinoma is the leading cause of mortality among all types of cancer in males (Mong et al., 2011). Non-small cell lung cancer (NSCLC), one lung cancer histology subtype, accounts for over 80% of all patients with lung cancer (Siegel et al., 2014). Patients may be eligible for current standard therapies ranging from surgical resection to radiation to chemotherapy, as well as targeted therapy, depending on the

stage of lung cancer (Lemjabbar-Alaoui et al., 2015). In the past 25 years, a notable improvement was made in diagnosis and therapy. Nonetheless, the prognosis for patients with lung cancer remains unsatisfactory (Lemjabbar-Alaoui et al., 2015). With the highly invasive, rapidly metastasising properties of lung cancer, 70% of patients diagnosed are presented with advanced-stage disease (stage III or IV) (Siegel et al., 2014). Our study has documented a high rate of *T. gondii* among lung cancer patients, and potentially adding symptoms of lung toxoplasmosis on top of already existing lung cancer manifestations could be expanding the diseased burden exerted on these patients. Thus, those patients should get access to proper screening, diagnosis and treatment for toxoplasmosis in order to improve the overall life quality of these patients. Unfortunately, there aren't any studies which document the outcomes of treating cancer patients with *T. gondii* infection, and what the effects are of using anti-*T. gondii* treatment, when used on cancer patients. In the future, it would be of great benefit to perform clinical trials on cancer patients who are infected with *T. gondii* and evaluate whether the two treatments have effects on each other. Moreover, to establish how much improvement lung cancer patients will experience when toxoplasmosis is treated.

So far, the relationship between *T. gondii* and cancers remains unclear. The majority of cancer patients have compromised cellular and humoral immune systems either from the primary cancer or from undergoing chemotherapy and/or radiotherapy. The mechanism of action of chemotherapeutic drugs is killing both fast-growing cancer cells as well as healthy white blood cells resulting in neutropenia. Hence, patients receiving chemotherapy are more prone to opportunistic infections, including toxoplasmosis**.** Nevertheless, the cancer samples obtained for this study were collected prior to any administration of cancer treatment or chemotherapy. One of the new approaches for lung cancer treatment is immunotherapy, which its main role is to enhance the weakened immune system (Shankaran et al., 2001). Studies have reported that after the injection with *T. gondii* viable parasite or antigen, the development of spontaneous mammary tumours and leukaemia, was suppressed in animal models (Shankaran et al., 2001). Moreover, in vitro, *T. gondii* infection and the cell-free parasite extract had the ability to reverse the multi-drug resistance in both human gastric cancers and in mouse lymphoma (Hibbs and Lambert, 1971). A study has investigated the mechanisms of the antitumor actions of *T. gondii* infection on Lewis lung carcinoma (LLC) bearing mice (Kim et al., 2007). *T. gondii* infection in LLC mice significantly increased the survival rates as well as serum IgG2a titers (Kim et al., 2007).

Furthermore, there was a significant increase in the expression of IFN-ϒ mRNA, CD8+ T-cell percentage, and caused inhibition of angiogenesis, indicating that *T. gondii* has triggered Th1 immune responses (Kim et al., 2007). These reports indicate that *T. gondii* is potentially a powerful tool for cancer immunotherapy, and it could be utilised as a stimulant of the cellular immune responses (Kim et al., 2007). Furthermore, a recent study has identified a network of 1178 genes in which *T. gondii* may affect control of tumour growth and clearance through these genes (Ngô et al., 2017). Moreover, the study suggested that following *T. gondii* infection, the altered levels of cytokines and other immune and inflammation-associated pathways, have the potential to support neoplastic transformation and neurodegeneration (Ngô et al., 2017).

In our study, we have established that the susceptibility of lung cancer patients to *T. gondii* infection may not only be determined by the balance between Arg-1 and iNOS but also cell type could contribute to the infection liability. Moreover, we have shown that although Arg-1 and iNOS were both expressed in alveolar macrophages and *T. gondii* cysts, quantitively, their expression was different. Such results support the data that suggest that *T. gondii* infection in different cell types could result in specific host cell–parasite interactions. On the other hand, in the alveolar knobs, no difference was established. It is clear that further evaluation is required in the future to fully understand the dynamics between *T. gondii* infection and lung cancer. A starting point could be increasing the number of our sample size for lung cancer patients as well as the controls and possibly expand the geographical distribution of the samples. In addition, developing cell culture lines of different lung cell types to establish how different Arg-1 and iNOS are expressed when cells are apart from the lung tissue. Moreover, obtaining non-cancer biopsies would provide benefits to compare with the lung cancer samples; however, with the difficulty of the feasibility of that approach, non-cancer cell cultures would be an acceptable alternative. Furthermore, another possible approach for the future is to link the findings of this study with the clinical data of each lung cancer patients. Investigating the patients' age, gender, smoking and diseases history, e.g. COPD and asthma, in relation to our data could reveal associations or expose patterns.

An important future consideration is the importance and relevance of a *T. gondii* infection in relation to the pathology of lung cancer. At present, testing for *T. gondii* infection is not part of the diagnostic regime for lung cancer patients in the UK. This study suggests that this should now be considered. In order to understand the relationship, testing at first diagnosis and at intervals

during treatment would provide information on the progression of the infection. An important question is whether the *T. gondii* infection occurs prior to the development of the cancer or during the progression of this disease. Prior testing would inform us about pre-existing chronic infection whilst detection of seroconversion during the development of the cancer might provide information on the susceptibility of lung cancer patients to infection. Further research might then be focussed on understanding whether infection affects the quality of treatment. Clinical trials could be carried out to investigate the role of treatment of *T. gondii* in lung cancer patients and document whether improvement is observed in the patients' overall life quality and survival. Further research is required to establish the broader importance of our findings. Nevertheless, we hope that this study increases our understanding of the many factors that influence the interaction between this highly successful parasite and one of the leading killer diseases in the world.

Bibliography

Abdallahi, O. M., Bensalem, H., Augier, R., Diagana, M., De Reggi, M. and Gharib, B. (2001) 'Arginase expression in peritoneal macrophages and increase in circulating polyamine levels in mice infected with Schistosoma mansoni.' *Cellular and molecular life sciences : CMLS*, 58(9) pp. 1350–7.

Adams, L. B., Hibbs, J. B., Taintor, R. R. and Krahenbuhl, J. L. (1990) 'Microbiostatic effect of murine-activated macrophages for Toxoplasma gondii. Role for synthesis of inorganic nitrogen oxides from L-arginine.' *Journal of immunology (Baltimore, Md. : 1950)*, 144(7) pp. 2725–9.

Adler, J. and Parmryd, I. (2010) 'Quantifying colocalization by correlation: The pearson correlation coefficient is superior to the Mander's overlap coefficient.' *Cytometry Part A*, 77(8) pp. 733–742.

Ahn, M., Lee, C., Jung, K., Kim, H., Moon, C., Sim, K. and Shin, T. (2012) 'Immunohistochemical study of arginase-1 in the spinal cords of rats with clip compression injury.' *Brain Research*. Elsevier B.V., 1445, March, pp. 11–19.

Akinosoglou, K. S., Karkoulias, K. and Marangos, M. (2013) 'Infectious complications in patients with lung cancer.' *European Review for Medical and Pharmacological Sciences*, 17(1) pp. 8–18.

Alghamdi, J., Elamin, M. H. and Alhabib, S. (2016) 'Prevalence and genotyping of Toxoplasma gondii among Saudi pregnant women in Saudi Arabia.' *Saudi Pharmaceutical Journal*. King Saud University, 24(6) pp. 645–651.

Ali, M. I., Abd El Wahab, W. M., Hamdy, D. A. and Hassan, A. (2019) 'Toxoplasma gondii in cancer patients receiving chemotherapy: seroprevalence and interferon gamma level.' *Journal of Parasitic Diseases*. Springer India, 43(3) pp. 464–471.

Amos, W. B. and White, J. G. (2003) 'How the confocal laser scanning microscope entered biological research.' *Biology of the Cell*, 95(6) pp. 335–342.

Andres, T. L., Dorman, S. A., Winn, W., Trainer, T. D. and Perl, D. P. (1981) 'Immunohistochemical demonstration of Toxoplasma gondii.' *American journal of clinical pathology*, 75(3) pp. 431–4.

Arya S., B. S. (2011) 'Lung Cancer and Its Early Detection Using Biomarker-Based Biosensors.'

Chem. Rev., 111(11) pp. 6783–6809.

Bajnok, J. (2017) *Development of Approaches for Investigating the Distrubution of Toxoplasma gondii in Natural Population if Animals and Humans*. University of Salford.

Bajnok, J., Boyce, K., Rogan, M. T., Craig, P. S., Lun, Z. R. and Hide, G. (2015) 'Prevalence of Toxoplasma gondii in localized populations of Apodemus sylvaticus is linked to population genotype not to population location.' *Parasitology*, 142(05) pp. 680–690.

Bajnok, J., Tarabulsi, M., Carlin, H., Bown, K., Southworth, T., Dungwa, J., Singh, D., Lun, Z.-R., Smyth, L. and Hide, G. (2019) ' High frequency of infection of lung cancer patients with the parasite Toxoplasma gondii .' *ERJ Open Research*, 5(2) pp. 00143–02018.

Bando, H., Lee, Y., Sakaguchi, N., Pradipta, A., Ma, J. S., Tanaka, S., Cai, Y., Liu, J., Shen, J., Nishikawa, Y., Sasai, M. and Yamamoto, M. (2018) 'Inducible Nitric Oxide Synthase Is a Key Host Factor for Toxoplasma GRA15-Dependent Disruption of the Gamma Interferon-Induced Antiparasitic Human Response.' Denkers, E. Y. and Boothroyd, J. C. (eds) *mBio*, 9(5) pp. 1–19.

Behl, D., Porrata, L. F., Markovic, S. N., Letendre, L., Pruthi, R. K., Hook, C. C., Tefferi, A., Elliot, M. A., Kaufmann, S. H., Mesa, R. A. and Litzow, M. R. (2006) 'Absolute lymphocyte count recovery after induction chemotherapy predicts superior survival in acute myelogenous leukemia.' *Leukemia*, 20(1) pp. 29–34.

Behr, J. and Furst, D. E. (2008) 'Pulmonary function tests.' *Rheumatology*, 47(Supplement 5) pp. v65–v67.

Bernal-Guadarrama, M. J., Salichs, J., Almunia, J., García-Parraga, D., Fernández-Gallardo, N., Santana-Morales, M. Á., Pacheco, V., Afonso-Lehmann, R. N., Déniz, D., Lorenzo-Morales, J., Valladares, B. and Martínez-Carretero, E. (2014) 'Development of an indirect immunofluorescence technique for the diagnosis of toxoplasmosis in bottlenose dolphins.' *Parasitology Research*, 113(2) pp. 451–455.

Black, M. W. and Boothroyd, J. C. (2000) 'Lytic cycle of Toxoplasma gondii.' *Microbiology and molecular biology reviews : MMBR*, 64(3) pp. 607–623.

Blaga, R., Aubert, D., Thébault, A., Perret, C., Geers, R., Thomas, M., Alliot, A., Djokic, V., Ortis, N., Halos, L., Durand, B., Mercier, A., Villena, I. and Boireau, P. (2019) ' Toxoplasma

gondii in beef consumed in France: regional variation in seroprevalence and parasite isolation .' *Parasite*, 26 p. 77.

Blanco, D., Vicent, S., Fragaz, M. F., Fernandez-Garcia, I., Freire, J., Lujambioz, A., Esteller, M., Ortiz-de-Solorzano, C., Pio, R., Lecanda, F. and Montuenga, L. M. (2007) 'Molecular analysis of a multistep lung cancer model induced by chronic inflammation reveals epigenetic regulation of p16 and activation of the DNA damage response pathway.' *Neoplasia*, 9(10) pp. 840–852.

Blows, F. M., Driver, K. E., Schmidt, M. K., Broeks, A., van Leeuwen, F. E., Wesseling, J., Cheang, M. C., Gelmon, K., Nielsen, T. O., Blomqvist, C., Heikkilä, P., Heikkinen, T., Nevanlinna, H., Akslen, L. A., Bégin, L. R., Foulkes, W. D., Couch, F. J., Wang, X., Cafourek, V., Olson, J. E., Baglietto, L., Giles, G. G., Severi, G., McLean, C. A., Southey, M. C., Rakha, E., Green, A. R., Ellis, I. O., Sherman, M. E., Lissowska, J., Anderson, W. F., Cox, A., Cross, S. S., Reed, M. W. R., Provenzano, E., Dawson, S.-J., Dunning, A. M., Humphreys, M., Easton, D. F., García-Closas, M., Caldas, C., Pharoah, P. D. and Huntsman, D. (2010) 'Subtyping of Breast Cancer by Immunohistochemistry to Investigate a Relationship between Subtype and Short and Long Term Survival: A Collaborative Analysis of Data for 10,159 Cases from 12 Studies.' Marincola, F. M. (ed.) *PLoS Medicine*, 7(5) p. e1000279.

de Boer, J., Duyvendak, M., Schuurman, F. E., Pouw, F. M. H., Zaagsma, J. and Meurs, H. (1999) 'Role of L-arginine in the deficiency of nitric oxide and airway hyperreactivity after the allergen-induced early asthmatic reaction in guinea-pigs.' *British Journal of Pharmacology*, 128(5) pp. 1114–1120.

Brandtzaeg, P. (1998) 'The increasing power of immunohistochemistry and immunocytochemistry.' *Journal of Immunological Methods*, 216(1–2) pp. 49–67.

Breedveld, F. (2000) 'Therapeutic monoclonal antibodies.' *The Lancet*, 355(9205) pp. 735–740.

Busby, M., Xue, C., Li, C., Farjoun, Y., Gienger, E., Yofe, I., Gladden, A., Epstein, C. B., Cornett, E. M., Rothbart, S. B., Nusbaum, C. and Goren, A. (2016) 'Systematic comparison of monoclonal versus polyclonal antibodies for mapping histone modifications by ChIP-seq.' *Epigenetics & Chromatin*. BioMed Central, 9(1) p. 49.

Butcher, B. A., Fox, B. A., Rommereim, L. M., Kim, S. G., Maurer, K. J., Yarovinsky, F., Herbert, D. R., Bzik, D. J. and Denkers, E. Y. (2011) 'Toxoplasma gondii Rhoptry Kinase ROP16

Activates STAT3 and STAT6 Resulting in Cytokine Inhibition and Arginase-1-Dependent Growth Control.' Hunter, C. A. (ed.) *PLoS Pathogens*, 7(9) p. e1002236.

Campbell, E. J. (2001) 'Physiologic Changes in Respiratory Function.' *Principles and Practice of Geriatric Surgery*, 60 pp. 396–405.

Canessa, A., Del Bono, V., De Leo, P., Piersantelli, N. and Terragna, A. (1992) 'Cotrimoxazole therapy of Toxoplasma gondii encephalitis in AIDS patients.' *European Journal of Clinical Microbiology & Infectious Diseases*, 11(2) pp. 125–130.

Carey, R. M., Kimball, A. C., Armstrong, D. and Lieberman, P. H. (1973) 'Toxoplasmosis Clinical Experiences in a Cancer Hospital.' *The American Journal of Mediciire*, 54(January) pp. 30–38.

Carruthers, V. B. and Suzuki, Y. (2007) 'Effects of Toxoplasma gondii infection on the brain.' *Schizophrenia Bulletin*, 33(3) pp. 745–751.

Chang, C.-I., Liao, J. C. and Kuo, L. (1998) 'Arginase modulates nitric oxide production in activated macrophages.' *American Journal of Physiology*.

Channon, J. Y., Seguin, R. M. and Kasper, L. H. (2000) 'Differential infectivity and division of Toxoplasma gondii in human peripheral blood leukocytes.' *Infection and Immunity*, 68(8) pp. 4822–4826.

Chaussabel, D., Semnani, R. T., McDowell, M. A., Sacks, D., Sher, A. and Nutman, T. B. (2003) 'Unique gene expression profiles of human macrophages and dendritic cells to phylogenetically distinct parasites.' *Blood*, 102(2) pp. 672–681.

Choi, S., Park, C., Ahn, M., Lee, J. H. and Shin, T. (2012) 'Immunohistochemical study of arginase 1 and 2 in various tissues of rats.' *Acta Histochemica*. Elsevier GmbH., 114(5) pp. 487–494.

Comeau, J. W. D., Costantino, S. and Wiseman, P. W. (2006) 'A guide to accurate fluorescence microscopy colocalization measurements.' *Biophysical Journal*. Elsevier, 91(12) pp. 4611–4622.

Cong, W., Liu, G.-H., Meng, Q.-F., Dong, W., Qin, S.-Y., Zhang, F.-K., Zhang, X.-Y., Wang, X.-Y., Qian, A.-D. and Zhu, X.-Q. (2015) 'Toxoplasma gondii infection in cancer patients: Prevalence, risk factors, genotypes and association with clinical diagnosis.' *Cancer Letters*.

Elsevier Ireland Ltd, 359(2) pp. 307–313.

Conley, F. K. and Jenkins, K. A. (1981) ‘Immunohistological study of the anatomic relationship of toxoplasma antigens to the inflammatory response in the brains of mice chronically infected with Toxoplasma gondii.’ *Infection and immunity*, 31(3) pp. 1184–92.

Coons, A. H., Leduc, E. H. and Connolly, J. M. (1955) ‘A Method for The Histochemical Demostration of Specific Antibody and its Application to a Study of The Hyperimmune Rabbit.’ *In Studies on Antibody Production*, pp. 49–60.

Coons, A. and Kaplan, M. (1949) ‘Localization of Antigen In Tissue Cells.’ *J. Immunol.*, 45(1) pp. 159–170.

Cordell, J. L. (1984) ‘II Iinmunoenzymatic of Monoclonal Antibodies of Alkaline Phosphatase.’ *Journal of Histochemistry and Cytochemistry*.

Cortina-Borja, M., Tan, H. K., Wallon, M., Paul, M., Prusa, A., Buffolano, W., Malm, G., Salt, A., Freeman, K., Petersen, E. and Gilbert, R. E. (2010) ‘Prenatal treatment for serious neurological sequelae of congenital toxoplasmosis: An observational prospective cohort study.’ *PLoS Medicine*, 7(10).

Costes, S. V., Daelemans, D., Cho, E. H., Dobbin, Z., Pavlakis, G. and Lockett, S. (2004) ‘Automatic and quantitative measurement of protein-protein colocalization in live cells.’ *Biophysical Journal*. Elsevier, 86(6) pp. 3993–4003.

Courret, N., Darche, S., Sonigo, P., Milon, G., Buzoni-Gâtel, D. and Tardieux, I. (2006) ‘CD11c- and CD11b-expressing mouse leukocytes transport single Toxoplasma gondii tachyzoites to the brain.’ *Blood*, 107(1) pp. 309–316.

Davies, D. R. (1993) ‘Antibody Structure.’ *Laboratory of Molecular Biology, National Institute of Diabetes, Digestive and Kidney Diseases, Bethesda, Maryland 20892 Received March 12,1993 421 Almost*, (26) pp. 421–427.

Denman, A. R., Rogers, S., Ali, A., Sinclair, J., Phillips, P. S., Crockett, R. G. M. and Groves-Kirkby, C. J. (2015) ‘Small area mapping of domestic radon, smoking prevalence and lung cancer incidence - A case study in Northamptonshire, UK.’ *Journal of Environmental Radioactivity*. Elsevier Ltd, 150 pp. 159–169.

Denton, G. R. W. and Namazi, S. (2013) 'Indoor Radon Levels and Lung Cancer Incidence on Guam.' *Procedia Environmental Sciences*. Elsevier B.V., 18 pp. 157–166.

Derouin, F., Howe, D. K. and Honore, S. (1997) 'Determination of genotypes of Toxoplasma gondii strains isolated from patients with Determination of Genotypes of Toxoplasma gondii Strains Isolated from Patients with Toxoplasmosis.' *Journal of Clinical Microbiology*, 35(6) pp. 1411–1414.

Derouin, F., Sarfati, C., Beauvais, B., Iliou, M. C., Dehen, L. and Lariviere, M. (1989) 'Laboratory diagnosis of pulmonary toxoplasmosis in patients with acquired immunodeficiency syndrome.' *Journal of Clinical Microbiology*, 27(7) pp. 1661–1663.

Dubey, J. P. (1996) 'WAAVP and Pfizer Award for excellence in veterinary parasitology research pursuing life cycles and transmission of cyst-forming coccidia of animals and humans.' *Veterinary Parasitology*, 64(1–2) pp. 13–20.

Dubey, J. P. (1998) 'Advances in the life cycle of Toxoplasma gondii.' *International Journal for Parasitology*, 28(7) pp. 1019–1024.

Dubey, J. P. (2004) 'Toxoplasmosis - A waterborne zoonosis.' *Veterinary Parasitology*, 126(1-2 SPEC.ISS.) pp. 57–72.

Dubey, J. P. (2009) 'History of the discovery of the life cycle of Toxoplasma gondii.' *International Journal for Parasitology*. Australian Society for Parasitology Inc., 39(8) pp. 877–882.

Dubey, J. P. and Jones, J. L. (2008) 'Toxoplasma gondii infection in humans and animals in the United States.' *International Journal for Parasitology*, 38(11) pp. 1257–1278.

Dubey, J. P., Lindsay, D. S. and Speer, C. a. (1998) 'Structures of Toxoplasma gondii tachyzoites, bradyzoites, and sporozoites and biology and development of tissue cysts.' *Clinical Microbiology Reviews*, 11(2) pp. 267–299.

Dubey, J. P., Tiwari, K., Chikweto, a., DeAllie, C., Sharma, R., Thomas, D., Choudhary, S., Ferreira, L. R., Oliveira, S., Verma, S. K., Kwok, O. C. H. and Su, C. (2013) 'Isolation and RFLP genotyping of Toxoplasma gondii from the domestic dogs (Canis familiaris) from Grenada, West Indies revealed high genetic variability.' *Veterinary Parasitology*, 197(3–4) pp. 623–626.

Duncanson, P., Terry, R. S., Smith, J. E. and Hide, G. (2001) 'High levels of congenital transmission of Toxoplasma gondii in a commercial sheep flock.' *International Journal for Parasitology*, 31(14) pp. 1699–1703.

Ellis, H. (2008) 'Lungs: blood supply, lymphatic drainage and nerve supply.' *Anaesthesia and Intensive Care Medicine*. Elsevier Ltd., 9(11) pp. 462–463.

Ermert, M., Ruppert, C., Günther, A., Duncker, H. R., Seeger, W. and Ermert, L. (2002) 'Cell-specific nitric oxide synthase-isoenzyme expression and regulation in response to endotoxin in intact rat lungs.' *Laboratory Investigation*, 82(4) pp. 425–441.

Ermert, M., Ruppert, C., Günther, A., Duncker, H., Seeger, W. and Ermert, L. (2002) 'Expression and Regulation in Response to Endotoxin in Intact Rat Lungs.' *Laboratory Investigation*, 82(4) pp. 425–441.

Eyzaguirre, E. and Haque, A. (2008) 'Application of Immunohistochemistry to Infections.' *Archives of pathology & laboratory medicine*, 132(3) pp. 373–83.

Forthal, D. N. (2014) 'Functions of Antibodies.' *Infectious Diseases, University of California, Irvine,* 2(4) pp. 1–17.

Franklin, R. A., Liao, W., Sarkar, A., Kim, M. V., Bivona, M. R., Liu, K., Pamer, E. G. and Li, M. O. (2014) 'The cellular and molecular origin of tumor-associated macrophages.' *Science*, 344(6186) pp. 921–925.

Fraser, R. S. (2005) *Histology and gross anatomy of the respiratory tract*. *Physiologic Basis of Respiratory*.

Frenkel, J. K. (1970) 'Pursuing toxoplasma.' *Journal of Infectious Diseases*, 122(6) pp. 553–559.

Frenkel, J. K. (1978) 'Toxoplasmosis in cats: diagnosis, treatment and prevention.' *Comparative immunology, microbiology and infectious diseases*, 1(1–2) p. 15.

Fritz, H. M., Buchholz, K. R., Chen, X., Durbin-Johnson, B., Rocke, D. M., Conrad, P. a. and Boothroyd, J. C. (2012) 'Transcriptomic analysis of toxoplasma development reveals many novel functions and structures specific to sporozoites and oocysts.' *PLoS ONE*, 7(2).

Fuks, J. M., Arrighi, R. B. G., Weidner, J. M., Kumar Mendu, S., Jin, Z., Wallin, R. P. A., Rethi,

B., Birnir, B. and Barragan, A. (2012) ‘GABAergic Signaling Is Linked to a Hypermigratory Phenotype in Dendritic Cells Infected by Toxoplasma gondii.’ *PLoS Pathogens*, 8(12).

Gajria, B., Bahl, A., Brestelli, J., Dommer, J., Fischer, S., Gao, X., Heiges, M., Iodice, J., Kissinger, J. C., Mackey, A. J., Pinney, D. F., Roos, D. S., Stoeckert, C. J., Wang, H. and Brunk, B. P. (2008) ‘ToxoDB: An integrated toxoplasma gondii database resource.’ *Nucleic Acids Research*, 36(SUPPL. 1) pp. 1–4.

Gallego, C., Saavedra-Matiz, C. and Gómez-Marín, J. E. (2006) ‘Direct genotyping of animal and human isolates of Toxoplasma gondii from Colombia (South America).’ *Acta Tropica*, 97(2) pp. 161–167.

Gao, J.-M., Xie, Y.-T., Xu, Z.-S., Chen, H., Hide, G., Yang, T.-B., Shen, J.-L., Lai, D.-H. and Lun, Z.-R. (2017) ‘Genetic analyses of Chinese isolates of Toxoplasma gondii reveal a new genotype with high virulence to murine hosts.’ *Veterinary Parasitology*. Elsevier, 241, July, pp. 52–60.

Gao, J.-M., Yi, S., Wu, M.-S., Geng, G.-Q., Shen, J.-L., Lu, F., Hide, G., Lai, D.-H. and Lun, Z.-R. (2015) ‘Investigation of infectivity of neonates and adults from different rat strains to Toxoplasma gondii Prugniaud shows both variation which correlates with iNOS and Arginase-1 activity and increased susceptibility of neonates to infection.’ *Experimental parasitology*, 149, February, pp. 47–53.

Gasperino, J. (2011) ‘Gender is a risk factor for lung cancer.’ *Medical Hypotheses*. Elsevier Ltd, 76(3) pp. 328–331.

Gerald, P. (1986) ‘Infection in Cancer Patients.’ *The American Journal of Medicine*, 13 Pt 2 pp. 175–208.

Gray, D. S., Selbie, D., Cooper, R. F., Williams, M. and Robson, G. (2006) ‘Simultaneous de-waxing and standardisation of antigen retrieval in immunohistochemistry using commercially available equipment’ pp. 93–97.

Habibi, G. R., Imani, a. R., Gholami, M. R., Hablolvarid, M. H., Behroozikhah, a. M., Lotfi, M., Kamalzade, M., Najjar, E., Esmaeil-Nia, K. and Bozorgi, S. (2012) ‘Detection and identification of Toxoplasma gondii type one infection in sheep aborted fetuses in Qazvin province of Iran.’ *Iranian Journal of Parasitology*, 7(3) pp. 64–72.

Haff, L. a (1994) ‘Improved quantitative PCR using nested primers.’ *PCR methods and applications*, 3(6) pp. 332–337.

Haines, D. M. and Chelack, B. J. (1991) ‘Technical considerations for developing enzyme immunohistochemical staining procedures on formalin-fixed paraffin-embedded tissues for diagnostic pathology.’ *J.Vet.Diagn.Invest.*, 3(1) pp. 101–112.

Haines, D. M., Clark, E. G. and Duboyi, E. J. (1992) ‘Monoclonal Antibody-based Immunohistochemical Detection of Bovine Viral Diarrhea Virus in Formalin-fixed , Paraffin-embedded Tissues.’ *Vet Pathol*, 29 pp. 27–32.

Halos, L., Thébault, A., Aubert, D., Thomas, M., Perret, C., Geers, R., Alliot, A., Escotte-Binet, S., Ajzenberg, D., Dardé, M. L., Durand, B., Boireau, P. and Villena, I. (2010) ‘An innovative survey underlining the significant level of contamination by Toxoplasma gondii of ovine meat consumed in France.’ *International Journal for Parasitology*. Australian Society for Parasitology Inc., 40(2) pp. 193–200.

Hamal, K. R., Wideman, R., Anthony, N. and Erf, G. F. (2008) ‘Expression of Inducible Nitric Oxide Synthase in Lungs of Broiler Chickens Following Intravenous Cellulose Microparticle Injection.’ *Poultry Science*, 87(4) pp. 636–644.

Hammermann, R., Stichnote, C., Closs, E. I. and Nawrath, H. (2001) ‘Inhibition of nitric oxide synthase abrogates lipopolysaccharides-induced up-regulation of L -arginine uptake in rat alveolar macrophages.’ *British journal of pharmacology*, 133 pp. 379–386.

Hanafiah, M., Nurcahyo, R. W., Siregar, R. Y., Prastowo, J., Hartati, S., Sutrisno, B. and Aliza, D. (2017) ‘Detection of Toxoplasma gondii in cat’s internal organs by immunohistochemistry methods labeled with-[strept] avidin-biotin.’ *Veterinary World*, 10(9) pp. 1035–1039.

Herce, H. D., Casas-Delucchi, C. S. and Cardoso, M. C. (2013) ‘New image colocalization coefficient for fluorescence microscopy to quantify (bio-)molecular interactions.’ *Journal of Microscopy*, 249(3) pp. 184–194.

Hey, C., Ignaz, W. and Kurt, R. (1995) ‘Nitric oxide synthase activity is inducible in rat , but not rabbit alveolar macrophages , with a concomitant reduction in arginase activity.’ *Naunyn-Schmiedeberg’s Arch Pharmacol*, 351 pp. 651–659.

Hibbs, J. and Lambert, L. (1971) ‘Resistance to Murine Tumors Conferred by Chronic Infection with Intracellular Protozoa, Toxoplasma gondii and Besnoitia jeeisoni,’ 124(6) pp. 587–592.

Hide, G. (2016) ‘Role of vertical transmission of Toxoplasma gondii in prevalence of infection.’ *Expert Review of Anti-infective Therapy*. Taylor & Francis, 14(3) pp. 335–344.

Hide, G., Morley, E. K., Hughes, J. M., Gerwash, O., Elmahsishi, M. S., Elmahsishi, K. H., Thomasson, D., Wright, E. A., Williams, R. H., Murphy, R. G. and Smith, J. E. (2009) ‘Evidence for high levels of vertical transmission in Toxoplasma gondii.’ *Parasitology*, 136(14) p. 1877.

Hide, G. and Tait, A. (1991) ‘The molecular epidemiology of parasites.’ *Experientia*, 47(2) pp. 128–42.

Hochstedler, C. M., Leidinger, M. R., Maher-Sturm, M. T., Gibson-Corley, K. N. and Meyerholz, D. K. (2013) ‘Immunohistochemical detection of arginase-I expression in formalin-fixed lung and other tissues.’ *Journal of Histotechnology*, 36(4) pp. 128–134.

Holec-Gąsior, L., Dominiak-Górski, B. and Kur, J. (2015) ‘First report of seroprevalence of Toxoplasma gondii infection in sheep in Pomerania, northern Poland.’ *Annals of Agricultural and Environmental Medicine*, 22(4) pp. 604–607.

Homan, W. L., Vercammen, M., De Braekeleer, J. and Verschueren, H. (2000) ‘Identification of a 200- to 300-fold repetitive 529 bp DNA fragment in Toxoplasma gondii, and its use for diagnostic and quantitative PCR.’ *International Journal for Parasitology*, 30(1) pp. 69–75.

Huang, H. J., Isakow, W., Byers, D. E., Engle, J. T., Griffin, E. A., Kemp, D., Brody, S. L., Gropler, R. J., Miller, J. P., Chu, W., Zhou, D., Pierce, R. A., Castro, M., Mach, R. H. and Chen, D. L. (2015) ‘Imaging Pulmonary Inducible Nitric Oxide Synthase Expression with PET.’ *Journal of Nuclear Medicine*, 56(1) pp. 76–81.

Humbert, C., Santisteban, M. S., Usson, Y. and Robert-Nicoud, M. (1992) ‘Intranuclear co-location of newly replicated DNA and PCNA by simultaneous immunofluorescent labelling and confocal microscopy in MCF-7 cells.’ *Journal of Cell Science*, 103(1) pp. 97–103.

Hunter, S. A. S. and Alley, M. R. M. (2014) ‘Toxoplasmosis in Wild Birds in New Zealand.’ *Kokako2*, 21(2) pp. 58–59.

Imam, A., Al-Anzi, F. G., Al-Ghasham, M. A., Al-Suraikh, M. A., Al-Yahya, A. O. and Rasheed,

Z. (2017) ‘Serologic evidence of toxoplasma gondii infection among cancer patients. A prospective study from Qassim region, Saudi Arabia.’ *Saudi Medical Journal*, 38(3) pp. 319–321.

Isidro, R. A., Isidro, A. A., Cruz, M. L., Hernandez, S. and Appleyard, C. B. (2015) ‘Double immunofluorescent staining of rat macrophages in formalin-fixed paraffin-embedded tissue using two monoclonal mouse antibodies.’ *Histochemistry and Cell Biology*. Springer Berlin Heidelberg, 144(6) pp. 613–621.

Israelski, D. M. and Remington, J. S. (1993) ‘Toxoplasmosis in Patients with Cancer.’ *Clinical Infectious Diseas*, 17(2) pp. S423-35.

Ivović, V., Vujanić, M., Živković, T., Klun, I. and Djurković-djaković, O. (2007) ‘Molecular Detection and Genotyping of Toxoplasma gondii from Clinical Samples.’

Jameson, D. M., Croney, J. C. and Moens, P. D. J. (2003) ‘Fluorescence: Basic concepts, practical aspects, and some anecdotes.’ *Methods in Enzymology*, 360 pp. 1–43.

Jemal, A., Siegel, R., Ward, E., Hao, Y., Xu, J., Murray, T. and Thun, M. J. (2008) ‘Cancer Statistics, 2008.’ *CA: A Cancer Journal for Clinicians*, 58(2) pp. 71–96.

Jenkinson, C. P., Grody, W. W. and Cederbaum, S. D. (1996) ‘Comparative properties of arginases.’ *Comparative Biochemistry and Physiology Part B: Biochemistry and Molecular Biology*, 114(1) pp. 107–132.

Jeon, S.-H. and Yong, T.-S. (2000) ‘Serological Observation of Toxoplasma Gondii Prevalence in Apodemus Agrarius, a Dominant Species of Field Rodents in Korea.’ *Yonsei Medical Journal*, 41(4) pp. 491–496.

Jiang, W. T., Liu, X. S., Xu, Y. J., Ni, W. and Chen, S. X. (2015) ‘Expression of nitric oxide synthase isoenzyme in lung tissue of smokers with and without chronic obstructive pulmonary disease.’ *Chinese Medical Journal*, 128(12) pp. 1584–1589.

Jianling, W. (1993) ‘Heme Coordination and Structure of the Catalytic Site in Nitric Oxide Synthase.’ *The Journal of Biological Chemistry*, 268(30) pp. 22255–22258.

Kakimoto, T. (2018) ‘Validation of an easily applicable three-dimensional immunohistochemical imaging method for a mouse brain using conventional confocal microscopy.’ *Histochemistry and Cell Biology*. Springer Berlin Heidelberg, 149(1) pp. 97–103.

Kaliyappan, K., Palanisamy, M., Duraiyan, J. and Govindarajan, R. (2012) 'Applications of immunohistochemistry.' *Journal of Pharmacy and Bioallied Sciences*, 4(6) p. 307.

Kang, K. M., Lee, G. S., Lee, J. H., Choi, I. W., Shin, D. W. and Lee, Y. H. (2004) 'Effects of iNOS inhibitor on IFN-gamma production and apoptosis of splenocytes in genetically different strains of mice infected with Toxoplasma gondii.' *The Korean journal of parasitology*, 42(4) pp. 175–183.

Khan, a, Su, C., German, M., Storch, G. a, Clifford, D. B. and Sibley, L. D. (2005) 'Genotyping of Toxoplasma gondii Strains from Immunocompromised Patients Reveals High Prevalence of Type I Strains Genotyping of Toxoplasma gondii Strains from Immunocompromised Patients Reveals High Prevalence of Type I Strains,' 43(12) pp. 5881–5887.

Kibbe, M. R., Li, J., Nie, S., Watkins, S. C., Lizonova, A., Kovesdi, I., Simmons, R. L., Billiar, T. R. and Tzeng, E. (2000) 'Inducible nitric oxide synthase (iNOS) expression upregulates p21 and inhibits vascular smooth muscle cell proliferation through p42/44 mitogen- activated protein kinase activation and independent of p53 and cyclic guanosine monophosphate.' *Journal of Vascular Surgery*, 31(6) pp. 1214–1228.

Kim, J. O., Jung, S. S., Kim, S. Y., Tae, Y. K., Shin, D. W., Lee, J. H. and Lee, Y. H. (2007) 'Inhibition of Lewis lung carcinoma growth by Toxoplasma gondii through induction of Th1 immune responses and inhibition of angiogenesis.' *Journal of Korean Medical Science*, 22(SUPPL.) pp. 38–46.

Kim, S. W., Roh, J. and Park, C. S. (2016) 'Immunohistochemistry for pathologists: Protocols, pitfalls, and tips.' *Journal of Pathology and Translational Medicine*, 50(6) pp. 411–418.

Kovari, H., Ebnöther, C., Schweiger, A., Berther, N., Kuster, H. and Günthard, H. F. (2010) 'Pulmonary toxoplasmosis, a rare but severe manifestation of a common opportunistic infection in late HIV presenters: Report of two cases.' *Infection*, 38(2) pp. 141–144.

Kroncke, K., Fehsel, K. and Kolb-Bachofen, V. (1998) 'Inducible nitric oxide synthase in human diseases.' *Clinical and Experimental Immunology*, 113(2) pp. 147–156.

Kugler, D. G., Flomerfelt, F. A., Costa, D. L., Laky, K., Kamenyeva, O., Mittelstadt, P. R., Gress, R. E., Rosshart, S. P., Rehermann, B., Ashwell, J. D., Sher, A. and Jankovic, D. (2016) 'Systemic toxoplasma infection triggers a long-term defect in the generation and function of naive T

lymphocytes.' *Journal of Experimental Medicine*, 213(13) pp. 3041–3056.

Lambert, H., Hitziger, N., Dellacasa, I., Svensson, M. and Barragan, A. (2006) 'Induction of dendritic cell migration upon Toxoplasma gondii infection potentiates parasite dissemination.' *Cellular Microbiology*, 8(10) pp. 1611–1623.

Lan, H. Y., Mu, W., Nikolic-Paterson, D. J. and Atkins, R. C. (1995) 'A novel, simple, reliable, and sensitive method for multiple immunoenzyme staining: use of microwave oven heating to block antibody crossreactivity and retrieve antigens.' *Journal of Histochemistry & Cytochemistry*, 43(1) pp. 97–102.

Last, R. D. and Shivaprasad, H. L. (2008) 'An outbreak of toxoplasmosis in an aviary collection of Nicobar pigeons (Caloenas nicobaria).' *Journal of the South African Veterinary Association*, 79(3) pp. 149–152.

Leal, F. E., Cavazzana, C. L., de Andrade, H. F., Galisteo, A. J., de Mendonça, J. S. and Kallas, E. G. (2007) 'Toxoplasma gondii pneumonia in immunocompetent subjects: case report and review.' *Clinical infectious diseases : an official publication of the Infectious Diseases Society of America*, 44(6) pp. e62–e66.

Lehrnbecher, T. and Laws, H. J. (2005) 'Infectious Complications in Pediatric Cancer Patients.' *Klinische Padiatrie*, 217(SUPPL. 1).

Lemjabbar-Alaoui, H., Hassan, O. U., Yang, Y.-W. and Buchanan, P. (2015) 'Lung cancer: Biology and treatment options.' *Biochimica et Biophysica Acta (BBA) - Reviews on Cancer*, 1856(2) pp. 189–210.

Lepidi, H., Fenollar, F., Dumler, J. S., Gauduchon, V., Chalabreysse, L., Bammert, A., Bonzi, M.-F., Thivolet-Béjui, F., Vandenesch, F. and Raoult, D. (2004) 'Cardiac Valves in Patients with Whipple Endocarditis: Microbiological, Molecular, Quantitative Histologic, and Immunohistochemical Studies of 5 Patients.' *The Journal of Infectious Diseases*, 190(5) pp. 935–945.

Li, H., Meininger, C. J., Kelly, K. A., Hawker, J. R., Morris, S. M. and Wu, G. (2002) 'Activities of arginase I and II are limiting for endothelial cell proliferation.' *American Journal of Physiology*, 282 pp. 64–69.

Li, M. H., Che, T. C., Kuo, T. T., Tseng, C. C. and Tseng, C. P. (2000) 'Real-time PCR for quantitative detection of Toxoplasma gondii.' *Journal of Clinical Microbiology*, 38(11) pp. 4121–4125.

Li, Z., Zhao, Z.-J., Zhu, X.-Q., Ren, Q.-S., Nie, F.-F., Gao, J.-M., Gao, X.-J., Yang, T.-B., Zhou, W.-L., Shen, J.-L., Wang, Y., Lu, F.-L., Chen, X.-G., Hide, G., Ayala, F. J. and Lun, Z.-R. (2012) 'Differences in iNOS and arginase expression and activity in the macrophages of rats are responsible for the resistance against T. gondii infection.' *PloS one*, 7(4) p. e35834.

Lipman, N. S., Jackson, L. R., Trudel, L. J. and Weis-Garcia, F. (2005) 'Monoclonal Versus Polyclonal Antibodies: Distinguishing Characteristics, Applications, and Information Resources.' *ILAR Journal*, 46(3) pp. 258–268.

van der Loos, C. M. (2009) 'User Protocol: Practical Guide to Multiple Staining.' *Cambridge Research & Instrumentation, Inc.*

van der Loos, C. M., Becker, A. E. and van den Oord, J. J. (1993) 'Practical suggestions for successful immunoenzyme double- staining experiments.' *Histochemical Journal*, 25 pp. 1–13.

Lu, N., Liu, C., Wang, J., Ding, Y. and Ai, Q. (2015) 'Toxoplasmosis Complicating Lung Cancer: a Case Report.' *International medical case …* pp. 37–40.

Luoma, J. S., Strålin, P., Marklund, S. L., Hiltunen, T. P., Särkioja, T. and Ylä-Herttuala, S. (1998) 'Expression of extracellular SOD and iNOS in macrophages and smooth muscle cells in human and rabbit atherosclerotic lesions: Colocalization with epitopes characteristic of oxidized LDL and peroxynitrite-modified proteins.' *Arteriosclerosis, Thrombosis, and Vascular Biology*, 18(2) pp. 157–167.

Ma, H., Wang, Z., Wang, C., Li, C., Wei, F. and Liu, Q. (2015) 'Fatal Toxoplasma gondii infection in the giant panda.' *Parasite*, 22.

Manders, E. M. M., Stap, J., Brakenhoff, G. J., Van Driel, R. and Aten, J. A. (1992) 'Dynamics of three-dimensional replication patterns during the S-phase, analysed by double labelling of DNA and confocal microscopy.' *Journal of Cell Science*, 103(3) pp. 857–862.

MANDERS, E. M. M., VERBEEK, F. J. and ATEN, J. A. (1993) 'Measurement of co-localization of objects in dual-colour confocal images.' *Journal of Microscopy*, 169(3) pp. 375–382.

Mason, D. Y., Micklem, K. and Jones, M. (2000) ‘Double immunoflurescence labelling of routinely processed paraffin sections.’ *Journal of Pathology*, 191 pp. 452–461.

Mason, D. Y. and Sammons, R. (1978) ‘Alkaline phosphatase and peroxidase for double immunoenzymatic labelling of cellular constituents.’ *Journal of Clinical Pathology*, 31(5) pp. 454–460.

Matossian, R. M., Nassar, V. H. and Basmadji, A. (1977) ‘Direct immunofluorescence in the diagnosis of toxoplasmic lymphadenitis.’ *Journal of Clinical Pathology*, 30(9) pp. 847–850.

McCabe, R. E. and Remington, J. S. (1986) ‘Mechanisms of killing of Toxoplasma gondii by rat peritoneal macrophages.’ *Infection and Immunity*, 52(1) pp. 151–155.

McDonald, C. F. and Atkins, R. C. (1990) ‘Defective cytostatic activity of pulmonary alveolar macrophages in primary lung cancer.’ *Chest*. The American College of Chest Physicians, 98(4) pp. 881–885.

McLeod, R., Van Tubbergen, C., Montoya, J. G. and Petersen, E. (2014) ‘Human Toxoplasma Infection.’ *In Toxoplasma Gondii*. Second Edi, Elsevier, pp. 99–159.

Melzer, T. . and Carnston, H. . (2012) ‘Host Cell Preference of Toxoplasma gondii Cysts in Murine Brain: A confocal Study.’ *Bone*, 23(1) pp. 1–7.

Mescher, A. L. (2016) *Junqueira ’ s Basic Histology Text & Atlas (14th ed .)*. *Mc Graw Hill*.

Meurs, H., Maarsingh, H. and Zaagsma, J. (2003) ‘Arginase and asthma: Novel insights into nitric oxide homeostasis and airway hyperresponsiveness.’ *Trends in Pharmacological Sciences*, 24(9) pp. 450–455.

Michel, T., Li, G. K. and Busconi, L. (1993) ‘Phosphorylation and subcellular translocation of endothelial nitric oxide synthase.’ *Proceedings of the National Academy of Sciences*, 90(13) pp. 6252–6256.

Mighell, A. (1998) ‘An Overview of The Complexities and Subtleties of Immunohistochemistry.’ *2Molecular Medicine Unit, The University of Lee&, Clinical Sciences Building, Si. James’s University Hospital, beds LS9 7TF. UK* pp. 217–223.

Mong, C., Garon, E. B., Fuller, C., Mahtabifard, A., Mirocha, J., Mosenifar, Z. and McKenna, R.

(2011) ‘High prevalence of lung cancer in a surgical cohort of lung cancer patients a decade after smoking cessation.’ *Journal of cardiothoracic surgery*. BioMed Central Ltd, 6(1) p. 19.

Montoya, J. G. (2002) ‘Laboratory Diagnosis of Toxoplasma gondii Infection and Toxoplasmosis.’ *The Journal of Infectious Diseases*, 185(s1) pp. S73–S82.

Morris, C. R., Poljakovic, M., Lavrisha, L., Machado, L., Kuypers, F. A. and Morris, S. M. (2004) ‘Decreased arginine bioavailability and increased serum arginase activity in asthma.’ *American Journal of Respiratory and Critical Care Medicine*, 170(2) pp. 148–153.

Morris Jr, S. M. (2009) ‘Recent advances in arginine metabolism: roles and regulation of the arginases.’ *British Journal of Pharmacology*, 157(6) pp. 922–930.

Morris, S. M. and Billiar, T. R. (1994) ‘New insights into the regulation nitric oxide synthesis of inducible nitric oxide synthesis.’ *American Journal of Physiology*.

Mussai, F. and Egan, S. (2015) ‘Arginine dependence of acute myeloid leukemia blast proliferation: A novel therapeutic target.’ *Blood*, 125(15) pp. 2386–2396.

Nakane, P. K. (1968) ‘Simultaneous Localization of Multiple Tissue Antigens Using The Peroxidase-Labeled Antibody Method: A Study on Pituitary Glands of The Rat.’ *The Journal of Histochemistry and Cytochemistry*, 16(9) pp. 557–560.

Nakazawa, M., Mukumoto, M. and Miyatake, K. (2010) ‘Production and Purification of Polyclonal Antibodies.’ *In Methods in Molecular Biology (Clifton, N.J.)*, pp. 63–74.

Ngô, H. M., Zhou, Ying, Lorenzi, H., Wang, K., Kim, T. K., Zhou, Yong, Bissati, K. El, Mui, E., Fraczek, L., Rajagopala, S. V., Roberts, C. W., Henriquez, F. L., Montpetit, A., Blackwell, J. M., Jamieson, S. E., Wheeler, K., Begeman, I. J., Naranjo-Galvis, C., Alliey-Rodriguez, N., Davis, R. G., Soroceanu, L., Cobbs, C., Steindler, D. A., Boyer, K., Noble, A. G., Swisher, C. N., Heydemann, P. T., Rabiah, P., Withers, S., Soteropoulos, P., Hood, L. and McLeod, R. (2017) ‘Toxoplasma Modulates Signature Pathways of Human Epilepsy, Neurodegeneration & Cancer.’ *Scientific Reports*, 7(1) pp. 1–32.

Nogareda, F., Le Strat, Y., Villena, I., De Valk, H. and Goulet, V. (2014) ‘Incidence and prevalence of Toxoplasma gondii infection in women in France, 1980-2020: Model-based estimation.’ *Epidemiology and Infection*, 142(8) pp. 1661–1670.

North, M. L., Amatullah, H., Khanna, N., Urch, B., Grasemann, H., Silverman, F. and Scott, J. A. (2011) 'Augmentation of arginase 1 expression by exposure to air pollution exacerbates the airways hyperresponsiveness in murine models of asthma.' *Respiratory Research*, 12(1) p. 19.

North, M. L., Khanna, N., Marsden, P. A., Grasemann, H. and Scott, J. A. (2009) 'Functionally important role for arginase 1 in the airway hyperresponsiveness of asthma.' *American Journal of Physiology - Lung Cellular and Molecular Physiology*, 296(6) pp. 911–920.

Panchuk-Voloshina, N., Haugland, Rosaria P., Bishop-Stewart, J., Bhalgat, M. K., Millard, P. J., Mao, F., Leung, W. Y. and Haugland, Richard P. (1999) 'Alexa dyes, a series of new fluorescent dyes that yield exceptionally bright, photostable conjugates.' *Journal of Histochemistry and Cytochemistry*, 47(9) pp. 1179–1188.

Pappas, G., Roussos, N. and Falagas, M. E. (2009) 'Toxoplasmosis snapshots: Global status of Toxoplasma gondii seroprevalence and implications for pregnancy and congenital toxoplasmosis.' *International Journal for Parasitology*. Australian Society for Parasitology Inc., 39(12) pp. 1385–1394.

Pearson, K. (1895) 'Mathematical Contributions to the Theory of Evolution.Regression, Heredity, and Panmixia.' *Philosophical Transactions of the Royal Society of London.*, 191 pp. 229–311.

Perlin, E., Bang, K. M., Shah, A., Hursey, P. D., Whittingham, W. L., Hashmi, K. and Campbell, L. (1990) 'The Impact of Pulmonary Infection on the Survival of Lung Cancer Patiens' pp. 1–4.

Pfefferkorn, E., Eckel, M. and Rebhun, S. (1986) 'Interferon-γ suppresses the growth of Toxoplasma gondii in human fibroblasts through starvation for tryptophan.' *Molecular and Biochemical Parasitology*, 20(3) pp. 215–224.

Plumb, J., Smyth, L. J. C., Adams, H. R., Vestbo, J., Bentley, A. and Singh, S. D. (2009) 'Increased T-regulatory cells within lymphocyte follicles in moderate COPD.' *European Respiratory Journal*, 34(1) pp. 89–94.

Pomeroy, C. and Filice, G. a (1992) 'Pulmonary toxoplasmosis: a review.' *Clinical infectious diseases : an official publication of the Infectious Diseases Society of America*, 14(4) pp. 863–870.

Pusch, L., Romelke, B., Deckert, M. and Mawrin, C. (2009) 'Persistent toxoplasma bradyzoite

cysts in the brain: Incidental finding in an immunocompetent patient without evidenceof a toxoplasmosis.' *Clinical Neuropathology*, 28(3) pp. 210–212.

Ramos-Vara, J. A. (2005) 'Technical Aspects of Immunohistochemistry.' *Veterinary Pathology*, 42(4) pp. 405–426.

Robert-Gangneux, F. and Dardé, M. L. (2012) 'Epidemiology of and diagnostic strategies for toxoplasmosis.' *Clinical Microbiology Reviews*, 25(2) pp. 264–296.

Roe, W. D., Howe, L., Baker, E. J., Burrows, L. and Hunter, S. A. (2013) 'An atypical genotype of Toxoplasma gondii as a cause of mortality in Hector's dolphins (Cephalorhynchus hectori).' *Veterinary Parasitology*. Elsevier B.V., 192(1–3) pp. 67–74.

Ross, M. H., Romrell, L. J. and Kaye, G. I. (1989) *Histology : a text and atlas*. Lippincott Williams and Wilkins.

Rottenberg, G. T., Miszkiel, K., Shaw, P. and Miller, R. F. (1997) 'Case report: Fulminant toxoplasma gondii pneumonia in a patient with AIDS.' *Clinical Radiology*, 52(6) pp. 472–474.

Sakikawa, M., Noda, S., Hanaoka, M., Nakayama, H., Hojo, S., Kakinoki, S., Nakata, M., Yasuda, T., Ikenoue, T. and Kojima, T. (2012) 'Anti-Toxoplasma antibody prevalence, primary infection rate, and risk factors in a study of toxoplasmosis in 4,466 pregnant women in Japan.' *Clinical and Vaccine Immunology*, 19(3) pp. 365–367.

Sarihan, S., Ercan, I., Saran, A., Çetintas, S. K., Akalin, H. and Engin, K. (2005) 'Evaluation of infections in non-small cell lung cancer patients treated with radiotherapy.' *Cancer Detection and Prevention*, 29(2) pp. 181–188.

Scerra, S., Coignard-Biehler, H., Lanternier, F., Suarez, F., Charlier-Woerther, C., Bougnoux, M.-E., Gilquin, J., Lecuit, M., Hermine, O. and Lortholary, O. (2013) 'Disseminated toxoplasmosis in non-allografted patients with hematologic malignancies: report of two cases and literature review.' *European Journal of Clinical Microbiology & Infectious Diseases*, 32(10) pp. 1259–1268.

Schacht, V. and Kern, J. S. (2015) 'Basics of Immunohistochemistry.' *Journal of Investigative Dermatology*. Elsevier Masson SAS, 135(3) pp. 1–4.

Scharton-Kersten, T. M., Yap, G., Magram, J. and Sher, A. (1997) 'Inducible nitric oxide is

essential for host control of persistent but not acute infection with the intracellular pathogen Toxoplasma gondii.' *Journal of Experimental Medicine*, 185(7) pp. 1261–1273.

Schroeder, H. W. and Cavacini, L. (2010) 'Structure and function of immunoglobulins.' *Journal of Allergy and Clinical Immunology*, 125(2) pp. S41–S52.

Secondini, C., Coquoz, O., Spagnuolo, L., Spinetti, T., Peyvandi, S., Ciarloni, L., Botta, F., Bourquin, C. and Rüegg, C. (2017) 'Arginase inhibition suppresses lung metastasis in the 4T1 breast cancer model independently of the immunomodulatory and anti-metastatic effects of VEGFR-2 blockade.' *OncoImmunology*. Taylor & Francis, 6(6) pp. 1–14.

Shan, D., Qian, W., Liu, J., Liu, R. and Liu, Q. (2015) 'Identification and co-localization of perforin-like (TgPLP1) protein in Toxoplasma gondii bradyzoites.' *Experimental Parasitology*. Elsevier Inc., 153 pp. 39–44.

Shankaran, V., Ikeda, H., Bruce, A. T., White, J. M., Swanson, P. E., Old, L. J. and Schreiber, R. D. (2001) 'IFNγ and lymphocytes prevent primary tumour development and shape tumour immunogenicity.' *Nature*, 410(6832) pp. 1107–1111.

Sheffield, H. G. and Melton, M. L. (1974) 'Immunity to toxoplasma gondii in cats' pp. 106–107.

Shen, W., Zhang, X., Fu, X., Fan, J., Luan, J., Cao, Z., Yang, P., Xu, Z. and Ju, D. (2017) 'A novel and promising therapeutic approach for NSCLC: Recombinant human arginase alone or combined with autophagy inhibitor.' *Cell Death and Disease*. Nature Publishing Group, 8(3) pp. e2720-11.

Sherman, T. S., Chen, Z., Yuhanna, I. S., Lau, K. S., Margraf, L. R. and Shaul, P. W. (1999) 'Nitric oxide synthase isoform expression in the developing lung epithelium.' *American Journal of Physiology*, 276(2 PART 1) pp. 383–390.

Shi, S. R., Cote, R. J. and Taylor, C. R. (2001) 'Antigen retrieval techniques: Current perspectives.' *Journal of Histochemistry and Cytochemistry*, 49(8) pp. 931–937.

Shi, S. R., Key, M. E. and Kalra, K. L. (1991) 'Antigen retrieval in formalin-fixed, paraffin-embedded tissues: An enhancement method for immunohistochemical staining based on microwave oven heating of tissue sections.' *Journal of Histochemistry and Cytochemistry*, 39(6) pp. 741–748.

Siegel, R., Ma, J., Zou, Z. and Jemal, A. (2014) 'Cancer statistics, 2014.' *CA: A Cancer Journal for Clinicians*, 64(1) pp. 9–29.

Silva, A. F., Oliveira, F. C. R., Leite, J. S., Mello, M. F. V., Brandão, F. Z., Leite, R. I. J. C. K., Frazão-Teixeira, E., Lilenbaum, W., Fonseca, A. B. M. and Ferreira, A. M. R. (2013) 'Immunohistochemical identification of Toxoplasma gondii in tissues from Modified Agglutination Test positive sheep.' *Veterinary Parasitology*. Elsevier B.V., 191(3–4) pp. 347–352.

Sims, T. A., Hay, J. and Talbot, I. C. (1989) 'An electron microscope and immunohistochemical study of the intracellular location of Toxoplasma tissue cysts within the brains of mice with congenital toxoplasmosis.' *British Journal of Experimental Pathology*, 70(3) pp. 317–325.

Singh, A., Sventek, P., Larivière, R., Thibault, G. and Schiffrin, E. L. (1996) 'Inducible nitric oxide synthase in vascular smooth muscle cells from prehypertensive spontaneously hypertensive rats.' *American Journal of Hypertension*, 9(9) pp. 867–877.

de Souza Giassi, K., Costa, A. N., Apanavicius, A., Teixeira, F. Bin, Fernandes, C. J. C., Helito, A. S. and Kairalla, R. A. (2014a) 'Tomographic findings of acute pulmonary toxoplasmosis in immunocompetent patients.' *BMC Pulmonary Medicine*, 14(1) p. 185.

de Souza Giassi, K., Costa, A. N., Apanavicius, A., Teixeira, F. Bin, Fernandes, C. J. C., Helito, A. S. and Kairalla, R. A. (2014b) 'Tomographic findings of acute pulmonary toxoplasmosis in immunocompetent patients.' *BMC Pulmonary Medicine*, 14(1) pp. 1–5.

Stack, E. C., Wang, C., Roman, K. A. and Hoyt, C. C. (2014) 'Multiplexed immunohistochemistry, imaging, and quantitation: A review, with an assessment of Tyramide signal amplification, multispectral imaging and multiplex analysis.' *Methods*. Elsevier Inc., 70(1) pp. 46–58.

Su, C., Shwab, E. K., Zhou, P., Zhu, X. Q. and Dubey, J. P. (2010) 'Moving towards an integrated approach to molecular detection and identification of Toxoplasma gondii.' *Parasitology*, 137(1) pp. 1–11.

Su, C., Zhang, X. and Dubey, J. P. (2006) 'Genotyping of Toxoplasma gondii by multilocus PCR-RFLP markers: A high resolution and simple method for identification of parasites.' *International Journal for Parasitology*, 36(7) pp. 841–848.

Tabbara, K., Al-Omar, M., Tawflk, A. and Al-shaiinnary, F. (1999) 'Toxoplasmosis in Saudi Arabia.' *Saudi Medical Journal*, 20(1) pp. 46–49.

Tabll, A., Abbas, A. T., El-kafrawy, S. and Wahid, A. (2015) 'Monoclonal antibodies : Principles and applications of immmunodiagnosis and immunotherapy for hepatitis C virus.' *World Journal of Hepatology*, 7(22) pp. 2369–2383.

Takir, S., Gürel-Gürevin, E., Toprak, A., Demirci-Tansel, C. and Uydeş-Doğan, B. S. (2016) 'The elevation of intraocular pressure is associated with apoptosis and increased immunoreactivity for nitric oxide synthase in rat retina whereas the effectiveness of retina derived relaxing factor is unaffected.' *Experimental Eye Research*, 145 pp. 401–411.

Tenter, A. M., Heckeroth, A. R. and Weiss, L. M. (2000) 'Toxoplasma gondii: From animals to humans.' *International Journal for Parasitology*, 30(12–13) pp. 1217–1258.

Thomas, F., Lafferty, K. D., Brodeur, J., Elguero, E., Gauthier-Clerc, M. and Misse, D. (2012) 'Incidence of adult brain cancers is higher in countries where the protozoan parasite Toxoplasma gondii is common.' *Biology Letters*, 8(1) pp. 101–103.

Tomashefski, J. F., Cagle, P. T., Farver, C. F. and Fraire, A. E. (2008) 'Anatomy and Histology of the Lung.' *Dail and Hammar's Pulmonary Pathology*, 1(November) pp. 1–1301.

Tomita, T., Bzik, D. J., Ma, Y. F., Fox, B. A., Markillie, L. M., Taylor, R. C., Kim, K. and Weiss, L. M. (2013) 'The Toxoplasma gondii Cyst Wall Protein CST1 Is Critical for Cyst Wall Integrity and Promotes Bradyzoite Persistence.' *PLoS Pathogens*, 9(12) pp. 1–15.

Toshiyuki, I., Naito, Z. and Nishigaki, R. (1997) 'Differential Distribution of ecNOS and iNOS mRNA in RAT Heart after Endotoxin Administraion.' *Japan Heart Journal* pp. 445–455.

Tousson, E., Ali, E. M., Ibrahim, W. and Ashraf, R. M. (2012) 'Histopathological and immunohistochemical alterations in rat heart after thyroidectomy and the role of hemin and ketoconazole in treatment.' *Biomedicine & Pharmacotherapy*. Elsevier Masson SAS, 66(8) pp. 627–632.

Travis, W. D. (2011) 'Classification of Lung Cancer.' *Seminars in Roentgenology*. Elsevier Inc., 46(3) pp. 178–186.

Travis, W. D., Brambilla, E., Müller-Hermelink, H. K. and Harris, C. C. (2004) 'Pathology and

genetics of tumours of the lung.' *Bulletin of the World Health Organization*, 50(1–2) pp. 9–19.

Travis, W. D., Brambilla, E., Nicholson, A. G., Yatabe, Y., Austin, J. H. M., Beasley, M. B., Chirieac, L. R., Dacic, S., Duhig, E., Flieder, D. B., Geisinger, K., Hirsch, F. R., Ishikawa, Y., Kerr, K. M., Noguchi, M., Pelosi, G., Powell, C. A., Tsao, M. S. and Wistuba, I. (2015) 'The 2015 World Health Organization Classification of Lung Tumors: Impact of Genetic, Clinical and Radiologic Advances since the 2004 Classification.' *Journal of Thoracic Oncology*. International Association for the Study of Lung Cancer, 10(9) pp. 1243–1260.

Tu, V., Mayoral, J., Sugi, T., Tomita, T., Han, B., Ma, Y. F. and Weissa, L. M. (2019) 'Enrichment and proteomic characterization of the cyst wall from in vitro toxoplasma gondii cysts.' *mBio*, 10(2) pp. 1–15.

Wang, L., He, L.-Y., Meng, D., Chen, Z.-W., Wen, H., Fang, G.-S., Luo, Q.-L., Huang, K.-Q. and Shen, J.-L. (2015) 'Seroprevalence and genetic characterization of Toxoplasma gondii in cancer patients in Anhui Province, Eastern China.' *Parasites & Vectors*, 8(1) p. 162.

Wang, T., Gao, J.-M., Yi, S.-Q., Geng, G.-Q., Gao, X.-J., Shen, J.-L., Lu, F.-L., Wen, Y.-Z., Hide, G. and Lun, Z.-R. (2014) 'Toxoplasma gondii infection in the peritoneal macrophages of rats treated with glucocorticoids.' *Parasitology research*, 113(1) pp. 351–358.

Wang, Z., Shi, X., Li, Y., Fan, J., Zeng, X., Xian, Z., Wang, Z., Sun, Y., Wang, S., Song, P., Zhao, S., Hu, H. and Ju, D. (2014) 'Blocking autophagy enhanced cytotoxicity induced by recombinant human arginase in triple-negative breast cancer cells.' *Cell Death and Disease*, 5(12).

Warford, A., Akbar, H. and Riberio, D. (2014) 'Antigen retrieval, blocking, detection and visualisation systems in immunohistochemistry: A review and practical evaluation of tyramide and rolling circle amplification systems.' *Methods*. Elsevier Inc., 70(1) pp. 28–33.

Weiss, L. M. and Dubey, J. P. (2009) 'Toxoplasmosis: A history of clinical observations.' *International Journal for Parasitology*. Australian Society for Parasitology Inc., 39(8) pp. 895–901.

Weissfeld, A. S., Forbes, B. A. and Sahm, D. F. (2007) *Bailey & Scott's Diagnostic Microbiology*. Twelfth, St. Louis: Mosby.

Wildhirt, S. M., Dudek, R. R., Suzuki, H., Pinto, V., Narayan, K. S. and Bing, R. J. (1994)

‘Immunohistochemistry in the identification of nitric oxide synthase isoenzymes in myocardial infarction.’ *Cardiovascular Research*, 28(9) pp. 526–531.

Wootla, B., Denic, A. and Rodriguez, M. (2014) ‘Polyclonal and Monoclonal Antibodies in Clinic.’ *In* Steinitz, M. (ed.) *Human Monoclonal Antibodies: Methods and Protocols, Methods in Molecular Biology*. Totowa, NJ: Humana Press (Methods in Molecular Biology), pp. 79–110.

Wu, G., Bazer, F. W., Davis, T. A., Kim, S. W., Li, P., Marc Rhoads, J., Carey Satterfield, M., Smith, S. B., Spencer, T. E. and Yin, Y. (2009) ‘Arginine metabolism and nutrition in growth, health and disease.’ *Amino Acids*, 37(1) pp. 153–168.

Xia, Y. and Zweier, J. L. (1997) ‘Superoxide and peroxynitrite generation from inducible nitric oxide synthase in macrophages.’ *Proceedings of the National Academy of Sciences*, 94(13) pp. 6954–6958.

You, J., Chen, W., Chen, J., Zheng, Q., Dong, J. and Zhu, Y. (2018) ‘The oncogenic role of ARG1 in progression and metastasis of hepatocellular carcinoma.’ *BioMed Research International*, 2018.

Young, B., Lowe, J., Stevens, A. and Heath, J. (2006) *Wheater’s Functional Histology: A Text and Colour Atlas*. 5th ed., Churchill Livingstone.

Yu, H., Yoo, P. K., Aguirre, C. C., Tsoa, R. W., Kern, R. M., Grody, W. W., Cederbaum, S. D. and Iyer, R. K. (2003) ‘Widespread Expression of Arginase I in Mouse Tissues : Biochemical and Physiological Implications.’ *The Journal of Histochemistry and Cytochemistry*, 51(9) pp. 1151–1160.

Yuan, Z., Gao, S., Liu, Q., Xia, X., Liu, X., Liu, B. and Hu, R. (2007) ‘Toxoplasma gondii antibodies in cancer patients.’ *Cancer Letters*, 254(1) pp. 71–74.

Zhang, X. and Homer, R. J. (2016) ‘Normal Development, Anatomy, Histology and Aging of the Lung.’ *The Aging Lungs* pp. 1–37.

Zhao, Z. J., Zhang, J., Wei, J., Li, Z., Wang, T., Yi, S. Q., Shen, J. L., Yang, T. B., Hide, G. and Lun, Z. R. (2013a) ‘Lower Expression of Inducible Nitric Oxide Synthase and Higher Expression of Arginase in Rat Alveolar Macrophages Are Linked to Their Susceptibility to Toxoplasma gondii Infection.’ *PLoS ONE*, 8(5) pp. 1–11.

Zhao, Z. J., Zhang, J., Wei, J., Li, Z., Wang, T., Yi, S. Q., Shen, J. L., Yang, T. B., Hide, G. and Lun, Z. R. (2013b) 'Lower Expression of Inducible Nitric Oxide Synthase and Higher Expression of Arginase in Rat Alveolar Macrophages Are Linked to Their Susceptibility to Toxoplasma gondii Infection.' Thomas, P. G. (ed.) *PLoS ONE*, 8(5) p. e63650.

Zhou, L. and Zhu, D. (2009) 'Nitric Oxide Neuronal nitric oxide synthase : Structure , subcellular localization , regulation , and clinical implications.' *Nitric Oxide*. Elsevier Inc., 20(4) pp. 223–230.

Appendices

Appendix A

High frequency of infection of lung cancer patients with the parasite *Toxoplasma gondii*

Jaroslav Bajnok[1], Muyassar Tarabulsi[1], Helen Carlin[1], Kevin Bown[1], Thomas Southworth[2], Josiah Dungwa[2], Dave Singh[2], Zhao-Rong Lun[1,3], Lucy Smyth[1] and Geoff Hide[1*]

[1] Biomedical Research Centre and Ecosystems and Environment Research Centre, School of Environment and Life Sciences, University of Salford, Salford, M5 4WT, UK

[2] The University of Manchester, Division of Infection, Immunity and Respiratory Medicine, School of Biological Sciences, Faculty of Biology, Medicine and Health, Manchester Academic Health Science Centre, The University of Manchester and University Hospital of South Manchester NHS Foundation Trust, Manchester, M23 9LT, UK

[3] Centre for Parasitic Organisms, State Key Laboratory of Biocontrol, School of Life Sciences and Key Laboratory of Tropical Diseases Control, Zhongshan School of Medicine, Sun Yat-Sen University, Guangzhou 510275, P.R. China

*Corresponding Author:

Professor Geoff Hide,

Biomedical Research Centre,

School of Environment and Life Sciences,

University of Salford, Salford, M5 4WT,

UK

email: g.hide@salford.ac.uk

"Take home" message: *Toxoplasma gondii* infection was found to be present in all lung tissue samples taken from 72 cancer patients (including active parasite stages in 96% of them).

ERJ open research

ORIGINAL ARTICLE
LUNG CANCER

High frequency of infection of lung cancer patients with the parasite *Toxoplasma gondii*

Jaroslav Bajnok[1], Muyassar Tarabulsi[1], Helen Carlin[1], Kevin Bown[1], Thomas Southworth[2], Josiah Dungwa[2], Dave Singh[2], Zhao-Rong Lun[1,3], Lucy Smyth[1] and Geoff Hide[1]

Affiliations: [1]Biomedical Research Centre and Ecosystems and Environment Research Centre, School of Science, Engineering and Environment, University of Salford, Salford, UK. [2]The University of Manchester, Division of Infection, Immunity and Respiratory Medicine, School of Biological Sciences, Faculty of Biology, Medicine and Health, Manchester Academic Health Science Centre, The University of Manchester and University Hospital of South Manchester NHS Foundation Trust, Manchester, UK. [3]Center for Parasitic Organisms, State Key Laboratory of Biocontrol, School of Life Sciences and Key laboratory of Tropical Diseases Control, Zhongshan School of Medicine, Sun Yat-Sen University, Guangzhou, P.R. China.

Correspondence: Geoff Hide, Biomedical Research Centre, School of Science, Engineering and Environment, University of Salford, Salford, M5 4WT, UK. E-mail: g.hide@salford.ac.uk

ABSTRACT

Background: *Toxoplasma gondii* is an intracellular protozoan parasite that can cause a wide range of clinical conditions, including miscarriage and pneumonia. The global prevalence is 30% in humans, but varies by locality (*e.g.* in the UK it is typically 10%). The association between lung cancer and *T. gondii* infection was investigated by direct detection in lung tissue samples.

Methods: Lung tissue samples were taken from patients undergoing lung resection surgery (n=72) for suspected lung cancer (infection prevalence 100% (95% CI: 93.9–100%)). All 72 participants were confirmed as having lung cancer following subsequent diagnostic tests. In addition, bronchial biopsy samples were collected from non-lung cancer healthy control subjects (n=10). Samples were tested for *T. gondii* using PCR amplification of *T. gondii* specific gene markers and *T. gondii* specific immunohistochemistry.

Results: All 72 lung cancer patients were infected with *T. gondii* (prevalence 100% (95% CI: 93.9–100%)). Of which, 95.8% (n=69) of patients showed evidence of active parasite stages. Infection prevalence in the controls (10%) was significantly lower ($p<0.0001$).

Conclusions: Clinicians treating lung cancer patients should be aware of the potential presence of the parasite, the potential for induction of symptomatic complications and interference with treatment success.

@ERSpublications
***Toxoplasma gondii* infection was found to be present in all lung tissue samples taken from 72 cancer patients (including active parasite stages in 96% of samples)** http://bit.ly/2DhPPRN

Cite this article as: Bajnok J, Tarabulsi M, Carlin H, *et al.* High frequency of infection of lung cancer patients with the parasite *Toxoplasma gondii*. *ERJ Open Res* 2019; 5: 00143-2018 [https://doi.org/10.1183/23120541.00143-2018].

This article has supplementary material available from openres.ersjournals.com

Received: Aug 29 2018 | Accepted after revision: March 23 2019

Introduction

Toxoplasma gondii is an intracellular protozoan parasite which can be found in all warm-blooded animals. This parasite can only complete its full life cycle in cats, but nevertheless around 30% of the human population, globally, is estimated to be infected [1–3]. Current estimates of human infection range from a relatively lower prevalence in countries like the UK (10%), China (10%) and the USA (10–20%) [2, 4] to areas where prevalence can exceed 40% (*e.g.* parts of continental Europe and South America) [2]. The main routes of transmission to humans are thought to be *via* ingestion of infective oocysts shed by infected cats or by ingestion of parasite cysts from undercooked meat. Congenital transmission, although reported to be infrequent, contributes to transmission and is often associated with significant neonatal pathology and possible miscarriage [5–8]. Other accidental routes of transmission have also been reported (*e.g.* blood transfusion and organ transplantation). With the exception of congenital transmission, primary infection in humans is usually asymptomatic in healthy individuals. If symptoms occur, they are usually mild influenza-like symptoms, occasionally accompanied by hepatosplenomegaly and lymphadenopathy, but are usually self-limiting [3, 9]. In immunosuppressed and immunodeficient patients *T. gondii* infection can have fatal consequences [10]. *T. gondii* can invade every type of nucleated cell in the body, but preferred target organs are the lymph nodes, brain, heart and lungs. Proliferation of tachyzoites results in the infection of neighbouring cells and necrosis [11, 12]. Common presentations include encephalitis, miscarriages, pneumonia and myocarditis [3].

Patients with cancer may have deficient cellular immunity that has allowed dysregulated proliferating cells to escape immune defences, and are potentially susceptible to opportunistic infections including *T. gondii* [5]. Not much is known about toxoplasmosis in this group of patients and few reports are available. As examples of studies of *T. gondii* infection in cancer patients [13], serological measurement of infection rates showed high prevalences in nasopharyngeal carcinoma (46.2%) and rectal cancer (63.6%), but lower rates in the other cancer groups, for example, pulmonary carcinoma (4.6%), breast cancer (9.5%), gastric carcinoma (10.0%), hepatocellular carcinoma (14.3%) and uterine cervix carcinoma (12.5%). This might suggest that there is an association between *T. gondii* infection and some types of cancer; however, these studies give little indication as to whether active infection is present, and they measure generic infection status rather than localised infection status in the cancer affected tissue. The objectives of this study were to use specific DNA based and immunohistochemical detection systems to detect the presence of the parasite, *T. gondii*, in lung biopsy samples taken from a well-characterised collection of patients with lung cancer. A secondary aim was to investigate any associations between parasite infection intensity or active/dormant infection and other recorded characteristics of these lung cancer patients (such as sex, age, presence of chronic obstructive pulmonary disease (COPD) and smoking history).

Materials and methods

Study subjects and sample processing

In total, 72 tissue samples were collected from patients undergoing lung resection surgery at University Hospital of South Manchester as part of their clinical care in the National Health Service (NHS). These patients were not specifically recruited for this study but were referred to the hospital with suspected lung cancer and biopsies were taken as part of the diagnostic process. This centre serves a large catchment area covering referrals for lung diseases across the north-west of England. The samples were taken for exploratory investigations as part of suspected lung cancer diagnosis and were taken prior to any anti-cancer drug therapy. All 72 patients were subsequently confirmed as having lung cancer following all subsequent diagnostic tests. Routine diagnosis for cancer does not involve serological testing for *Toxoplasma* infection, thus none of these patients were tested in this way. To act as controls, a further 10 bronchial biopsy samples were obtained from healthy subjects without any history or evidence of lung cancer who were recruited specifically as healthy controls. The potential risk of biopsy to healthy subjects made it difficult to gain a large sample size of control subjects. The control subjects were selected from the same population catchment area as the lung cancer patients and covered a comparable age range, although they have a lower average age (table 1). We recognise the limitations of the control sample, the relatively small numbers, the younger average age range and different tissue type (bronchial rather than lung biopsy), but it was not possible with this study to recruit more appropriate controls. These limitations are discussed later in this article. The overall study methodology is presented in figure 1. The studies were approved by the local South Manchester research ethics committee (03/SM/396, lung tissue collection) and the NRES Committee North West – Greater Manchester South (06/Q1403/156, control sampling). All subjects provided written informed consent. The study also received ethical approval from the University of Salford Research Governance and Ethics (CST 12/37 and ST16/124). For each sample, data was available on age, sex, lung conditions (*e.g.* COPD) if present, pack-years smoking history, and inhaled medication use including bronchodilators and inhaled corticosteroids.

TABLE 1 Summary of patient demographics

	Males/ females	Age years	FEV_1 L	FEV_1 %pred	FVC L	FEV_1/FVC ratio	Smoking history pack-years	Lung cancer lesion	Recorded medications		
									SAB	LAB	ICS
COPD, current smoker	10/6	70.9 (60–82)	1.9 (0.9–3.5)	74.6 (53–96)	3.3 (1.7–5.4)	59.0 (46–75)	56.9 (9–124)	Yes	7	4	4
COPD, ex-smoker	17/2	72.1 (60–80)	1.7 (1.3–2.5)	64.8 (45–118)	3.0 (2.4–4.5)	56.3 (42.5–69.3)	48.7 (11–112)	Yes	9	12	9
No airflow obstruction, current smoker	4/13	64.4 (44–78)	2.3 (1.6–3.3)	105.2 (70–131)	3.1 (2.1–4.4)	73.1 (66.9–82.5)	44.2 (15–90)	Yes	0	0	0
No airflow obstruction, ex-smoker	9/8	72.1 (57–84)	2.1 (1.2–3.2)	91.9 (47–127)	2.9 (1.8–4.1)	71.2 (55–85.8)	37.3 (2.1–117)	Yes	1	1	1
Never smoker	0/3	68.3 (65–71)	1.9 (1.8–2.0)	108.3 (100–113)	2.7 (2.2–3.6)	82.5 (77–91)	0 (0)	Yes	1	0	1
Average for lung cancer group	40/32 (total)	69.8 (44–84)	2.0 (0.87–3.5)	84.8 (45–131)	3.1 (1.69–5.4)	65.5 (42.5–90.9)	44.1 (0–124)	Yes	18	17	15
Healthy, never smoker controls	7/3	52.2 (31–75)	3.3 (2.3–4.18)	107 (82.7–148.6)	4.3 (2.9–5.6)	78.6 (70.8–95.1)	0.0 (0)	No	0	0	0

Subject demographics of cancer patients (n=72) and healthy nonsmoker control subjects (n=10). Data are presented as the mean (range) or n. FEV_1: forced expired volume in 1 s; FVC: forced vital capacity; SAB: short-acting bronchodilators; LAB: long-acting bronchodilators; ICS: inhaled corticosteroid.

Tissue sections were obtained from the lung as far distal to the tumour as possible, as determined by an NHS pathologist. Lung tissue was washed in sterile PBS prior to use. A portion of the tissue was fixed with 10% formalin in PBS buffer and embedded in paraffin, using a Leica TP1020 automatic tissue processor (Leica Microsystems (UK) Ltd, Milton Keynes, UK). Tissues were sectioned into 5 µm slices and lifted

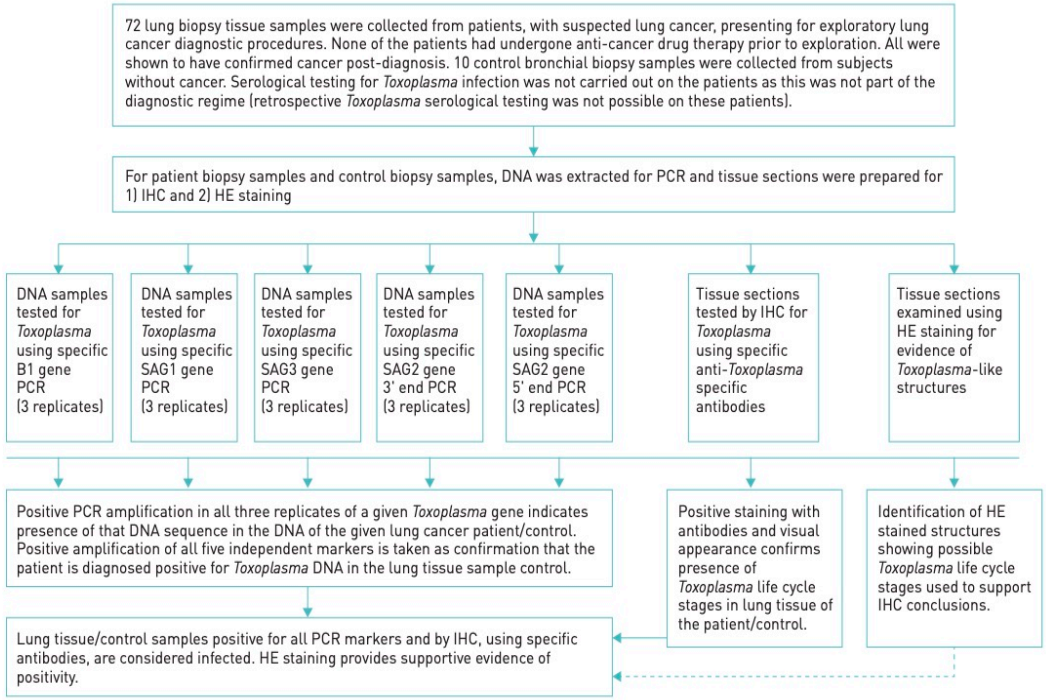

FIGURE 1 Flowchart showing the study methodology. IHC: immunohistochemistry; HE: haematoxylin and eosin.

onto poly-L-lysine glass slides. Portions of tissue were snap frozen in liquid nitrogen, stored at −80°C and used later for DNA extraction. Control bronchial biopsies were collected from subjects and immediately fixed using 10% neutral buffered formalin (CellPath, Newtown, UK), processed and paraffin embedded. 4 µm sections were cut and lifted onto poly-L-lysine coated glass slides (Surgipath, Peterborough, UK).

PCR detection of T. gondii *in human lung samples*

DNA from 72 lung cancer patients and 10 control subjects was extracted from small blocks of snap frozen tissue or directly from sections on poly-L-lysine microscope slides, using proteinase K lysis followed by phenol/chloroform extraction as previously described [14]. Extracted DNA was tested using a mammalian α-tubulin PCR to ensure the viability of the DNA for PCR amplification [15]. Protocols and processes were applied to prevent cross contamination of PCR reactions as previously described [16–19]. The presence of the parasite was tested with five markers at four genetic loci: SAG1, SAG2 (the 3′ and 5′ ends were tested separately), SAG3 and B1 [20–22] as previously described [19]. All of these markers are commonly used specific PCR diagnostic markers for *T. gondii*. Pure parasite DNA from the *T. gondii* RH strain and from a type II strain, isolated from a goat in Slovakia [19] were used as positive controls. Negative controls (water) were interspersed throughout the PCR reactions to detect any possible false amplification and DNA extraction controls from sham blocks were also included as negative controls. Any experiment in which the negative controls showed amplification was discarded and repeated. PCR amplifications were conducted in replicates; each sample was tested three times. PCR products were visualised by agarose gel electrophoresis using standard methods and were sequenced to confirm that the correct amplicons were amplified. The DNA samples were considered to be positive for *T. gondii* if they successfully amplified in all three reactions with all five *Toxoplasma* specific markers.

Immunohistochemical detection of T. gondii *in human lung sections*

Using established approaches [23], immunohistochemistry (IHC) was performed on paraffin embedded tissue using commercial anti-*T. gondii* polyclonal antibodies produced in rabbits (Thermo Fisher Scientific, Catalogue number PA1-38789, Rockford, IL, USA). This antibody was generated from a whole *Toxoplasma gondii* lysate, has been validated for IHC (Thermo Fisher) and used in previous studies (*e.g.* [24]). The 5 µm tissue sections were cut and mounted on positively charged glass slides then dewaxed in Histoclear (2×5 min), rehydrated in alcohols (ethanol), 100% (5 min), 90% (3 min), 75% (2 min) and 50% (1 min). They were finally rinsed in tap water to remove the ethanol for 5 min. Antigen retrieval was performed in 1% trypsin/calcium chloride (pH 7.8) at 37°C for 30 min in a humidified chamber [25]. After incubation, the sections were left to cool at room temperature for 10 min, then washed in PBS Tween 20 twice for 2 min. Endogenous peroxidase activity was blocked by incubating slides in 0.3% hydrogen peroxide for 30 min at room temperature followed by washing in TBS. Nonspecific antibody binding was blocked using normal goat serum (Vectastain ABC Systems, Vector Laboratories, Peterborough, UK) for 30 min at room temperature and followed by incubation in diluted (1/100) polyclonal rabbit anti-*T. gondii* antibodies for 1 h at room temperature. Following this incubation, the slides were washed in TBS Tween for 3×3 min and incubated in biotinylated goat anti-rabbit secondary antibody (Vectastain ABC Systems) for 30 min at room temperature followed by another wash in TBS Tween (3×3 min). Slides were incubated in ABC-Px mix (Vectastain ABC Systems) for 30 min, and re-washed ×3 in TBS. The resulting complex was visualised using 3-3′-diaminobenzidine (DAB) for a maximum of 10 min. The intensity of the tissue staining was monitored using light microscopy and the DAB reaction quenched in distilled water when optimal staining was reached. Sections were then washed with running water for 5 min, counterstained with haematoxylin for 45 s, washed with water for another 5 min, dehydrated with alcohols, 50% (1 min), 75% (2 min), 95% (4 min), and 100% (5 min), cleared in Histoclear (2×5 min) and mounted, using cover slips, in DPX. Three negative controls were used for each staining. These were lung sections from *T. gondii* negative wood mouse (*Apodemus sylvaticus*), human lung sections with primary antibodies omitted and cells derived from a C2C12 culture (mouse myoblast cell line, free of *T. gondii*) with both primary antibodies present and absent. Specific *T. gondii* staining was not observed in any negative controls. Cell culture derived *T. gondii* RH strain tachyzoites and lung tissue from a *T. gondii* infected wood mouse were used as positive controls [19]. Specific *T. gondii* staining was observed in all positive controls. Immunostained slides were also assessed using quantitative criteria. The program ImageJ (https://imagej.nih.gov/ij/) was used to calculate a percentage score which described the degree of coverage of infected tissue on each slide. For each patient, three microscope fields of view (×400 magnification) were randomly selected, photographed and quantified using ImageJ software (as a percentage of stained pixels with respect to total pixels). The mean percentage of pixels in the stained areas was calculated for each slide. According to the calculated mean (a measure of parasite intensity) the patients were divided into three grades of staining. Grade 1 had a staining of <10% of the area covered, grade 2 between 10 and 20% and grade 3 intensity of >20%. In addition to overall percentage cover, slides were analysed in more detail and percentage coverage for different parasite life cycle stages were recorded

(*T. gondii* cysts, intracellular infection of macrophages (or other cell types) and free tachyzoites). Finally, haematoxylin and eosin (HE) staining was used to confirm that structures compatible with *T. gondii* stages could be observed within sections [26].

Statistical analyses

To compare infection status of lung cancer patients (n=72) and non-lung cancer control patients (n=10), 2×2 contingency tables were used. Fisher's exact test was used to calculate p-values and values of <0.05 were considered statistically significant. In order to investigate any relationships between *T. gondii* infection and demographic data collected from within the lung cancer patient cohort (n=72), logistic regression (generalised linear model with a binomial distribution) was used to avoid the statistical pitfalls of conducting multiple univariate analyses. Model selection was based on backwards selection with only those factors remaining significant at a level of $p<0.05$ being included in the final model. This approach was used to avoid the pitfalls of confounding variables. As all lung cancer patients were infected, this analysis used the following variables for parasite infection status: *Toxoplasma* infection intensity (*i.e.* grades 1–3) and active/inactive parasite stages. Intensity grades were assessed by IHC staining using Image J analysis of pixel coverage, as described above, and also included distinction between active (presence of tachyzoites and infected cells) and inactive stages (presences of cysts alone). Dependent variables used in the model for parasite infection were inactive *versus* active infection. Data on patient status was also recorded as follows: sex, age, presence of COPD and smoking history. Lung cancer patients were placed into two categories (dependent variables), "No COPD" subjects (no airflow obstruction as determined by normal spirometry) or "COPD" subjects (Global Initiative for Chronic Obstructive Lung Disease criteria), and considered against factors that predicted individuals in each category. Factors considered included age, sex of the individual and a number of measures of smoking and *Toxoplasma* infection intensity and active/inactive stage status. Patient-associated dependent variables were as follows: smoker, "pack-year history" (1 pack-year is defined as 20 cigarettes per day for 1 year) and non-smoker; current smoker *versus* non-smoker; prior medication *versus* non-medication. Only one patient- or *Toxoplasma*-associated variable was considered at a time and all combinations were considered. Model selection was based on backwards selection with only those factors remaining significant at a level of $p<0.05$ being included in the final model. All analyses were undertaken using R 3.01 (RCore Team, 2013) [27].

Results

DNA and tissue samples, for IHC, were collected from resected lung tissues from lung cancer patients (n=72) and non-lung cancer healthy control subjects (n=10). Patient demographics are shown in table 1 and figure 1 illustrates the overall methodology used to examine the samples. Initially, DNA was extracted successfully from tissue from all subjects. All samples were tested for the absence of PCR inhibition using amplification of the mammalian α-tubulin gene. All samples showed successful PCR amplification of the α-tubulin gene and were used for *T. gondii* DNA PCR detection using three replicated experiments of five genetic markers at four independent loci: SAG1, SAG2 (3′ and 5′ ends), SAG3 and B1. Multiple independent markers were used to rule out the possibility that individual markers could nonspecifically amplify as can happen with *Toxoplasma* in single marker PCR or qPCR. All tested lung cancer patient samples (32 females, 40 males) were found to be *T. gondii* positive, giving a prevalence of 100% with all five genes. Of the 10 healthy control subjects, one sample showed positive amplification for all *T. gondii* markers and the remaining nine did not amplify with any of the *T. gondii* specific primers. To confirm the presence of the parasite, using an independent detection system, the tissue sections were examined by IHC using specific anti-*T. gondii* antibodies. This was followed by secondary confirmation using HE staining. IHC was performed on all tissue sections enabling both detection of the parasite and identification of the life cycle stage. Infected tissue could be identified as containing *T. gondii* cysts, intracellular infection of macrophages (or other cell types) and free tachyzoites (figure 2). All 72 lung cancer patient tissue samples showed positive staining with the anti-*T. gondii* antibody and thus confirmed the PCR detection results of 100% (95% CI: 95.19–100%) prevalence in this cohort. Only one sample in the control group showed specific staining with the anti-*T. gondii* antibody and this was the same sample that showed positive amplification for the five *T. gondii* specific PCR amplifications. There was an extremely significant difference in prevalence between the lung cancer group (n=72) and the non-cancer control group (n=10) ($p<0.0001$, Fisher's exact test). A surprisingly high proportion of lung cancer patients (95.8%; n=69) showed evidence of an active form of infection, as defined by the presence of tachyzoites or infected alveolar macrophages (or other cell types). Only three lung cancer subjects (4.2%) had the dormant cyst stage as the only stage present. This is indicative of a latent infection in these three patients. Image J was used to measure the proportion of infected cells and infected areas of the lung tissue. A quantitative score was calculated for each type of life cycle stage individually and an overall score determined (see materials and methods) for each lung tissue sample (table 2). Both *T. gondii* cysts and infected cells were observed in the single infected non-cancer control sample. All samples were also stained with HE and observed

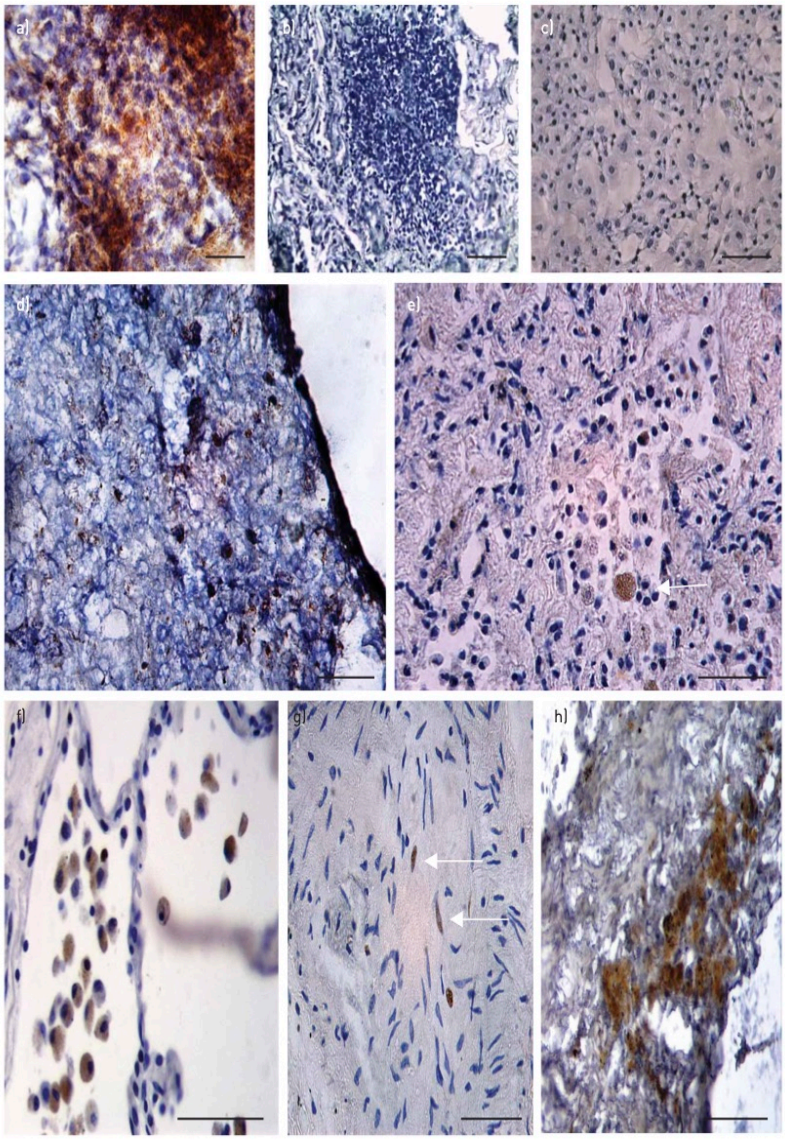

FIGURE 2 Anti-*Toxoplasma gondii* antigen immunostaining of human lung and control tissues. a) Cell culture derived *T. gondii* RH strain tachyzoites stained with polyclonal anti-*T. gondii* antibodies. Brown staining indicates detection of *T. gondii.* Positive control (×400 magnification, scale bar = 100 µm). b) Human lung section stained with polyclonal anti-*T. gondii* antibodies with primary antibodies omitted. Negative control (×400 magnification, scale bar = 100 µm). c) Cells derived from a C2C12 culture (mouse myoblast cell line) which is *T. gondii* free and stained with polyclonal anti-*T. gondii* antibodies. Negative control (×400 magnification, scale bar = 100 µm). d) Lung tissue from a *T. gondii* infected wood mouse (*Apodemus sylvaticus*) stained with polyclonal anti-*T. gondii* antibodies. Brown staining indicates detection of *T. gondii*. Positive control (×400 magnification, scale bar = 100 µm). e) Human lung section, from subject 1045, stained with polyclonal anti-*T. gondii* antibodies. *T. gondii* cysts can be seen (examples indicated with white arrows) (×400 magnification, scale bar = 100 µm). f) Human lung section, from subject 1040, stained with polyclonal anti-*T. gondii* antibodies. Alveolar macrophages infected with *T. gondii* can be seen (×400 magnification, scale bar = 100 µm). g) Human lung section, from subject 1028, stained with polyclonal anti-*T. gondii* antibodies. By observation of cell morphology, fibroblasts infected with *T. gondii* can be seen (examples indicated with white arrows) (×400 magnification, scale bar = 100 µm). h) Human lung section, from subject 975, stained with polyclonal anti-*T. gondii* antibodies. Ruptured *T. gondii* cysts and free *T. gondii* tachyzoites can be seen (×400 magnification, scale bar = 100 µm).

TABLE 2 Life cycle stages of *Toxoplasma gondii* and type of infection in lung cancer patients (n=72) as identified by immunohistochemistry

Infection type	Subjects n	Range of percentage score[#]	Infection status
Cysts	3	0.2–2.9%	Inactive
Tachyzoites	3	0.8–8.7%	Active
Macrophages or other cells	18	0.6–34.2%	Active
Mixture	48	1.1–44.0%	Active
Total infections	72		

[#]: the score was determined as described in the materials and methods.

under the light microscope. Although less specific as a diagnostic technique than the IHC and PCR, the presence of structures consistent with infection by the parasite was confirmed in 67 out of 72 tissue sections from the lung cancer patients and in one out of 10 of the non-cancer control group. In the latter case, this corresponded to the sample that was positive for the PCR amplifications and IHC. The remaining lung cancer samples could not be reliably confirmed as potentially infected by this method, but could have possessed less visible structures such as tachyzoites. Using the HE staining technique, infected cells, macrophages and some tissue cysts were observed (figure 3) but no free tachyzoites could be detected.

By quantifying the *Toxoplasma* infection intensity among the 72 lung cancer patients, we were able to evaluate any relationship between parasitic load and presence of COPD or other demographic factors. Our cohort did not show any significant association between *Toxoplasma* infection load with patient smoking history (both total exposure ($p>0.05$) or current exposure ($p>0.05$)) or airflow obstruction in COPD ($p>0.05$). All other analyses conducted had non-significant p-values ($p>0.05$) except for a parasitologically unrelated association between COPD and sex (males>females; $p<0.05$).

Discussion

In this study, we investigated the prevalence of *T. gondii* in clinical samples from patients with lung cancer using PCR and *T. gondii* specific IHC. Surprisingly, of the 72 subjects admitted to hospital for examination for lung cancer, all (100%) showed evidence of infection of lung tissue by the parasite *T. gondii*. A significant difference was observed between the prevalence in these lung cancer patients and in a non-cancer control group. Of the lung cancer patients, 95.8% showed evidence of active infection as opposed to being in the dormant (cyst) stage. Four stages of infection were observed by IHC: cysts, infected macrophages, other cell types infected and free-living tachyzoites. Given that the background levels of infection in the UK are considered to be low at 10% and the global infection rate is 30% [2], this represents an extremely high infection rate in these cancer patients. While detailed prevalence figures have not recently been determined for the catchment area sampled, it is unlikely that it significantly deviates

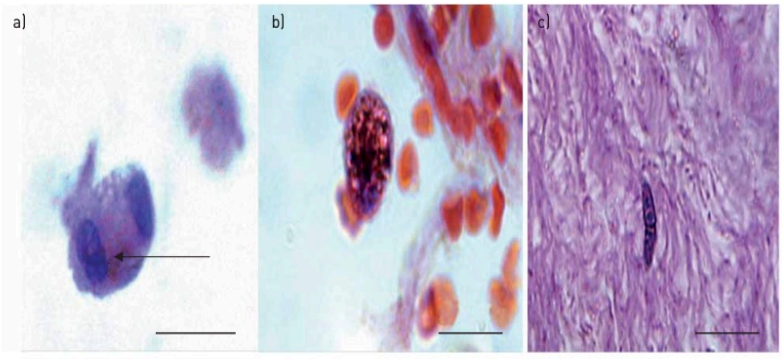

FIGURE 3 Haematoxylin and eosin staining of human lung sections. a) Infected alveolar macrophage with four visible tachyzoites (red arrow) in subject 1040 (×400 magnification, scale bar = 10 µm). b) Tissue cyst from subject 1070 (×400 magnification, scale bar = 10 µm) and (c) young tissue cyst in subject 1028 (×400 magnification, scale bar = 10 µm).

from the national average. The most recent studies in the UK show infection in a range of 7–34% [2, 28–30]. In our study, we were able to evaluate *Toxoplasma* infection in 10 samples from healthy subjects without cancer who were specifically recruited as controls and were similarly age range matched with the cancer patients (although with a lower average age). We acknowledge some limitations in the control group; however, it was difficult to achieve a suitably sized and matched control group due to the potential risks of lung biopsy techniques. For example, one limitation was the comparison of lung tissue *versus* bronchial tissue. However, as *T. gondii* can infect any nucleated cell types and that both tissue types will have the same exposure to parasite infection, we consider minimal impact of these limitations on the conclusions. We also acknowledge potential bias due to the relatively small control sample size and younger average age of the control population, which is again related to the difficulty and risks associated with sampling healthy subjects. However, taken alongside the many studies of prevalence in the UK [2, 28–30], this study has demonstrated an unexpectedly high prevalence of *Toxoplasma* infection in lung cancer patients compared with control subjects and with the expected UK prevalence in people without cancer.

Toxoplasmosis has been reported to increase the fatality rate in a variety of cancers such as Hodgkin's disease, leukaemia, melanoma and brain cancer [31–35]. However, *Toxoplasma* infection causing complications in lung cancer has been reported only rarely. A case report demonstrated that a *T. gondii* infection was detected in a patient with lung cancer [36]. The diagnosis was based on tachyzoites present in bronchoalveolar lavage and detection of specific IgM antibodies. Most of the studies that investigate the link between cancer and *T. gondii* infection are based on serological prevalence detection of the parasite in cohorts of cancer patients rather than by direct investigation of tissue samples. Overall 8.38% of examined patients with malignant neoplasms in China were seropositive for antibodies against *T. gondii*. However, when nested PCR detection was used on the same samples, only 3.55% of these patients were positive [37]. In another study from China [38], much higher prevalence was detected, with 35.56% of the cancer patients overall being positive for anti-*T. gondii* IgG. The highest prevalence of infection, in this study [38], was observed in lung cancer patients (60.94%) followed by cervical cancer patients (50%). Among 356 cancer patients, 21 (5.9%) cases were found to be IgG-positive and 8 (2.3%) were IgM-positive, and five of them were found to have both IgG and IgM antibodies [39]. The total seroprevalence of *Toxoplasma* infection in this study was 6.8% [39]. A study in Iran concluded that 45.2% of cancer patients were seropositive for *T. gondii* [40]. High seropositivity rates were detected in women with breast cancer (86.4%) [41]. In a study comparing national figures from 37 countries [42], it was found that brain cancers are 1.8 times more common in countries where *T. gondii* infections are more prevalent than in those where it is virtually absent. Overall, the studies that investigate cancer and *T. gondii* infection generally show no particular link, although these studies are rarely specifically addressing the link or are controlled against a healthy cohort. As far as we can determine, our study is the first that specifically investigates the link between cancer affected lung tissue and *T. gondii*. Unfortunately, while we recognise the value of it, we were not able to investigate the seropositivity of our cohort of cancer patients since there is no formal process of *Toxoplasma* testing as part of lung cancer diagnostic protocols. Subsequent follow-up is not possible due to some subjects having passed away since diagnosis and the length of time since diagnosis could complicate the serological outcomes. Our study suggests that routine serological testing for *Toxoplasma* may be of value in lung cancer diagnostic protocols.

Using additional data associated with our sample set, the relationship between patient health and *T. gondii* infection was investigated to see if there were any further factors associating with patient health. We investigated which factors were associated with predicting whether an individual had normal lung function (no COPD) or "patients" (COPD) using logistic regression. This multiple regression analysis takes into account that the data are not normally distributed and follows a binomial distribution. We investigated the effects of age and sex, as well as a range of different smoking parameters (smoker, non-smoker and pack-year smoking history) and *Toxoplasma* infection measures (*Toxoplasma* intensity of infection, presence of free tachyzoites, acute or active infection). We only looked at one smoking and one infection related measure at a time, but considered all possible combinations (*e.g.* smoker and parasite intensity, then smoker and free tachyzoites, then smoker and acute infection) and each factor on its own (*e.g.* smoker). The final model we selected included only sex as a factor and we showed that males were more likely to have an obstruction than females in our cohort. There was no significant effect of smoking or stage/extent of *Toxoplasma* infection on the likelihood of being a lung "patient" (*i.e.* having COPD) in this sample set. While the sex relationship is clearly of interest in relation to lung disease, it does not have relevance to the *T. gondii* infection reported here. COPD has been linked to a higher risk in the male population, until more recently when it is now predicted that incidence in females will overtake that of males as a possible result of an increased proportion of female smokers in Western societies [43]. We recognise that there are limitations in our regression analyses and there were many potentially confounding parameters where no data were available. For example, most studies on *T. gondii* infection

include risk factors for infection. As no previous studies on lung cancer patients have revealed such striking prevalence levels as this study, there has been little reason to investigate parasitological parameters. In the future, detailed studies are required which involve more specific questions pertinent to the results presented here.

The high frequency of *T. gondii* infection in these lung cancer patients raises questions about whether the two conditions are linked. It is unlikely that there is a direct cause and effect linkage as there are no reported causative effects of *T. gondii* infection on producing cancers, as far as we are aware. However, many types of cancer can cause immunomodulatory effects on affected tissues and individuals [44] and *Toxoplasma* infection may also provoke a state of immunosuppression by affecting thymic related T-cell activity as systemic *Toxoplasma* infection triggers a long-term defect in the generation and function of naïve T-lymphocytes [5, 45–48]. Furthermore, pulmonary toxoplasmosis is generally considered to be rare in immunocompetent hosts [49], further supporting the idea that these patients are immunocompromised (at least locally within the lung tissue). Based on the observations reported in this article, a high proportion of lung cancer patients potentially could be at risk of acute infection or reactivation of chronic infection from *T. gondii*. This could lead to complications such as pulmonary toxoplasmosis, a serious condition causing a high mortality rate, which could seriously affect general wellbeing and interfere with treatment. Further research is required to establish the wider significance of these findings but in the meantime, we suggest that all lung cancer patients (and possibly patients with other cancers) should be considered at risk of *T. gondii* infection and, if necessary, monitored to prevent further complications during their treatments.

Acknowledgements: We would like to thank those people who have participated anonymously in this study, Geoff Parr (School of Science, Engineering and Environment, University of Salford, UK) and Salford Analytical Services for their expertise in microscopy and image capture, and Ross Gordon (School of Science, Engineering and Environment, University of Salford, UK) for his help with the project.

Conflict of interest: J. Bajnok reports grants from British Society of Parasitology (provision of a travel grant to attend a conference), during the conduct of the study. M. Tarabulsi reports grants from Saudi Arabian Cultural Bureau (PhD studentship funding), during the conduct of the study. H. Carlin has nothing to disclose. K. Bown has nothing to disclose. T. Southworth has nothing to disclose. J. Dungwa has nothing to disclose. D. Singh reports personal fees from Apellis, Cipla, Genentech, Peptinnovate and Skyepharma, grants and personal fees from AstraZeneca, Boehringer Ingleheim, Chiesi, GlaxoSmithKline, Glenmark, Menarini, Merck, Mundipharma, Novartis, Pfizer, Pulmatrix, Teva, Therevance and Verona, all outside the submitted work. Z-R. Lun reports their laboratory is supported by a National Key R&D Program of China (2017YFD0500400), outside the submitted work. L. Smyth reports grants from Kidscan (charity grant funds for leukaemia research), outside the submitted work. G. Hide reports grants from Saudi Arabian Cultural Bureau (provision of funding to cover one of the authors' PhD fees and research costs. Some of these research costs were used to purchase consumables to support this project. The funding was to support M. Tarabulsi and research consumables used by her and her PhD supervisor (G.Hide), grants from British Society of Parasitology (provision of a travel grant to J. Bajnok for attendance at a conference), during the conduct of the study.

Support Statement: The authors would like to thank the University of Salford, The Saudi Arabian Cultural Bureau and the British Society of Parasitology for funding this research. This report is independent research supported by the National Institute for Health Research South Manchester Respiratory and Allergy Clinical Research Facility at the University Hospital of South Manchester NHS Foundation Trust. The views expressed in this publication are those of the authors and not necessarily those of the NHS, the National Institute for Health Research or the Department of Health. Funding information for this article has been deposited with the Crossref Funder Registry.

References

1 Peyron F, Wallon M, Kieffer F, *et al.* Toxoplasmosis. *In:* Wilson CB, Nizet V, Maldonado Y, *et al.*, eds. Infectious Diseases of the Fetus and Newborn Infant. Philadelphia, Elsevier Saunders, 2015; pp. 949–1042.
2 Pappas G, Roussos N, Falagas M. Toxoplasmosis snapshots: global status of *Toxoplasma gondii* seroprevalence and implications for pregnancy and congenital toxoplasmosis. *Int J Parasitol* 2009; 39: 1385–1394.
3 Dubey J. Toxoplasmosis of Animals and Humans. Boca Raton, CRC Press, 2010.
4 Gao X, Zhao Z, He Z, *et al. Toxoplasma gondii* infection in pregnant women in China. *Parasitology* 2011; 139: 139–147.
5 Montoya J, Liesenfeld O. Toxoplasmosis. *Lancet* 2004; 363: 1965–1976.
6 Giakoumelou S, Wheelhouse N, Cuschieri K, *et al.* The role of infection in miscarriage. *Hum Reprod Update* 2015; 22: 116–133.
7 Haq S, Abushahama M, Gerwash O, *et al.* High frequency detection of *Toxoplasma gondii* DNA in human neonatal tissue from Libya. *Trans R Soc Trop Med Hyg* 2016; 110: 551–557.
8 Hide G. Role of vertical transmission of *Toxoplasma gondii* in prevalence of infection. *Expert Rev Anti Infect Ther* 2016; 14: 335–344.
9 Krick J, Remington J. Toxoplasmosis in the adult an overview. *N Engl J Med* 1978; 298: 550–553.
10 Robert-Gangneux F, Sterkers Y, Yera H, *et al.* Molecular diagnosis of toxoplasmosis in immunocompromised patients: a 3-year multicenter retrospective study. *J Clin Microbiol* 2015; 53: 1677–1684.
11 Evans T, Schwarztman J. Pulmonary toxoplasmosis. *Semin Respir Infect* 1991; 6: 51–57.
12 Peng H, Chen X, Lindsay D. A review: competence, compromise, and concomitance-reaction of the host cell to *Toxoplasma gondii* infection and development. *J Parasitol* 2011; 97: 620–628.
13 Yuan Z, Gao S, Liu Q, *et al. Toxoplasma gondii* antibodies in cancer patients. *Cancer Lett* 2007; 54: 731–774.

14 Duncanson P, Terry R, Smith J, *et al.* High levels of congenital transmission of *Toxoplasma gondii* in a commercial sheep flock. *Int J Parasitol* 2001; 31: 1699–1703.
15 Terry R, Smith J, Duncanson P, *et al.* MGE-PCR: a novel approach to the analysis of *Toxoplasma gondii* strain differentiation using mobile genetic elements. *Int J Parasitol* 2001; 31: 155–161.
16 Williams R, Morley E, Hughes J, *et al.* High levels of congenital transmission of *Toxoplasma gondii* in longitudinal and cross-sectional studies on sheep farms provides evidence of vertical transmission in ovine hosts. *Parasitology* 2005; 130: 301–307.
17 Hughes J, Thomasson D, Craig P, *et al. Neospora caninum*: Detection in wild rabbits and investigation of co-infection with *Toxoplasma gondii* by PCR analysis. *Exp Parasitol* 2008; 120: 255–260.
18 Morley E, Williams R, Hughes J, *et al.* Evidence that primary infection of Charollais sheep with *Toxoplasma gondii* may not prevent foetal infection and abortion in subsequent lambings. *Parasitology* 2008; 135: 169–173.
19 Bajnok J, Boyce K, Rogan M, *et al.* Prevalence of *Toxoplasma gondii* in localized populations of *Apodemus sylvaticus* is linked to population genotype not to population location. *Parasitology* 2015; 142: 680–690.
20 Su C, Zhang X, Dubey J. Genotyping of *Toxoplasma gondii* by multilocus PCR-RFLP markers: a high resolution and simple method for identification of parasites. *Int J Parasitol* 2006; 36: 841–848.
21 Shwab E, Zhu X, Majumdar D, *et al.* Geographical patterns of *Toxoplasma gondii* genetic diversity revealed by multilocus PCR-RFLP genotyping. *Parasitology* 2013; 141: 453–461.
22 Jones C, Okhravi N, Adamson P, *et al.* Comparison of PCR detection methods for B1, P30, and 18S rDNA genes of *T. gondii* in aqueous humor. *Investigative Ophthalmol Visual Sci* 2000; 41: 634–644.
23 Plumb J, Smyth L, Adams H, *et al.* Increased T-regulatory cells within lymphocyte follicles in moderate COPD. *Eur Respir J* 2009; 34: 89–94.
24 Work TM, Massey JG, Lindsay DS, *et al.* Toxoplasmosis in three species of native and introduced Hawaiian Birds. *J Parasitol* 2002; 88: 1040–1042.
25 Roe WD, Howe L, Baker E, *et al.* An atypical genotype of *Toxoplasma gondii* as a cause of mortality in Hector's dolphins (*Cephalorhynchus hectori*). *Vet Parasitol* 2013; 192: 67–74.
26 Lynch M, Raphael S, Mellor L, *et al.* Medical Laboratory Technology and Clinical Pathology. 2nd Edn. Philadelphia, London, Toronto, WB Saunders Co, 1969.
27 R Core Team. R: A language and environment for statistical computing. Vienna, Austria, R Foundation for Statistical Computing, 2013. www.R-project.org/
28 Joynson D. Epidemiology of toxoplasmosis in the U.K. *Scand J Inf Dis* 1992; 8: 65–69.
29 Flatt A, Flatt A, Shetty N. Seroprevalence and risk factors for toxoplasmosis among antenatal women in London: a re-examination of risk in an ethnically diverse population. *Eur J Pub Health* 2013; 23: 648–652.
30 Public Health Wales. Toxoplasmosis: how common is it? 2010. www.wales.nhs.uk/sitesplus/888/page/44347. Date last accessed: June 14, 2018. Date last updated: May 05, 2017.
31 Vietzke W, Gelderman A, Grimley P, *et al.* Toxoplasmosis complicating malignancy. Experience at the National Cancer Institute. *Cancer* 1968; 21: 816–887.
32 Carey R, Kimball A, Armstrong D, *et al.* Toxoplasmosis. Clinical experiences in a cancer hospital. *Am J Med* 1973; 54: 30–38.
33 Israelski D, Remington J. Toxoplasmosis in patients with cancer. *Clin Inf Dis* 1993; 17: S423–S435.
34 Zhou P, Chen Z, Li H, *et al. Toxoplasma gondii* infection in humans in China. *Parasit Vectors* 2011; 4: 165.
35 Scerra S, Coignard-Biehler H, Lanternier F, *et al.* Disseminated toxoplasmosis in non-allografted patients with hematologic malignancies: report of two cases and literature review. *Eur J Clin Microbiol Infect Dis* 2013; 32: 1259–1268.
36 Lu N, Liu C, Wang J, *et al.* Toxoplasmosis complicating lung cancer: a case report. *Int Med Case Rep J* 2015; 8: 37–40.
37 Wang L, He L, Meng D, *et al.* Seroprevalence and genetic characterization of *Toxoplasma gondii* in cancer patients in Anhui Province, Eastern China. *Parasit Vectors* 2015; 8: 162.
38 Cong W, Liu G, Meng Q, *et al. Toxoplasma gondii* infection in cancer patients: prevalence, risk factors, genotypes and association with clinical diagnosis. *Cancer Lett* 2015; 359: 307–313.
39 Shen Q, Wang L, Fang Q, *et al.* [Seroprevalance of *Toxoplasma gondii* infection and genotyping of the isolates from cancer patients in Anhui, Eastern China]. *Zhongguo Ji Sheng Chong Xue Yu Ji Sheng Chong Bing Za Zhi* 2014; 32: 366–370.
40 Ghasemian M, Maraghi S, Saki J, *et al.* Determination of Antibodies (IgG, IgM) against *Toxoplasma gondii* in patients with cancer. *Iranian J of Parasitol* 2007; 2: 1–6.
41 Kalantari N, Ghaffari S, Bayani M, *et al.* Preliminary study on association between toxoplasmosis and breast cancer in Iran. *Asian Pacific J Trop Biomed* 2015; 5: 44–47.
42 Thomas F, Lafferty K, Brodeur J, *et al.* Incidence of adult brain cancers is higher in countries where the protozoan parasite *Toxoplasma gondii* is common. *Biol Lett* 2012; 8: 101–103.
43 Gan WQ, Man SF, Postma DS, *et al.* Female smokers beyond the perimenopausal period are at increased risk of chronic obstructive pulmonary disease: a systematic review and meta-analysis. *Respir Res* 2006; 7: 52.
44 Franklin R, Liao W, Sarkar A, *et al.* The cellular and molecular origin of tumor-associated macrophages. *Science* 2014; 344: 921–925.
45 Canessa A, Bono V, Leo P, *et al.* Cotrimoxazole therapy of *Toxoplasma gondii* encephalitis in AIDS patients. *Eur J Clin Microbiol Inf Dis* 1992; 11: 125–130.
46 Ajzenberg D, Yera H, Marty P, *et al.* Genotype of 88 *Toxoplasma gondii* isolates associated with Toxoplasmosis in immunocompromised patients and correlation with clinical findings. *J Infect Dis* 2009; 199: 1155–1167.
47 Ahmadpour E, Daryani A, Sharif M, *et al.* Toxoplasmosis in immunocompromised patients in Iran: a systematic review and meta-analysis. *J Infect Dev Ctries* 2014; 8: 1503–1510.
48 Kugler D, Flomerfelt F, Costa D, *et al.* Systemic toxoplasma infection triggers a long-term defect in the generation and function of naive T lymphocytes. *J Exp Med* 2016; 213: 3041–3056.
49 de Souza Giassi K, Costa A, Apanavicius A, *et al.* Tomographic findings of acute pulmonary toxoplasmosis in immunocompetent patients. *BMC Pulmon Med* 2014; 14: 185.

Appendix B

Research, Innovation and Academic Engagement Ethical Approval Panel

Research Centres Support Team
G0.3 Joule House
University of Salford
M5 4WT

T +44(0)161 295 5278

www.salford.ac.uk/

14 December 2016

Muyassar Tarabulsi

Dear Muyassar,

RE: ETHICS APPLICATION ST16/124– Investigation of Toxoplasma gondii infection in humans with lung cancer

Based on the information you provided, I am pleased to inform you that your application ST16/124 has been approved.

If there are any changes to the project and/ or its methodology, please inform the Panel as soon as possible by contacting S&T-ResearchEthics@salford.ac.uk

Yours sincerely,

Prof Mohammed Arif
Chair of the Science & Technology Research Ethics Panel
Professor of Sustainability and Process Management
School of Built Environment
University of Salford
Maxwell Building, The Crescent
Greater Manchester, UK M5 4WT
Phone: + 44 161 295 6829
Email: m.arif@salford.ac.uk
www.salford.ac.uk/ethics

University of Salford MANCHESTER

Ethical Approval Form for Post-Graduate Researchers

Ethical approval must be obtained by all postgraduate research students (PGR) prior to starting research with human subjects, animals or human tissue.

A PGR is defined as anyone undertaking a Research rather than a Taught masters degree, and includes for example MSc by Research, MRes by Research, MPhil and PhD. The student must discuss the content of the form with their dissertation supervisor who will advise them about revisions. A final copy of the summary will then be agreed and the student and supervisor will 'sign it off'.

The signed Ethical Approval Form and application checklist must be e-mailed to your Research Centre Support team in the Research & Enterprise Division:

School of Arts & Media:

Julie Connett – A&M-ResearchEthics@salford.ac.uk

Salford Business School:

Julie Connett – SBS-ResearchEthics@salford.ac.uk

School of the Built Environment

Nathalie Audren-Howarth – S&T-ResearchEthics@salford.ac.uk

School of Computing, Science & Engineering

Nathalie Audren-Howarth – S&T-ResearchEthics@salford.ac.uk

School of Environment & Life Sciences

Nathalie Audren-Howarth – S&T-ResearchEthics@salford.ac.uk

For applications to the **School of Health Sciences** and **School of Nursing, Midwifery, Social Work & Social Sciences**, please follow the process mentioned at http://www.salford.ac.uk/chsc/research/staff-pgr-students-research-ethics

or contact Sarah Starkey – Health-ResearchEthics@salford.ac.uk

The forms are processed online therefore without the electronic version, the application cannot progress.

Please ensure that all references to you or anyone else involved in the project must be removed from the documents as the application has to be anonymised before the panel considers it.

Where you have removed your name, you can replace with a suitable marker such as […..] Or [Xyz], [Yyz] and so on for other names you have removed too.

Please refer to the **'Notes for Guidance'** if there is doubt whether ethical approval is required.

The form can be completed electronically; the sections can be expanded to the size required.

Name of Student:	Dr Muyassar Tarabulsi MB ChB
Name of Supervisor:	Professor Geoff Hide
School:	Environment and Life Science
Course of study:	PhD

Name of Research Council or other funding organisation (if applicable):	Saudi Arabian Cultural Bureau

1a. Title of proposed research project

Investigation of *Toxoplasma gondii* infection in humans with lung cancer

1b. Is this Project Purely literature based?

NO (delete as appropriate)

2. Project focus

Investigation of parasite infection in lung tissue from human subjects with cancerous or non-cancerous lungs. The project will involve diagnostic PCR detection of the parasite, strain typing of the parasite and investigation of the host immune gene diversity in relation to infection. Diagnostic immunochemistry and the bioassay of lung tissue in cell culture will also be used to verify infection.

3. Project objectives

Specific objectives: (1) use standard PCR and immunohistochemistry to investigate infection in non-cancerous and cancerous lungs, (2) develop quantitative methods (e.g. q PCR) to quantify infection levels (3) possibly develop culture methods for *Toxoplasma* or other parasites to assist in quantifying and exploring infection (4) investigate using in vitro or collected lung tissue to investigate the relationship between infection and cancer.

4. Research strategy

(For example, outline of research methodology, what information/data collection strategies will you use, where will you recruit participants and what approach you intend to take to the analysis of information / data generated)

The broad aims of this study are to (1) investigate infection in human lung tissue from a cancerous and non-cancerous origin (2) investigate parasite infection in lung tissue with reference to understanding infection levels and possible modes of infection and (3) to make

some progress towards understanding the nature of the link between lung cancer and *T. gondii* or other parasitic infections. Specific methodologies: (1) Use an existing collection of human lung tissue (cancerous and non-cancerous) which has been obtained as part of a larger lung disease research program. This project has already been scrutinised and has obtained ethical approval for the investigation of a wide range of conditions (e.g. COPD, smoking behaviours, asthma and also including infections) and the host responses and health. The work is conducted in collaboration with Professor XXX of Manchester University, Dr ZZZ Salford University and South Manchester Hospitals Trust. All due ethical considerations (e.g. informed consent, subject anonymity, data protections etc) have been considered as part of this project. It has received ethical approval by the South Manchester research ethics committee (03/SM/396). This work continues on from work carried out by a previous PhD student who received ethical approval from the University of Salford (CST 12/37). We are seeking to extend this approval to new PhD student YYY to continue this work. (2) To use standard PCR and immunohistochemistry to investigate infection levels and prevalences in non-cancerous and cancerous lungs. (3) Develop quantitative methods (e.g. q PCR) to quantify infection levels (4) develop culture methods for *Toxoplasma* or other parasites to assist in quantifying and exploring infection (5) investigate, using in vitro or collected lung tissue, to investigate the relationship between host genes, infection and cancer.

The results will be analysed in an anonymous manner – data on prevalence on infection will appear as a percentage infection within the population and will not refer to individual subjects. The anonymity of samples means that data collected on parasite genotypes or host immune gene information (expression levels, diversity) cannot (and will not) be linked back to individual subjects. Publication of results will be confined to population studies rather than individual case reports. Health status data is available for the subjects and may be used in this study – however, this is also anonymised to prevent any linkage to individuals.

5. What is the rationale which led to this project?

(For example, previous work – give references where appropriate. Any seminal works must be cited)

Approach to Research: *Toxoplasma gondii* is an important pathogen of humans and all warm blooded animals. In humans it is a cause of miscarriage and congenital defects. In domestic

animals it is of major economic and livestock welfare importance. The parasite is zoonotic – interacting transmission cycles include both animal and humans - with three main transmission routes – infected oocysts from cats, eating undercooked infected meat and vertical transmission (mother to offspring). The importance of each of these routes of transmission is unclear and difficult to measure. Vertical transmission is thought to occur infrequently although the high prevalence of *Toxoplasma* in human and animal populations (often >30%) encourages us to revisit this. One of the key difficulties is that the parasite has to be detected directly from infected tissue samples. In natural infections, some humans and animals are clearly highly infected while others are not. Previous research within our group has established that human subjects that have been diagnosed with lung cancer are infected with high prevalence as established by PCR and immunohistochemistry. At present, it is unclear whether this high prevalence represents background infection levels in the human population in the UK nor is it clear whether lung tissue is a representative tissue for *T. gondii* infection. Furthermore, the links between lung cancer and *Toxoplasma* infection (or any other parasites) are unknown.

6. **If you are going to work within a particular organisation do they have their own procedures for gaining ethical approval**
   (For example, within a hospital or health centre?)

   YES (delete as appropriate)

   If YES – what are these and how will you ensure you meet their requirements?

The work will be conducted in Salford, however, it is conducted in collaboration with Professor XXX of Manchester University, Dr ZZZ Salford University and South Manchester Hospitals Trust. All due ethical considerations (e.g. informed consent, subject anonymity, data protections etc) have been considered as part of this project. It has received ethical approval by the South Manchester research ethics committee (03/SM/396). This work continues on from work carried out by a previous PhD student who received ethical approval from the University of Salford (CST 12/37)

7. **Are you going to approach individuals to be involved in your research?**
   NO (delete as appropriate)

If YES – please think about key issues – for example, how you will recruit people? How you will deal with issues of confidentiality / anonymity? Then make notes that cover the key issues linked to your study

8. More specifically, how will you ensure you gain informed consent from anyone involved in the study?

For the existing samples, subjects have already been recruited and ethical approval has been received from the South Manchester research ethics committee (03/SM/396) to cover this.

9. How are you going to address any Data Protection issues?
See notes for guidance which outline minimum standards for meeting Data Protection issues

All data will be securely stored on University of Salford computing systems. No subject identity is available and no personal details of individuals are held.

10. Are there any other ethical issues that need to be considered? For example - research on animals or research involving people under the age of 18.

None

11. (a) Does the project involve the use of ionising or other type of "radiation"

NO

(b) Is the use of radiation in this project over and above what would normally be expected (for example) in diagnostic imaging?

NO

(c) Does the project require the use of hazardous substances?

NO

(d) Does the project carry any risk of injury to the participants?

NO

(e) Does the project require participants to answer questions

that may cause disquiet / or upset to them?

NO

If the answer to any of the questions 11(a)-(e) is YES, a risk assessment of the project is required and must be submitted with your application.

12. How many subjects will be recruited/involved in the study/research? What is the rationale behind this number?

For this specific study, we require 200 samples. This number is based on the 88 we currently have as part of an existing study and the potential for future studies. These numbers were calculated based on the average prevalence of *Toxoplasma* infection in the UK and the necessary statistical power required to distinguish infected and non-infected population groups.

13. Please state which code of ethics has guided your approach (e.g. from Research Council, Professional Body etc).

Please note that in submitting this form you are confirming that you will comply with the requirements of this code. If not applicable please explain why.

South Manchester research ethics panel, University of Manchester guidance, University of Salford Guidance. MRC ethics series Human Tissue and Biological Samples for Use in Research: Operational and Ethical Guidelines

Remember that informed consent from research participants is crucial; therefore all documentation must use language that is readily understood by the target audience.

Projects that involve NHS patients, patients' records or NHS staff, will require ethical approval by the appropriate NHS Research Ethics Committee. The University Ethics Panel will require written confirmation that such approval has been granted. Where a project forms part of a larger, already approved, project, the approving REC should be informed about, and approve, the use of an additional co-researcher.

Application Checklist

Ref No: *Office Use Only*

Name of Applicant: Dr Muyassar Tarabulsi MB ChB

The checklist below helps you to ensure that you have all the supporting documentation submitted with your ethics application form. This information is necessary for the Panel to be able to review and approve your application. Please complete the relevant boxes to indicate whether a document is enclosed and where appropriate identifying the date and version number allocated to the specific document (*in the header / footer*), Extra boxes can be added to the list if necessary.

Document	**Enclosed?** **(indicate appropriate response)**				**Date**	**Version No**
Application Form	Mandatory			If not required please give a reason		
Risk Assessment Form			Not required for this project	This project uses existing samples collected from previously recruited subjects		
Participant Invitation Letter			Not required for this project	This project uses existing samples collected from previously recruited subjects		
Participant Information Sheet		No	Not required	This project uses existing samples collected from		

			for this project	previously recruited subjects		
Participant Consent Form		No	Not required for this project	This project uses existing samples collected from previously recruited subjects		
Participant Recruitment Material – e.g. copies of posters, newspaper adverts, website, emails		No	Not required for this project	This project uses existing samples collected from previously recruited subjects		
Organisation Management Consent / Agreement Letter		No	Not required for this project	This project uses existing samples collected from previously recruited subjects		
Research Instrument – e.g. questionnaire		No	Not required for this project	This project uses existing samples collected from previously recruited subjects		
Draft Interview Guide		No	Not required for this project	This project uses existing samples collected from previously recruited subjects		

National Research Ethics Committee consent	Yes			This has been obtained. South Manchester research ethics committee (03/SM/396).	05/12/2003 14/09/2005	Version 1 Amendment 1
Note: If the appropriate documents are not submitted with the application form then the application will be returned directly to the applicant and will need to be resubmitted at a later date thus delaying the approval process						

South Manchester Local Research Ethics Committee
Room 181
Gateway House
Piccadilly South
Manchester
M60 7LP
Telephone: 0161 237 2153
Fax: 0161 237 2383
kath.osborne@gmsha.nhs.uk

Dr SD Singh
Senior Lecturer & Cons Resp Pharmacologist
Medicines Evaluation Unit
North West Lung Research Centre
Wythenshawe Hospital
Southmoor Road
Manchester M23 9LT

Our ref: *03/SM/396*

05 December 2003

03/SM/396 - Please quote this number on all correspondence

Dear Dr Singh

The Role Of Lymphocytes And Macrophages In The Pathogenesis Of COPD; Immunological And Molecular Analysis Of Samples Obtained After Lung Surgery

The Chairman of the South Manchester Local Research Ethics Committee has considered the amendments submitted in response to the Committee's earlier review of your application on 9th October 2003 as set out in our letter dated 24th October 2003. The documents considered were as follows:

- **LREC Application Form (dated 23/7/03)**
- **Patient Information sheet (version 1, dated July 2001)**
- **Consent form (version 1, dated July 2001)**
- **GP Letter**
- **Protocol (dated 23/7/03)**

The Chairman, acting under delegated authority, is satisfied that these accord with the decision of the Committee and has agreed that there is no objection on ethical grounds to the proposed study. I am, therefore happy to give you the favourable opinion of the committee on the understanding that you will follow the conditions of approval set out below.

Conditions of Approval

- You do not recruit any research subjects within a research site unless favourable opinion has been obtained from the relevant local research ethics committees.

- You do not undertake this research in an NHS organisation until the relevant NHS management approval has been gained as set out in the *Framework for Research Governance in Health and Social Care*.

Appendix C

Table 7.1 Summary of patient demographics.

	Gender	Age	FEV1	FEV1 (%pred)	FVC	FEV1/FVC ratio	PYH	Lung Cancer lesion	SAB	LAB	ICS
CCS	10/6	70.9 **(60-82)**	1.9 **(0.9-3.5)**	74.6 **(53-96)**	3.3 **(1.7-5.4)**	59.0 **(46-75)**	56.9 **(9-124)**	y	7	4	4
CEX	17/2	72.1 **(60-80)**	1.7 **(1.3-2.5)**	64.8 **(45-118)**	3.0 **(2.4-4.5)**	56.3 **(42.5-69.3)**	48.7 **(11-112)**	y	9	12	9
NCS	4/13	64.4 **(44-78)**	2.3 **(1.6-3.3)**	105.2 **(70-131)**	3.1 **(2.1-4.4)**	73.1 **(66.9-82.5)**	44.2 **(15-90)**	y	0	0	0
NEX	9/8	72.1 **(57-84)**	2.1 **(1.2-3.2)**	91.9 **(47-127)**	2.9 **(1.8-4.1)**	71.2 **(55-85.8)**	37.3 **(2.1-117)**	y	1	1	1
NS	0/3	68.3 **(65-71)**	1.9 **(1.8-2.0)**	108.3 **(100-113)**	2.7 **(2.2-3.6)**	82.5 **(77-91)**	0 **(0)**	y	1	0	1
Average for lung cancer group	**40/32 (Total)**	**69.8 (44-84)**	**2.0 (0.87-3.5)**	**84.8 (45-131)**	**3.1 (1.69-5.4)**	**65.5 (42.5-90.9)**	**44.1 (0-124)**	**y**	**18**	**17**	**15**
HNS controls	**7/3**	**52.2 (31-75)**	**3.3 (2.3-4.18)**	**107 (82.7-148.6)**	**4.3 (2.9-5.6)**	**78.6 (70.8-95.1)**	**0.0 (0)**	**n**	**0**	**0**	**0**

Notes: Subject demographics of cancer patients (n=72) and healthy non-smoker control subjects (n=10). Gender: male/female. Groups: CCS, COPD current smoker; CEX, COPD ex-smoker; NCS, no airflow obstruction current smoker; NEX, no airflow obstruction ex-smoker, NS, never smoked; HNS, healthy never smoked. Characteristics: FEV1 (forced expired volume in 1 second), %Pred (Percentage of the predicted value), FVC (Forced Vital Capacity), PYH (Pack Year History). Recorded patient use of medications includes SAB (short-acting bronchodilators), LAB (long-acting bronchodilators), ICS (inhaled corticosteroid). Average values for each group are shown (range in brackets).

Appendix D

Table 7.2 Correlation coefficients of macrophages from lung cancer samples double labelled with *T.gondii* and iNOS

iNOS	PCC	overlap-co	K1	K2	M1	M2	Costas	*p*-value
989	r=0.221	r=0.69	0.542	0.88	0.58	0.883	-0.001±0.384	1
1025	r=0.162	r=0.45	0.34	0.596	0.625	0.522	0.0±0.138	1
1040	r=0.229	r=0.42	0.46	0.383	0.605	0.522	0.0±0.146	1
1040	r=0.276	r=0.496	0.159	1.552	0.501	0.726	0.002±0.458	1
1069	r=0.146	r=0.604	0.392	0.93	0.321	0.734	0.0±0.05	1
1040	r=0.193	r=0.508	0.279	0.924	0.751	0.448	0.001±0.337	1
1040	r=0.21	r=0.736	0.733	0.739	0.837	0.706	0.001±0.34	1
1064	r=0.122	r=0.401	0.182	0.883	0.877	0.396	0.004±0.845	1
1064	r=0.234	r=0.571	0.077	4.213	0.737	0.794	0.003±0.706	1
664	r=0.187	r=0.487	0.277	0.856	0.801	0.652	0.001±0.341	1
757	r=0.094	r=0.189	0.008	4.164	0.12	0.611	0.0±0.151	1
757	r=0.216	r=0.761	0.598	0.967	0.591	0.957	0.001±0.282	1
757	r=0.114	r=0.165	0.005	4.99	0.028	0.34	0.002±0.498	0.99
757	r=0.14	r=0.517	0.312	0.857	0.986	0.639	0.004±0.948	0.96
813	r=0.234	r=0.804	0.824	0.785	0.825	0.772	0.003±0.636	1
1043	r=0.224	r=0.708	0.664	0.755	0.641	0.713	0.0±0.046	1
1043	r=0.237	r=0.611	0.615	0.607	0.613	0.595	0.003±0.686	1
1032	r=0.099	r=0.555	0.804	0.383	0.744	0.353	0.002±0.433	1
1068	r=0.121	r=0.463	0.328	0.653	0.938	0.499	0.0±0.138	1
1033	r=0.214	r=0.44	0.145	1.336	0.645	0.723	0.001±0.375	1
1033	r=0.238	r=0.71	0.53	0.95	0.694	0.913	0.0±0.139	1
1033	r=0.162	r=0.434	0.075	2.507	0.371	0.973	0.001±0.364	1
1043	r=0.247	r=0.572	0.569	0.575	0.57	0.565	-0.002±0.563	1
1072	r=0.164	r=0.355	0.379	0.332	0.361	0.428	0.001±0.376	1
1032	r=0.131	r=0.446	0.333	0.596	0.36	0.198	0.004±0.937	1
1032	r=0.194	r=0.385	0.511	0.29	0.429	0.155	0.0±0.056	1
1004	r=0.269	r=0.447	0.489	0.41	0.592	0.125	0.0±0.044	1
1068	r=0.095	r=0.411	0.595	0.284	0.405	0.187	0.0±0.141	0.97
813	r=0.096	r=0.611	0.384	0.972	0.309	0.621	0.0±0.042	0.99
757	r=0.071	r=0.191	0.008	4.164	0.067	0.197	0.0±0.139	1
757	r=0.139	r=0.69	0.503	0.945	0.501	0.93	0.0±0.14	1
757	r=0.217	r=0.375	0.11	1.276	0.217	0.204	-0.003±0.689	1
1033	r=0.159	r=0.44	0.144	1.344	0.316	0.278	-0.002±0.409	1
1033	r=0.18	r=0.622	0.395	0.977	0.329	0.781	0.001±0.334	1

Table 7.3 Correlation coefficients of macrophages from lung cancer samples double labelled with *T.gondii* and Arg-1

Arg-1	PCC	overlap-co	K1	K2	M1	M2	Costas	*p*-value
1025.00	r=0.421	r=0.581	0.42	0.81	0.81	0.73	-0.004±0.845	1.00
1025.00	r=0.622	r=0.741	0.73	0.76	0.82	0.73	0.001±0.285	1.00
1025.00	r=0.592	r=0.711	0.67	0.75	0.82	0.66	-0.001±0.304	1.00
1025.00	r=0.67	r=0.669	0.05	8.49	0.15	0.95	0.0±0.199	1.00
1040.00	r=0.215	r=0.73	0.58	0.92	0.64	0.90	0.0±0.035	1.00
1040.00	r=0.471	r=0.643	0.29	1.41	0.77	0.61	0.002±0.451	1.00
1040.00	r=0.436	r=0.641	0.30	1.37	0.75	0.65	0.0±0.08	1.00
1040.00	r=0.566	r=0.742	0.50	1.10	0.92	0.82	-0.001±0.385	1.00
757.00	r=0.543	r=0.781	0.17	3.64	0.77	0.97	0.003±0.613	1.00
757.00	r=0.57	r=0.791	0.17	3.76	0.76	1.00	0.0±0.15	1.00
813.00	r=0.539	r=0.651	0.18	2.39	0.73	0.86	-0.001±0.34	1.00
813.00	r=0.513	r=0.575	0.15	2.15	0.53	0.73	-0.003±0.754	1.00
813.00	r=0.423	r=0.591	0.27	1.31	0.81	0.60	0.0±0.061	1.00
1068.00	r=0.334	r=0.727	0.27	1.95	0.88	0.98	0.0±0.121	1.00
1068.00	r=0.607	r=0.742	0.28	1.96	0.73	0.98	0.0±0.129	1.00
1068.00	r=0.52	r=0.775	0.31	1.95	0.89	0.95	0.001±0.241	1.00
1072.00	r=0.41	r=0.798	0.74	0.86	0.91	0.82	0.001±0.389	1.00
1072.00	r=0.46	r=0.678	0.13	3.52	0.92	0.93	-0.004±0.966	1.00
1033.00	r=0.543	r=0.754	0.50	1.15	0.85	0.73	-0.001±0.251	1.00
1037.00	r=364	r=0.397	0.22	0.72	0.76	0.37	0.0±0.09	1.00
1037.00	r=0.304	r=0.517	0.23	1.15	0.91	0.50	-0.002±0.483	1.00
1014.00	r=0.487	r=0.885	0.79	1.00	0.89	0.99	0.001±0.274	1.00
1014.00	r=0.534	r=0.842	0.80	0.88	0.86	0.91	0.002±0.542	1.00
1014.00	r=0.497	r=0.839	0.86	0.82	0.91	0.83	0.003±0.648	1.00
1032.00	r=0.401	r=0.729	0.78	0.68	0.85	0.64	0.003±0.67	1.00
1052.00	r=0.564	r=0.676	0.15	3.14	0.66	0.87	-0.002±0.423	1.00
1072.00	r=0.493	r=0.756	0.59	0.97	0.54	0.95	0.003±0.769	1.00
1072.00	r=0.437	r=0.756	0.77	0.75	0.49	0.58	0.001±0.257	1.00
1072.00	r=0.413	r=0.709	0.13	3.85	0.36	0.51	-0.011±2.353	1.00
1068.00	r=0.489	r=0.726	0.27	1.97	0.44	0.44	0.002±0.49	1.00
1068.00	r=0.606	r=0.777	0.31	1.93	0.56	0.58	0.003±0.62	1.00
1068.00	r=0.589	r=0.74	0.28	1.96	0.42	0.57	-0.001±0.312	1.00
1068.00	r=0.418	r=0.819	0.64	1.05	0.56	0.96	0.002±0.499	1.00
813.00	r=0.54	r=0.645	0.42	0.99	0.36	0.91	0.005±1.162	1.00
813.00	r=0.437	r=0.846	0.86	0.84	0.85	0.82	0.006±1.295	1.00
813.00	r=0.415	r=0.559	0.38	0.83	0.31	0.70	0.003±0.796	1.00
813.00	r=0.551	r=0.652	0.18	2.39	0.32	0.41	-0.001±0.344	1.00
813.00	r=0.514	r=0.548	0.14	2.15	0.25	0.46	0.0±0.118	1.00
813.00	r=0.564	r=0.643	0.18	2.29	0.70	0.77	0.001±0.367	1.00
813.00	r=0.527	r=0.639	0.32	1.27	0.90	0.58	0.001±0.205	1.00
813.00	r=0.581	r=0.67	0.20	2.23	0.68	0.80	-0.002±0.456	1.00

Table 7.4 Correlation coefficients of a cyst from lung cancer samples double labelled with *T.gondii* and iNOS

Arg-1	PCC	overlap-co	K1	K2	M1	M2	Costas	*p*-value
1008	r=0.116	r=0.408	0.3	0.556	0.864	0.535	0.001±0.217	1
1045	r=0.076	r=0.369	1.054	0.129	0.688	0.307	0.003±0.748	1
1028	r=0.51	r=0.816	0.879	0.757	0.793	0.545	0.0±0.196	1

Table 7.5 Correlation coefficients of a cyst from lung cancer samples double labelled with *T.gondii* and Arg-1

iNOS	PCC	overlap-co	K1	K2	M1	M2	Costas	*p*-value
1008	r=0.67	r=0.669	0.248	1.801	0.96	0.615	0.003±0.678	1
1045	r=0.435	r=0.921	0.899	0.944	0.741	0.691	0.001±0.32	1
1028	r=0.037	r=0.322	0.4	0.258	0.38	0.291	0.0±0.071	1

Table 7.6 Correlation coefficients of alveolar walls (knobs) from lung cancer samples double labelled with *T.gondii* and iNOS

iNOS	PCC	overlap-co	K1	K2	M1	M2	Costas	*p*-value
972	0.171	r=0.899	0.868	0.931	0.806	0.861	0.0±0.091	1
985	0.294	r=0.378	0.23	0.62	0.274	0.169	-0.001±0.358	1
1005	0.172	r=0.324	0.266	0.394	0.176	0.231	0.0±0.044	1
1030	0.298	r=0.393	0.395	0.391	0.137	0.282	0.003±0.6	1
1054	0.394	r=0.47	0.197	1.119	0.315	0.218	-0.005±1.044	1
757	0.276	r=0.555	0.219	1.404	0.381	0.234	0.002±0.563	1
813	0.633	r=0.713	0.547	0.928	0.506	0.365	0.0±0.179	1
1004	0.516	r=0.769	0.351	1.681	0.453	0.329	-0.002±0.419	1

Table 7.7 Correlation coefficients of alveolar walls (knobs) from lung cancer samples double labelled with *T.gondii* and Arg-1

Arg-1	PCC	overlap-co	K1	K2	M1	M2	Costas	*p*-value
985	0.212	r=0.38	0.46	0.31	0.209	0.192	0.008±1.61	0.99
988	0.47	r=0.51	0.39	0.67	0.62	0.181	-0.003±0.7	1
1013	0.58	r=0.71	0.98	0.51	0.826	0.242	0.021±4.25	1
664	0.304	r=0.40	0.40	0.40	0.17	0.307	-0.001±0.4	1
813	0.474	r=0.55	0.733	0.414	0.901	0.165	-0.004±0.8	1